Analyzing the regional long-term development of the German power system using a nodal pricing approach

Zur Erlangung des akademischen Grades eines
Doktors der Wirtschaftswissenschaften
(Dr. rer. pol.)

von der Fakultät für Wirtschaftswissenschaften
des Karlsruher Instituts für Technologie (KIT)

genehmigte
DISSERTATION
von

Dipl.-Wi.-Ing. Anke Eßer-Frey

Referent:
Prof. Dr. Wolf Fichtner

Korreferenten:
Prof. Dr. Dominik Möst
Prof. Dr. Werner Rothengatter

Tag der mündlichen Prüfung: 7. Mai 2012

Vorwort

Die vorliegende Arbeit entstand während meiner Tätigkeit am Institut für Industriebetriebslehre und Industrielle Produktion (IIP) des Karlsruher Instituts für Technologie. Die Grundlage bildeten Arbeiten im Rahmen der Young Investigator Group „New methods for energy market modelling“ unter Leitung von Prof. Dr. D. Möst (jetzt TU Dresden), die mit Geldern der Exzellenzinitiative des Bundes und der Länder zur Förderung von Wissenschaft und Forschung an deutschen Hochschulen gefördert wurden.

Die Fertigstellung dieser Arbeit wäre ohne die Unterstützung einer Vielzahl von Menschen nicht möglich gewesen, denen ich in diesem Rahmen danken möchte. Besonderer Dank gilt meinem Doktorvater Prof. Dr. W. Fichtner für die Betreuung der Arbeit. Gleichfalls gilt mein Dank Prof. Dr. O. Rentz für die Unterstützung und Betreuung in den ersten Jahren meiner Tätigkeit am IIP. Beim ehemaligen Leiter meiner Arbeitsgruppe “Energiesystemanalyse und Umwelt” Prof. Dr. D. Möst bedanke ich mich für seine Unterstützung, konstruktive Diskussionen sowie die Übernahme des Korreferats. Zudem gilt mein Dank Prof. Dr. W. Rothengatter für die Übernahme des Korreferats.

Des Weiteren möchte ich mich bei meinen ehemaligen Kollegen, insbesondere den Mitgliedern meiner Arbeitsgruppen “Energiesystemanalyse und Umwelt” sowie “Dezentrale Energiesysteme und Netze”, für die gute Zusammenarbeit sowie zahlreiche Anregungen und Diskussionen bedanken. Für die prüfende Durchsicht des Manuskripts bedanke ich mich bei Sonja Babrowski, Heidi Heinrichs, Dr. Anne Held, Dr. Russell McKenna, Christoph Nolden sowie Kerstin und Christopher Wilson.

Nicht zuletzt danke ich meinem Mann Andreas, meiner Familie sowie meinen Freunden für ihr Verständnis und ihre Unterstützung während der Fertigstellung der Arbeit.

Steinweiler, Mai 2012   Anke Eßer-Frey

Contents

List of Figures

List of Tables

Nomenclature

Indices

ec	Index of energy carriers
ex	Index of export nodes, i.e. the sinks of the graph
ext	Index of external grid nodes, i.e. transmission grid nodes
$heattype$	Index of heat types
im	Index of the sources of the graph
int	Index of internal grid nodes
$nuts1$	Index of NUTS1-region
$nuts3$	Index of NUTS3-regions
$proc$	Index of processes
$prod$	Index of producers
reg	Index of regions
$seas$	Index of time slots
sub	Index of subregions
t	Index of years
$unit$	Index of units

Set of indices

$DEMPROC_{proc,ec}$	Set of demand processes
EC	Set of energy carriers
EX	Sinks of the graph
EXT	Set of external grid nodes
$GENPROC$	Set of generation processes

$HEATPROC$	Set of heat generation processes
$HEATTYPE$	Set of heat types
IM	Set of sources of the graph
INT	Set of internal grid nodes
$NUTS1$	Set of NUTS1-regions
$NUTS3$	Set of NUTS3-regions
$PROC$	Set of processes
$PROD$	Set of producers
REG	Set of regional indices
$SEAS$	Set of time slots
SUB	Set of subregions
T	Set of periods
$UNIT$	Set of units

Parameters

α_t	Discount factor
$\beta_{ec,reg1,reg2}$	Share of the subregion *reg1* of region *reg2* in the energy carrier potential of region *reg2*
$\delta^{CI}_{nuts3,electr,t}$	Annual power consumption of commerce and industries in in time slot t within the region nuts3.
$\delta^{HH}_{nuts3,electr,t}$	Annual power consumption of commerce and industries in in time slot (t,seas) within the region nuts3.
$\eta_{proc,ec}$	Efficiency of the process *proc* using energy carrier ec
$\eta_{prod,prod',ec,t}$	Transport efficiency of the flow *(prod,prod',ec,t)*
$\lambda_{proc,ec}$	Share of energy carrier *ec* related to the total input / output of a process *proc* (convention: negative sign for input, positive sign for output)
$\omega_{proc,t}$	Power production equivalent of the process *proc* in period t
$\sigma^{CI}_{nuts1,t}$	Specific power consumption of commerce and industries in a NUTS1-region in period t

$\sigma^{HH}_{nuts1,t}$	Specific power consumption of households in a NUTS1-region in period t
$A_{ec,reg}$	Area potential of a region *reg* regarding the installation of ec-fueled power stations
$Avai_{unit,t}$	Average availability of a unit *unit* in period t
$b_{ext,ext',t}$	Element of the admittance matrix in period t
C_{km}	Themal limit of the power line *km*
$CapMax_{unit,t}$	Upper limit for the totally installed capacity of a unit in period t (including capacity additions)
$CapMin_{unit,t}$	Lower limit for the totally installed capacity of a unit in period t capacity additions
$CapRes_{unit,t}$	Capacity of a unit already installed in period t (residual capacity)
$Cfix_{unit,t}$	Fixed annual maintainance and operation costs of the unit in period t
$Cfuel_{prod,ec,t}$	Costs for delivering the fuel *ec* to producer *prod* in period t
$Cinv_{unit,t}$	Specific investment for commissioning the unit in period t
$Cload_{unit,t}$	Load change costs of the unit in period t
$Cvar_{prod,prod',ec,t}$	Variable transport costs of the flow *(prod,prod',ec)* in period t
$Cvar_{prod,ex,ec,t}$	Variable transport costs of the export flow *(prod,ex,ec)* in period t
$Cvar_{proc,t}$	Variable operating costs of the process *proc* in period t
$D_{reg,ec,t,seas}$	Demand of region *reg* for energy carrier *ec* in time slot *(t,seas)*
$D_{nuts3,electr,t,seas}$	Power demand of a NUTS3-region *nuts3* in time slot *(t,seas)*
$f_{proc,t,seas}$	Load profile of a demand process (as weight of the time slot *(t,seas)* as related to the total annual demand)
$f_{nuts3,t,seas}$	Load profile of the county *nuts3* (as weight of the time slot *(t,seas)* as related to the total annual demand)
$FLLEV_{prod,prod',ec,t}$	Binding flow level for flow *(prod,prod',ec,t)*
$FLMAX_{prod,prod',ec,t}$	Maximum flow level for flow *(prod,prod',ec,t)*

$FLMIN_{prod,prod',ec,t}$	Minimum flow level for flow *(prod,prod',ec,t)*
$GDP_{nuts3,t}$	Gross domestic product of the county *nuts3* in period t
$h_{ext,ext',ext'',t}$	Element of the transfer admittance matrix in period t belonging to line *ext,ext'* and grid node *ext"*
$HGF_{unit,t,seas,heattype}$	Load profile of a heat demand unit in time slot *(seas,t)* of a specific heattype
h_{seas}	Number of hours in season *seas*
h_{year}	Number of hours of the year
$INH_{nuts3,t}$	Number of inhabitants of the NUTS3-region (county) in period t
LT_{unit}	Life time of the unit *unit*
$MaxAdd_{unit,t}$	Maximum allowed capacity addition of a unit *unit* in period t
$NewCap_{ec,reg,t}$	Sum of all new power generating capacities using fuel *ec* that are constructed in region *reg* in period t
$No_{seas-1,seas}$	Number of transitions between time slots *seas-1* und *seas* in the course of one year
$Rcap_{(pr/sr)tr,unit,seas,t}$	Maximume contribution of a unit's capacity to a type of reserve in time slot *(seas,t)*
$Rdem_{(pr/sr)tr,unit,seas,t}$	Total demand for a type of reserve in a region *reg* in a time slot *seas* in a period t
$Slack_{ext}$	Parameter indicating the slack bus at the external grid node *ext*
$ThLim_{ext,ext',t}$	Thermal limit of the transmission line (ext,ext') in period t
$VlhMax_{proc,t}$	Maximally allowed full load hours of the process *proc* in period t
$VlhMin_{proc,t}$	Minimally required full load hours of the process *proc* in period t

Variables

$\theta_{ext,t,seas}$	Phase angle difference at grid node *ext* in timeslot *(t,seas)*
$Cap_{unit,t}$	Installed capacity of a unit in period t

$CapNew_{unit,t}$	Newly installed capacity of a unit *unit* in period t (capactiy addition)
$CapNew_{unit,t}$	Newly installed capacity of a unit in period t
$FL_{prod,ex,ec,t}$	Level of the export flow *ex* of energy carrier *ec* from producer *prod* in period t
$FL_{ext,ext',elec,t,seas}$	Level of the power flow over a transmission line *(ext,ext')* in time slot *(t,seas)*
$FL_{im,prod,ec,t}$	Level of an import flow of the energy carrier *ec* into producer *prod* in period t
$FL_{prod,prod',ec,t}$	Flow level of energy carrier *ec* from producer *prod* to producer *prod'* in period t
$FL_{prod,prod',ec,t,seas}$	Seasonal flow level of energy carrier *ec* from producer *prod* to producer *prod'* in season *seas* of the period t
$LVdown_{unit,seas-1,seas,t}$	Negative load change of a unit between the time slots *sesas-1* and *seas*
$LVup_{unit,seas-1,seas,t}$	Positiv load change of a unit between the time slots *sesas-1* and *seas*
$NetIn_{ext,elec,t,seas}$	Net injection of electricity into the grid node *ext* in time slot *(t,seas)* (Electricity that is produced within a subregion)
$PL_{proc,t,seas}$	Activity level of the process *proc* in time slot *(t,seas)*
$PL_{proc,t}$	Activity level of the process *proc* in period t

List of abbreviations

AC	alternating current
AM/FM	automated mapping / facility management
AMP	automated ex ante market power mitigation measure
APX	Amsterdam Power Exchange
A/S	ancillary services
ATC	available transmission capacity
BAT	best available technology
BeNeLux	Belgium, the Netherlands, and Luxembourg
BMU	Bundesministerium für Umwelt, Naturschutz und Reaktorsicherheit - Federal Ministry for the Environment, Nature Conservation and Nuclear Safety
CCGT	combined cycle gas turbine
CCS	carbon capture and storage
CHP	combined heat and power
CWE	Central West European market coupling
CRR	congestion revenue rights
DC	direct current
DCOL	direct current ohmic losses
EC	European Commission
ECCP	European Climate Change Program
EEX	European Energy Exchange
EFOM	Energy Flow Model
ELMOD	Electricity Market Model
EMCC	European Market Coupling Company
ENTSO-E	European Network of Transmission Ssystem Operators for Electricity
EPEX	European Power Exchange
ETSO	European Transmission System Operators
ETS	Emission Trading Scheme
EU	European Union
EUA	EU Emission Allowance
EXAA	Energy Exchange Austria

FERC	Federal Energy Regulatory Commission
FNP	full nodal pricing
FTR	financial transmission right
GAMS	General Algebraic Modeling System
GDP	gross domestic product
GEM	general equilibrium model
GENCO	generating company
GHG	greenhouse gas
GIS	geographic information system
GRIDCO	grid operating company
GT	gas turbine
GWP	global warming potential
HPS	hydro-electric pumped storage
HV	high voltage
HVDC	high voltage direct current
ICT	information and communication technology
IGCC	integrated gasification combined cycle
IO	input-output (model)
ISO	independent system operator
LMP	locational marginal pricing
LNG	liquefied natural gas
MC	marginal cost
MCDA	multi criteria decision analysis
MCF	market coupling flows
MIP	mixed integer programming
MOREHyS	Model for Optimization of Regional Hydrogen Supply
MV	medium voltage
MRTU	Market Redesign and Technology Upgrade
NAP	National Allocation Plan
NGCC	natural gas combined cycle
NUTS	Nomenclature of Territorial Units for Statistic: NUTS0 = country, NUTS1= federal state, NUTS2 = administrative region, NUTS3 = county.
OPF	optimal power flow
OR	Operations Research
OTC	over-the-counter, meaning off-market
PCC	pulverized coal combustion
PERSEUS	Program Package for Emission Reduction Strategies in Energy Use and Supply
PFC	power flow controlling

PTDF	power flow distribution factors
PV	photovoltaic
RDCOL	restricted direct current ohmic losses (model)
RES	renewable energy sources
RES-E	electricity generated from renewable energy sources
RSC	regional system coordinator
RTD	research and technology development
SADI	system average duration of interruptions
SCED	security constrained economic dispatch
SCUC	security constrained unit commitment
SO	system operator
StromNEV	Stromnetzentgeltverordnung - German System Usage Fee Ordinance
StromNZV	Stromnetzzugangsverordnung - German Electricity Grid Access Ordinance
TCC	tradable congestion contract
TLC	trilateral market coupling - coupling of the power markets of Belgium, France, and the Netherlands
TSO	transmission system operator
UCTE	Union for the Coordination of the Transmission of Electricity
UML	unified modeling language

1. Introduction

1.1. Motivation

The German power system is subject to extensive structural changes. In its latest reform of the Renewable Energy Act, the German government set the target to increase the share of renewable energies in power supply to 35% by 2020 and to 50% by 2030 (EEG [2011]). This target shall be reached, above all, by installing large offshore wind parks in the North Sea and in the Baltic Sea. The annually published lead study of the German Federal Ministry for the Environment, Nature Conservation and Nuclear Safety projects a total offshore wind turbine capacity of 25 GW for 2030, which is to produce 95 TWh/a. By 2050 power generation of offshore wind farms is projected to reach 157 TWh/a. Moreover, the installed capacities of roof-top photovoltaic are expected to rise significantly from 17 GW in 2010 to 60 GW by 2030 (DLR et al. [2010]). The increasing use of renewable energies in power generation will, on the one hand, involve a further decentralization of the German power system. On the other hand, the construction of large offshore wind farms on the coasts will involve a shift of generation capacities from Southern parts of Germany to regions in the North that are faraway from the large load centers. This will require the conduction of large amounts of electricity from the North to large load centers in South and West Germany. As a consequence, the grid load in the German system will rise to an extent that is not manageable with existing power grid capacities any more. Latest studies determine a need for additional grid capacity with a route length of at least 3,600 km by 2020 (DENA [2010a]).

As a response to the nuclear disaster at Fukushima, the German government and prime ministers of the federal states decided upon a three month moratorium of the seven oldest operating German nuclear power stations in March 2011. Before the end of the moratorium the German legislator passed an amendment to the Nuclear Power Act, which declares that the nuclear power stations affected by the moratorium as well as one further, which already had been shut down due to technical problems, will not be reactivated again. Moreover, it sets a schedule for the shut down of the remaining nuclear power stations, according to which the last nuclear power stations will be finally taken offline at the end of 2022. Since, again, power generation close to the large load centers in the southern parts of Germany is affected, the abrupt shut down of nuclear power stations leads to a significantly increased system loading of the German power system, which is expected to result in increased congestion in the cooler months of the years 2011 and 2012 (Bundesnetzagentur [2011b]). Due to the shut-down of nuclear power stations the need for new power generating capacity rises. The demand for new generating capacity is exacerbated by the fact that the technical lifetime of a huge share of existing power stations will be reached by 2030. Since the remaining bottleneck capacity will not suffice to meet the anticipated demand by 2030, 31 GW - 44 GW of new fossil-fueled power station capacity will have to be commissioned in Germany (BDEW [2011]).

To evaluate the potential development path of the restructuring of the German power system a profound energy system analysis should be conducted. One of its main focuses should be to provide for decision support in power station investment planning. The models used for such types of energy system analysis are called power plant or capacity expansion planning models. They are applied to determine the optimal size and point in time of power station capacity expansion as well as the optimal fuel mix. Yet, due to the structural changes in the German power system new requirements for energy system modeling arise. For a comprehensive assessment of future developments in the German power system, grid constraints have to be taken into account. The power system cannot be regarded as a copperplate anymore, but congestion in the grid will rather necessitate the modeling of power flows and grid constraints. Besides the need for capacity expansion, the location of the new capacities becomes of importance, given the increasing decentralization of electricity supply systems. Therefore the integration of regional aspects, such as regional availabilities of renewable and fossil energy sources or the location of power stations, into capacity expansion planning models is imperative to cope with these new requirements for energy system models.

Yet, common modeling approaches used today to analyze the power system development consider both aspects only in an insufficient way. Energy system models generally deal with the power systems in a rather aggregated way, in which whole countries are virtually collapsed into a single grid node and neither regional aspects nor power flows and grid constraints within the countries are taken into account. In recent years, first approaches to adequately consider the power grid as well as regional power system characteristics in energy system modeling have been made (cf. e.g. Schönfelder et al. [2011]). Yet, these approaches focus on evaluating the situation in single years and thus do not allow for the analysis of the optimal long-term development of the German power system.

1.2. Objective and methodological approach

The objective of this work is therefore to develop a modeling approach for the analysis of the long-term development of the German power supply system that allows for an adequate consideration of the power grid as well as the regional characteristics of the power system. The focus of the modeling approach will be on analyzing the regional development of the German power system, paying special regard to the optimal expansion of power stations from a techno-economic point of view. Moreover, the regional development of the marginal cost for power supply shall be analyzed. This requires locational price signals for decision support that reflect the locational marginal costs of electricity supply and provide a basis for decisions regarding a regionally optimal power plant expansion.

This thesis offers a novel approach to obtain the required regional prices signals for power station capacity investments. A nodal pricing approach, which consists of a grid node-based representation of a power system, is integrated into the bottom-up energy system model PERSEUS. Moreover, the power flows in the system are determined using a direct current (DC) optimal power flow approach. Using the developed modeling approach, the locational marginal costs of power supply can be obtained, which comprise the marginal cost of generation as well as the marginal cost of congestion in the power grid.

It is not the objective of this work to evaluate whether a nodal pricing-based market system is better suited for Germany than the existing centralized one. The nodal pricing-based energy system model will be rather used within this thesis to analyze possible development paths of the German power system.

To meet the objective of this work, the following procedure has been chosen:

In chapter 2 the political framework conditions formed by European and German legislature and the resulting challenges for power station capacity investment planning in Germany are outlined.

The theoretical background on power markets and price signals is given in chapter 3. It comprises a summary of the principles of the determination of electricity prices and the relevance of power market price signals, as well as a description of the architecture of the German power market. Moreover, the concept of locational marginal pricing as an alternative market approach is introduced and applications of locational marginal pricing are described.

Based on this theoretical background, chapter 4 describes first modeling approaches to include the concept of locational marginal pricing in multi-period power system analysis. Initially, the requirements for a spatio-temporal energy system model are outlined. Then, optimal power flow models are presented, which allow for an integration of power flow calculations and grid constraints in energy system models. Special attention is paid to the electrotechnical principles of optimal power flow models as well as to different power flow model types. Moreover, a literature survey on applications of locational marginal pricing and optimal power flow approaches in energy system analysis is given. The last part of chapter 4 deals with tools to edit, manipulate, and store data describing the regional characteristics of the energy system. In the context of geographic modeling, in particular, database-based geographic information systems have been proven most useful. Therefore, in the last part of this chapter, a literature survey on existing approaches using geographic information systems in power system analysis is given.

Based on the literature surveys on existing modeling approaches, a nodal pricing-based energy system model to analyze the spatio-temporal development of power systems is developed in chapter 5. After a short overview of the model's structure and components and the energy system models serving as precursors of the developed modeling approach, the mathematical description of the multi-period linear optimization model is presented. It comprises the objective function specifying all relevant costs of power generation and transmission as well as the system equations for power generation and transmission. The latter represents the power flow equations of a DC optimal power flow model.

Within this thesis, the model developed in chapter 5 is used to analyze the long-term regional development of the German power system. The structure and data basis for this analysis is described in chapter 6. It comprises the time horizon and temporal resolution of the model as well as the technical specification and regional distribution of the power grid model and power generation technologies. Moreover, the derivation of the regional distribution of power generating capacities using renewable energy sources and power demands is explained.

Using the optimizing energy system model developed in chapter 5 and the input data described in chapter 6, the regional development of the German power system till 2030 is analyzed in chapter 7. The base scenario describes the development of the input parameters assumed to be most likely. To account for different developments, alternative scenarios covering gas price variations, as well as variations in the prices of EU allowances are analyzed. Moreover, the influence of delays in grid extensions as well as significantly increasing power imports is analyzed.

In chapter 8, the model is critically reflected. In chapter 9, the results obtained with the model application are compiled and discussed.

Moreover, in chapter 10 conclusions that can be drawn from the model application regarding the future development of the German power system as well as the adequacy of the chosen modeling approach are outlined. The thesis concludes with an outlook on future research perspectives.

2. Political context for investment decisions in the power sector

Studies suggest that until 2030, up to 100 GW of new power generating capacity will have to be commissioned in the German power system to replace existing power stations and to meet increasing demand (cf. e.g. DENA [2008]). Since the construction of e.g. a coal power station requires approximately ten years, a large part of the investment decisions has to be prepared or taken within the next ten to fifteen years. As part of the strategic planning, investment decisions determine the direction in which a company will develop in the future. By contrast to other sectors, investments in power system infrastructure are characterized by a high capital intensity and long payback periods as well as long operational lifetimes of the assets (cf. Rosen [2007, p. 9]). Furthermore, since electricity is grid-bound, inter-dependencies between the investment decisions of individual actors exist. Investment decisions have to be taken behind the framework of changing economic, political, and social framework conditions. The decisions to invest in new power system infrastructure are affected to a high degree by political and legal framework conditions. On the one hand, strong political influence is exerted on the actors in the electricity sector, on the other hand, uncertainties arise due to changing political framework conditions.

In the following, the main political framework conditions which contribute to possible future developments in the energy sector will be outlined. In the second part of this chapter, the resulting challenges for power generating capacity investment planning will be discussed.

2.1. Factors of change in energy and environmental policy in Germany and Europe

Electricity is used in almost all processes of industrial production as well as for most household appliances. With about 20% in Germany's final energy consumption, it is the third most important final energy carrier (cf. AGEB [2011b]). Therefore, securing an economically efficient electricity supply traditionally is one of the major concerns of policy makers (cf. COM(2000)769, p. 11ff.). Energy supply companies in Germany act within the political and legal framework of the European Union.[1] Since the 1990s

[1] EU legislation constitutes the legal framework for national law. It has priority over state regulation. The two most important pillars of EU legislation are Regulations and Directives. Regulations are immediately effective, whereas Directives have to be transfered into national law. They declare binding objectives for the EU Member States.

the European energy policy is affected by three major efforts (cf. e.g. COM(2000)769, COM(2006)105, COM(2007)1):

- introducing competition in the European energy markets,
- reducing the EU's external energy dependency, and
- reducing greenhouse gas (GHG) emissions.

The latter two ambitions are supported by increasing the share of renewable energy sources (RES) in power generation as well as by increasing energy efficiency in power generation and demand. To introduce competition, the European gas and power markets have been gradually liberalized in the last 20 years. In Germany, the common European efforts are completed by a fourth endeavor, the phase-out of nuclear power station. Altogether, these political intentions have led to substantial changes in the structure of the energy sector that strongly affect energy systems operation and planning.

In the following sections, the main issues of energy and environmental policy will be addressed, that is the liberalization of the electricity market, the security of supply with primary energy sources, energy efficiency, renewable energy sources in power generation and the nuclear phase-out in Germany. In doing so, special regard will be paid to their relevance for the long-term development of the German power system.

2.1.1. The process of liberalization in the European electricity market

The objective of the liberalization of the European power markets was to replace the existing monopolies by competitive, open, and integrated energy markets, as to achieve competitive prices and higher standards of service and security of supply. Before the liberalization process of the European energy sector was initiated in the 1990s, electricity was provided by vertically integrated energy utilities, dealing with the production, transmission, trading, and distribution of electricity. Energy prices were determined using a cost-based approach and had to be approved by the state.

The first important European remittal with the intention to increase competition in the European energy markets and to reduce inefficiencies, was Directive EC [1996] concerning common rules of the internal market in electricity. Above all, it was to initiate the liberalization of the European electricity market by creating a free and competitive single European market. It established common rules for the generation, transmission, and distribution of electricity and set up the liberalization of retail markets. In addition, Directive 96/92/EC initiated the financial unbundling of vertically integrated energy supply industries, by requiring separate accounting for the generation, transmission, and distribution of energy products. Moreover, the Member States were requested to establish a non-discriminatory grid access, for all eligible power producers, including independent power producers as well as producers located outside the national power systems, by implementing either a regulated or negotiated grid access model. Member States were urged to implement measures to guarantee the construction of sufficient transmission, distribution, and interconnecting capacity. Furthermore, the use of market-based methods for congestion management was set out. In the years following the enactment of Directive 96/92/EC, almost all Member States passed appropriate regulations for the transmission of the Internal Market Directive into national law - in Germany with the Energy Act of 1998 (EnWG [1998]).[2]

Since several years after the liberalization process started, a number of obstacles to competition persisted, the first Internal Market Directive was replaced by the so-called Acceleration Directive (EC [2003a]), which became effective on July 1, 2004.[3] It was transposed into German national law by the Energy Act of 2005 (EnWG [2005]). Above all, Directive 2003/54/EC committed the Member States to accelerate the financial unbundling of energy supply companies and ordered the legal and organizational unbundling of system operators. In addition, it fostered the electricity market opening.[4]

Regarding grid regulation, new rules for the access to power grids as well as the determination of transmission fees were set out. Conditions for access to the grid for cross-border exchanges that enhance competition within the Internal Energy Market were specified in Regulation EC [2003b]. Among other things, rules regarding the establishment of a compensation mechanism for cross-border flows were established. Moreover, harmonized principles on cross-border transmission charges and on the allocation of interconnection capacities were created. Regarding congestion management, non-discriminatory market based solutions which give efficient economic signals to the market participants and transmission system operators were required (EC [2003b]). In Germany, the directives regulating power grid access (StromNZV [2005]), defines i.a. principles for congestion management, according to which network or market related methods for congestion management have to be used in Germany, if they are economically reasonable. The German regulation of system usage fees is specified in StromNEV [2005], according to which the level of system usage fee that has to be paid for contemporaneous feeding in and extraction of power is determined by the voltage levels affected and is thus independent from the distance over which power has to be transported. Moreover, in 2005 a Federal Network Agency took up work, e.g. to control the process of unbundling and the levels of transmission fees. In addition, it is responsible for the monitoring of security of power supply. In 2007, the German parliament enacted the Ordinance Concerning an Incentive Regulation (AregV [2007]). It implies that from 2009 on, a revenue cap regulation for gas and power grids controlled by the Federal Network Agency applies, according to which individual revenue caps are defined for each system operator in a way to reduce inefficiencies in the energy supply systems of the system operators.

In 2009, the European Commission passed the third Internal Market Package (EC [2009d]) i.a. to enforce a stricter (vertical) unbundling of power grid owners and operators. In addition, the creation of an Agency for the Cooperation of Energy Regulators

[2] In the EnWG [1998], Germany chose a negotiated access model for grid access at the beginning.

[3] Among the obstacles ranked excessively high grid transmission fees and undisclosed and unapproved transmission fee structures, high market power in combination with a lack of liquidity on power markets, as well as an insufficient unbundling of energy supply companies (cf. e.g. SEC(2001)1957 [2001], SEC(2002)1038 [2002], SEC [2004]).

[4] Since July 1, 2004 non-household customers and since July 1, 2007 household customers are free to choose their supplier in Germany.

was initiated and the duties and power of the National Regulatory Authorities were specified. Furthermore, in a new Directive on conditions for access to the network for cross-border exchanges (EC [2009e]) was issued. Among other things, it establishes a European Network of Transmission System Operators for Electricity (ENTSO-E). Moreover, general principles for a market-based congestion management are laid down and new guidelines on the management and allocation of cross-border grid capacities are specified. In particular, the European Parliament and the Council of the EU emphasize on the need for *"efficient locational signals"* (EC [2003b, art. 4]) for grid access and congestion management methods that give signals *"for efficient network and generation investment in the right location."* (EC [2003b, Annex])

Concerning this work, in particular the unbundling of power station and grid owners is of importance. Since power station and grid operation and expansion are not performed by the same entity any more, economic inefficiencies caused by suboptimal unit commitment or infrastructure siting are likely to occur. This challenge could be met by locational price signals. One example of such price signals are the market-based congestion management method favored by the European Commission.

2.1.2. Security of supply with primary energy sources

Ensuring an economically and ecologically efficient energy supply counts among the most important efforts of European economic policy. In 2000, the Commission of the European Communities published its first Green Paper on the security of energy supply (COM(2000)769), which addressed the subject of the increasing dependence of the European Union on external energy supplies. In a broader sense, security of supply in the electricity sector can be defined as an uninterruptedly power supply, which implies that consumers are able to meet their demand at all times, at present as well as in the future.[5] Hurdles to security of supply can be e.g. physical risks, such as the exhaustion of energy sources that can be exploited at reasonable costs, or economic risks, such as erratic price fluctuations (cf. COM(2006)105).

At present, Germany's supply with primary energy carriers can be considered as being secured. However, Germany is becoming increasingly dependent on external supplies.[6] Traditionally, power generation in Germany is based on fossil fuels and uranium. In 2010, lignite had the highest share in electricity generation (23.7%), followed by uranium (22.6%) and hard coal (18.7%) (cf. AGEB [2011a]). The share of RES in power generation amounted to 16.5%, while the share of natural gas amounted to 13.6%.

5 Small-scale, short-lived interruptions that only marginally effect consumers' demand fulfillment, are generally not considered to affect the overall security of supply (cf. CONSENTEC et al. [2008]), but are rather referred to as the reliability of supply, which is quantified in the System Average Interruption Duration (SADI). In 2007, the SADI of the German power system amounted to 19.5 min. per end customer, which reflects a very high reliability of power supply. For comparison, the SADI in the Netherlands amounted to 33.1 min. per end customer and in Austria to 45.47 min. per end customer (cf. Bundesnetzagentur [2009], p. 126).

6 Likewise, the European Union is becoming increasingly dependent on external energy sources, however to a lower extent compared to Germany. Forecasts assuming a business as usual scenario show that the EU's dependence on fuel imports will reach 65% in 2030 (cf. COM(2000)769, p.13; COM(2007)1, p. 3).

The demand in lignite is met nearly to 100% by domestic production. Due to its low energy density the transport of lignite over long distances is not economically advantageous. Therefore, the security of supply with lignite relies on the rate of consumption of the residual reserves (and resources). Since the ration of proven reserves to annual production of lignite in Germany amounts to approximately 226 years, a high degree of supply security can be assumed (cf. AGEB [2009]). Likewise, a high degree of supply security can be assumed for uranium and hard coal, which are at present imported by approximately 100% and 67%, respectively. The supply sources of both energy carriers are sufficiently diversified and thus no dependencies on individual politically unstable countries exist. Moreover, the relatively stable market prices reduce the economical risks to security of supply (cf. BGR [2007]; CONSENTEC et al. [2008]). One third of Germany's coal demand is met from indigenous mining. The rest is imported i.a. from Russia, South Africa, and Poland. Further, even though the abandoning of hard coal extraction in Germany until 2018 (cf. SteinkohleFinG [2007]) will lead to a further increase of imports during the next years, the high reserves in politically stable countries as well as indigenous coal reserves, which could be extracted if needed, will prevent problematic dependencies. Regarding uranium, the highest amount of uranium is found in Australia, Canada, and Kazakhstan. Yet, the phase-out (see section 2.1.6) of nuclear power stations will probably remove all import dependencies, on the long run. By contrast, gas imports, which have been increasing during the last years, will need to be further diversified. Today gas is imported to 81%, mainly from Russia, Norway, and the Netherlands. Yet, the indigenous gas resources of the EU-27 (and Norway) are declining. If the construction of additional gas-fired power stations is intended, new liquefied natural gas (LNG) terminals as well as new pipelines should be constructed to further diversify sources of supply (cf. COM(2000)769, CONSENTEC et al. [2008]).[7] Regarding power generation, fuel oil can be neglected, since it only plays a minor role.[8]

Since Germany has only limited scope to influence the conditions of the supply with conventional primary energy carriers, increasing overall energy efficiency, on the one hand, and increasing the share of RES in power generation, on the other hand, are considered essential means to guarantee for future security of supply. Both will lead to a further decentralization of the German power system. Yet, even though the share of RES in power generation is expected to continue to rise in the next years, carbon fuels and uranium will most likely continue to play an important role in future German power supply, at least until 2020. Germany's ambitions to increase the use of RES in power generation will be further discussed in section 2.1.5.

[7] Yet, E.ON Ruhrgas plans to construct a LNG terminal at Wilhelmshaven have been given up.

[8] Yet, with a share of almost 100% in road traffic and approximately 77% in total traffic, it is still the most important fuel in the traffic sector (cf. BMVBS [2009]). As the German government wishes to reduce Germany's dependence on oil imports and the associated risks of oil price fluctuation, it has set up a Development Plan for Electric Mobility, in which it announces the ambition to support research and development in the field of electric mobility so that electric mobility will account for one million vehicles by 2020 and five million vehicles by 2030 (cf. Bd.-Reg. [2009b], p. 18). Thus, Germany's ambition to reduce its dependence on oil imports might lead to an increase in power demand in the future. In addition to electric vehicles, the use of biodiesel, bioethanol (cf. BioKraftQuG), biogas, and gas (cf. FÖS [2002]) is supported to reduce Germany's dependence on oil exports and to decrease GHG emissions.

2.1.3. Climate change policy

With the ratification of the Kyoto Protocol in 2002, the EU-15 committed itself to reduce its greenhouse gas emissions till 2012 by 8% compared to the level of 1990 (EC [2002a]).[9] The Burden Sharing Agreement (EC [2002b]) defines how the -8% target of the EU is shared among the Member States (see Annex A). The national targets range from +25% for Greece to -28% for Luxembourg. Germany has to meet a reduction target of -21% in 2012. Alarmed by scientific studies about the costs of climate change, the EU declared in 2007 the objective to limit the global climate change to less then 2 degrees Celsius compared to pre-industrial levels (cf. COM(2007)2). In addition, the European Council agreed to reduce EU's greenhouse gas emissions by at least 20% by 2020 (compared to 2005 level). Moreover, the German government set the target to reduce Germany's GHG emissions by at least 40% by 2020.

Since CO_2 emissions account for approximately 89% (Germany: 88%) of the global warming potential weighted GHG emissions in Europe (cf. EEA [2009]),[10] their reduction takes the center stage of the European climate protection policy. The electricity industry is one of the key emitters of greenhouse gases, combined with large scale facilities which are easy to control. In Germany the public electricity and heat supply contribute to 33.89% to total CO_2 emissions. Therefore, special attention has been given to emission reductions in this sector. Already in 2000, the European Commission launched the first European Climate Change Program (ECCP) (COM(2000)88 [2000]), which aimed at identifying and implementing measures to reduce GHG emissions in the energy, transport, and industry sector. In the first phase of the ECCP, the European Commission brought forward a package of measures (COM [2001]). Among them count the implementation of an emission allowance trading scheme, which was intended to complement the flexible mechanisms of the Kyoto protocol, as well as an action plan to tackle climate change. The action plan outlines priority actions to increase energy efficiency in energy supply and consumption as well as to increase the share of RES in energy supply (COM(2001)580 [2001]). (The measures regarding RES and energy efficiency, which were proposed in the European action plan are discussed in section 2.1.4 and section 2.1.5, respectively.)

---

9 In 1992 the Rio Summit signed the United Nations Framework Convention on Climate Change (UN [1992]). It forms the framework for the UN climate change conferences, which were set up to find measure for mitigating the harmful effects of the antropogenously provoked climate change. At the third conference of parties in Kyoto in 1997, the industrialized nations committed themselves to reduce their overall emission of the six most important GHG from 2008 to 2012 by at least 5% compared to 1990 level (UN [1998]). The six GHG listed in the Kyoto protocol are carbon dioxide (CO_2), methane (CH_4), nitrous oxide (N_2O), fluoridated hydrocarbons (HFC), perfluorinated hydrocarbons (PFC), and sulfur hexafluoride (SF_6). The Kyoto Protocol entered into force in 2005 after being adopted by 150 contracting member states, which are responsible for more than 60% of the greenhouse gas emissions.

10 The global warming potenital (GWP) quantifies to which extent a specified amount of a greenhouse gas, generally expressed in CO_2 equivalents, contributes to the greenhouse effect.

2.1.3.1. The EU Emission Trading Scheme

Following the suggestion in the ECCP report, the European Parliament and the Council established in October 2003 a cap-and-trade system for greenhouse gas emission allowances in the Community (EC [2003]). Contrary to the emission trading on national level, which is proposed within the Kyoto Protocol, the EU Emission Trading Scheme (ETS) obliges companies of the energy sector and in energy intensive industries to hold EU allowances (EUA) covering their GHG emissions. The system designed in Directive 2003/87/EC is to cover at least two periods, a three-year period from 2005 to 2007, which was considered a test period, and a five-year period from 2008 to 2012, which corresponds to the first Kyoto commitment period. A further link of the EU ETS and the Kyoto Protocol was created by Directive 2004/101/EC, which recognizes the latter's project-based mechanism credits as equivalent to EUAs in the second ETS period. The total quantities of EUAs allocated by each Member States as well as the allocation rules applied are published in so-called National Allocation Plans (NAP).[11] In Germany, EUAs corresponding to 510 Mt. p.a. of CO_2 emissions have been allocated for the first ETS period, of which 21% have been assigned to energy intensive industries and 79% to the energy sector (cf. BMU [2004]). According to the German NAP II emission allowances corresponding to 482 Mt. p.a. will be allocated in the period 2008 - 2012 (cf. BMU [2006b]). Regarding the allocation of emission allowances to new power plants, a 14 year free-allocation based on a BAT-benchmark with ex-post adjustment[12] has been chosen for the period 2005 - 2007, while a fuel dependent BAT-benchmark[13] has been chosen for the period 2008 - 2012.

The limitation of GHG emissions to the level of allowances allocated involves significant changes for the production planning of electricity generators and energy intensive industries. As a price evolves for scarce resources, the formerly free and unlimited resource CO_2 emission is accounted for as a production factor. Since the launch of the European emission trading scheme in 2005, a market for EUAs has developed. Figure 2.1 shows the development of carbon index prices at the German power exchange EEX between Jan. 2006 and Apr. 2009. The significant drop in prices in 2007 can be explained by an overallocation of EUAs in the first ETS period. Independent of whether the emission allowances are allocated free of charge or not, the entity owning the emission allowance always has the choice either to use the allowance to cover its CO_2 emissions or to sell it at the market. Therefore, the opportunity costs of the use of CO_2 emission allowances are part of the electricity generation costs. The so-called "windfall profits" generated that way have been widely discussed as one of the main shortfalls of the grandfathering allocation method.[14] Moreover, the free allocation for new installations based on a

---

[11] An overview of the NAPs of the Member States is offered on the EU website on climate change (http://ec.europa.eu/environment/climat/emission/emission_plans.htm).

[12] The German benchmark for electricity generation units amounts to 750 t CO_2 equivalents per kWh. If a new installation emits less, the allocation is adjusted ex-post, but amounts at least to 365 t CO_2 equivalents per kWh (cf. BMU [2006a]).

[13] The allocation to new installation in the electricity sector based on a fuel dependent benchmark amounts to 365 g CO_2 equivalents per kWh for gas-fired power plants and 750 g CO_2 equivalents per kWh for coal-fired power plants, with corresponding utilization factors.

[14] Cf. e.g. Möst et al. [2008]

Figure 2.1.: Carbon Index at the EEX (based on EEX [2009])

fuel-dependent benchmark, which is specified in the German NAP II, can have a significant impact on the structural evolution of the power plant mix. The free allocation of EUAs for new installations can be considered as an investment grant. Since coal and lignite-fired power plants receive a higher allocation than gas-fired power plants, the incentives for the investment in low-emission-intensive generation technologies is reduced (cf. Möst et al. [2008]).

2.1.3.2. Status quo of greenhouse gas emission reductions and further action

According to the EU reports on the progress towards achieving the Kyoto objectives (cf. COM(2008)30, SEC(2009)1581 [2009]), total GHG emissions of the EU-15 (EU-27) were 2.7% (10.8%) below the base year emissions in 2006. Projections show that the European Community will miss its Kyoto target with the existing policies and measures. If the use of Kyoto mechanisms, carbon sinks, and additionally planned measures is considered, the EU-15 (EU-27) projections show GHG emission reductions of 11.3% (16.3%). Germany ranks among the Member States which have projected emissions that would allow them to achieve their targets. According to the Commission's benchmarking report Germany will reduce its GHG emissions by 23.5% considering the existing policies and measures and by 26.2% when taking into account Kyoto mechanisms, carbon sinks, and the effect of all additional measures planned. Thus it will reach its share in emission reductions according to the Burden Sharing Agreement (cf. SEC(2008)2636 [2008]). An overview of the detailed contribution of each Member State is given in Annex A.

Yet, new measures are needed to meet the target of a 20% reduction of GHG emissions by 2020.[15] Therefore, the European Commission prepared an climate and energy package,

[15] The EU climate and energy package was based on the second European Climate Change Pro-

which passed the European Parliament in December 2008. Regarding the electricity sector, it defines three mayor lines of actions: Firstly, the EU climate and energy package comprises a directive concerning the implementation of an improved post-Kyoto EU ETS (EC [2009c]). Secondly, a regulatory framework for geological storage of CO_2 is created (EC [2009a]).[16] Additionally, it contains a Directive on the promotion of the use of energy from RES (EC [2009b]; see section 2.1.5).

The improved ETS (EC [2009c]) differs from its former version above all by specifying stricter emission caps. Starting in 2013 the quantity of EUA issued each year will decrease by a linear factor of 1.74%, which is supposed to lead to a 21% cut by 2020.[17] In addition, an increased level of auctioning is planned. While in 2013 80% of the EUA will be allocated free of charge, the quantity of free allocation is to decrease each year *"resulting in 30% free allocation in 2020 with a view to reaching no free allocation in 2027."* (EC [2009c]) Furthermore, EU-wide valid rules for allowance allocation will be defined.

In Germany, a corresponding national integrated Energy and Climate Program has been passed (Bd.-Reg. [2009a]). Among its basic elements rank the promotion of combined heat and power generation, the promotion of RES in power generation, low carbon power generation technologies, including more energy efficient power generation as well as carbon capture and storage technologies, intelligent metering systems, the introduction of innovative energy management systems, the promotion of energy efficient products, and electric mobility. Furthermore, measures to reduce GHG emissions in transport and in the building sector are planned (Bd.-Reg. [2009a]).

2.1.4. Energy efficiency

In response to the oil crises in the 1970s, energy efficiency became a major subject in European energy policy. With the objective of decoupling economic growth and energy demand, first efforts were made to foster a more rational use of energy. Today increasing energy efficiency contributes notably to meet the European energy policy objectives security of supply, competitiveness, and environmental protection. In March 2007, the

gramme (ECCP II), which was launched in Ocotber 2005.

[16] A corresponding German bill has been approved by the federal cabinet in April 2009. For economical as well as for geopolitical and technological reasons, the EU and in particular Germany will continue to rely on coal-fired power stations. They consider CCS to be a bridging technology which will contribute to mitigating climate change. Supporters of CCS claim that if deployed in all industry sectors, CCS could reduce CO_2 emissions in the EU by 54% by 2050 (Stangeland [2007], Capros [2007]). Critics of the geological storage of CO_2 refer to the high additional investments, costs, and risks involved, as well as long-term liability issues. In addition they point to the lower thermal efficiency of CCS power plants (cf. e.g. Capros [2007], Cremer et al. [2008]). To further investigate the potential deficits of CCS, more than 40 demonstration plants are being planned or in consideration in the EU (cf. ZEP [2008]).

[17] Additional binding targets have been set for the reductions of GHG emission from installations not covered in Directive 2003/87/EC, which are, small-scale emitters in sectors including transport, building, agiculture, and waste. By 2020 emissions from those emitters have to be reduced by 10% compared to 2005. This EU target is shared out between the Memeber States based on the differences in GDP per capita. The German target amounts to a GHG reduction of 14% (cf. EC [2009a])

European heads of state and government agreed on reducing energy consumption by 2020 by 20%.[18] The target is part of the EU's "20-20-20 by 2020" climate and energy targets. Among other things, fostering energy efficiency is expected

- to reduce GHG emissions and thus to contribute to prevent climate change (cf. COM(2005)265 [2005] and EC [2006a]),
- to lead to a more sustainable energy policy,
- to enhance security of supply and reduce energy dependency (COM(2005)265 [2005], p37; EC [2006a]),
- to keep technological leadership (COM(2005)265 [2005], p. 17), increase Europe's innovativeness and competitiveness (COM(2005)265 [2005], p. 37; EC [2006a]), and thus to facilitate the attainment of the goals underlined in the Lisbon strategy.

In 1998 the European Commission identified an available economic potential for energy demand reduction, which could be realized between 1998 and 2010, of 18%[19] (COM(1998)246 [1998]). To realize this potential, the European Commission worked out its first action plan for energy efficiency (COM(2000)247 [2000]), in which it affirmed the ambition to reduce energy intensity by an additional 1% per year compared to a business as usual scenario. The action plan of 2000 was succeeded by a second EU action plan, which was published in October 2006 (COM(2006)545 [2006]). In it, the EU Commission announced to take measures in the following fields of action: energy-efficient products and buildings, energy services, energy transformation processes, transport means, energy behavior, financing, and international partnerships. Regarding energy efficiency in transmission and distribution an incentive based transmission system regulation to reduce losses has been proposed (COM(2005)265 [2005] p. 25ff.) In 2006, the EU passed the Directive 2006/32/EC (EC [2006c]) on energy end-use efficiency and energy services which sets an overall indicative energy savings target of 9%[20] is to be reached in the ninth year of the adoption of the directive.[21]

Since there are limited prospects to influence energy supply conditions on the short to medium term, most efforts to increase energy efficiency focus on increasing energy end-use efficiency, and managing energy demand (EC [2006a]). The highest potential of increasing energy efficiency in a cost efficient manner can be realized in the building and transport sector, e.g. by retrofitting wall and roof insulation and efficiency requirements for cars (cf. COM(1998)246 [1998], COM(2000)247 [2000], COM(2000)769).

To foster the market penetration of energy efficient technologies, the EU as well as the German government started several initiatives to rise awareness, e. g. of the energy demand of household appliances, electronic equipment, or light bulbs, such as the Energy Efficiency Initiative of the German Energy Agency (cf. DENA [2009]) or the Intelligent

[18] Compared to the projected energy demand in 2020

[19] Compared to 1995 level

[20] Compared to January 1st 2008.

[21] To achieve the energy savings target the Member States shall work out national Energy Efficiency Action Plans, in which they outline their intermediate targets as well as their strategy for the achievement of their targets (cf. EC [2006c]).

Energy Europe Program of the EU (EC [2009b]).[22] Moreover, the installation of so-called smart Information and Communication Technology (ICT), in combination with load- and time-dependent tariffs reflecting the actual costs of power supply is promoted (EC [2006a]).[23] Some countries, such as France, have implemented market oriented mechanisms, called white certificates schemes, to support demand side actions (cf. Rentz et al. [2004]).[24]

Thus, by the means of the implementation of demand side measures, energy intensity is decreasing in Germany. Between 1990 and 2007 it has decreased by approximately 37%. The energy productivity has increased by approximately 40% between 1990 and 2008 AGEB [2008], DESTATIS [2009].

Regarding the supply side, above all, the liberalization of the energy markets is expected to increase energy efficiency. On the one hand, competition is expected to increase energy efficiency, and on the other hand, competition is expected to produce market prices that better reflect the true cost of energy supply (COM(1998)246 [1998]). Furthermore, the EU and Germany promote research and technology development (RTD) programs, which aim at increasing fuel efficiency in electricity generation (cf. e.g. BMWi [2007], EC [2006b]). In particular, improvements in the energy yield of coal-fired power plants beyond 50% are aspired (cf. e.g. Bd.-Reg. [2009a], COM(2005)265 [2005]). In addition, the European Commission wishes to ensure that only the most fuel-efficient technologies, namely Combined Cycle Gas Turbines (CCGT) are being used in Europe (COM(2005)265 [2005], p.27).[25] Furthermore, increasing the share of RES as well as of co-generation rank among the most prominent measures to increase energy efficiency in energy supply. Therefore, the EU enacted Directive 2004/8/EC (EC [2004]) on the promotion of co-generation based on a useful heat demand in the internal energy market. Moreover, it agreed upon raising the use of co-generation to 18% of EU electricity production by 2010 (COM(2000)247 [2000]). To foster the use of co-generation in Germany, a system of feed-in tariffs has been implemented.[26] Power generation in co-generation

---

[22] In addition, several measures for the labeling of energy efficient end-use appliances and equipment have been initiated, such as the statutory energy consumption label for large household appliances (EEC [1992], EnVKW [1997]) or the voluntary Energy star program for office equipment (cf. EC [2009a]).

[23] In Germany, smart metering systems have to be installed in all new or renovated buildings as from 1. January 2010 (EnWG [2005] §21b). In addition, as from 30. December 2010, energy utilities are obliged to offer tariffs that give incentives for energy savings or to demand management (EnWG [2005] § 40). Furthermore, the implementation of modern energy management systems will be mandatory for manufacturing companies as from 2013 (Bd.-Reg. [2009a]). Those measures are expected to decrease the overall power demand by increasing awareness of its actual costs. In addition, the time-dependent tariffs are supposed to motivate consumers to shift their power demand to more cost and energy efficient points in time.

[24] White certificates are issued for realized energy efficiency measures. Like in other quota systems, such as emission trading, the participants are obliged to hold a certain number of certificates per period. They obtain white certificates by either conducting energy efficiency measure or by obtaining them on the market.

[25] Due to their high fuel-efficiency and due to the fuel based benchmark in Germany, combined cycle gas turbines are already favored within the European Emission Trading Scheme.

[26] In the *Kraft-Wärme-Kopplungsgesetz (Cogeneration Act)* (KWKG [2002]) feed-in bonuses are defined to foster the installation of co-generation plants. The date of the start of operation as well as the capacity of the power are decisive for the determination of the level of remuneration, which

plants increased from 41.8 TWh in 1998 to 77.5 TWh in 2007 (EUROSTAT [2009], EC [2001a]) and thus had a share of 12.2% in electricity generation in Germany. According to political targets, it is to reach a share of 25% by 2020 (cf. UBA [2009], p. 65).

To subsume, increasing energy efficiency can be expected to decrease power demand on the long-term. Moreover, on the supply side, increased efficiency of power stations as well as a rise in the use of co-generation (and RES) can be expected.

2.1.5. Power generation based on renewable energy sources

In the EU, accelerating the penetration of RES is considered as an important step towards reducing energy imports and therefore increasing security of supply. At the same time, it can contribute to reducing the EU's greenhouse gas emissions as well as regional and local pollutants. Furthermore, supporting RES technologies is expected to have positive effects on employment as well as on social and economic cohesion (cf. e.g COM(1997)599 [1997], EC [2001b], COM(2005)627 [2005]). In its 1986 resolution (EC [2009]), the European Council listed the development of new and RES among its energy policy objectives. Based on the debate initiated by the Green Paper, the Commission published in 1997 a White Paper (COM(1997)599 [1997]) laying down a Community strategy on RES. Therein, the Commission set a goal *"of achieving 12% penetration of renewable energy sources in the Union by 2010"* (COM(1997)599 [1997], p. 10), which meant doubling the share of RES in its gross internal energy consumption by 2010.[27] To achieve this goal, the White Paper proposed an action plan as well as a campaign to promote RES. Following up the White Paper, the European Union adopted a Directive (2001/77/EC) on the promotion of electricity produced from RES (RES-E) (EC [2001b]), in which it set indicative targets regarding the share of RES-E in gross electricity consumption by 2010. For the EU-15 a contribution of 22.1% was fixed. The national indicative targets for the contribution of electricity produced from RES range from 5.7% for Luxembourg to 78.1% for Sweden. The German target amounts to 12.5%.[28] In March 2007 the EU Council agreed to set the target to reach a share of 20% of renewable energies in EU energy consumption by 2020. Amongst the EU's climate and energy package of 2008, a directive has been adopted to intensify the promotion of the use of energy from renewable sources (EC [2009b]), which sets national targets for the share of energy from renewable sources in gross final consumption by 2020. Regarding Germany, the share amounts to 18%. Moreover, it creates a cooperation mechanism for the Member States, calls for national action plans, and removes administrative barriers to prepare the ground to reach the EU target of a 20% share of renewable energy by 2020.

Following the Directive 2001/77/EC the EU Member States installed a variety of support measures to promote the use of RES in electricity supply. Among the most prominent count feed-in tariffs, quota obligations, investment subsidies, and fiscal incentives.

range from 0.56 Ct./kWh for old units to 5.11 Ct./kWh for new units with a capacity of less then 50 kW.

[27] The 12% target is a political, not a leagally binding objective.

[28] With a share of 16.5%, Germany reached its indicative RES-E 2010 target.

An overview and a evaluation of the different support measure is given e. g. in Ragwitz et al. [2007], COM(2005)627 [2005], and Rosen [2007].

With the objective of doubling the share of RES in electricity supply, the German legislative body passed the Act on Granting Priority to Renewable Energy Sources (EEG (2000))[29], which defined minimum feed-in tariffs for RES-E.[30] Furthermore, it obligates system operators to connect RES-E units and accept electricity generated from renewable sources. In addition it regulated a nationwide cost balancing. After two amendments it was replaced by a renewal, which became effective in August 2004 (EEG [2004]). The scope of the EEG (2004) was to transpose Directive 2001/77/EC into national law and thus to set the stage to achieve Germany's 12.5% target. In addition, it stated the ambition to increase the share of electricity generated from RES to at least 20% by 2020. To prepare the ground for Germany's contribution to the EU climate protection targets, a second revised version of the EEG has been passed in 2008, which came into force in January 2009 (EEG). In §1 of the EEG, the previous target of a 20% of RES-E by 2020 was replaced by a more ambitious 30% target. Further amendments compared to EEG are i.a. adapted feed-in fees, modified gradual decrease of the feed-in fees, an obligation for grid operator to provide for grid expansion if needed, and the regulation of financial compensations in case of feed-in management. In the latest reform of the EEG (EEG [2011]), which has been passed in July 2011, the German parliament raised the 2020 target, again. According to EEG [2011], the share of RES-E in power supply shall amount to 35% by 2020. Moreover, a 50% target has been defined for 2030, while by 2040 and by 2050 the shares of RES-E in power supply shall amount to 65% and 80%, respectively (EEG [2011]).

Triggered by these support measures, the share of RES has increased significantly in the last two decades. Figure 2.2 shows the development of RES-E since 1990. In 2010 RES-E accounted for 16.5% of the total electricity consumption. The total installed capacity of RES-E technologies in Germany amounted to 44,772 MW in 2009 (wind: 25,777 MW; solar: 9,800 MW; water: 4,760; biomass: 4,429 MW; geothermal energy: 6,6 MW). Since 2004, wind energy holds the top position in gross electricity consumption. In 2010 it amounted to 36.5 TWh, corresponding to 5.9% in total power generation. Power generation from biomass added up to 28.5 TWh (4.6%), while hydro power generation amounted to 19.7 TWh (3.2%). Solar power increased significantly and accorded for 12.0 TWh (1.9 %). In terms of contribution to gross electricity consumption, geothermal power only plays a remote role, with 0.028 TWh (0,0%) (cf. AGEB [2011a]). Regarding the future development, the share of RES in gross electricity consumption would have to continue to increase to more than 50% to reach the ambitious GHG emission reduction targets (cf. BMU [2008]).

29 Gesetz für den Vorrang Erneuerbarer Energien (EEG)

30 The EEG 2000 replaced the *Stromeinspeisungsgesetz* of 1990 EEG [2004], which regulated the feed-in and renumeration of power from generated from RES.

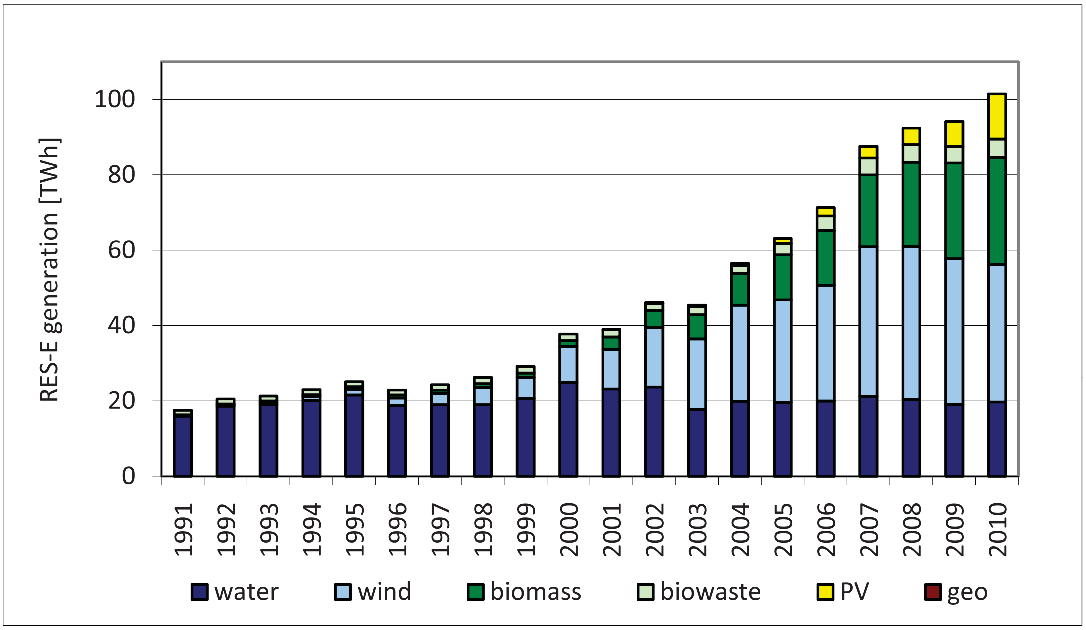

Figure 2.2.: Development of power generation from renewable energy sources in Germany (based on AGEB [2011a])

2.1.6. Use of nuclear power

With an average load factor of up to 90% (COM(2006)844 [2006]) nuclear power stations are a typical base load technology. In 2005, nuclear power generation amounted to approximately 163.1 TWh in Germany. Thus, with a gross production share of approximately 27%, it is one of the largest sources of carbon free energy (EUROSTAT [2007b]). In addition, with operational cost of nuclear power generation amounting to 40 - 45 €/MWh, it is one of the cheapest sources of low carbon energy in the EU (cf. COM(2007)1, p. 16ff.). In addition, the European Commission points out the economic benefits in maintaining and developing the technological lead of the EU in the field of nuclear technology (cf. EURATOM [2007], p. 16).

However, the use of nuclear power generation also bears considerable drawbacks, such as security risks in plant operation and the necessary long-term storage of spent nuclear fuel. Therefore, in June 2000 the German federal government reached an agreement with the power supply companies, to phase-out all nuclear power plants (BMU [2000]).[31] In the agreement, the construction of new nuclear power stations is ruled out. In addition,

[31] Unlike Germany, other European countries continue to rely on nuclear energy. In the EU-27 a total of 152 nuclear power stations are in operation in 15 Member States. Thus, nuclear energy contributes to 30.6% in gross power generation (EUROSTAT [2007b]). Yet, currently only in France and Finnland new nuclear stations are under construction (cf. COM(2006)844 [2006]). Furthermore, Bulgaria, Romania, the Czech Republic, and the United Kingdom are planning the construction of new nuclear power stations. Furthermore the Netherlands, Slovenia, and Hungary have signed declarations of intent to build new nuclear power stations. The power

Table 2.1.: Nuclear power plants in Germany (AtG [1959], BMU [2000], AtG [2002], BFS [2011], BMU [2011, 2009], AtG [2010], Bd.-Reg. [2011])

Name	Capacity [MW]	Date of commissioning	Remaining generation [TWh]	Estimated year of decommissioning	Remaining generation 01.01.2011 [TWh]	Additional generation [TWh]	Estimated year of decommissioning	Latest year of decommissioning
			BMU [2000], AtG [2002]			AtG [2010]		AtGÄndG [2011]
Obrigheim	367	01.04.1969	8.70	-	-	-	-	-
Stade	672	19.05.1972	23.18	-	-	-	-	-
Biblis A	1225	26.02.1975	62.00	2010	3.47	68.617	2018	2011
Neckarwestheim I	840	01.12.1976	57.35	2010	0.0	51.000	2020	2011
Biblis B	1300	31.01.1977	81.46	2010	8.55	70.663	2018	2011
Brunsbüttel	806	09.02.1977	47.67	2012	11.00	41.038	2019	2011
Isar 1	912	21.03.1979	78.35	2011	2.93	54.984	2018	2011
Unterweser	1410	06.09.1979	117.98	2012	12.61	79.104	2020	2011
Phillipsburg 1	926	26.03.1980	87.14	2012	9.23	55.826	2020	2011
Grafenrheinfeld	1345	17.06.1982	150.03	2014	40.93	135.617	2028	2015
Krümmel	1402	28.03.1984	158.22	2019	88.25	124.161	2032	2011
Gundremmingen B	1344	19.07.1984	160.92	2015	49.26	125.759	2028	2017
Philippsburg 2	1458	18.04.1985	198.61	2018	79.47	146.956	2031	2019
Grohnde	1430	01.02.1985	200.90	2018	80.65	150.442	2032	2021
Gundremmingen C	1344	18.01.1985	168.35	2016	57.56	126.938	2029	2021
Brokdorf	1440	22.12.1986	217.88	2019	93.05	146.347	2032	2021
Isar 2	1475	09.04.1988	231.21	2020	103.77	144.704	2032	2022
Emsland	1400	20.06.1988	230.07	2020	108.12	142.328	2033	2022
Neckarwestheim 2	1400	15.04.1989	236.04	2022	119.58	139.793	2035	2022
Mühlheim-Kärlich	1302	-	107.25	-	99.15	-	-	-
Sum	23798	-	2623.3	-	967.58	2763.48	-	-

it restricts the remaining electricity generation in nuclear power plants to 2623.3 TWh as from January 2000. In 2010, a total gross nuclear capacity of 20.5 GW has been in service. The last German nuclear power plant will phase-out in 2022. Yet, behind the framework of increasing electricity prices, as well as of increasingly ambitious GHG reduction targets, a new debate on the extension of the life of the remaining nuclear power stations arose in 2010. It resulted in an amendment of the nuclear power act, in which the operational lifetime of the still operating power stations was expended by an average of twelve years (AtG [2010]). However, after the nuclear accidents in Fukushima, those plans have been revised, again. First, in March 2011, the German government passed a moratorium, on which basis the seven oldest German nuclear power stations were taken out of service for three month. At that time, the nuclear power station Krümmel, which was shut down after a fire in July 2009, was already disconnected. In June 2011, the German government decided upon a new nuclear power act, according to which the remaining operating nuclear power stations will phase-out in 2022 at the latest (AtGÄndG [2011]). Moreover, the nuclear power station which have been set out of service in March 2011 will not go operational again. An overview of the nuclear stations in Germany, their remaining terms as well as of their (estimated) phase-out dates is given in Table 2.1

2.2. Resulting challenges for power system planning

By 2030, almost two thirds of the generating capacities installed in 2005 in Germany will have retired. Figure 2.3 shows the development of existing conventional power generating capacities in Germany without expansion.[32] Since the remaining bottleneck capacity will not suffice to meet the anticipated demand, 31 GW - 44 GW of new fossil-fueled power plant capacity have to be be commissioned (BDEW [2011]).[33][34] Moreover, the capacity demand in Germany will be met by the construction of power generating capacities using RES. According to the latest amendment of the EEG (EEG [2011]), the share of RES in power supply shall amount to 50% by 2030. Nevertheless, there will still be a need for additional conventional power station capacity.

The decisions for investment in new power stations have to be taken against the background of the liberalization of the European energy systems as well as of geopolitical

stations being constructed in France and Finnland belong to the supposedly more safe and more efficient 'Generation IV'. An overview on Generation IV nuclear systems is given in NERAC and GIF [2002].

32 In general, power stations are shut-down for age-related reasons, if they do not generate an adequate contribution margin. Thus, the life-time of a power station is not or not only determined by technical criteria (cf. Pfaffenberger and Hille [2004]).

33 In case not enough generating capacity is commissioned to close the capacity gap in Germany, the power demand has to be met by foreign power suppliers. Since this would increase inter-regional power transfers, additional transmission capacities, in particular at the inter-connectors, would have to be built.

34 Similar developments are expected for the rest of Europe. The Directorate-General for Energy and Transport of the EC estimates that in the next two decades 881 GW of new power plants will have to be built in the EU15, to meet the expanding demand and replace old stations (cf. DG for Energy and Transport [2003])

and environmental challenges. The resulting challenges for capacity investment will be described in the following. They are summarized under the headlines “decentralization of power systems” and “increasing relevance of grid constraints”.

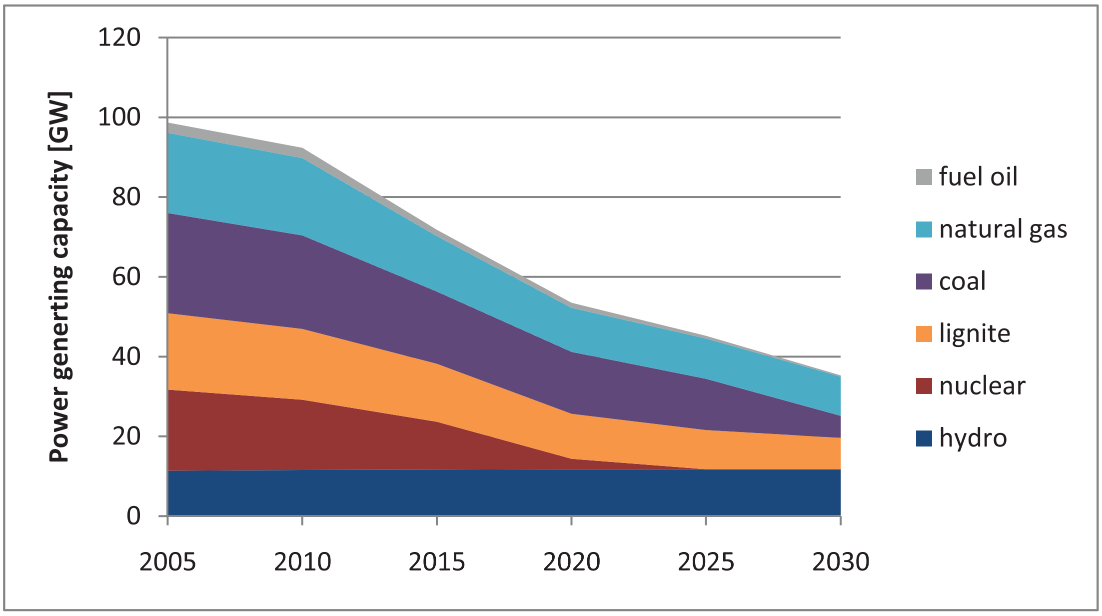

Figure 2.3.: Development of the installed capacity of existing power stations in Germany (based on DENA [2008], Enquete-Kommission [2002])

2.2.1. Decentralization of power systems

A great number of the new power stations will be based on RES, which can be characterized by regionally strongly differing potentials and, for the most part, comparatively small unit sizes, which implicates a connection to the low voltage grid.[35] Regarding the regionally differing potentials, the highest wind power potentials, for example, are situated in Northern Germany, whereas PV or small hydro power station potentials are to a large extent found in Southern Germany (see chapter 6). In addition, particularly wind power and photovoltaic feature only stochastic availabilities, which will require system operators to hold additional power plants in readiness.

Moreover, an increasing number of co-generation facilities will be constructed to increase the fuel efficiency of conventional power stations. The end-use efficiency will be increased e.g. through the gradual substitution of old inefficient consumer loads by new efficient ones and is thus expected to lower the overall power demand. Furthermore, the use of information and telecommunication technologies (ICT) to control end-use is expected to smooth the load curves. Hence, the structure of the German power system is most likely to shift from centralized power stations that are situated close to large demand

[35] This does not apply for off-shore wind farms.

centers to distributed generation that are characterized by a dependency on regional characteristics.

Yet, coal, in particular low carbon technologies, and uranium will most likely continue to play an important role in future German power supply. The new EUA allocation rules are due to favor power plants with high fuel efficiencies, such as combined cycle gas turbines. Furthermore, CCS facilities, which reduce CO_2-emissions of coal-fired power plants, are expected to be in service by 2020. Thus, regional aspects that go beyond the availability of fuel supply will play a role in the siting of future coal-fired power plants.

2.2.2. Increasing relevance of power grid constraints

Regarding power transmission and distribution, a potential inversion of power flows from the low voltage to the high voltage grid will require an enhancement even of low voltage grids with intelligent grid control elements, which will give rise to the so-called smart grids. In addition, power transition, in particular in north-south direction, will increase, due to increasing wind power feed-ins in Northern Germany as well as due to increasing inter-regional power flows resulting from the single European market. At present no structural bottlenecks exist within the German transmission system (cf. e.g. Bundesnetzagentur [2011c], Frontier Economics and CONSENTEC [2011]). Yet, in times of low load and high wind power feed-in locational bottlenecks occur in the transmission grid. In addition, increasing international power transitions and a further renunciation of power generation close to consumption, e.g. through the construction of further wind power capacities in Northern Germany, will necessitate an expansion of the transmission system to avoid the occurrence of structural bottlenecks in the future (cf. CONSENTEC et al. [2008], Bundesnetzagentur [2009]). Therefore, the four German Transmission System Operators have announced to rise their investments in new transmission capacities from 398 M. EUR in 2007 to 685 M. EUR in 2009. Moreover, they budget 7,801 M. EUR for the expansion and modernization of grid infrastructure. Their endeavors are supported by the Energy Line Expansion Act (EnLAG [2009]), with which the procedures regarding 24 grid expansion projects are sped up. Yet, delays in the construction of grid infrastructure, in particular for the grid integration of offshore wind farms, can be observed. Thus, the prospective availability of sufficient line capacity is questionable and structural bottlenecks in the German transmission system will probably not be avoided.

Moreover, since the unbundling of power system and power plant operation prevents an integrated power system planning, the location planning of power plants does not take grid restriction into account. Thus, increasing costs of grid operation that are due to suboptimal power plant location are being socialized.

In summary, regional aspects, e.g. regarding demand forecasts, or RES potentials as well as grid constraints should play an important role in the analysis or planing of future power systems. Therefore, locational prices reflecting the true cost of electricity supply by integrating those aspects should be used as decision criterion.

3. Power markets and price signals

Power markets play a decisive role for the planning process in the electricity sector. Market prices are determined by matching demand and supply. Typically, the price levels induce reactions on the supply as well as on the demand side. Prices rise, if supply capacity is scarce. As a result investments in new generation capacity become economically beneficial. Thus power prices signalize the need for capacity investments. Given a price-elastic demand, demand will adapt to prices changes, too. In particular, demand levels might decrease if prices are high, which would possibly render investments in new capacity unnecessary.

In general, two levels of power markets, wholesale and retail markets, can be distinguished. On wholesale markets, electricity generation companies and re-distributors trade electricity and other power related services. By contrast, retail markets match demand and supply on end-customer level. Thereby, retailing comprises the financial transaction between a retailer and the end-customer, which includes billing and, sometimes, meter reading.

In the following, the levels and tasks of planning in the electricity sector will be described. Special interest will be given to the markets, which influence the decisions on different planning levels. Further, the rational of electricity pricing and price signals will be addressed. Among other things, the concept of locational marginal pricing (LMP) will be introduced. It allows for regionally differentiated price signals by taking aspects of generation and grid operation into account. In the following parts of this work locational marginal pricing will be used to analyze the future development of the German power system. In section 3.3 the German power markets, which build the context of the following investigations, will be described. In particular, the architecture of power markets in Germany as well as the concepts of wholesale and retail pricing will be addressed. In the last part of this chapter, the transmission pricing in Germany and applications of LMP schemes will be briefly discussed.

3.1. Levels and tasks of planning in the electricity sector

Power supply undertakings maximize profits by providing for a sufficient supply with electric energy at any time. This demands for an optimal planning of their power system on the short-run as well as on the long-run. The planning process affects all elements of the supply chain, including the generation, transmission, and distribution of electric energy. Since power station and grid operation and planning can not be regarded independently, an integrated consideration of generating capacity and power grid operation and planning is necessary. Due to the high capital costs associated with

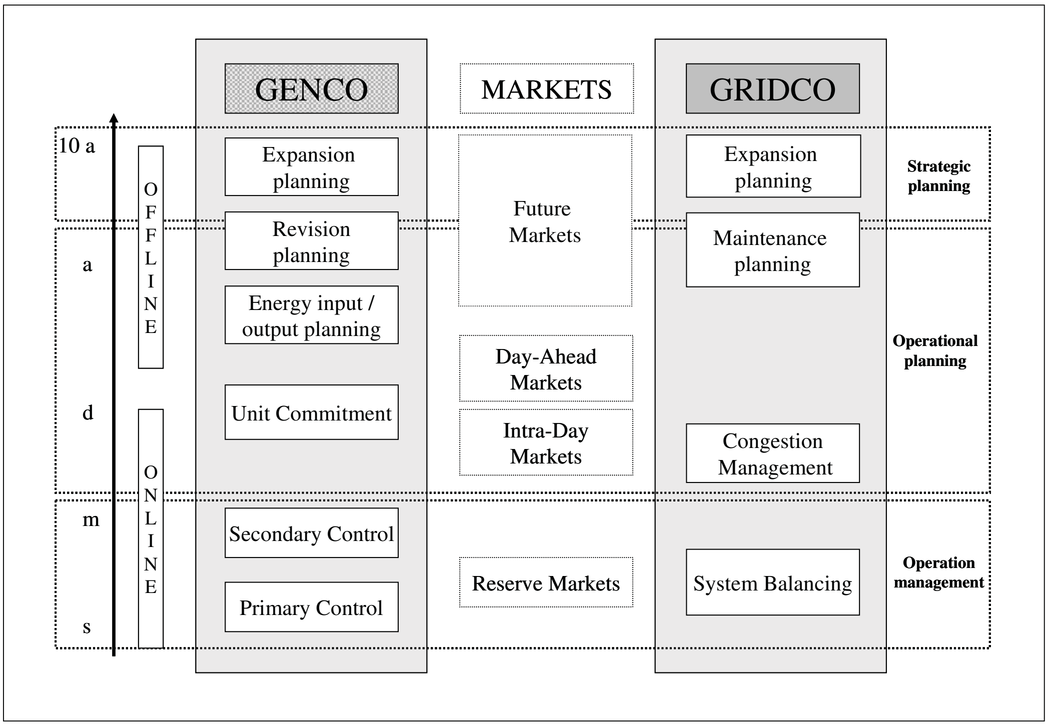

Figure 3.1.: Planning tasks of power supply companies (based on Rosen [2007], p. 64)

electricity supply, power supply planning differs a lot from the planning process in other industries (cf. Wolter and Reuter [2005], p. 51). Before the liberalization of electricity markets, the integrated planning tasks were part of the planning process of vertical integrated utilities. In the course of the unbundling of energy utilities, power station and grid ownership and operation have been separated (see section 2.1.1). Therefore, today the tasks of power supply system operation and planning are divided between electricity generating companies (GENCO) and grid operating companies (GRIDCO) (see Figure 3.1).

Within the planning process, different time horizons can be distinguished (short-term, medium-term, long-term). According to these the complex planning process can be divided into individual sub-problems (cf. Flechner [1996], Möst [2006]). From this, several planning tasks of energy supply companies can be derived. Furthermore, specific power markets exist, where products with different maturities are traded.[1]

Regarding the long-run, generating companies are concerned with questions of strategic planning of electricity generation, which comprises, above all, the planning of investment in electricity generating capacity. At this planning stage, capacity as well as activity based costs are considered. Generating companies have to decide in which new technologies to invest. Such decisions are taken up to 30 years ahead of time. Necessary input in the planning process are i.a. long-term forecasts of demand and peak load

[1] In this section, they will only be classed in terms of time. A more detailed description of the markets will be given in section 3.3.

developments, future fuel and electricity price forecasts, technology developments, and policy issues. Future markets give indications for electricity price developments (see section 3.3.1).

However, not only the correct choice of technology and time of investment is of interest, but also the siting of the new power stations. Due to regional conditions, potential sites differ in many sort of ways. Issues of choice in power plant siting are i.a. resource and cooling water availabilities, environmental constraints, or public acceptance as well as existing grid connections and transmission capacity availabilities (cf. e.g. Cremer [2005]).

The medium-term planning stage is called operational planning. On the part of generating companies it comprises different tasks of unit commitment planning. In revision planning, which can be ranked between strategic and operational planning, i.a. maintenance schedules of power plants are established. Medium-term planning tasks include energy input and output planning. That is, the medium-term planning of power plant operation, emphasizing the optimal distribution of energy inputs and outputs. Which units are operated at which time and at which load is defined in short-term unit commitment. Short-term unit commitment is decided upon, while taking the status quo of unit operation as well as revision schedules and energy planning issues into account.[2] While in long-term capacity expansion planning, capacity as well as activity based costs are considered, capacity based costs have no influence on unit commitment decisions.

The shortest-term planning tasks of generating companies is the power plant operation management. Since demand fluctuates and thus can not be forecasted exactly, power generation has to be adjusted permanently. On the one hand unit commitment schedules have to be modified on short-notice, on the other hand electricity generating companies provide ancillary services to balance demand and supply at any point in time.

Analogous to generating company's planning tasks, grid operating company's planning tasks can be subdivided into several levels, according to the time horizon of the planning process. Like in generating companies, the main long-run planning task is the system expansion planning. In addition to the replacement and expansion of old existing grid infrastructure, in particular grid connections of new power plants are projected. In addition, the construction of a new power plant might induce the construction of additional grid capacity. Thus, the strategic planning of generating companies interferes with the strategic planning of the grid operation companies. The long-term nature of the planning process is last but not least due to the long-taking approval process. On the medium-term, the planning of the maintenance of grid equipment and power lines matches generating company's revision planning. The main short-term planning tasks comprise power system balancing and congestion management. On this level, the planning tasks of generating companies and grid operating companies are most closely linked, since the congestion management and balancing processes entail the deliver-

[2] Various methods of solution in short-term unit commitment planning exist, using mathematical as well as heuristic methods. In general, the whole planning task is decomposed into sub-problems. The most common method for short-term unit commitment planning is the Lagrange Relaxation. An overview of methods for unit commitment planning is given in Hobbs et al. [2001], while a quantitative evaluation of different solution procedures is given in Jürgens [1994].

ance of ancillary services. All grid operation and expansion planning processes are supported by network analysis tools, such as topology processors, state estimators, or optimal power flow simulations (cf. Song and Wang [2003], p. 5 ff.).

3.2. Electricity prices and price signals

In economics, prices indicate the scarcity of goods. In the following, the rational of electricity price and price signals in competitive power markets will be described. In particular the inter-dependencies of electricity prices and unit commitment, investments, and power demand will be addressed.

3.2.1. Marginal costs, merit order, and investments

In the course of the liberalization of the European market for electricity, common marketplaces for electricity trading have been established in many European countries, including Germany. Most deregulated power markets rely on central day-ahead auctions, which are realized on power exchanges.[3] In these auctions suppliers bit their individual supply curves, that are, in a competitive market,[4] the same as the supplier's marginal cost curves. In general, short-term and long-term marginal costs can be distinguished. While short-term marginal costs cover only the variable operational costs, such as costs of fuels and emission allowances, long-term marginal costs additionally cover future capacity cost.

The driving force in power supply systems is the power demand. It is characterized by cyclical variations[5] and short-term stochastic fluctuations. Power demand depends on the time of day, the weekday, the season, etc. Since it is not economically justifiable to store large amounts of electricity, power has to be produced at the time it is consumed. To determine the market price, the market operator aggregates all supply curves to a single market supply curve, called merit order curve, by ranking them from those with the lowest costs to those with the highest costs (see Figure 3.2). The supply curves are generally drawn either with a gradually increasing or as a flat slope that takes an infinite upward leap when it reaches the maximum output.[6] The cost minimizing market price is found at the intersection of the aggregated supply and the demand curve (equilibrium price). Since in most markets the short-run price elasticity of power demand is almost zero demand curves are almost vertical. To provide for a cost efficient energy supply,

[3] Further common electricity market types are bilateral markets or power pools. Power exchanges are in general preferred to bilateral trading or power pools, if a facile short-term energy trading and a high degree of transparency in price formation is of importance. For a detailed description of the different market types, including their advantages and disadvantages cf. e.g. Stoft [2005].

[4] A competitive market is characterized by price taking traders, good information, and well-behaved costs (cf. e.g. Stoft [2005], p. 52ff).

[5] Power demand follows seasonal, weekly, and daily patterns (cf. VDEW [1999]).

[6] In reality this assumption does not correctly reflect power generation costs. Cost components such as start-up and load change costs might cause decreasing marginal costs. Yet, to simplify matters they are often neglected.

different types of power plants are used for different demand situations. While e.g. run-of-river and nuclear power stations, which feature low variable costs of generation, are generally used in base load periods, e.g. gas-turbines, which are characterized by higher variable generation costs, are used only during peak load periods. In Figure 3.2[7] a merit order curve for a market with multiple suppliers is shown. With an increase or decrease, respectively, of demand, generators with higher or lower generation costs determine the equilibrium price.

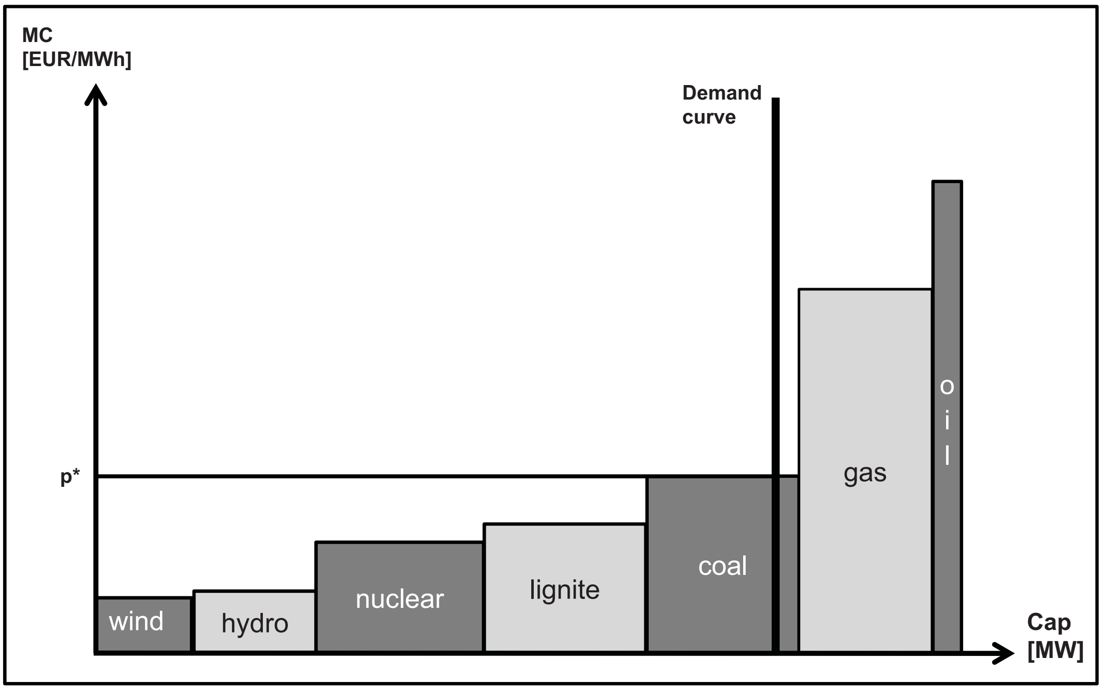

Figure 3.2.: Determination of market prices using a merit order curve

The short-run profits of a supplier can be determined as revenue minus the variable costs. In economic theory, they are called scarcity rent or infra-marginal rent (see figure 3.2). Since in the long-run competitive equilibrium, suppliers exactly recover their fixed costs, the short-run profits have to equal the fixed costs.[8]

Competitive power market prices induce short-run (dispatch) efficiency as well as long-run (investment) efficiency. Hence, in power systems with overcapacity where no adjustments of the capital stock are necessary, efficient market prices correspond to the

[7] It should be noted that in the chosen representation, changes in the supply curves have been neglected. However, such changes frequently occur in reality, above all due to fluctuating primary energy prices or power station availabilities. For a more detailed discussion please refer to Weber [2004].

[8] It is often wrongly claimed that the peaker does not recover its fixed costs. For a detailed discussion of this issue and an explanation of how a peaker recovers its fixed costs please cf. Stoft [2005], p. 120ff.

short-run marginal costs of power production, that is the marginal operational costs. However, if adjustment of the capital stock is needed, market prices have to recover the full costs of power production, including operational costs as well as capital costs and a normal return on investment. If marginal prices are high enough to over-recover fixed costs, new suppliers would enter the market. However, as generating capacity increases, market prices will ease and the incentives for investors to build new capacity will decrease. As the overcapacity will be reduced to nil over time, short-run profits will again exactly recover fixed costs. Thus the "invisible hand" of the market signalizes if investment in new generating capacity is needed (cf. e.g. Stoft [2005], pp. 52ff.).[9]

3.2.2. The price-elasticity of power demand and retail pricing

In economics, the relation of relative changes in quantity demanded to relative changes in market price is called price elasticity. It expresses the responsiveness of consumers demand to price changes.[10] Like other fuels, power is not consumed directly. In fact, consumers prepare food or do their laundry and thereby use electricity. Thus, power demand elasticity implicates that consumers are able to or want to alter the use of their electric appliances, because of higher prices.

In general, economists distinguish short-run and long-run demand elasticity. In power markets a certain degree of long-run price elasticity can be assumed (cf. Wietschel [1995]). If power prices increased significantly, consumers would buy more efficient household appliances or substitute electricity by another energy carrier (e.g. for room heating or hot water generation) over the years. By contrast, power demand is presently almost inelastic on the short-term, which is viewed as an important structural problem of power markets (cf. Stoft [2005]).[11]

The main reason for this short-run inelasticity is that the variations in generation costs, which are mirrored in wholesale prices, are not passed down to the retail customers. In general, most retail customers are billed on a time-invariant (flat) tariff. Thus, retail prices do not reflect the costs of consuming an additional unit of power at that specific point in time and thus, retail customers have no incentive to alter their power consumption. In particular, no incentives are set to reduce consumption when power generation is most costly. In addition, the inability of consumers to respond the on short-run to high market prices favors the exercise of market power.

The short-term inelasticity of power demand could be reduced, by introducing time-varying power prices for retail customers that reflect the temporal cost structure of

[9] At the beginning of the liberalization process in the 1990s, the German power supply system was characterized by overcapacity that amounted to approximately between 10,000 MW to 20,000, that is 10% - 15% of the total net generating capacity (cf. Rychwalski [2005], Matthes and Cames [2000], Jochem et al. [2000, p. 1]). Yet, if we assume a competitive power market in Germany the decline in generating capacities, should lead to a rise in market prices. In fact, power market prices in Germany have begun to reflect this reality (cf. Ockenfels et al. [2005]), and, as a consequence, European utilities have begun to plan the construction of new capacities.

[10] In price quantity diagrams, the elasticity of power demand can be read from the gradient of the demand curve.

[11] Therefore, the demand curve in figure 3.2 is virtually vertical.

Table 3.1.: Characteristics and results of German field trials

Fiel trial	Tariff	Period	Participants	Load reductions	Demand reductions
Freiburg	TOU	1989-1990	266	5.3% - 6.6%	8.0% - 13.5%
Saarland	TOU	1990-1991	1405	6.5% - 8.7%	0%
Berlin	TOU/CPP	1991-1992	480	1.3% - 1.6%	2% - 3%
Rheine	RTP	1989-1991	100	13.4%	NA
Eckernförde	RTP	1994-1996	1000	5%	0%

power supply. Given time-varying retail prices, retail customers could react to high prices either by modifying their usage of electric appliances (e.g. by dimming lights) or by rescheduling usage (e.g. by shifting the laundry to low price times). Thus, direct and indirect price elasticities have to be distinguished. The direct price elasticity is defined as the relative change in quantity demanded of a good in relation to relative changes in its price. It is also called demand elasticity. By contrast, the indirect or cross price elasticity is defined as the relative change in quantity demanded of a good in relation to relative changes in the price of another good. Thereby, the two goods have to be either complements or substitutes. Regarding power demand, the demand elasticity represents the relative **reduction** in power demand in relation to relative price changes. By contrast, the **shifts** in power demand are measured by the cross price elasticity.[12]

In the following, first experiences with time-varying electricity prices are outlined in an excursus. They comprise results of field tests as well as results obtained with the demand side optimization model DS-Opt that indicate the potential of household load shifting stimulated by time-varying electricity prices.

Excursus: Experiences with time-varying electricity prices During the past few years, first experiences with time-varying electricity prices have been made. Since the 1980s several field trial with time-varying electricity prices have been undertaken in Germany. The main objectives of all of them was on the one hand to offer an incentive for customers to shift their consumer loads from the peak load hours during lunchtime and in the early evenings to off-peak hours and to the weekend. On the other hand the time-varying prices are to provide an incentive to reduce the power demand by signaling its actual costs. In the following table the four major German field trials with their main characteristics and results are summarized (see 3.1). Within these field trials peak load reductions of up to 13.4% have been realized.

In 2008, the German Ministry of Economics and Technology and the German Ministry of Environment, Nature Conservation and Nuclear Safety launched the research program E-Energy[13], in which solutions for future energy systems based on smart information and communication technology are developed in six projects and tested in corresponding

[12] Potential impacts of dynamic pricing on the load curves of final consumers are evaluated in Eßer et al. [2006b, 2008].

[13] http://www.e-energy.de/

smart grid model regions. One focus of the projects is on equipping end consumers with smart meters and control devices so that they can react on time-varying electricity price signals. Hillemacher et al. [2011] present first results of the E-Energy project MEREGIO. They measure a peak load reduction during evening hours of up to 19% along with an load increase in the morning and afternoon hours.[14]

Similar results have been obtained using simulations of households' demand shifting potentials. Eßer et al. [2006b] present a mixed-integer linear optimization approach to investigate if and to what extent price signals can be used to control power demand in an energy system. They assume, that hourly prices are transmitted to the customers by their power suppliers one day in advance. Based on these prices, the customers decide whether to use their appliances at the usual time, or to reschedule the usage. They do so by weighting-up their temporal preferences and the time-dependent costs of the use of the appliance. This way Eßer et al. [2006b] show that a high potential to shave off the lunch-time and evening peak exists in households and that price signals can be an adequate instrument to control the temporal distribution of power demand of households. In Figure 3.3 the load smoothing for different values of the preference α is presented.

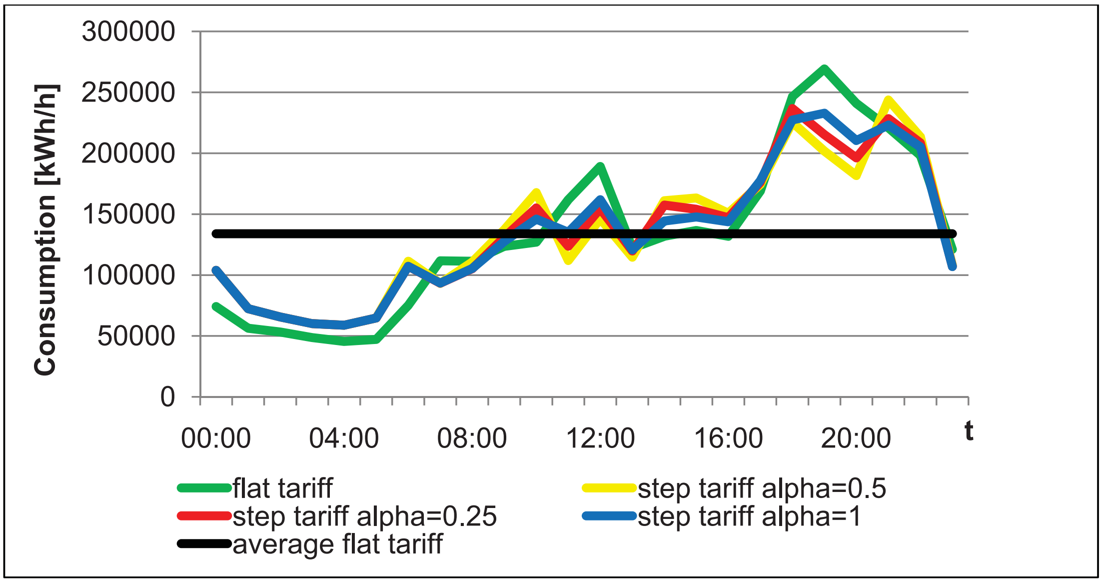

Figure 3.3.: Simulation of households load changing potential (Eßer et al. [2006b])

The preference α expresses the weighting of the importance of using appliances at the preferred time slot in relation to monetary savings realized by shifting demand to a

[14] Outside of Germany similar field tests have been conducted, e.g in California, Norway, Denmark or Switzerland. In the biggest test in California, including 606 households, for example, a peak load reduction of up to 13.1% was attained in 2003 / 2004. The high peak load reduction was mainly due to the automated control of air conditioners. In Scandinavia the high potential of direct an indirect control of storage heating systems for peak load reduction was shown.

time slot with lower electricity prices. A preference of 1 signifies that for the household using its appliances at the preferred time of use is always more important than any amount of money gained by shifting the appliances to a low-price time slot. It becomes apparent that in all optimized scenarios both the lunch peak and the evening peak are smoothed by more than 10%. Load rises mainly occur at night and in the afternoon. The former are caused by a rescheduling of the cooling devices, the latter by the big household appliances. With an integration of a load management system for cooling devices, an average household in our model area realizes savings of 15.03 Euros p.a., that is about 15,000 Euros per year for all households of the model area. If a household begins to schedule a part of its big household appliances on the basis of price signals, further savings are possible, e.g. savings of 6.86 Euros per year with α=0.75 and 13.12 Euros per year with α=0.5.

3.2.3. Locational marginal pricing

Locational marginal pricing (LMP) refers to the principle of calculating optimal price signals with respect to space and time of use. The intention is, to allow for an economic efficient use of electric energy, in terms of space and time of use, by considering the interconnections and interdependecies in between generation, transmission, and distribution of power. In the purest form of locational marginal pricing, which is called nodal pricing, a time-dependent spot price is calculated for each network bus or grid node.[15] These prices incorporate generation costs as well as the costs of transmission losses and congestion. *"When the transmission system is congested (or if losses are charged for as they should be) energy at location A is technically a different product from energy at location B. (...) A completely unregulated bilateral market will price energy different at the two locations. Consequently, an energy market is a multiproduct market with internal linkages between the products."* (Stoft [2005, p. 89])

One of the major benefits of applying LMP is that on the short term it guarantees a dispatch that considers physical power flows and line flow constraints. Thus, no further congestion management is needed and the costs of re-dispatch and voltage control are significantly reduced. In addition, it gives incentives for capacity expansion of locational generation. Regarding this work, LMP is of special interest, because it renders locational price signals while taking grid constraints into account.

3.2.3.1. The principles of locational marginal pricing

The principle of LMP was first introduced in power system economics by Schweppe et al. [1988]. The nodal pricing concept referred to in this work is based on his model.

[15] A bus (or bus bar) is the part of electrical equipment that is used to build connections between several power lines, generators, etc. In mathematics, a node refers to the intersection of connecting graphs. In energy economics, the terms "bus" and "node" are often used synonymously (cf. Stoft [2005], p. 390).

According to marginal cost pricing, the time-dependent price $p_k(t)$ of supplying customer at node k in period t with electric energy equals the marginal power supply cost. Neglecting revenue reconciliation, the marginal cost is

$$p_k(t) = \frac{\partial C_{Total}}{\partial d_k(t)}. \tag{3.1}$$

C_{Total} are the total costs of power supply and $d_k(t)$ is the power demand [kWh] at node k in period t. Since locational marginal pricing considers the whole energy system, the locational prices are calculated subject to generation and transmission constraints. These comprise energy balance constraints, generation limits, line flow limits as well as Kirchhoff's laws. The marginal costs of providing customer k with electric power in period t are composed of the marginal values of power station and grid operation (cf. Schweppe et al. [1988], p. 34 ff.):

$$p_k(t) = g(t) + n(t). \tag{3.2}$$

The generation component *g(t)* comprises i.a. marginal fuel and marginal maintenance cost. The marginal costs of grid operation *n(t)* are composed of a loss component and a quality of supply component. The marginal costs of quality of supply arise when thermal limits of grid operation are being approached, that is, if the power grid is congested. The transmission congestion price between any two nodes corresponds to the electricity price difference at the buses.

Like competitive power market prices, nodal prices induce in an ideal case short-run as well as long-run efficiency, by defining a location-specific market price. Nodes with high prices attract investments, which, again, will increase supply and lower nodal prices. Regarding the short-run efficiency relevant literature concludes that LMP is an efficient method for managing existing infrastructure or congestion management (cf. e.g. Hogan [1992], Chao and Peck [1996], Brunekreeft et al. [2005]). Yet, there is an ongoing discussion whether LMP renders optimal price signals for power infrastructure investments. It concerns the interaction of short-term pricing and long-term capacity planning and the question whether LMP do recover total network costs.[16] This problem will be discussed in more detail in chapter 8. In an ideal case, in which a central planner *"accurately forecasts the (optimal) sequence of generation and network investments"* (Brunekreeft et al. [2005]) based on accurate load forecasts, the LMP derived from the optimal dispatch do reflect the marginal costs, irrespective of fixed infrastructure cost. Brunekreeft et al. [2005] call this case the central planned benchmark.

Example: To give an example of how costs arise because of grid constraints, let us consider a three-line network. Such a network consisting of three buses (*N1, N2, N3*), which are interconnected by three lines, is the simplest network permitting loop flows (see Figure 3.4).

[16] This discussion is in line with the ongoing debate about the failure of power markets to provide adequate incentives for capacity investments (cf. e.g. Joskow [2008]).

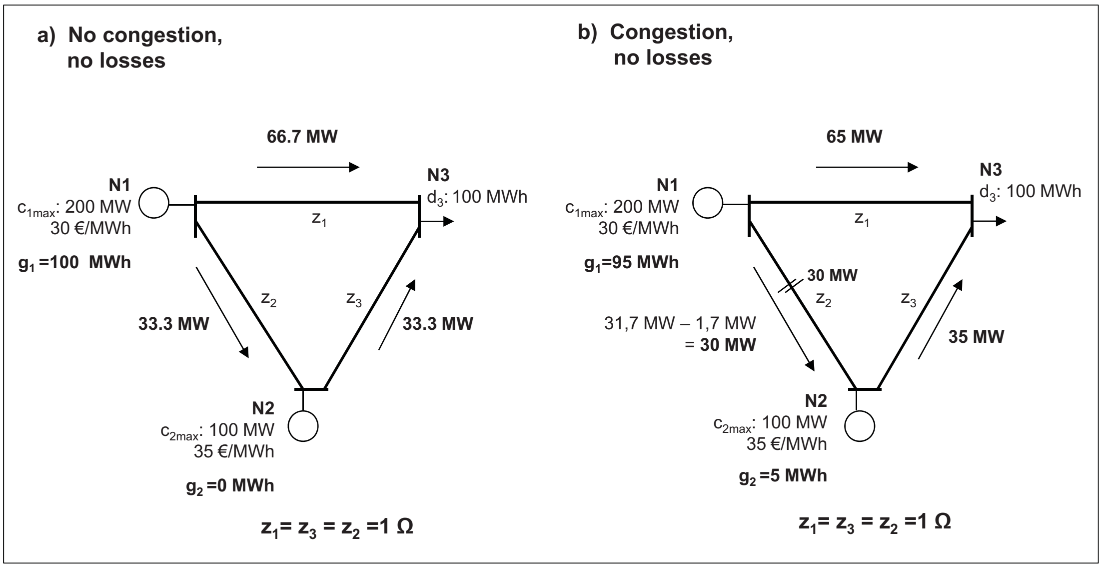

Figure 3.4.: Example for line flows and nodal price distribution in a three node network

In our three-line network, there are two generators with a maximum generating capacity of 200 MW and 100 MW, at the network buses *N1* and *N2*, while there is a power demand of 100 MWh at *N3*. A power flow, which is injected into bus *N1* of such a looped power network and which is extracted at bus *N3*, takes all possible paths between *N1* and *N3*. The impedances of the power lines determine how the power flow splits up. For simplification, the impedances z_i of the power lines in our model are all equal and amount to 1 Ω.

Let us first neglect line losses and assume that no line constraints exist.[17] The marginal costs of supplying bus *N3* with power is determined by the marginal generation cost of the system. Since no line constraints exist, the load is met by generator g_1 alone. The corresponding power flow over the power lines is shown in Figure 3.4 a). The locational marginal prices at the network buses, which equal the costs of providing one (incremental) unit more at that node, are all equal and amount to 30 €/MWh.

Let us now consider that line $\overline{N1N2}$ has a thermal line limit of 30 MW (see Figure 3.4 b)). Now, generator g_1 alone cannot meet the total demand of 100 MWh any more. If he did, the thermal limit of line $\overline{N1N2}$ would be exceeded. Therefore, the high-cost generator g_2 has to partly replace the low-cost generator g_1. Maximizing the share of the low-cost generator g_1, we obtain a share in power generation of the additional unit of g_1 of 95% and of g_2 of 5%. The corresponding line flows are shown in figure 3.4 b). Since it would be possible to meet the demand of a load at node *N1* the cost of providing one unit more at bus N1 still amounts to 30 €/MWh. Yet, an additional unit at bus *N2* could only be fed by generator g_2. Therefore, the price at node *N2* would

17 In this example, revenue reconciliation will not be considered. For examples considering revenue reconciliation the interested reader may consult Schweppe et al. [1988].

adjust to 35 €/MWh. Finally, to supply bus *N3* with an additional unit, the power flows from generator g_1 to generator *N2* has to net the power flow from g_2 to *N1*, in order that the line limit is respected. Consequently, the price at bus *N3* amounts to 32.5 €/MWh.[18]

3.2.3.2. Price determination in coupled markets

Grid nodes, like the nodes in the previous example, can also be considered as individual markets, on which market prices are simultaneously determined in implicit auctions. Let us consider to markets, market A and market B that are linked by a transmission line. Moreover, let us assume that the market price p_A on market A is lower than the price p_B on market B. If there is no congestion on the line connecting the markets, market A exports electricity to market B, which causes a shift in the demand curve of market a and a shift in the supply curve of market B until the price on market A $p_A{}^*$ equals the price on market B $p_B{}^*$ (see figure 3.5).

By contrast, if a line capacity limitation exists that is not sufficient to ensure price harmonization, the amount of electricity exchanged between the two markets is then equal to the available transfer capacity (ATC). The market prices $p_A{}^*$ and $p_B{}^*$ are given by the intersection of the demand and supply curves as illustrated in figure 3.6. Moreover, the price difference between the prices $p_A{}^*$ and $p_B{}^*$ corresponds to the implicit cost of the transmission capacity.

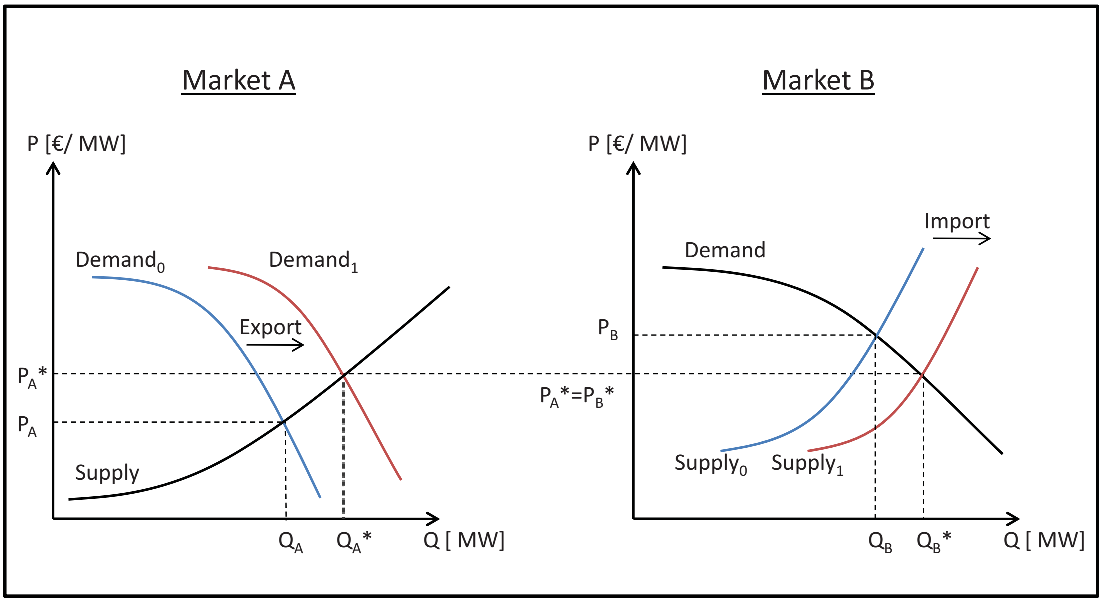

Figure 3.5.: Price determination at the coupled markets A and B - no congestion (based on CWE MC Project [2010, p. 8f.])

[18] In this example the nodal price a bus *N3* can be determined as follows: $p_3 = 0.5 \cdot p_1 + 0.5 \cdot p_2$.

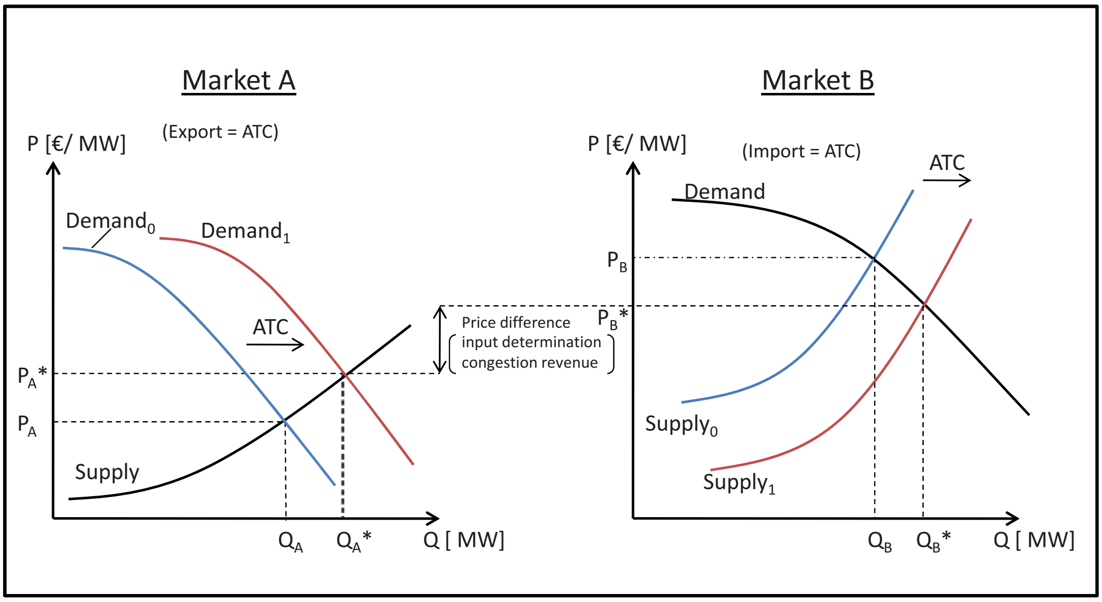

Figure 3.6.: Price determination at the coupled markets A and B - congestion (based on CWE MC Project [2010, p. 8f.])

3.2.3.3. Full nodal pricing versus zonal pricing

The purest form of locational marginal pricing is the (full) nodal pricing, in which locational prices are determined for each network bus. However, it is often claimed that in large networks with hundreds of network buses the great number of nodal prices would cause high administrative expenses and transaction costs and would result in illiquid markets at the nodes. To reduce the number of relevant prices, zonal pricing approaches have been developed. In zonal pricing several network buses and lines are consolidated in one grid node. Only power exchanges between those zones are considered, while intra-zonal power exchanges are disregarded. Since only one locational price is calculated for each zone, the number of prices is significantly reduced, compared to full nodal pricing. However, in order to assume that zonal pricing leads to correct results, some fundamental requirements have to be fulfilled. To obtain correct price signals, only nodes that would receive the same nodal price can be grouped into a zone. Thus, intra-zonal congestion and losses have to be negligible. Yet, if intra-zonal congestion occurs, the zone has to be split up (cf. Ping and Sekar [2002], Stoft [2005]).

Generally, locational marginal pricing is used for congestion management in combination with unit dispatch. Therefore, only congestion management methods, in which transmission capacities and electricity are acquired in one single operation are classified as zonal or nodal pricing approaches.[19]

[19] This classification of a congestion management methods is based on Krause [2005]. Some authors maintain, that other congestion management methods such as explicit auctions also qualify as zonal pricing methods.

Typically nodal pricing approaches are realized as fully coordinated implicit auctions,[20] in which electricity and transmission capacity are auctioned at the same time. They are realized e.g. by implementing security constrained unit commitment (SCUC) or security constrained economic dispatch (SCED). Using SCUC the start-up and shut-down schedules of generation units are determined on a short-term operational level considering grid constraints (cf. e.g. Zhang et al. [2006], Sun et al. [2005]). In a similar way, SCED determines the energy and reserve transaction schedule (cf. e.g. Xin et al. [2006]). Thereby, power flow models are used to determine transmission constraints.

Zonal pricing does not consider the whole grid, but focuses on certain flow gates. Therefore it is applied e.g. for cross-border congestion management or for transactions between control areas. The most common market instruments used are flow-based market coupling without separate bids for transmission capacities or market splitting. In market splitting schemes, at first the market is cleared without considering grid constraints. If, in consequence, demand for transmission capacity exceeds the available capacity, the market is split in price zones connected by the congested transmission line. By contrast, market coupling approaches consist of two clearing processes: power market clearing and the clearing of trades in between the power markets. Yet, as there is no separate bid for transmission capacity, flow-based market coupling ranks among the implicit auctioning concepts. This is realized either as a price-based market coupling, in which both, flows and prices, are determined by the coupler or as a volume-based market coupling, in which flows are determined by the coupler and prices on the power exchanges concerned (cf. EuroPEX and ETSO [2009], p. 18ff.; Krause [2005], p. 28ff.).

The main advantage of zonal pricing compared to nodal pricing is that due to the concentration of network buses into a zone, implicating the higher number of buyers and sellers in a zone compared to an individual node, the liquidity at the zonal market is generally higher. This allows for more retail competition and a more effective risk management. However, zonal markets might give perverse incentives for generation expansion (Ding and Fuller [2005]) and also have proven to be very susceptible for gaming, which is impossible in nodal pricing approaches.

A further discussion of the advantages and disadvantages of nodal and zonal pricing schemes can be found in Hogan [1999] and Ding and Fuller [2005].

3.3. The power markets architecture in Germany

In Germany, three main types of power markets can be distinguished: scheduled energy markets on wholesale level, balancing energy markets, and retail markets. In the following section, the different power markets that are found in Germany are introduced. In addition, transmission capacity allocation will be addressed.

[20] In implicit auctions, transmission capacity is integrated in electricity trading. By contrast, in explicit auctions electricity and transmission capacity are traded separately.

3.3.1. Scheduled energy markets

Utilities plan providing the power needed to maximize their profits one day in advance, at the latest. Based on price forecasts they arrange schedules for energy delivery. The electricity that has to be provided to meet these schedules is obtained on different types of wholesale markets. In addition, power trading is used for speculation or to hedge against the risks of energy supply, such as price fluctuations or unforeseen changes in the demand structure. Based on the time lags between closing day and delivery, principally, three types of so-called scheduled energy markets can be distinguished:

- *Day-ahead market:* On spot markets power contracts with (physical) fulfillment on the subsequent day are traded. For each day, there are 24 hourly contracts. In addition, baseload and peakload block contracts are traded, in which the delivery of baseload or peakload energy for serveral hours or days is arranged.
- *Future market:* On future markets contracts are traded, whose fulfillments lie weeks or months ahead. Contrary to spot markets either physical or financial fulfillment is possible. Futures with physical and without delivery are used to hedge against quantity and price risks.
- *Intra-day market:* Power markets for short-dated power trading are called intra-day markets. Power traded on these markets has to be delivered within the next few hours. Delivery periods range from several hours to 15 minutes. Intra-day markets are used for sub-daily balancing of demand and supply imbalances, e.g. caused by fluctuating wind energy availabilities.

In general, markets for scheduled energy are realized on power exchanges. To guarantee a high degree of transparency only standardized contracts are traded. The German power exchange, called European Energy Exchange (EEX), was founded in 2001. It offers a future market, and an OTC clearing house for electricity.[21] Regarding day-ahead and intraday trading, the EEX cooperates with the French Power Exchange Powernext in the joint venture European Power Exchange (EPEX) Spot SE, of which they each hold 50% of the shares. Since 2009 EPEX organizes the day-ahead and intraday trading for Germany, France, Austria and Switzerland. Other important European power exchanges are i.a. the NordPool (Norway), the Amsterdam Power Exchange (APX), and the Energy Exchange Austria (EXAA). However, utilities usually obtain only a fraction of the scheduled energy on power exchanges. In 2009 the share in total power demand of the EEX / EPEX spot- and intraday-market for the trade area Germany and Austria amounted to 25.5% (cf. EUROSTAT [2011], Bundesnetzagentur [2011a, p. 32]).[22] The remaining electric energy is obtained over-the-counter (OTC), that is off-market. In contrast to the standardized contracts traded on power exchanges, the design characteristics of the OTC-contracts, such as price, volume, or place and time of delivery are negotiated between the two contracting parties.

[21] In addition, spot and future contracts for gas, coal futures, and EUA are traded at the EEX.

[22] In 2008 the share of the EEX spot-market in total power demand amounted to 19.6%, while in 2008 it amounted to 23.7% Bundesnetzagentur [2010, p. 83f.].

Table 3.2.: Spot market volumes and prices at selected European power exchanges (Rahn [2008])

Power exchange	**Spot market volumes** [TWh]				**Spot market prices** [EUR/MWh] (Annual avg.)			
	2004	2005	2006	2007	2004	2005	2006	2007
APX	13.4	16.4	19.0	21.0	31.59	52.38	64.60	41.90
EEX	59.4	85.7	89.0	123.7	28.52	45.98	50.80	38.00
EXAA	1.7	1.5	1.7	6.2	28.59	46.57	50.97	38.96
NordPool	165.0	176.0	250.0	292.0	28.57	29.33	48.60	27.90
Powernext	14.2	19.7	30.0	44.0	28.13	46.65	47.20	40.90

Measured by the traded volume (see Table 3.2), NordPool (292.0 TWh in 2007) and the EEX (123.7 TWh in 2007) are the top-selling power exchanges in Europe. Moreover, it can be noted that since 2004 the volumes traded at the European power markets are continuously increasing, which can be interpreted as a sign of an increasing market liquidity. In 2007 the average spot market price at the EEX amounted to 38,00 €/MWh, with a spread of 18,15 €/MWh on Mai 17^{th} and 158,97 €/MWh on December 19^{th} (cf. Rahn [2008]). The decrease in prices between 2006 and 2007 can be explained by more favorable weather conditions, while the price spread between the different European power exchanges is explicable by different levels of deregulation and different generation mixes, in connection with insufficient inter-regional power exchange capacity.

3.3.2. Market for control reserve

The German power transmission and distribution grid contributes to transfer electric energy from power plants to ultimate consumers. It is part of the European Network of Transmission System Operators for Electricity (ENTSO-E), which links up 34 national grids in continental Europe, Great Britain, and Scandinavia. As part of the ENTSO-E network, the German power system is connected to the Dutch, Belgian, French, Swiss, Austrian, Czech, Polish, and Danish transmission grids via AC-interconnection. In addition, DC-interconnectors to the Swedish transmission grid exist (see Figure 3.7).

In transmission systems both the system reliability and the quality of supply have to be guaranteed. Concerning system reliability, the number of outages has to be minimized. Regarding quality of supply, above all, a constant network frequency is required. Deviations of the network frequency from the nominal value cause malfunctions or damages on electrical appliances. Frequency deviations are mainly caused by variations in power production and consumption. If there is an oversupply of electric output, the network frequency rises above the nominal value, if there is insufficient supply, the frequency drops below its nominal value. Due to demand variations, forecasting errors or unforeseen events, demand and supply are virtually always in disequilibrium. Therefore, extra generating capacity for balancing power production and consumption on very short notice is needed. In Germany three types of balancing (or control) power are distinguished (cf. ETSO [2003]):

- primary control, which is the automatic reaction of generating sets to frequency deviations,
- secondary control, the instructed action of generation sets, to move the overall system deviation of the control area towards zero, and
- minutes reserve, which is activated at the latest after 15 minutes in case of plant losses or major forecasting errors.

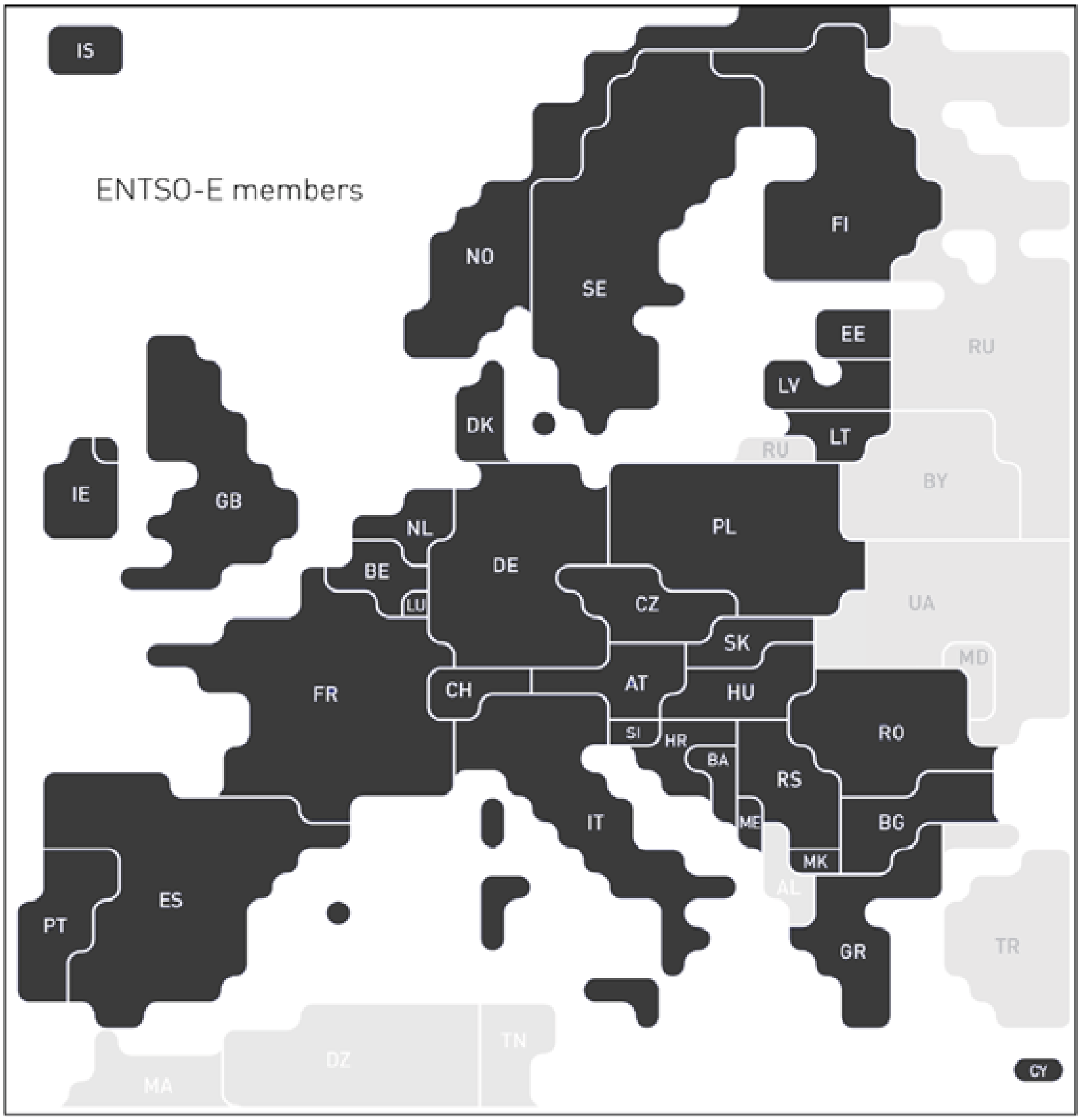

Figure 3.7.: The European Network of Transmission System Operators for Electricity (source: www.entsoe.eu)

The call-off orders for balancing energy are realized according to the merit order. While primary and secondary control are needed every day, minutes reserve is called only a few times per month or year. Secondary and minutes reserve are provided by power stations on request of the transmission system operator (TSO), to countervail variations of balancing groups.[23] Therefore, balancing energy provided as secondary or minutes control is cleared at the expenses of the balancing groups. By contrast, primary control is one of the system services provided for by power station on request of the TSO, which is why costs of providing primary control are included in the system usage fees (cf. StromNZV [2005]). In 2007 the overall costs for the provision of the three types of balancing power amounted to 777 million Euros (cf. CONSENTEC et al. [2008], p. 7).

As the number of installed RES-E capacities with fluctuation feed-in is increasing, a rising demand for reserve capacity is expected (cf. Rosen [2007], pp. 51ff.). It will be met by keeping additional conventional capacity available, such as flexible gas or coal power stations in partial load. Assuming that the number of distributed micro generation capacities and flexible consumer load will significantly rise, the balancing power could also be provided by distributed loads or generation units (cf. e.g. Klobasa [2009]).

3.3.3. Retail markets

Since 1999 the basic principle of freedom of contract applies in the German power market. It grants all customers the freedom to choose their electricity supplier.[24] In addition, utilities are free to supply customers throughout Germany. Along with the unbundling of energy supply companies and the prohibition of the regional monopolies, this has let to considerable changes in the retail power market structure. Before liberalization local utilities controlled the retail markets for electricity. Today, they have to compete with the distribution companies of the four large energy producers, pure redistributors as well as other players such as green electricity suppliers. Regarding the demand side, basically two end-customer groups can be differentiated. On the one hand, special contracts are concluded with customers, which are connected to the medium voltage levels (special contract customers). In the main, industries rank among the group of special contract customers. On the other hand, standard contracts are concluded with customers connected to the low voltage grid, such as private households or small businesses (standard customers).

At the end of 2007, the average price for industrial consumers amounted to 10.13 Ct/kWh, which was 5.63% above the European average (EU27) (cf. Goerten and

[23] A balancing group is an aggregation of feed-in and extraction points, which serves the purpose to balance power feed-in and extraction and which enables transactions procedures (cf. EnWG [2005]).

[24] By the end of 2006, almost all special contract customers in Germany have exercised their right to choose a supplier. Approximately 66% have chosen a new supplier. The remaining 34% have concluded new contracts with their old supplier (cf. EUROSTAT [2007a]). By contrast, by the end of 2006 only 25% of all private households have exercised their right to change their contract, thereof 5% have chosen a new supplier. Regarding SME, 50% have changed their power supply contract, and 7% have changed their supplier (cf. EUROSTAT [2007a]).

Clement [2008]). The average electricity price for private households amounted to 21.05 Ct./kWh in 2007, which is more than 30% higher than the average price in the European Union. Above all, this is due to the high share of taxes in the prices paid by end-customers (cf. Goerten and Clement [2008]), which amounted to 38% in 2007 (cf. BMWi [2008]). The second most important position in households electricity prices are the network costs. To allocate the costs of transmission and distribution as equitably as possible, the amount of network costs a consumer has to pay is dependent on the voltage levels affected by the supply. While end-consumers connected to the high voltage grid only have to cover transportation costs associated with this voltage level, end-consumers connected to the low voltage grid have to cover the costs incurring at the extra high, high, medium, and low voltage level (cf. Wolter and Reuter [2005]). The third position in households' electricity prices are the costs for power generation and distribution, which depend, above all, on the type of power plant used to generate the electric energy.

3.3.4. Transmission capacity allocation

The German transmission grid is divided into four control areas operated by Tennet, 50Hertz Transmission, Amprion GmbH, and EnBW Transportnetze AG. As at present no structural bottlenecks exist (cf. e.g. Bundesnetzagentur [2011c], Frontier Economics and CONSENTEC [2011]),[25] transmission capacities within the German transmission grid are not allocated individually. Congestion is rather managed using cost-based redispatch.[26] Moreover, the German TSO in coordination with the network agency intend to avoid potential future bottlenecks in the transmission grid by means of investing in new grid infrastructure in line with the times and needs (cf. BNetzA [2008], Inderst and Wambach [2007]).

Other than line capacity within Germany, interconnector capacity between Germany and its neighboring countries, except Austria, is scarce. Since this hinders the achievement of an increased power market integration, the EU endeavor to bring forward the construction of additional interconnector capacity. Furthermore, the EU sets rules for the allocation of scarce interconnector capacity, by defining harmonized principles on cross-border transmission charges and on the allocation of interconnector capacities and congestion management (cf. EC [2009e]). According to this, non-discriminatory market based solutions which give efficient economic signals to the market participants and transmission system operators have to be established (EC [2003b]). Capacity allocation methods that are considered to meet these conditions are explicit auctions and implicit auctions either with volume or price coupling. For the future, EuroPEX and ENTSO-E aspire a "glide-path" towards implicit auctions with price coupling - pan-European or at least between ENTSO-E Market Regions - and thus wish to introduce locational pricing within the European power markets (cf. EuroPEX and ETSO [2009]).

[25] According to recent studies on the further development of the German power system, structural bottlenecks are to be expected until 2020, above all, due to increasing offshore wind power feed-in (cf. e.g. DENA [2010a])

[26] According to the Ordinance on Grid Connection of New Power Plants (KraftNAV [2007]) new power plants are given a preferential treatment in redispatch in Germany.

As for Germany, explicit auctions are used for capacity allocation and congestion management of interconnectors to the transmission systems of the Czech Republic, Poland, and Switzerland.[27] Furthermore a volume based market coupling between Denmark and Germany started in 2009. In addition, a market coupling approach between Germany, France, Belgium, and the Netherlands (Central West European (CWE)) (cf. EuroPEX and ETSO [2009], p. 29f.) has been launched in 2010. It will be described in more detail in the next section.

3.4. Application of locational marginal pricing approaches

Schweppe et al. [1988] developed a spot pricing approach for deregulated power markets, in which prices of power supply are calculated for each bus of the power system network. By means of considering grid constraints, congestion is managed and transmission is implicitly priced. Based on the work of Schweppe, manifold theoretical contributions on potential designs and applications of nodal or zonal pricing schemes have been published. Most of them praise the gain in economic efficiency and social benefit of locational marginal pricing. In spite of those theoretical efficiency gains, only a small number of nodal and zonal pricing concepts have been realized. LMP schemes are generally implemented in the form of fully coordinated implicit auctions. An overview of nodal and zonal approaches is given in Table 3.3.

So far, the most sophisticated locational marginal pricing schemes have been developed in the United States. Therefore, the schemes operated by PJM[28] and the California ISO (CAISO) as well as the standard market design of the US Federal Energy Regulation Commission (FERC) are described.

3.4.1. Selected examples of nodal pricing schemes in the US

Today's largest full nodal pricing (FNP) based market structure was established by PJM in 1997. It consists of a day ahead and a real time market that are both operating with locational marginal prices which are composed of a generation as well as a congestion and a loss component. The hourly day ahead market is cleared using a least-cost security constrained unit commitment that simultaneously optimizes power generation and reserve capacity dispatch. To hedge congestion, financial transmission rights are issued. In addition, the LMP at the real time market are determined taking current grid conditions into account (cf. Hausman et al. [2006], Zhou [2003]). LMP are calculated for each bus and also for aggregate load buses and hubs. Yet, the implementation of PJM's LMP based market approach shows a number of deficiencies compared to the theoretical model developed by Schweppe et al. [1988].

[27] Since there is no congestion on the line capacities between Germany and Austria, no market based congestion management methods are used.

[28] PJM was founded as the ISO and market operator of **P**ennsylvania, **J**ersey, and **M**aryland. Today it is in charge of the market operation of 13 US States plus the District of Columbia.

Table 3.3.: Applications of locational pricing based market structures

Market	Start of operation	Reference
Nodal Pricing:		
New Zealand	1996	Zhou [2003]
PJM, USA	1998	Hausman et al. [2006]
New York, USA (generation)	1999	Zhou [2003]
New England, USA	2003	Hausman et al. [2006]; Zhou [2003]
Singapore (generation)	2003	Frontier Economics [2009]
Midwest, USA & Canada	2003	Zhou [2003]
California, USA	2009	CAISO [2009, 2008]; Isemonger [2009]
Zonal Pricing:		
Nordel	1991	Zhou [2003] Stamtsis et al. [2004] Kristiansen [2004] Björndal and Jörnsten [2007]
Australia	1998	Zhou [2003]
California, USA	1998	Isemonger [2009]
Spain / Iberian Peninsula	1998	EuroPEX and ETSO [2009]
New York, USA (loads)	1999	Zhou [2003]
Texas, USA	2001	Zhou [2003]
Italy	2004	EuroPEX and ETSO [2009]
France, Belgium, the Netherlands (TLC)	2006-2010	EuroPEX and ETSO [2009]
Denmark, Germany	2009	EMCC [2009]
CWE-region	2010	EuroPEX and ETSO [2009] EMCC [2009]

First, even though PJM's LMP approach favors a lowest cost dispatch, suboptimal optimization results might occur, because only approximations of system conditions are used. Moreover, since a large part of load is served off market, no genuine system-wide optimization is possible. Second, PJM's LMP signals do not guarantee neither generation nor transmission infrastructure investments that are optimal regarding time or location. The main reason for this is that LMP price signals are only one among many factors upon which the investment decisions are based. Moreover, as in all markets, the contrast between retrospective price signals and prospective investments leads to a disconnection of LMPs and investments. A final deficiency of PJM's nodal pricing based market is that it is not guaranteed that it is sufficiently competitive to render correct LMPs. On the one hand this is due to the lack of demand response. On the other hand the opportunity to exercise market power exists as generators in constraint areas are allowed bid adders of up to 10% (cf. Hausman et al. [2006]).

PJM's nodal-based market structure is the basis for other LMP approaches, e.g. standard market design of the Federal Energy Regulation Commission (FERC) (cf. FERC [2002], Fraser [2010]). The design of the FERC standardized LMP based electricity market is shown in Figure 3.8. The only difference between the PJM and the FERC approach is that PJM's market design misses the Automated Ex Ante Market Power Mitigation Measure (AMP). Like PJM's electricity market, it comprises day-ahead and real time LMP based electricity markets, possibilities to hedge congestion with so-called congestion revenue rights (CRR), and demand side participation (cf. Zhou [2003], pp. 3ff.).

The most recent implementation of a full nodal pricing scheme based on PJM's approach is the Market Redesign and Technology Upgrade (MRTU) of the California ISO (CAISO). On April 1, 2009 the CAISO started up a new nodal-based power market, which replaced the pre-existing zonal design. The nodal design was chosen to encompass the inadequacies of the zonal scheme, especially concerning the congestion management. Like PJM's market, CAISO's new scheme features a cost minimizing SCUC, in which locational prices are calculated for each grid node using a full grid model. Additionally, Ancillary Services Marginal Prices are calculated for each ancillary service provider with a real-time state estimator (cf. Alaywan and Wu [2004], Price [2007]). The main difference between the MRTU and other presently existing models is that an AC power flow simulation is used that allows for a correcter forecasting of power flows than power flow approximations calculated with DC power flow models. In the first few month of operation, the Californian FNP scheme has proven to be robust.

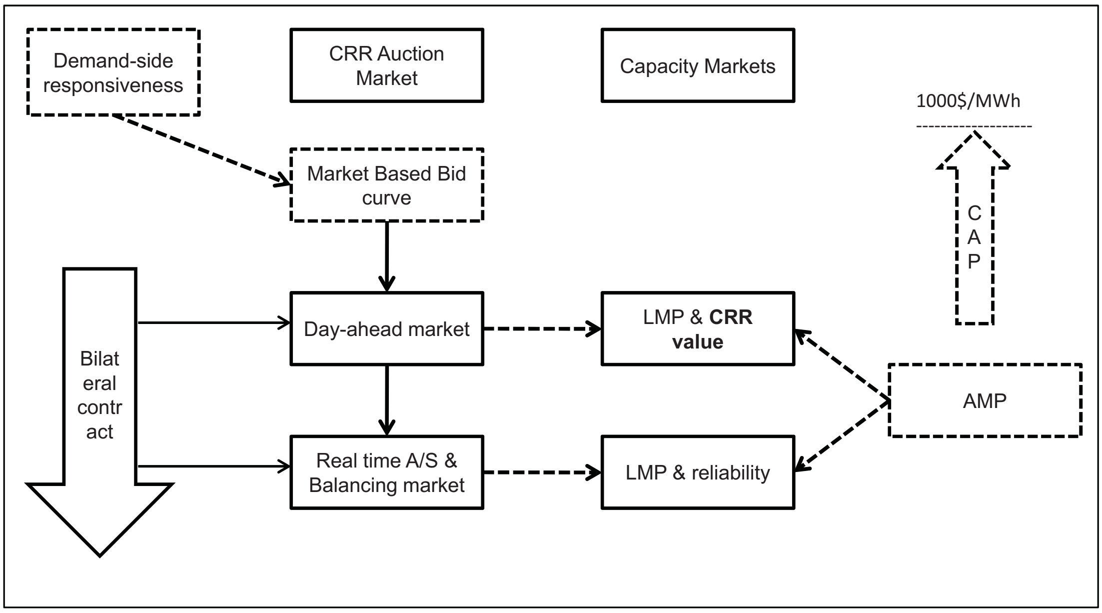

Figure 3.8.: FERC Standardized Market Design (Zhou [2003])

3.4.2. Zonal pricing in Europe

In the case of the European system networks (ENTSO-E), the implementation of a full nodal pricing scheme seems rather unrealizable. For one thing, the European grid consists of no integrated market to start with, but rather of a highly meshed, but only to a limited extent integrated national or regional transmission systems. For another thing, there are political restrictions and conflicting interests of the national system operators (cf. e.g. ETSO [2001], Leuthold and Todem [2007], Pérez-Arriaga and Olmos [2005]). Furthermore, even though zonal pricing approaches use strong simplifications of the power grid and consequently can lead to false price signals, they still can lead to more transparency in capacity allocation, compared to no congestion management at all or even to explicit auctions. Therefore, several zonal pricing approaches for inter-regional congestion management have been implemented in Europe in recent years (cf. Krause [2007], EuroPEX and ETSO [2009]).

The first European zonal pricing scheme, a market splitting approach, called area pricing model, was launched by Nordel in 1991. Until 2009, Nordel was the body for the transmission system operators in the common Nordic energy market, which comprised Norway, Sweden, Finland, and Eastern Denmark. Unlike the above mentioned LMP schemes implemented in the U.S., the area pricing model is a zonal pricing approach. It is based only on financial transactions while neglecting the actual power flows. The market, which is divided into several bidding areas, may be split into several price zones if congestion between the bidding areas occurs. However, only congestion between the zones is considered. Congestion occurring within the zones still has to be managed using conventional, more inefficient methods, such as counter trading (cf. Björndal and Jörnsten [2007], Kristiansen [2004], Stamtsis et al. [2004]).

A similar market splitting approach is used for the day-ahead market of the Italian Power Exchange. Like in the Nordic energy market, the market is first cleared without respecting transmission constraints. In a second step, it is checked if congestion occurs at the flow gates of seven predefined zones. If so, the market is split into separate price zones with different selling prices. The purchasing price, however, remains uniform (cf. EuroPEX and ETSO [2009], p. 26).

The Spanish Market accepts bids for energy produced or consumed outside Spain, that is in any country with which Spain has a border, since 1998. Moreover, in 2007, a full market splitting scheme has been launched for Spain and Portugal.

In 2004 EuroPEX and ENTSO-E proposed a zonal pricing approach in the form of a flow-based market coupling, which has been further elaborated during the last years (cf. EuroPEX and ETSO [2009]). In their theoretical model, they regard the European System as a number of single price regions, which should be linked through this market coupling approach. It includes two clearing processes, implicit or explicit auctions.

In 2006, France, Belgium and the Netherlands started the so-called Trilateral Market Coupling (TLC), to establish an optimal management of interconnecting capacity between these countries. The TLC is realized via a price coupling of the three day-ahead electricity markets. Each day, the order books of the day-ahead auctions of Powernext, Belpex, and APX are aggregated. Then the market prices as well as import / export flows are calculated while respecting the available transfer capacities between the countries (Powernext [2010]). In November 2010, the Trilateral Market Coupling was replaced by a new market coupling initiative of the TSOs (Creos, Elia, EnBW Transportnetze AG, Transpower, RTE, Amprion and TenneT) in the Central West European Electricity market (CWE -Belgium, France, Germany/Austria, Luxembourg, and the Netherlands). Since then, the newly-founded Capacity Allocation Service Company for the CWE (CASC-CWE) conducts daily implicit auctions for interconnecting capacities in between the five countries. It is based on the aggregated order information from the participating power exchanges (EPEX, Belpex, APX/ENDEX) and the available transmission capacities ATC determined by the corresponding TSO. In the near future, it is planned to switch from ATC values to flow-based parameters (CWE MC Project [2010]).

Another operating market coupling with German participation started in 2009. Using a tight volume coupling approach, the European Market Coupling Company (EMCC) links the German and the Danish power markets. Since May 2010, the market coupling is also applied on the Baltic cable linking Germany and Sweden. In this volume-based coupling, the EMCC calculates cross border flows (market coupling flows (MCF)) or market coupling bids based on the order book data (Nord Pool and EPEX) and the available daily capacity data. In a second step, the market coupling bids are integrated in the clearing process of the two power exchanges (EuroPEX and ETSO [2009], EMCC [2009]). In case market prices on the coupled markets differ, the EMCC collects a congestion rent amounting to the product of the MCF and the price difference and passes it on to the owners of the interconnection.

4. The consideration of system properties and regional price signals in energy system modeling

In the previous chapters, the changing framework conditions for power supply have been outlined. Above all, they lead to an increasing decentralization of the power system as well as to a growing relevance of power grid constraints. Consequently, existing approaches in energy system modeling have to be adapted to meet the new requirements. The alternative locational marginal pricing market model, which has been presented in chapter 3, is most suitable to meet the new requirements, because the power flows are directly considered and grid congestion can be identified. This leads to the fact that locational prices can be determined which give incentives for an efficient capacity utilization and expansion planning in terms of time and space. Moreover, since individual grid nodes are regarded, the regional characteristics of the power system, which are the basis for a further decentralization, are taken into account.

In the following sections, firstly the requirements for a model for regional expansion planning will be outlined. Secondly, an overview over existing approaches for decision support in capacity expansion planning is given. Then, ways to integrate a LMP approach into energy system models are presented. In doing so, special attention is paid to the modeling of the power grid. In the last section geographic information systems (GIS) are presented as a tool to collect and manage location dependent data reflecting the regional properties of the energy system.

4.1. Requirements for a regional power plant expansion planning model

Center stage in this analysis is the long-term regional power plant expansion planning. Therefore, the model to be developed has to be able to represent all relevant techno-economical characteristics of the power supply system in a sufficiently detailed way.

In addition to the detailed representation of techno-economic and ecological properties of power generating units, which is common in energy system modeling today, a from an engineering point of view accurate representation of the power grid is necessary. While energy system models with a long-term focus generally neglect transmission restrictions as well as the physical characteristics of power transmission, power flow models do not determine optimal infrastructure investments. The model which will be developed in the following sections allows for a combination of both modeling approaches.

Moreover, in increasingly decentralizing power systems, the location of existing infrastructure as well as regional characteristics gain in importance, such as regional potentials of renewable energy sources (e.g. wind and biomass) or regional characteristics of power demand. Therefore, the modeling approach has to allow for an adequately differentiated representation of the spatially inhomogeneous distribution of RES potentials, consumer loads, and power station sites. Furthermore, the model shall render spatially and temporally differentiated price signals to guide unit commitment and capacity expansion planning.

In addition to the sufficiently accurate modeling of the engineering properties of the power grid and a geographically detailed representation of existing infrastructure and regional characteristics, the modeling approach for regional power plant investment planing under grid constraints should

- respect the technical restrictions of power generation and transmission, which are based on the physical characteristic of the power system,
- include unit commitment as well as capacity expansion planning,
- cover a sufficiently long time horizon (e.g. 20 to 30 years),
- be easily adaptable to changing framework conditions, such as changing prices of energy carriers or EUAs,
- allow for the integration of seasonal load profiles,
- permit to meet planning uncertainties with sensitivity analysis, and
- create a balance between a high degree of detail regarding power system representation and the computational effort in terms of computing time and RAM capacity requirements.

4.2. Overview of modeling approaches for decision support in capacity expansion planning

Models for decision support are employed at all levels of power system planning (see section 3.1). However, while a multitude of models exists for decision support in short to medium-term operation planning, comparatively fewer models exist for investment and production program planning (cf. Göbelt [2001]). Presumably this is due to the complexity of adequate model representations of investment decisions. Moreover, existing overcapacity from the pre-liberalization era lessened the necessity of extensive long-term models up to now. In general energy models are distinguished in macroeconomic top-down and bottom-up power market models.[1] Figure 4.1 shows an overview of decision support models in energy modeling. The model classification presented in the following is mainly based on Möst [2010], Ventosa et al. [2005], Weigt [2009].

[1] In recent years, hybrids of top-down and bottom-up models have been set up with the intention to combine the advantages of both modeling types. Examples of these hybrid modeling approaches are presented e.g. in Böhringer and Rutherford [2008], Wing [2008], Frei et al. [2003], Messner and Schrattenholzer [2000].

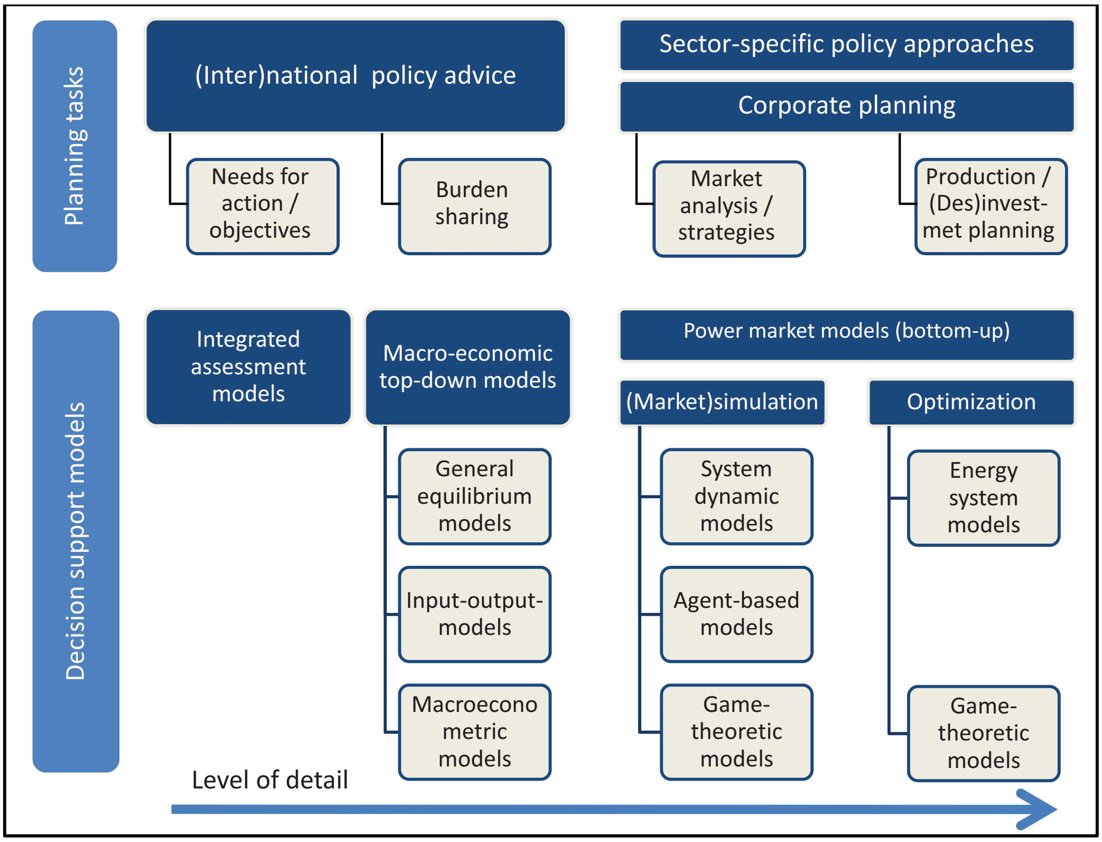

Figure 4.1.: Models for decision support in energy planning (based on Möst [2010])

4.2.1. Macro-economic top-down approaches

Macro-economic top-down approaches represent the national economies in a holistic and highly aggregated way. In general, top-down approaches do not consider individual technologies. Technical characteristics of the production processes are rather modeled using production functions. A differentiation of individual technologies, however, is unusual. The main focus of top-down models is on analyzing price developments and the trade-offs between the different factor markets, subject to different framework conditions. Among them rank general equilibrium models (GEM) and Input-output (IO) models.

GEM consider one economy or competiting economies that are structured into different branches featuring a demand-supply equilibrium. They are generally used in policy consultancy, e.g. to determine the long-term world-wide burden sharing in climate policy. Smeers [1997] and Ventosa et al. [2005] present a good overview of different types of general equilibrium models.

IO models represent the exchange relationships between different branches of economies. By contrast to GEM, IO models are generally used to analyze short through medium term sectoral effects in the context of changing political frameworks. The focus of IO models is on the detailed modeling of the quantity and usage of resources (cf. Möst and Fichtner [2008]). Due to the highly aggregated way to model individual technologies, both, GE and IO models disregard technological aspects, e.g. of the power system. Likewise technological changes are in general not considered in top-down approaches.[2]

4.2.2. Bottom-up approaches

By contrast to top-down approaches, bottom-up approaches represent the relevant techno-economic characteristics of the production processes of the modeled system, whereas inter-sectoral trade-offs are generally neglected. The main target of these process analytical approaches is to provide a basis for a detailed analysis of the (technological) development of the system, depending on changing framework conditions. The most prominent types of bottom-up models are optimizing energy system models and market simulations. Since bottom-up approaches model only one branch of the economy while neglecting inter-sectoral exchanges and interdependecies with other branches, they are also called partial models.

4.2.2.1. Optimizing energy system models

Using optimizing energy system models, optimal, e.g. cost-efficient or welfare maximizing, unit commitment and power plant investment strategies can be determined for a given set of predefined techno-economic input data. The main objective of these process analytical approaches is to provide a basis for detailed evaluations of the (technological) development of the system, subject to changing framework conditions (cf. Ventosa et al. [2005]).[3]

Optimizing energy system models are generally realized as energy and material flow models. Mathematically, they are implemented as linear or mixed integer linear programming. They are based on the assumption of a perfectly competitive market, in which all market participants have the same target function. Moreover, most optimizing energy system models assume a perfect foresight. The strength of optimizing energy system models is the high level of detail with which a multitude of complex technical and economical restrictions can be modeled, their flexibility in the model structure, the possibility to easily adjust the optimization model to new research questions, the available optimization algorithms that permit to solve large scale models, and the transparency of the modeling results. One of their weaknesses is that the strategic behavior of market actors cannot be considered in optimizing energy system models. Furthermore, the assumptions of perfect competition and perfect foresight are questionable.[4]

A detailed overview of energy system models with a long-term focus on optimal investment strategies is given in section 5.4.

[2] In some macro-economic top-down approaches technological changes are considered by modeling individual sectors using a bottom-up approach.
[3] A detailed classification and valuation of energy system models is given in Enzensberger [2003].
[4] This is further discussed in chapter 8.

4.2.2.2. Market simulations

Market simulations do not render an optimal course of action, but model the impacts of a given set of framework conditions.[5] The most prominent representatives of market simulation models are system dynamic and agent-based approaches.

In system dynamic models the interactions between the different 'players' in the energy system are described using differential equations. Typically, system dynamic simulations are used to model market imperfections or strategic behavior of market actors. While, the underlying decision rules of system dynamic simulations are generally comprehensible, the overall results are often difficult to interpret. In particular, if system dynamic simulations are used in long-term modeling, the assumptions made about the future behavior of market actors must be judged critically.

The main characteristic of agent-based simulations is the representation of market actors as so-called agents that each have their own bidding strategies, which they can adjust (learning) in answer to market signals. In general, agent-based simulations have a short-term scope. An example of an agent-based simulation model with a long-term scope is presented in Genoese et al. [2008]. A detailed overview of agent-based modeling can be found in Sensfuß et al. [2008].

4.2.2.3. Game-theoretic models

Game-theoretic models can be realized either as simulations or as optimizing models, in which supply curve approaches are used, on whose basis sets of equilibria are determined. Typically they are used to model price effects and market power in oligopolistic market structures, e.g. to evaluate different possible market designs. Thereby, normally mainly qualitative statements are made, while quantitative studies are made for illustration purposes only. The main disadvantage of those models is, that inter-temporal effects are often neglected. An overview of game-theoretic models is given in Ventosa et al. [2005] and Weigt [2009].

4.3. Locational marginal pricing in power system analysis

In energy system modeling various approaches exist to derive regionally resolved electricity prices. They can be grouped into two main model classes: Transshipment models and optimal power flow (OPF) models. In transshipment models, the power transmission is modeled in a highly simplified way and the physical laws and constraints of power flows are neglected. By contrast, optimal power flow models calculate the optimal generation dispatch while considering Kirchhoff's law as well as power line limitations. In the following, both approaches are introduced.

---

[5] A comparison of the main characteristics of optimizing energy system models and market simulations can be found in Möst and Fichtner [2008].

4.3.1. Transshipment models

In transshipment models the sources and sinks of the energy system and the energy and mass flows between them are modeled using direct graphs. However, the power transmission and distribution grids are normally modeled in a very simplified way. Often, a country is represented by one regional grid node and only the inter-connectors between the countries are modeled. In addition, the physical constraints of power flows such as Kirchhoff's laws are neglected. Power transfers from one region to another are rather modeled like transfers of any other commodity (Examples: Quelhas et al. [2006], Meiborn et al. [2006], MEX IV [2004]).

Regional electricity prices are calculated for each region, including i.a. fuel costs and variable and fixed conversion costs. Electricity transmission and distribution costs are approximated, e.g. using cost factors for power transmission and fixed penalty factors for line losses. Thus, the real costs of electricity transmission and distribution, which also comprise congestion costs and the actual costs of grid losses, are only approximated.

Therefore, transshipment models rank among the transportation problems. Mathematically they can be described as follows:

$$
\begin{aligned}
min \sum_{i=1}^{m} \sum_{j=1}^{n} c_{ij} \cdot x_{ij} & \\
\text{s.t.} \sum_{j=1}^{n} x_{ij} \leq s_i & \qquad \forall i = 1, ..., m \\
\sum_{i=1}^{m} x_{ij} = d_j & \qquad \forall j = 1, ..., m \\
x_{ij} \geq 0 & \qquad \forall i = 1, ..., m \ \forall j = 1, ..., n
\end{aligned}
$$

The sum of the costs of transporting all units x_{ij} from the suppliers i to the producers j is minimized, while supply capacities s_i are respected and the demand d_j is exactly met. Since in power systems the amount of electricity supplied has to equal the amount of electricity in demand[6] $(d_{ij} = s_{ij})$, transshipment models are balanced transportation problems.

The main advantage of transshipment models is that they are linear or mixed integer linear problems and, as such, easy to solve, e.g. using the simplex algorithm. Thus, various applications of transshipment models in energy system analysis exist (cf. e.g. MEX IV [2004]). A severe disadvantage is however the oversimplification of the energy system. Above all, disregarding the actual electrical characteristics of the system and of the laws of power flow, leads to falsified price signals. Furthermore, the high level of aggregation of the system network does not give detailed regional price signals. In addition, transshipment models cannot accurately model loop flows[7] or detailed interactions between line limits (cf. CAISO [2008]).

[6] Here, transmission losses are neglected.

[7] Loop flows occur in inter-meshed transmission grids. Since they superimpose on other power flows,

4.3.2. Optimal power flow models

Recently, attempts have been made to overcome the above mentioned shortfalls of transshipment models, by integrating OPF approaches into energy system models. OPF models are cost-minimizing energy system models subject to transmission system constraints. On the one hand, these models feature a higher degree of detail in the representation of the power transmission system, e.g. by modeling power lines individually. On the other hand, they allow for a more accurate representation of the system's characteristics and behavior by including constraints that model the physical laws of power flow as well as thermal power line limitations in the optimization problem. Thus, in particular grid restrictions are modeled more correctly.

Figure 4.2 shows the difference in solution space between a transshipment model and an OPF energy model. By way of example, the three node network (see section 3.2.3.1) is considered again. In addition to the previous example, it is assumed that the lines *N2N3* and *N3N1* are limited to 100 MW. Again, the feasible sets of injections are restricted by the constraints of the power lines. In a power flow based model, in which the power flow splits according to Ohm's law, the maximum feasible power injection of generator 1, is 90 MW (restriction *N2N1* binds), if generator 2 is not producing (and vice versa). The region of feasible injections considering all line constraints is shown in figure 4.2 a). By contrast, in transshipment models, in which the physical laws of power flow are ignored, it would be assumed that 130 MW could be produced by generator 2, if generator 1 is not producing (and vice versa). Thus, by not considering power flow constraints, the region of feasible injections is enlarged (see Figure 4.2 b)).

In general, OPF based nodal pricing approaches can be distinguished either by the type of power flow model used or by the type of model coupling. Concerning the types of power flow models, alternating current (AC) or direct current (DC) models are employed. Regarding the model integration, integrated approaches, in which the restrictions of optimal power flow are added to the energy system model constraints, and hybrid approaches interlinking the individual submodels via the exchange of result files exist.

As pointed out previously, in LMP approaches the marginal costs of supplying electricity to a specific node of the power grid are determined. For this purpose, the optimal power flow in the power system is calculated. In optimal power flow models, the system is analyzed in a symmetrical steady state. *"The OPF problem can be described as the cost of minimization of real power generation in an interconnected system where real and reactive power, transformer taps, and phase-shift angles are controllable and a wide range inequality constraints are imposed. It is a static optimization problem of minute-by-minute operation."* (Das [2002], p. 525) Examples of optimal power flow model objectives, constraints, and controls are shown in Table 4.1.

In the following, different types of power flow models are presented. Based thereupon, existing approaches of integrating power flow based locational pricing approaches into techno-economic energy system analysis are summarized.

loop flows can cause equipment overload, a limitation of free transmission capacity, and higher grid losses.

Table 4.1.: Objectives, constraints, and control variables of optimal power flow models (Das [2002], p. 528)

Objectives	**Constraints**	**Control variables**
- Min. generation costs - Min. transmission losses - Opt. voltage profile - Min. shunt reactive power compensation - Min. load shedding - Min. emissions - Min. control shifts	- Power flow equations - Limits on control variables - Circuit loadings - Reserve limits - Power compensation - Unit capacity - Active power exports - Bus voltage magnitudes - Voltages angles limits - Spinning reserve - Contingency constraints - Environmental and security constraints	- Real and reactive power generation - Voltage profile at a bus - Load transfers - Line flows - LTC transformer tap positions - Net interchanges - Load shedding - Line switching - Standby start-up units

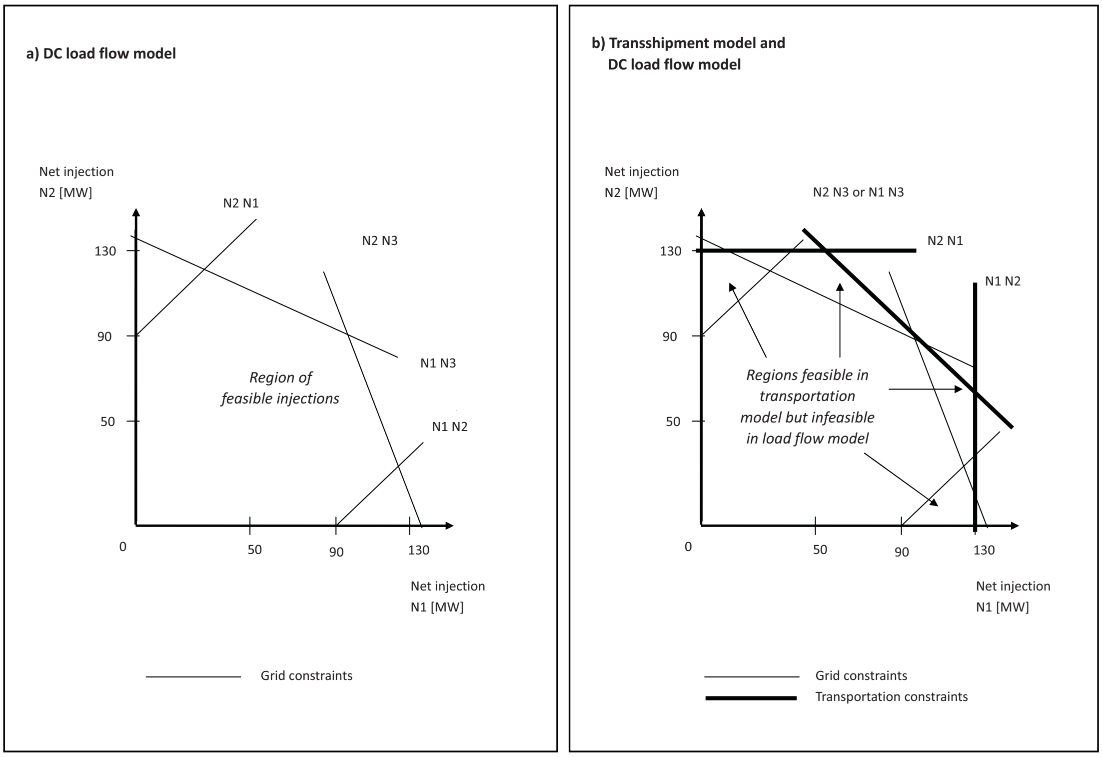

Figure 4.2.: Feasible injections resulting from power flow and transportation model (based on Wolak et al. [2004])

4.3.2.1. Alternating current power flow models

In power systems, generators are regarded as voltage sources capable of supplying the required quantity of active and reactive power to the systems. They are specified by their terminal voltage magnitude $/V/$ and the amount of real power P required to be supplied (P, $/V/$ bus bars). Network loads are specified by their real P and reactive Q power requirements for each bus-bar (P, Q bus bars), cables, lines and transformers by their impedances.

To accurately calculate the power flow in an electricity network, an AC model has to be used. In general, complex numbers are used for the presentation of the power flows in AC networks.[8] In AC-systems, the apparent power $\underline{S_k}$ at node k is calculated as the product of the voltage $\underline{U_k}$ at node k and the current $\underline{I_k}^*$ at node k (see Eq. 4.1). It can be split into an active part P_k called active or real power and a complex part Q_k called reactive power. The node voltage consists of the absolute voltage value U_k and the phase angle θ_k.

$$\underline{S_k} = \underline{U_k} \cdot \underline{I_k}^* = P_k + jQ_k \quad \forall k \in K \tag{4.1}$$

First, the power flow over a power line is considered. For simplification, only one line of the power system is accounted for, which is represented by its π-equivalent (see Figure 4.3).[9] Since we assume a balanced load, it is possible to use the single phase equivalent of the three-phase line. Besides, per-unit quantities are used (cf. e.g. Powell [2004]).[10]

The real and reactive power at node k (P_k and Q_k) equal the sums of active (p_{km}) and reactive (q_{km}) power flows on lines adjacent to node k (see Eq. 4.2 and 4.3).

$$P_k = \sum_{m \epsilon N_k} p_{km} \quad \forall k \in K \tag{4.2}$$

$$Q_k = \sum_{m \epsilon N_k} q_{km} \quad \forall k \in K \tag{4.3}$$

---

8 The underline indicates that complex values are used, while the asterisk denotes conjugate complex values.

9 The π-equivalent model is used for power lines with a line length up to 250 km. Longer power lines are sectioned into a series of π-equivalents. In the π-equivalents model power lines are described by their series resistance (ohmic resistance and inductance) and by their shunt resistance. The shunt resistance results of the capacitance of the line against the other lines and the ground. It is equally allocated to the ends of the line.

10 In a per unit system the system quantities are expressed as a fraction of the base quantities (cf. e.g. Powell [2004]).

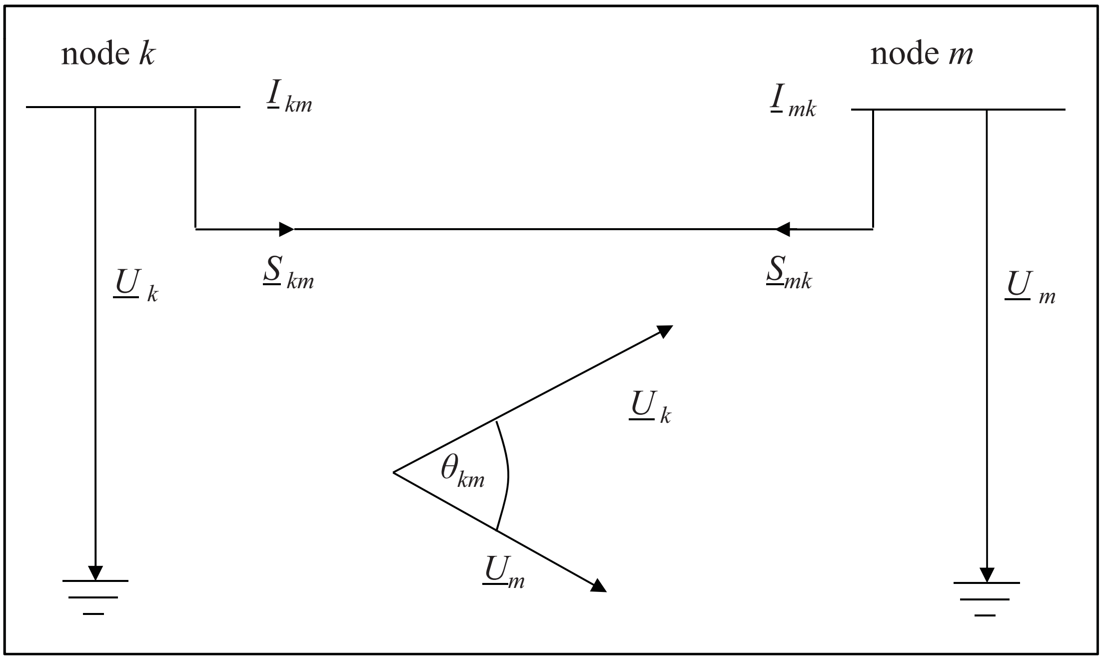

Figure 4.3.: Power flow over a line

The apparent power on a power line amounts to $\underline{s}_{km} = U_k \underline{I}^*_{km}$. According to Ohm's law, the complex conjugate of the current flow is $\underline{I}^*_{km} = \frac{\underline{U}^*_k - \underline{U}^*_m}{\underline{Z}^*}$. Furthermore, the conjugated voltage vectors are $\underline{U}^*_k = U_k$ for the left end of the power line and $\underline{U}^*_m = U_m(cos\theta_{km} + j\, sin\theta_{km})$ for the right end of the power line. Replacing $\underline{Z}^*$ by $R - j\,X$ and expanding the fraction by $R + j\,X$ the power flow over a line as a function of the voltage levels U_k and U_m, the phase angle difference of the node voltages θ_{km}, and the line characteristics results (Das [2002]). Equations 4.4 - 4.6 describe these nonlinear relationships between the power flows on a line, the voltages of the nodes adjacent to the line, and the line characteristics. The power flow s_{km} on line km can be calculated as shown in Equation 4.4. The real term of the equation represents the active power p_{km} (see Eq. 4.5) and the complex term of the equation represents the reactive power q_{km} (see Eq. 4.6). The power flows at all other nodes and power lines of the network can be calculated analogously.

$$\begin{aligned} \underline{s}_{km} = \;& g_{km}U_k^2 - g_{km}U_kU_m cos\theta_{km} - b_{km}U_kU_m sin\theta_{km} \\ & + j\left(b_{km}U_kU_m cos\theta_{km} - g_{km}U_kU_m sin\theta_{km} - U_k^2(b_{km}^q + b_{km})\right) \end{aligned} \tag{4.4}$$

$$p_{km} = g_{km}U_k^2 - g_{km}U_kU_m cos\theta_{km} - b_{km}U_kU_m sin\theta_{km} \tag{4.5}$$

$$q_{km} = b_{km}U_kU_m cos\theta_{km} - g_{km}U_kU_m sin\theta_{km} - U_k^2(b_{km}^q + b_{km}) \tag{4.6}$$

$$\forall k \in K,\ \forall m \in N_k$$

The line characteristics describe the transfer capability of the line km. They comprise the conductance g_{km}, the inductive susceptance b_{km}, and the capacitive susceptance b_{km}^q of the line (cf. e.g. Das [2002], Powell [2004]) that can be calculated using the resistance R_{km}, the reactance X_{km}, the capacitance $C_{B_{km}}$ and the angular velocity ω (see Eq. 4.7 - 4.9).

$$g_{km} = \frac{R_{km}}{R_{km}^2 + X_{km}^2} \tag{4.7}$$

$$b_{km} = \frac{-X_{km}}{R_{km}^2 + X_{km}^2} \tag{4.8}$$

$$b_{km}^q = \frac{\omega C_{B_{km}}}{2} \tag{4.9}$$

$$\forall k \in K,\ \forall m \in N_k$$

Furthermore, the active and reactive power flows over a line have to respect the thermal line limitations C_{km}.

$$\sqrt{p_{km}^2 + q_{km}^2} \leq C_{km} \quad \forall k \in K,\ \forall m \in N_k \tag{4.10}$$

The resulting power flow equations, which have to be solved in the OPF model are nonlinear and neither convex nor concave. Thus, an iterative, computationally intensive approach has to be used to solve the problem. Today in general the Newton-Raphson

Method is used (cf. e.g. Powell [2004]). Its convergence performance depends largely on the starting values chosen (Powell [2004]). Especially for large systems, the duration of the solution process can be very long.

To reduce computing time and consequently enable to solve larger network problems, several simplified modeling approaches are suggested in literature. The most mentioned simplified approach are the DC power flow models. Furthermore, extended DC power flow models, which additionally consider e.g. transmission losses, and the PR-model are mentioned in literature.

4.3.2.2. Direct current power flow models

In DC power flow models[11] several assumptions are made to simplify the solution process. Thus, DC models provide approximations of the relationships between demand and generation levels at network buses and the power flows between the buses in AC power networks. Since as a result, DC models are linear in contrast to AC models, no iterative solution procedure is necessary, but direct solutions are obtained.

The approximations that are generally made in DC models to simplify the calculation are (cf. Powell [2004], Handschin et al. [2009b], Sun and Tesfatsion [2006]):

1. The voltage angle differences θ_{km} are assumed to be very small, so that the $cos\theta_{km} \approx 1$ and the $sin\theta_{km} \approx \theta_{km}$.[12]
2. A high $X : R$ ratio is assumed. As a result, g_{km} is very small compared to b_{km} and can be neglected.
3. An equal distribution of loads and power injections is assumed, so that $b^q_{km} = 0$.
4. All node voltages U_k equal one in relation to the nominal node voltage (per unit system).[13]

As a result of these simplifications, the reactive power flow q_{km} becomes zero. The active power flow p_{km} can be calculated as stated in equation 4.11.

$$p_{km} = b_{km} \cdot \theta_{km} \quad \forall k \in K,\ \forall m \in N_k \tag{4.11}$$

In addition, due to the high $X{:}R$-ratio, it is assumed that $p_{km} = -p_{mk}$ and thus all line losses can be ignored.

[11] *"The term "DC" comes from an old method of computing a solution using an "analog computer" built of resistors and batteries where direct currents were measured."* (Schweppe et al. [1988, p. 313]

[12] That implies that changes in voltage angle have little effect on reactive flows, but a large effect on active flows.

[13] Changes in voltage magnitude have little effect on active flows.

The main advantage of DC models is their very high speed in solving the problem (cf. Powell [2004]). Therefore, they are primarily used for large systems like large energy system models.[14] However, DC models only give approximations of the actual power flows in a network. Therefore, the validity of their application in power system analysis has been questioned. For a further discussion of the adequacy of DC OPF in techno-economic power system modeling see section 8.3.

4.3.2.3. Extended direct current models

To overcome some of the drawbacks of DC models and to provide for a more accurate representation, several approaches were made to extend direct current models, e.g. by integrating constraints for power losses or by additionally considering reactive power flows. However those extensions involve that the model becomes nonlinear and thus has to be solved using an iterative approach.

Direct current models with ohmic losses Handschin et al. [2009a] and Barth et al. [2007] apply an extended DC approach that takes approximated ohmic losses (DCOL) ν_{km} of a line km as the difference of p_{km} and p_{mk} into account. The ohmic losses ν_{km} are calculated based on Eq. 4.12.

$$\nu_{km} = 2g_{km}(1 - cos\theta_{km}) \quad \forall k \in K,\, \forall m \in N_k \tag{4.12}$$

To obtain a convex problem, Handschin et al. [2009a] restrict θ_{km} to $\theta_{km}\epsilon[-\frac{\pi}{2}, \frac{\pi}{2}]$ and solve the resulting non-convex restricted DCOL model (RDCOL) using an iteratively approximation approach. However, Handschin et al. [2009a] apply a RDCOL to a 28 bus model of the German transmission system to determine the optimal unit commitment respecting the grid restrictions. They find that depending on the level of wind power feed-in, the difference of the level of grid losses between an optimal AC and the RDCOL model ranges between -0.8% and -2.4%.

Stigler and Todem [2004] propose another approximation to consider ohmic losses in a DC model. Using an approximation of the cosine function ($cos\theta_{km} = 1 - \frac{\theta_{km}^2}{2}$) and taking into account that the resistance is much smaller than the reactance they approximate the ohmic loss of the DC power flow by Eq. 4.13.

$$\nu_{km} = r_{km}P_{km}^2 \quad \forall k \in K,\, \forall m \in N_k \tag{4.13}$$

[14] In addition to its application in the (economic) analysis of large energy system, DC power flow models are used to derive starting voltages for AC power flow calculations (cf. e.g. Powell [2004]).

Yet, Barth et al. [2007] find that for a 20 kV medium voltage distribution grid, with wind power feed in as well as real and reactive power, DCOL significantly underestimates line losses and thus is not satisfying.

Power flow models considering only active power flows and line impedances For distribution grid design problems Handschin et al. [2009b] propose another simplified power flow model, which they call PR-model. In the PR-model only the real parts of the power flows and line impedances are considered. As a result, the voltage angle differences as well as the susceptances become zero. The active power flows are then calculated according to Eq. 4.14.

$$p_{km} = u_k^2 g_{km} - u_k u_m g_{km} cos\theta_{km} \quad \forall k \in K,\ \forall m \in N_k \tag{4.14}$$

This simplified non-linear modeling approach is suited for problems in which the $X:R$ ratio is small (in their case it was approximately one), in which losses cannot be neglected, and in which node voltages cannot be assumed to be constant.

4.3.2.4. Realizations of optimal power flow and locational marginal pricing approaches in techno-economic energy system analysis

In literature several modeling approaches using OPF analysis and / or LMP approaches in techno-economic energy system analysis could be identified (see Table 4.2). A selection of these studies is outlined in the following paragraphs. The focus is on studies on the German power system and the system of the ENTSO-E.[15]

In the context of proposing locational spot prices of electricity, Schweppe et al. [1988] set up the equations necessary to integrate DC power flow constraints into a techno-economic energy system model. Schweppe's approach was adapted by Stigler and Todem [2004][16] to investigate the optimal use of existing resources subject to network shortages. They realized the integration of the DCOL power flow model into an energy system model for Austria. Concerning the grid model, 165 and 135 lines of the control area of the Austrian TSO Verbund AG are taken into account. As in Schweppe's formulation a quadratic loss function is considered. The nonlinear model is solved in a stepwise

[15] Further contributions to inter-zonal congestion management without special focus on the UCTE transmission grid were made, e.g. by Aguada et al. [2001] and Hao [2005]. Aguada et al. [2001] propose an optimization-based auction mechanism for inter-zonal congestion management. The auction is coordinated by a Regional System Coordinator (RSC), who sets and adjusts frontier bus spot prices till a convergences with ISO price responses is achieved. Hao [2005] presents a DC-OPF-based decentralized congestion management approach for meshed energy markets. He introduces a general approach for the coordination of overlapping markets, which he divides into a master problem for the determination of prices for congested lines and sub problems to determine individual market dispatches and prices.

[16] The model development is also described in Todem [2004].

approach. First a linear MIP disregarding transmission losses is solved to determine the optimal binary conditions of the thermal power plants. In a second step the nonlinear formulation is solved using the fixed binary condition to estimate the transmission losses. Applying it to the Austrian electricity market they show that a new 380-kV transmission line connecting the northern and southern part of Austria removes congestion in the control zone of the Verbund AG. With their modeling approach Stigler and Todem [2004] propose a practical methodology which allows for an easy integration of Schweppe's DC network constraints into techno-economic energy system models. It can be used to calculate welfare minimizing unit commitments for a definite energy system topology. Additionally nodal prices, line flow levels, etc. can be derived.

Based on the work of Stigler and Todem [2004], a DCOL European Electricity Market Model (ELMOD) incorporating the continental European high voltage grid has been developed at Dresden University (cf. Leuthold [2010]). As in Stigler et al. [2004], a quadratic loss function is taken into account. So far, it has been used for various welfare-economic analyzes focusing mainly on grid constraints and the influences of wind power feed-in. In the following exemplary applications of the model are presented.

In Weigt [2006], a short-term time-variant optimization using ELMOD is presented to analyze the impact of wind feed-in in North Germany on the German transmission system. Moreover, he determines the increase in social welfare which could be reached using nodal pricing instead of uniform pricing in Germany. Furthermore, he identifies three necessary grid extensions to integrate offshore wind power and analyzes their effect on nodal prices and social welfare. Leuthold and Todem [2007] investigate different income distribution schemes of flow-based coordinate explicit auctions. They find that income allocations to power flows resulting from accepted bids are preferable while the distribution scheme defined in ETSO [2001] sets false incentives. Leuthold et al. [2008] compare the gains in welfare that could be obtained by replacing the existing uniform pricing scheme in the German power market by a nodal pricing approach. Furthermore, they investigate the effects of offshore wind parks in the German North Sea on congestion in the German and Benelux power grid. Weigt et al. [2010] evaluate alternative extension measures in the German transmission system to integrate the offshore wind power available by 2015. Furthermore, they compare the respective welfare gains under a uniform, zonal, and nodal pricing regime. They find that installing three HVDC lines connecting the offshore wind parks in the North Sea with large demand centers in Central and South Germany is advantageous to the transmission system extension suggested by the first DENA study (DEWI et al. [2005]). Furthermore, they show that nodal pricing is superior to uniform and zonal pricing. Dietrich et al. [2010] convert the social welfare into a cost minimizing approach and analyze the location of optimal investments in power plants between 2007 and 2012 using a version of the ELMOD model (cf. Leuthold [2010]) restricted to Germany and its surrounding countries. They find that optimal investment placing does not reduce average prices significantly compared to a base scenario in which the actually planned investments are considered if only power stations in Germany are optimized. Yet, if additional power station investments in the surrounding countries are taken into account, average prices decrease by approximately 7 €/MWh (-16%). Leuthold [2010] uses a simplified version of the ELMOD model to quantify the amount of necessary grid extension in the UCTE high voltage

Table 4.2.: Overview of selected OPF and LMP approaches in energy system analysis (based on Groschke et al. [2009])

Subject	**Geographic focus**	**Type of OPF**	**LMP**	**Study**
Congestion management and optimal dispatch under grid constraints	East Germany and15-bus test system	AC	nodal	Stamtsis et al. [2002]
	Austria	DCOL	nodal	Stigler and Todem [2004]
	Italy	DCOL	nodal, uniform	Ding and Fuller [2005]
	UCTE	DC	zonal	Purchala et al. [2005a]
	Germany, surrounding countries as single node	DCOL	uniform, nodal	Weigt [2006]
	CWE Denmark, alpine countries	DCOL	uniform, nodal	Leuthold et al. [2008]
	Germany	RDCOL	-	Handschin et al. [2009a]
	UCTE	AC	-	Duthaler [2009]
	EU27	-	zonal	Barth et al. [2009]
	CWE	DCOL, AC	-	Waniek et al. [2010]
	UCTE	DCOL	uniform, nodal	Leuthold et al. [2010]
Transmission pricing	NordPool	AC	nodal	Stamtsis [2004]
	England and Wales	DC	zonal	Green [2004]
Power plant expansion	Germany and surrounding countries	DCOL	nodal, zonal	Dietrich et al. [2010]
	Germany	DC	nodal	Apfelbeck [2009]
Grid extension	Germany, surrounding countries as single node	DCOL	uniform, nodal	Weigt [2006]
	UCTE	DCOL	nodal	Leuthold [2010]
	Germany	DCOL	uniform, zonal, nodal	Weigt et al. [2010]
	Germany	DC	nodal	Apfelbeck [2009]

system induced by increasing wind energy feed-in. He uses an iterative approach in which he extends the transmission grid on those lines connecting the two grid nodes with the highest nodal price difference until no welfare gains can be realized any more.

Another OPF model of the German power system has been developed at the University of Dortmund (cf. Waniek et al. [2008]). Waniek et al. [2008] apply a RDCOL to a 28 bus model of the German transmission system with a preset development of the German power generation system to evaluate the development of re-dispatch costs between 2005 and 2020. They compare a business-as-usual grid scenario to scenarios in which (1) several power grid upgrades in north-south direction and (2) the installation of power flow controlling (PFC) in 2015 devices are made. They model the power flows using an AC model, paying special regard to the system's compliance with the (n-1) criterion. Their results show that due to increasing wind power feed-in at German coasts as well as due to increasing power transitions through Germany the re-dispatch costs will increase significantly till 2020. Both, grid upgrades as well as PFC devices lead to a considerable decrease in congestion probability as well as an increase of maximum relative wind power feed-in. Handschin et al. [2009a] use the same 28-bus RDCOL model of the German grid to determine the optimal unit commitment respecting the grid restrictions for three wind energy feed-in scenarios. Waniek et al. [2010] develop a flow based method for cross-border transmission capacity allocation and test it on a 68 nodes network of the CWE region and their neighboring countries. They compare the results of a DCOL SC-OPF approach that respects the (n-1) criterion, to the existing NTC model and a linearized PTDF approach in which each country is represented by one grid node. In particular the SC-OPF, but also the PTDF approach lead to higher economic welfare and to a better utilization of the cross-border inter-connectors. Analyzing the linearization error, they further find that from a technical point of view, the *"linearization of the AC load flow equation leads to a comparatively low deviation"* from the optimal AC SC-OPF solution.

Apfelbeck [2009] develops an energy system model that considers DC power flows to determine the optimal adaptation of the German power system. The model is first optimized to determine the optimal unit commitment and optimal investments in power stations under grid constraints and then to determine optimal grid extensions. In the first case, the power grid is considered as given while the power plant park is optimized, in the second case the power station capacities are kept unchanged, while grid expansions are optimized. The focus of the investigation is on the optimal grid extension. This is why power plant expansion is considered in a very restricted way. The model covers the time horizon until 2031, using eight representative years, each being modeled by a representative week. In doing so, also time slots with moderate wind power feed-in and low system load as well as with high wind power feed-in and moderate system load is considered. The grid model is a simplified version of the German transmission grid consisting of 210 grid nodes and 251 transmission lines. Regarding power plant expansions, investments with a total capacity of approximately 36 GW are exogenously given. Furthermore no nuclear phase-out is assumed and nuclear power stations are operated until the end of their technical lifetime. In applying the model, they determine 19 grid extensions, most of them in north-south direction and between Thuringia and Bavaria. Furthermore, the optimizer builds 5600 MW of coal-fired power station capacity, in particular at the German coast and in the economic hotspots in Southern Germany. The very low level of power station capacity investment is due to the extremely high number of predefined expansion projects.

Further studies using LMP or OPF simulation with a focus on other parts of the European power system have been realized by Stamtsis et al. [and 2002, 2004], Green [and 2004], Pérez-Arriaga and Olmos [and 2005], Purchala et al. [and 2005a], Ding and Fuller [and 2005], Duthaler [and 2009]

Stamtsis et al. [2002] explore the share of market participants in nodal pricing by analyzing the market participants' bid behavior on congestion. They test their approach using an AC OPF on a 15-nodes network and the VEAG grid in East Germany.

Stamtsis [2004] developed a simulation model for operation mode assessment of Nord Pool's zonal pricing based transmission pricing and congestion management methods. Unlike the other approaches, he uses an AC power flow simulation to derive nodal prices. In addition, Stamtsis develops a fixed cost allocation approach based on a combination of an AC OPF model with a game theoretic model.

Green [2004] presents a welfare economic analysis of different transmission pricing schemes, for England and Wales. Using a DCOL model he shows that moving from uniform to nodal pricing would increase social welfare.

Pérez-Arriaga and Olmos [2005] discuss several approaches for inter-zonal (single price area) DC power flow-based congestion management in the context of their possible implementation in the Internal Electricity Market of the European Union. They further state that, even though nodal pricing-based joint auctions would be ideal in terms of market efficiency, point-to-point coordinated explicit transmission auctions seem to be a more realistic alternative due to political restrictions.

Purchala et al. [2005a] developed a DC power flow based congestion management model for the UCTE high voltage grid, in which for simplicity (and political) reasons each country is supposed to be one zone and the zonal exports and imports are transferred into flows on virtual border links. For a more accurate reflection of the actually available transfer capacity they use a stochastic variable indicating the *"maximal power flow possible through a given border at which a predefined probability of occurrence of congestion is reached"*. (Purchala et al. [2005a])

Ding and Fuller [2005] compare the economic surplus distribution of a nodal, zonal, and uniform pricing approach. They suggest a combination of uniform (zonal) pricing and OPF calculation, in which a uniform (zonal) price is calculated using the results of an OPF model. Generators whose dispatch quantities differ from the zonal or uniform price settlement are compensated. They illustrate that such a uniform or zonal pricing scheme gives perverse incentive regarding the optimal location of new power stations and test their approach on a 129-bus model of the Italian 400-kV grid.

Duthaler [2009] uses a full network model of the UCTE transmission system to conduct security constrain optimal AC power flow simulations under different load situations. He thus identifies areas exporting power and areas with lack of generation capacities.

Barth et al. [2009] integrates a PTDF approach into a power market model for the EU27 (including Norway, Switzerland, and the Balkan countries, excluding Malta, Cyprus, and the Baltic countries) to analyze the effects of a European flow-based market coupling. In their model each country is represented by one zone that are linked by the existing inter-connectors modeled with their total available transfer capacity.

To summarize, even though various studies using power flow based LMP approaches or OPF models have been made, only one publication on integrating an OPF approach into a techno-economic energy system expansion planning model with a long-term time horizon could be found. However, its focus is on the determination of an optimal grid extension plan, while its significance regarding optimal power station capacity investments is limited.

4.4. Using geographic information systems to represent spatial information

Due to the further decentralization of power systems as well as the increasing relevance of grid constraints, geographic aspects of power systems should be considered in energy systems analysis. Geographic Information Systems (GIS) are most suitable to represent detailed geographic aspects in energy models.

The applications of GIS in operational and strategic energy system planning are manifold, such as management of natural resources or engineering applications. For years special GIS-applications called Automated Mapping / Facility Management (AM/FM) are used in the inventory management of power delivery assets. AM /FM systems store georeferenced data of all grid facilities and provide for an easy mapping of the energy systems (cf. e.g. Dolezilek and Ayers [2005], Wu et al. [1999]). In addition, they are employed to visualize the power system and thus help in power system topology analysis.[17]

Regarding the strategic planning of energy systems, GIS are used to determine regional potentials, e.g. of renewable energy sources, support electrification planning in developing countries, or to select feasible (or optimal) sites for new infrastructure. In addition to those technical application, GIS can be used e.g. for marketing and customer management purposes.

In the following sections, a short introduction to GIS in power system modeling is given.[18] First, selected works on GIS-based approaches to determine regional RES potentials are presented. Then, literature examples for the coupling of techno-economic

[17] Moreover, AM/FM systems provide a basis for further GIS-based network operation analysis, such as power flow analysis, circuit rating, and reliability analysis (cf. Kuo and Chao [2010], Mohar et al. [2000], Fleeman [1997]). GIS-based distribution system models are used to provide spatial load models for HV/MV stations (cf. e.g. Stojkovska et al. [2002], Wu et al. [1999], Yeh and Tram [1996]) or as visualization aid in fault diagnosis and outage management (cf. e.g. Fleeman [1997], Kearney [1998]).

[18] For a more detailed description of the functionalities of GIS the interested reader may refer to Galati [2006].

energy system models with a GIS are given. Finally, three GIS-based power system models used for power flow simulations are described.

4.4.1. Introduction to geographic information systems

GIS are computer-aided systems to digitize, edit, save, reorganize, analyze, and visualize all forms of geographically referenced data. Moreover, they enable the developer to overlay information from different sources by means of layers and thus facilitates comprehensive analysis and visualization of the data (cf. Galati [2006], Schmedding [2006]). The element of the GIS to store georeferenced data is called geodatabase. A geodatabase is *"a collection of geographic data sets, real-world object definitions and geometric features."* (Galati [2006, p. 5]) Georeferenced data is data which is spatially transformed into a defined reference system. The geographic data model of a GIS is either based on a grid (raster) structure or a coordinate point (vector) structure (see Figure 4.4).

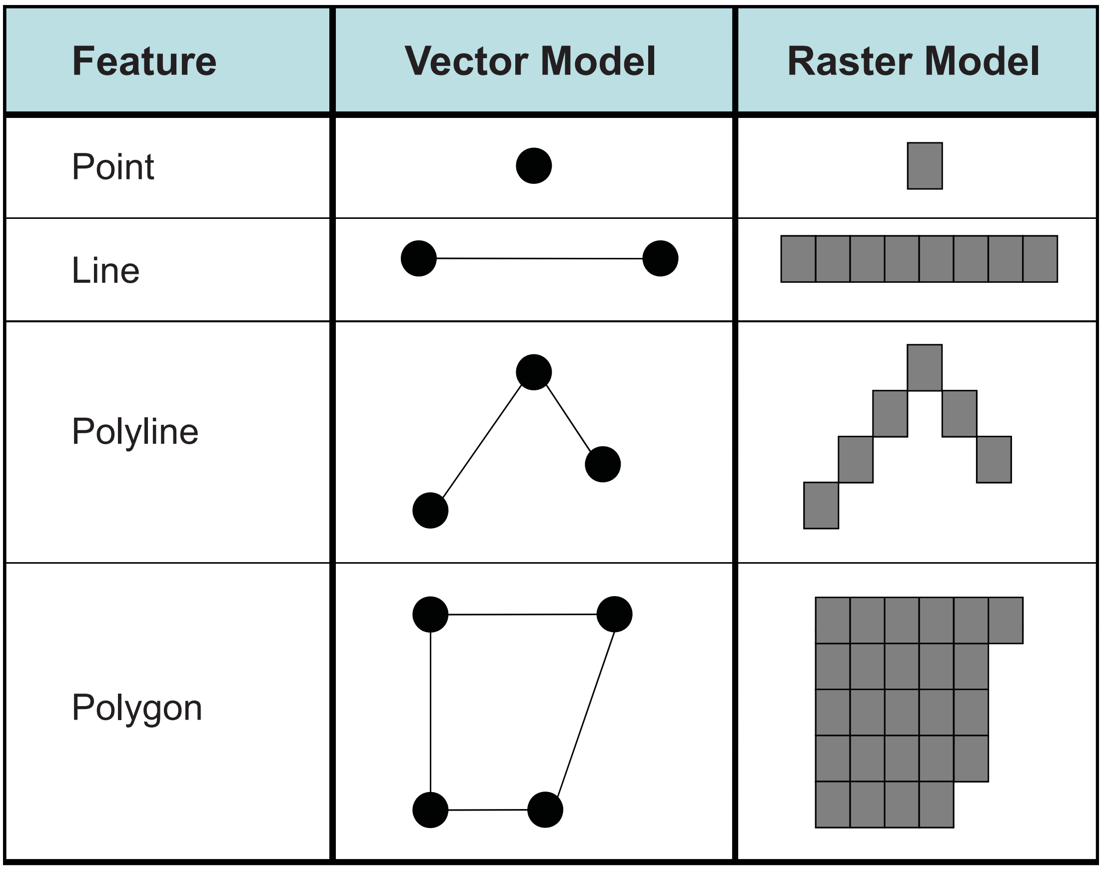

Figure 4.4.: Modeling of features using vector and raster data (Galati [2006], p. 32)

Vector data formats use x-y (or x-y-z) coordinates to depict Earth features. They comprise a feature file, containing the geographic feature information, an index file that serves as unique identifier, and a linked attribute table containing descriptive attributes of a set of features. To detail the objects, different feature geometry types are used: points, lines, polylines, and poligones. Vector data formats are most suitable to represent discrete data with distinct boundaries and well-defined point info, such as roads or gas pipelines and thus to create geographic networks of existing infrastructure.

By contrast, in raster data format digital images are depicted by a grid of pixels or cells. The raster data format is especially well suited for images involving continuous data, e.g. aerial photographs or scans (Galati [2006]). Furthermore, cost raster maps are sometimes used in energy system models to determine minimum route related costs, such as resource transportation costs or grid connection costs. For this purpose, lowest cost paths are calculated with the aid of cost surface maps. Using similar approaches, minimum emission solutions can be obtained.

Because vector data have a more complex data structure, they require much more powerful computational resources for processing and analyzing than raster data.

Since in such GIS-based energy system planning models a multitude of criteria is used, they can be classed into the group of GIS-based multi-criteria decision analysis (MCDA) models. An overview of GIS-based MCDA is given in Malczewski [2006].

4.4.2. Applications of GIS-based location planning

Regarding infrastructure siting, GIS are used by energy utilities and consulting engineers amongst other things to exclude unsuitable sites and to determine distances to calculate costs, e.g. for grid connections. Siting of RES-E generating units but also conventional power stations can be challenging and may encounter difficulties, such as topographic challenges, environmental constraints, geographic constraints, but also public opposition, inter agency coordination problems, or regulatory barriers (Vajjhala [2006]).[19] Moreover, GIS have been proven helpful in the design of new or extensions of existing distribution grid and in electrification planning in developing countries, respectively.[20]

4.4.2.1. Determination of renewable energy potentials and plant siting

In energy system analysis, geographic information systems are commonly used to determine the regional availabilities of resources, in particular of RES. Thus, they help to

[19] Especially to encounter the latter three Miranda et al. [2002] developed a GIS-based negotiation aid system for investors, environmental groups, and governmental agencies who negotiate the optimal location and size of RES-E installations.

[20] This comprises the determination of load centers (cf. e.g. Govender et al. [2001]), providing support with the routing of power grids (cf. e.g. Luchmaya et al. [2001], Fronius and Gratton [2001]), or the selection of economic beneficial generation and distribution modes (cf. e.g. Fronius and Gratton [2001], Monteiro et al. [2001]). Further GIS-based approaches are used to determine the optimal types and locations of substations (cf. e.g. Zifa and Jianhua [2006]) or cables (cf. e.g. Ferreira et al. [1997]).

derive suitable locations for RES-E conversion technologies and to determine the cost of grid connection for potential sites. In these studies, layers with the regional characteristics, such as global radiation, wind speed or land use data, demographic information, and geological data are interlinked and analyzed. Furthermore, exclusion zones such as natural reserves or water bodies, existing infrastructure, power grid constraints, tolerance of interest groups maps, or spatial load patterns are considered.

In the following typical examples of GIS-based approaches to determine RES potentials and sides are listed:

- Bellucci et al. [2003] assess the potential of PV installation on noise barriers along Italian roads using GIS to create buffer zones along roads with heavy noise emissions.
- Fiorese et al. [2007] determine the energetic potentials of short-rotation forestry in the Italian region Emilia-Romagna by overlaying pedological, phytoclimatic, and land use data.
- Hammons [2007] uses GIS to identify possible sites for wind mills on Greek islands by overlaying wind speed and flow accumulation layers, distances from roads and data excluding sites in visibility from monuments. Furthermore he determines distances of feasible sites to the next substation for an economic evaluation of the feasible sites.
- Prest et al. [2007] use GIS to evaluate possible locations for wave farms. In particular they determine optimal cable routes while taking exclusion zones, such as national parks, submarine cables, and regional reserves into account.
- Förster et al. [2008] determine biomass potentials in the Havelland region by using land use data and soil geo-factors for selected crops.
- Yue and Yang [2009] evaluate wind-energy potentials in Taiwan using wind speed and exclusion zone raster data.
- Held [2011] uses regional wind speed, solar radiation, and land use data to determine national cost-resource curves for onshore wind power and PV.

Further examples on the use of GIS-based MCDA in RES-based capacity and grid connection siting are presented in Prest et al. [2007].

4.4.2.2. Siting of large power system infrastructure

To assess the costs and potentials of investments in carbon capture and storage technologies (CCS) at geographically restricted nodes in the German energy system Cremer [2005] coupled a version of the open source partial equilibrium model Balmorel[21] (Ravn [2001]) with a geographic ArcGis based model. The employed version of the energy and material flow model Balmorel allows for a stepwise multi-period linear optimization of the energy system. The optimization is characterized by a myopic dynamic approach.

[21] Baltic Model of Regional Energy Market

The GIS is used to select feasible sites for carbon fueled power plants, to allocate the cost optimal storage sites to feasible power plants, and to select the overall optimal combination of power plant and storage sites. The feasible sites have to fulfill a set of location-specific preconditions. The allocation of storage reservoirs is realized by applying a cost raster based weighted distance function. To select the overall optimal site, all potential sites are put in a merit order and the site with the overall minimal costs is chosen.

The main innovation of Cremer's approach is that the GIS is directly integrated into the optimization process of the partial equilibrium model. The energy system model routine calls the geographic model in the first year of optimization for initial data concerning feasible CCS investment options. During the further optimization process Balmorel calls the geographic model for data update once investments in CCS technologies are realized.

Cremer's approach is well suited for energy system analysis with special regard to technologies characterized by regionally strongly varying potentials and investment decision inter-dependencies. However, if a multitude of possible sites existed and numerous investments in technologies with geographic relation were realized, the iterative model coupling would significantly slow down the optimization (Cremer [2005]).

Another combination of a version of the open-source energy system model Balmorel with a GIS called MOREHyS (Model for Optimization of Regional Hydrogen Supply) is presented in Ball [2006]. Ball developed a model-based approach to optimize the spatial and temporal construction of a hydrogen supply infrastructure with special emphasis on the quantitative analysis of effects on the energy system. The analysis is conducted for Germany, taking the period from 2010 to 2030 as a time horizon. Center stage in the model representation of the production, transport, and distribution of hydrogen was the integration of geographic references. On the one hand, GIS was used to determine demand centers for hydrogen. On the other hand transport distances were calculated using GIS. In addition, the GIS served as visualization tool. Thus, in contrast to Cremer's modeling approach no site optimization or the like was conducted using the GIS. In the MOREHyS model the geographic and the optimization sub-model is interconnected via a soft link, that is, the sub-models are run separately and only result data is exchanged.

Seydel et al. [2007] enhanced the model to analyze the role of regional energy carriers in the development of a hydrogen infrastructure. In particular, they added a resource sub-module to GIS.

Biberacher [2008] couples GIS and a version of the TIMES model (see section 5.2) to determine whether the global power demand can be covered by solar, wind, and hydro power in combination with power storage and power generated in fusion power stations. GIS is used to store, manage, and display all input and output data. Regarding the regional potentials of wind and PV, 6-hour wind speed maps, with a grid distance of 2.5 degree in longitude and latitude, and solar radiation data provided by NASA, with a geographic resolution of 1 degree in longitude and latitude are used. Hydro-power potentials are derived using accumulated annual precipitation data. Biberacher's findings are that especially the entrance of fusion power is very sensitive to increasing costs of fusion technology and the availability of transport capacity between the considered regions. If sufficient transport capacity is available, the power demand is entirely covered by RES, while fusion power disappears completely. Furthermore, his results emphasis that hydro-power would always be competitive.

Johnson et al. [2008] set up a simpler techno-economic GIS-based model to determine the cost-minimizing locations of hydrogen production and distribution facilities in the state of Ohio. They take into account the techno-economic data of coal gasification installations, CCS and hydrogen storage facilities, as well as of a distribution grid consisting of trucks, pipelines, and refueling stations. They use GIS to georeference the input data, determine demand centers, and to determine transportation distances. Unlike Ball [2006] and Seydel et al. [2007] they do not consider implications on the long-term development of the power system.

4.4.3. Large grid models and GIS-based power flow simulations

In addition to the GIS applications described above, several power flow simulation tools, which are based on GIS, could be identified in literature. In the following, the most prominent approaches realized by Zhou and Bialek [2005] and Rudkevich et al. [2007] are described.

Zhou and Bialek [2005] developed an approximate GIS-based power flow model of the UCTE transmission grid. They combined a PowerWorld[22] DC power flow simulator with a geodatabase, in which all relevant information of the UCTE energy system is stored. To obtain the relevant grid data, they digitized the UCTE 400 kV grid map. In total 1254 load buses and 378 generators were edited. Each power plant is related to a bus bar of the grid model. Generation data, such as capacities, fuel types, or cost curve information of the individual power plants are stored in the geodatabase. Spatial demand data was determined using national demand statistics. It was distributed among regions on the supposition that demand in a region is proportional to the population of that region. Concerning the allocation of demand to the load buses, it was assumed that the load buses share the regional load equally. The simulation results obtained with the Zhou-Bialek model comprise i.a. power generation levels, power loads on transmission lines, power flow directions, and power transfer distribution factors (PTDF)[23] for given load levels. An integration of this power flow simulator and a long-term energy system model could be realized by exchanging the PTDF values. However, the high price of the commercial simulator does not seem appropriate and is thus a big drawback of this

[22] PowerWorld is a commercial power system simulation tool offered by PowerWorld Cooperation. Optimal power flow simulations can be conducted using an OPF add-on. For more information please confer http://www.powerworld.com/products/simulator.asp.

[23] Power Transfer Distribution Factors (PTDF) describe the physical flow on specific lines that are provoked by a commercial exchange between two regions. Thus *"PTDF translate a commercial transaction between two hubs into the expected physical flows over the entire network."* ETSO [2007]

approach.[24]

Rudkevich et al. [2007] present a similar approach for the Eastern US grid. They interlink a geographic model with the commercial energy market simulator GE MAPS[25]. The geographic model is used to cluster buses into hubs and to identify transmission corridors. The market simulation model was then used to identify most critical transmission constraints. The integration of the model with a long-term energy system optimization could be realized by exchanging PTDF, too.

4.5. Summary

In this chapter, the requirements for an energy model for regional expansion planning have been outlined. Special focus was on the requirements regarding the integration of power grid constraints and regional system characteristics. In particular the need to integrate the technical characteristics of the power grid has been addressed.

In the second part of this chapter, an overview of different types of modeling approaches for decision support in energy system planning has been given. While top-down approaches model the energy sector in an aggregated way, bottom-up models are characterized by describing all relevant techno-economic characteristics of the energy system. Among the most prominent types of bottom-up approaches rank optimizing energy system models and market simulation models. The choice of model depends on the (research) question to be answered.

In the third part of this chapter, the application of locational marginal pricing in power system analysis has been discussed. First, the advantage of power flow-based approaches over transshipment models in depicting the actual constraints of the power grid were discussed. Based thereupon, different types of power flow models as well as their applications in techno-economic energy system analysis has been discussed. The literature survey shows that so far, no application of a techno-economic energy system expansion planning models with a real focus on long-term power station expansion planning could be found.

In the last part of this chapter, geographic information systems have been introduced as a tool to model regional power system characteristics. Moreover, selected examples of typical application with reference to the focus of this work have been presented.

In the following, these literature surveys are the basis to develop a modeling approach for the analysis of the long-term development of power systems that considers grid constraints as well as the regional characteristics of the power system in an adequate way.

---

[24] The geographic model of the UCTE transmission systems developed in Zhou and Bialek [2005] is also used in the EFOM model (cf. Leuthold [2010]).

[25] cf. http://www.gepower.com/prod_serv/products/utility_software/en/ge_maps/index.htm

5. Development of a nodal pricing based optimizing energy system model

The focus of this work is to develop a techno-economic model, which can be used to analyze the long-term development of an increasingly decentralized power system. In the context of the liberalization of energy markets and an increasing decentralization of power systems, new challenges for energy system modeling arise. Among them counts in particular the need to consider power grid constraints in an adequate way.

In the following sections, the optimizing energy model PERSEUS-NET, which has been developed to meet the requirements outlined above will be presented. Firstly, an outline of the model will be described in section 5.1. Then, existing energy and material flow models, which are the precursors for the developed model are presented. Since the optimization model developed in this work is part of the model family PERSEUS, in particular applications and methodological approaches of other models of the model family are addressed. In section 5.3, the mathematical description of the model PERSEUS-NET is given. Firstly, the objective function and the system of equations for power generation, which are common for many other models of the PERSEUS model family are described. Finally, the system of equations for power transmission, which are the innovative part of this work, is presented.

5.1. Realization of the modeling concept

In the section 4.1, the requirements for a nodal pricing based optimizing energy system model have been elaborated. To meet those requirements techno-economic bottom-up-models that combine system expansion with unit dispatch planning seems most suitable. Top-down approaches seem less appropriate, mainly due to their aggregated point of view. In this work, a hybrid modeling approach has been developed, which consists of the energy and material flow model PERSEUS-NET that is coupled to a geodatabase containing all georeferenced input data (see Figure 5.1).

The PERSEUS-NET model was developed to analyze possible trajectories of a decentralizing energy system. Based on experiences made with existing models of the PERSEUS family (see section 5.2), it integrates a unit dispatch and expansion planning. While the long-term unit commitment planning determines which of the available units should contribute to what extent and at which point in time to fulfill a given demand, the expansion planning investigates in which power plants to invest.

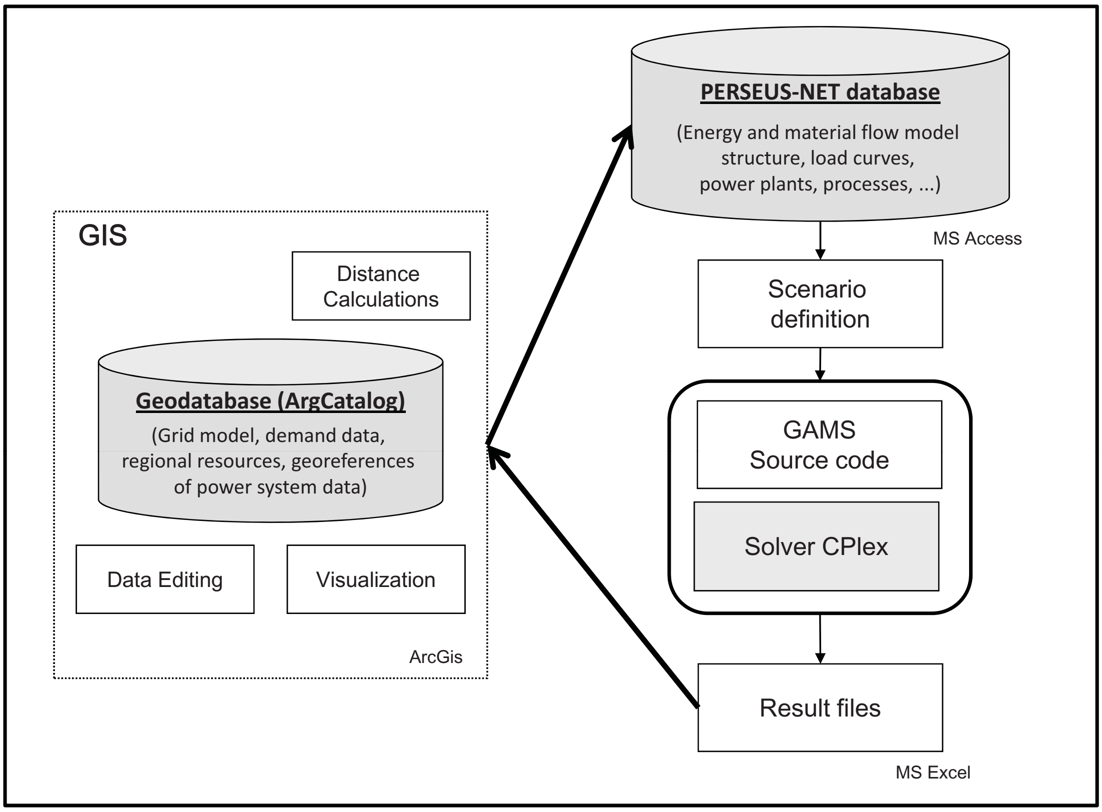

Figure 5.1.: Outline of the modeling approach

PERSEUS-NET enhances this optimization approach by considering the regional distribution of power generation, demand, and investments, as well as the DC power flows arising in the power system. Therefore, PERSEUS-NET is most suited to analyze the following matters:

- The optimal evolution of the German power system regarding generating capacity distribution,
- the timely and spatial integration of RES-E and its impact on the generation and transmission system,
- the regional distribution of the marginal cost of electricity supply,
- the influence of grid congestion and transmission grid requirements, and
- the influence of different scenarios concerning EUA and energy carrier prices.

PERSEUS-NET is an energy and material flow model applying a multi-period linear programming approach, which requires the minimization of all decision relevant costs within the energy system. The target function comprises fuel supply and transport costs, fixed and variable costs of the physical assets, such as operation, maintenance and load variation costs, and investments in new power stations. The driving force of the PERSEUS-NET model is the exogenously given demand that is represented by annual, regionally differentiated demand levels and load profiles for characteristic days. Within the optimization, a cost-minimizing supply structure to meet this demand is determined.

Moreover, the main techno-economical and ecological characteristics of the energy system are considered by further equations. They allow for a realistic representation of the energy system. The most important technical equations, which are common to all PERSEUS models, are the energy and material flow balances, which match demand and supply while taking into account the above mentioned load profiles, generating capacity restrictions, such as the availabilities of installed capacities and the physical lifetime of power stations, and restrictions of process utilization, e.g. load variation restrictions, maximum and minimum full load hours, or co-generation options. In PERSEUS-NET they are completed by technical constraints describing the DC power flows within the power grid, the restriction resulting from the thermal limits of the power lines, and the slack bus definition.

Investments in new transmission lines are not determined in PERSEUS-NET, because the focus of this work lies on power plant expansion planning. Furthermore the exogenous definition of grid extensions is beneficial in terms of calculating time and RAM requirements. Moreover, the decisions where to invest in new transmission lines are only partly based on economic criteria, but rather politically influenced, and should thus not be determined using purely economic decision criteria. If, in further investigations the optimal expansion of the transmission system shall be determined an appropriate extension of the PERSEUS-NET model could easily be implemented.

The optimization problem is written in GAMS (General Algebraic Modeling System). and is solved by using a version of the simplex algorithm (CPLEX).

To facilitate a realistic representation of the geographic characteristics of the power system, and thus to lay the groundwork for a correct determination of DC power flows, all generating, demand, and transmission facilities are specified not only regarding their techno-economic characteristics, but also regarding their physical location. The data management is based on a relational database, containing the techno-economic and ecological characteristics of the units, processes, and energy carrier flows. It is coupled to a geodatabase containing the geographic references of the input and output data (see section 6.2). For this purpose, the software ArcGis (ESRI) is used. In detail, GIS is used

- to digitize a map of the German transmission system,
- to georeference unreferenced input data,
- to store and manage georeferenced data,
- to calculate the length of the transmission lines, and
- to visualize the geographic structure of the energy system as well as the results of the modeling work.

The ArgGis component ArgMAP is used to edit and visualize the German power supply system. To store the data, the ArcGis component ArgCatalog is used. The power supply system can be described as a geographic network consisting of power lines and grid nodes, each with its specific characteristics. Therefore, using a vector data format seems most appropriate for this modeling approach. The power lines are modeled as line-type data, while the grid nodes are modeled as point-type data. The database based systems provide for a detailed and correct mapping of regional potentials, transmission line lengths, etc. and thus allow for a geographically optimal location planning of energy system infrastructure. ArgCatalog stores the data in .mdb-files, which are compatible with the existing databases of the PERSEUS model family. The data stored in the PERSEUS-NET database can be linked to the data edited with ArcMap. This allows the visualization of all model data, with geographic reference, such as power plant sites or regional power demands.

5.2. Optimizing energy system models as the precursors to the developed model PERSEUS-NET

Since the first oil crises in the 1970s, energy system models have been increasingly used for corporate planning and policy support. At first, their main field of application was the development of strategies for restructuring the energy systems to reduce the nations' oil dependency. Later on, energy system models were used to help to cope with new political and environmental challenges, such as SO_2, NO_x, or GHG reduction. In general, those energy and material flow models based on OR methods have the advantage of a very detailed representation of the techno-economic characteristics of the energy conversion chain, and thus provide a good understanding of the circumstance-based evolution of energy systems. Due to their highly technological reference system they are often referred to as "engineering models".

Today, a large number of energy systems models exist. Among the internationally most widespread approaches, on which many of the models used today are based, rank EFOM[1] (cf. Finon [1974], E. Van der Voort [1984]), MESSAGE[2] (cf. Agnew et al. [1979], Messner [1984], Messner and Strubegger [1999]) and MARKAL[3] (cf. Fishbone and Abilock [1981]). Their basic versions have been developed in the framework of European research projects. Over the years, they have been enhanced and adapted to altering circumstances and newly emerging problems, such as environmental defiances, by various research institutions.

In Germany the models IKARUS (cf. Martinsen et al. [2007]), E³-Net (cf. Fahl and Blesl [2002]), EMS (cf. Gerdey and Pfaffenberger [2002]), EIREM/EUDIS (cf. Hoster [1996]) as well as the PERSEUS model family count among those derivatives.[4]

1 Energy Flow Optimisation Model
2 Model for Energy Supply System Alternatives and their General Environmental impact
3 Market Allocation Model
4 An overview of the energy system models developed and applied at German research institutions

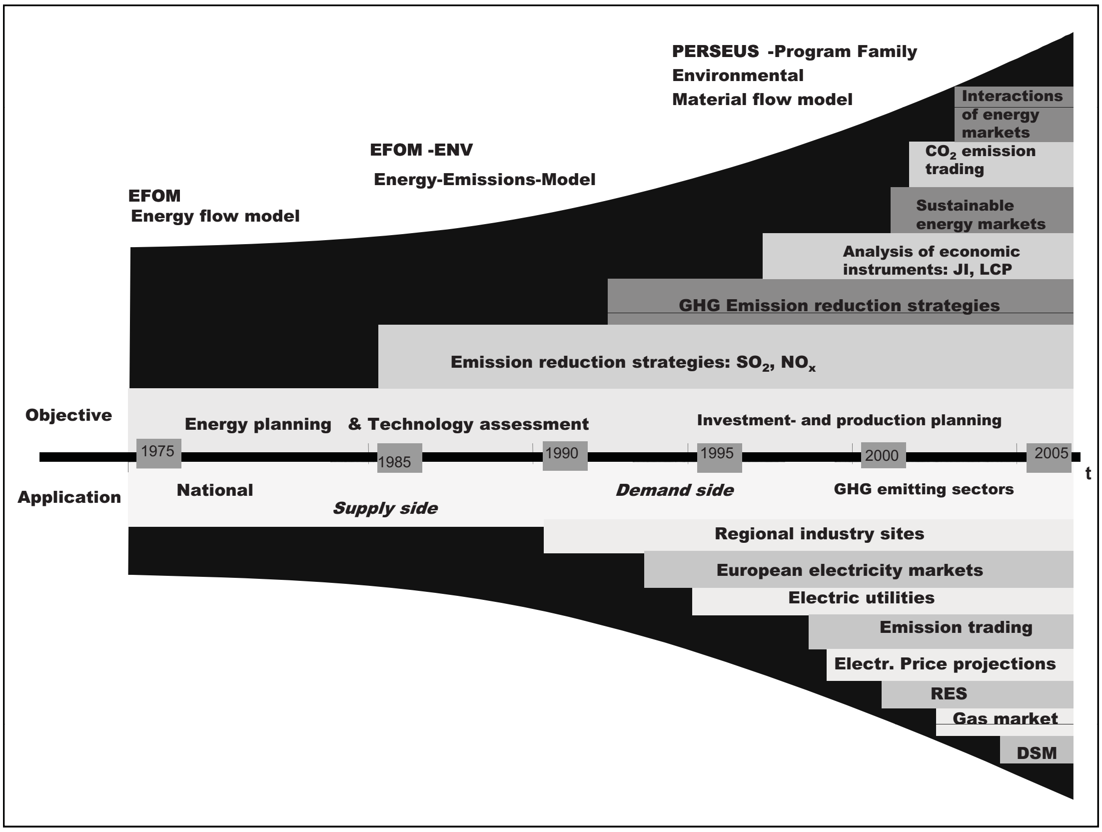

Figure 5.2.: Development of the PERSEUS model family (based on Rosen [2007])

The PERSEUS (Program Package for Emission Reduction Strategies in Energy Use and Supply) model family, has been developed at the Institute of Industrial Production (IIP) of the Karlsruhe Institute of Technology. PERSEUS is based on the EFOM-ENV model (see Figure 5.2). The EFOM model was developed in the early 1970s at the Institute Economique et Juridique de l'Energie in Grenoble. In a consistent approach, the whole energy system of a country, with its different conversion levels, is represented in the model. On the basis of the existing structure of the contemplated energy system, the cost minimizing system development is determined for a given energy demand. Considering individual investment alternatives as well as their interdependencies, the model EFOM has been used by policy advisers to identify systematic optimization potentials of the energy system evolution. Besides, in the derivative EFOM-ENV, emission reduction strategies, e.g. for SO_2, NO_x, and CO_2 can be considered. The results obtained with this model were e.g. considered in the determination of legal limits for SO_2 and NO_x of power plants. The PERSEUS group of models based on EFOM is described in Wietschel et al. [1997]. Since its development, it

is given in MEX III [2004], MEX IV [2004], MEX I [1999], MEX II [2002]. MEX I [1999] addresses structural and macroeconomic effects of the climate change, and in MEX II [2002] the consequences of the German nuclear phase out plans. MEX III [2004] deals with the role of RES and MEX IV [2004] with the German contribution to the EU climate change policy.

Table 5.1.: Modules of the PERSEUS model family - methodological modules (based on Rosen [2007, p. 101])

Optimization alg.	**Application**	**Selected References**
Linear programming	Different countries, utilities of Karlsruhe and Rottweil, RWE AG, EdF	Fichtner [1999a], Enzensberger [2003], Rosen [2007]
Decomposition algorithm	i.a. Germany, Russia, Indonesia	Ardone [1999], Morgenstern [1991]
Iterative optimization	Germany	Wietschel [1995]
Mixed-integer linear optimization	i.a. Energy utilities, RWE AG, Industrial zone Karlsruhe Rhine Harbor, Switzerland	Lüth [1997], Fichtner [1999a], Göbelt [2001], Tietze-Stöckinger [2005], Möst et al. [2004]
Stochastic linear programming	Energy utilities	Göbelt et al. [2000b,a]
Target function	**Application**	**Selected References**
Minimization of expenditures	Different countries, regions, and utilities	Rosen [2007], Fichtner [1999a], Enzensberger [2003]
Profit maximization	Different utilities	Göbelt [2001], Göbelt et al. [2000a]
Goal programming	France	Fleury [2005]

has been enhanced in various dissertation projects, e.g. Fichtner [1999b], Ardone [1999], Göbelt [2001], Dreher [2001], Enzensberger [2003], Frank [2003], Fleury [2005], Tietze-Stöckinger [2005], Möst [2006], Perlwitz [2007], or Rosen [2007]. The focuses of those projects comprise energy planning and technology assessment, analyses of the effects of the European Emission Trading Scheme, or the assessment of the interactions of the different energy markets. The fields of applications of the various model specifications are, e.g. the supply and / or demand side of a national energy system, the European electricity markets, the gas markets, or regional industrial parks.

The different modules of the technology-based energy and material flow model can be distinguished into methodological and application orientated modules (see Tables 5.1 and 5.2). Regarding the methodological approaches, the optimization algorithm or the target function is the main distinctive feature. The application modules are either characterized by their focus of application or their system boundaries. The focuses of application rank from capacity expansion planning and the evaluation of abatement strategies to the design of regional energy networks. System boundaries vary from company to EU level. Concerning the optimization algorithms linear programming, decomposition algorithms, iterative optimization, mixed-integer linear programming and stochastic linear programming have so far been applied. As target functions the minimization of total system expenditures, profit maximization as well as goal programming have been employed.

Table 5.2.: Modules of the PERSEUS model family - application oriented modules (based on Rosen [2007, p. 101])

Focus of application	**Application**	**Selected References**
Emission abatement strategies	Different countries, baseline calculations	Ardone [1999]
CO_2 certificate market	EU 25	Enzensberger [2003]
LCP / IRP strategies	Utilities of Karlsruhe and Rottweil	Schöttle [1998]
Analysis of flexible instruments for climate change	Germany, Russia, Indonesia, India	Ardone [1999]
External costs	Germany, Slovenia, France	Lüth [1997], Fleury [2005]
Capacity expansion and decommissioning planning	Different utilities, RWE AG, Wingas GmbH	Fichtner [1999a]
Contracting	Utilities of Karlsruhe and Rottweil	Wietschel et al. [1999]
Evaluation of environmental policy instruments	Germany, Baden-Wuerttemberg	Dreher [2001]
Developments of sustainable strategies	France	Fleury [2005]
Design of (regional) energy networks	Industrial Zone Karlsruhe Rhine Harbor, EU natural gas market	Tietze-Stöckinger [2005], Frank [2003], Perlwitz [2007]
Renewable energies	Switzerland, EU15	Rosen [2007], Möst [2006]
System boundaries	**Application**	**Selected References**
International	Europe	Enzensberger [2003]
National	Several countries	Ardone [1999]
Regional	Northern Germany, Baden-Wuerttemberg	Dreher [2001]
Sectoral	Wood finishing	Wietschel et al. [1997]
Inter-company networks	Industrial Zone Karlsruhe Rhine Harbor, cooperations in the energy sector	Tietze-Stöckinger [2005], Frank [2003]
Company level	Utilities of Karlsruhe and Rottweil, RWE AG, Wingas GmbH	Dreher [2001]

5.3. Mathematical description of the optimization model

In the following, the model structure, parameters, and variables will be introduced. Then, the objective function and the system equation for power generation, which are common in many offshots of the PERSEUS model family, are described. In the last part of this section, the system of equations for the modeling of the DC power flows and the grid restrictions are presented. They are the elements integrated in the optimization model within this work.

5.3.1. Model structure, parameters, and variables

The energy system model PERSEUS-NET is divided into five hierarchical levels (see Figure 5.3). At the top level, the regions $reg \in REG$ considered in the model are specified. Those regions, in this case in particular Germany, are subdivided into geographic subsystems $sub \in SUB \subset REG$ which represent the sub-regions determined by the grid nodes of the transmission grid. Each sub-region is assigned to exactly one region, while a region contains several sub-regions. The first and the second level of the model form the so-called aggregational level. Underneath producers $prod \in PROD$ and flows of energy carriers $ec \in EC$ compose the structural level. In PERSEUS-NET the producers convert, store, or transfer energy, and thus represent the power generators, retail customers, transmission, and distribution system grid nodes, etc.

At the detailed level, the conversion and transmission units $unit \in UNIT$ are defined. Since Germany's power supply system is represented in a very detailed way, all large power and heat producing units are modeled individually. Furthermore, the flows of energy carriers, which are characterized by their flow levels, variable costs, efficiencies, and seasonality, are defined at the detailed level.

The processes $proc \in PROC$ at the lowest hierarchical level are the material and energy conversion processes within the units, such as processes for the conversion of energy carriers, electricity generation, or electricity consumption. All technological parameters, which characterize the operation mode of a unit, are defined within the process level. Typically, different operating modes within a unit are distinguished, e.g. variable output combinations of a CHP unit are considered.

The structure of the energy model PERSEUS-NET corresponds to a digraph. Herein, the nodes of the digraph correspond to producers $prod \in PROD$, whereas the edges represent the energy flows between those producers. The flows represent the transport of the different energy carriers $ec \in EC$. Inside the nodes of the digraph, no flows are allowed. Their utilization is subject to the optimization. The sources of the graph are represented by the different types of energy sources. The sinks of the model are the end-uses of power.

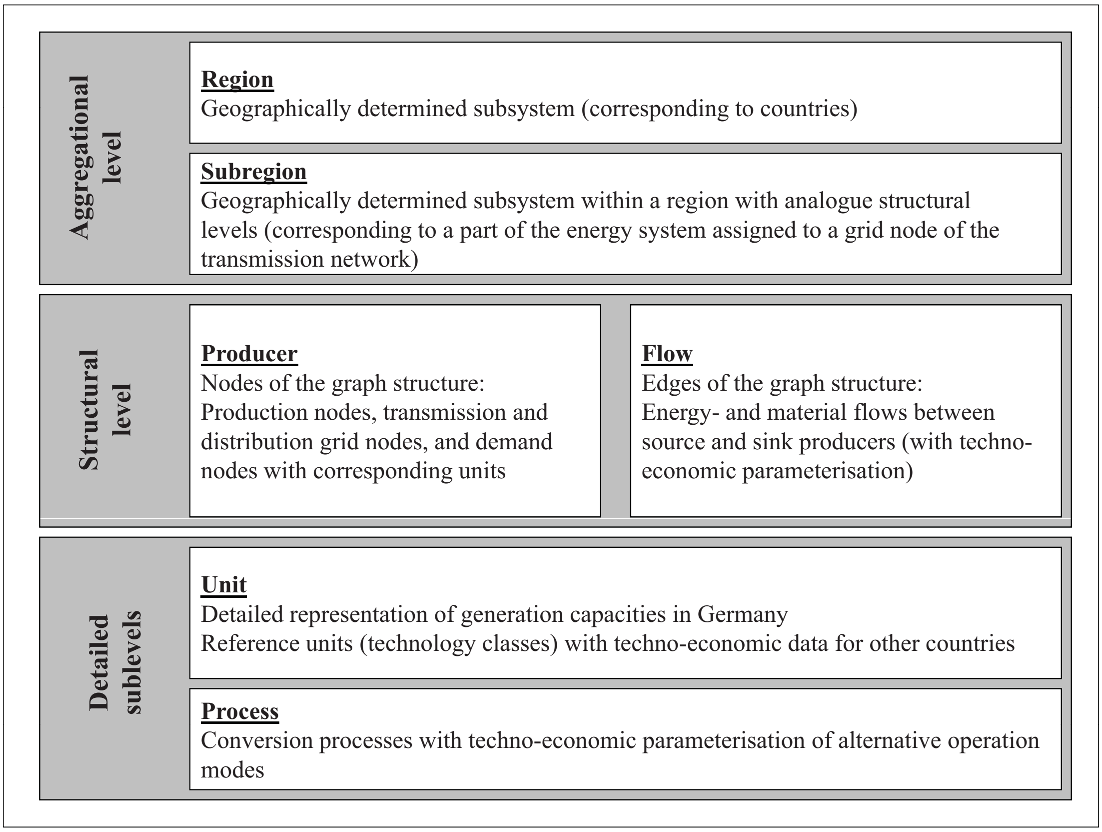

Figure 5.3.: Hierarchy of the model elements (based on Rosen [2007, p. 105])

In PERSEUS-NET, the grid nodes of the electricity grid are modeled using subsets of the set of producers. So-called external grid nodes ($ext \in EXT \subset PROD$) correspond to the grid nodes of the high voltage or transmission grid, while the internal grid nodes ($int \in INT \subset PROD$) are an aggregated representation of the lower voltage levels. The power lines of the transmission grid are modeled as flows connecting two external grid nodes ($FL_{ext,ext',elec,t,seas}$).

The basic structure of the PERSEUS-NET model for Germany, with its detailed representation of the power grid is depicted in Figure 5.4.

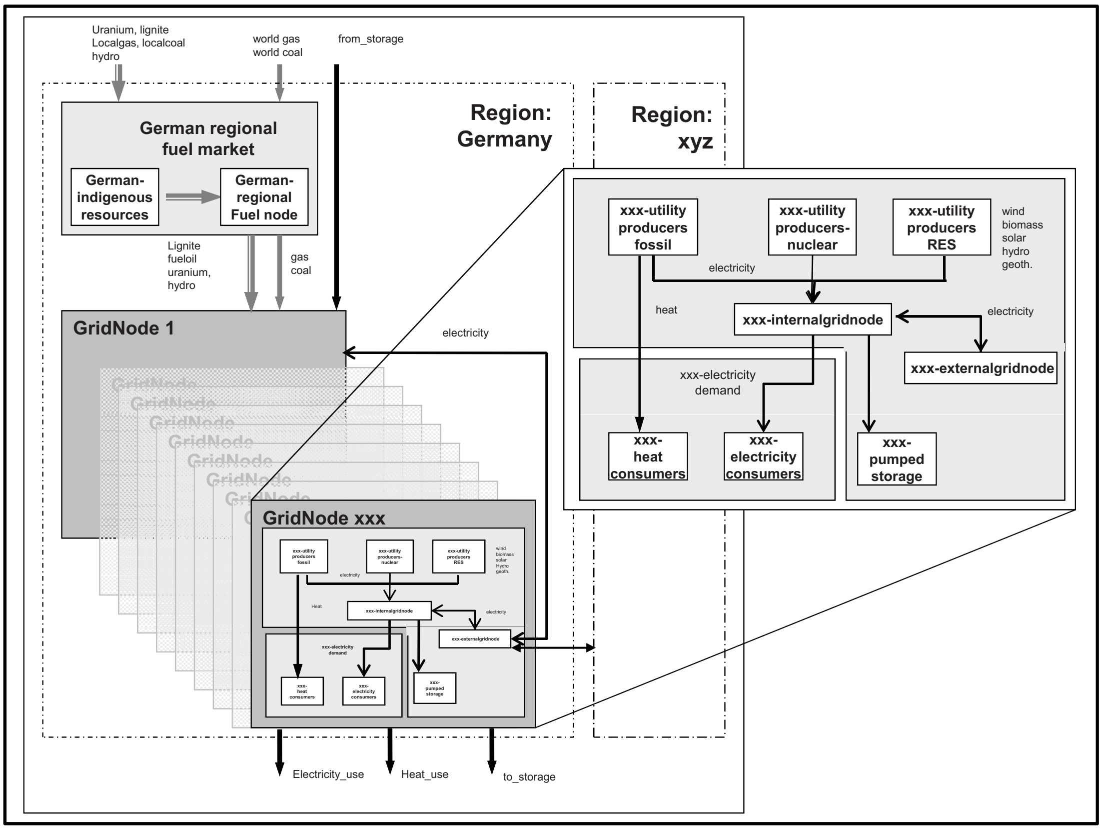

Figure 5.4.: Generalized PERSEUS-NET model structure (cf. Rosen [2007])

5.3.2. Objective function

In the optimization model PERSEUS-NET all system expenditures are minimized on the condition that the exogenously given electricity demand is satisfied. The value of the objective function is the sum of all system relevant expenditures, discounted to the base year (see Equation 5.1).

The first group of summands contains all expenditures concerning supply, transport, and transmission of energy and material. They are all related to the energy and material FL flows in the model. The first summand describes the fuel expenditures as a product of the flow level of the import flows $FL_{im,prod,ec,t}$ and the fuel specific expenditures $Cfuel_{prod,ec,t}$, which include related expenditures for EU emission allowances. The second summand contains variable expenditures associated with the transport and transmission of energy carriers between the nodes of the digraph ($FL_{prod,prod',ec,t} \cdot Cvar_{prod,prod',ec,t}$). The last summand of this group of expenditures represents the variable expenditures linked to the transport of energy carriers to its final destination ($FL_{prod,ex,ec,t} \cdot Cvar_{prod,ex,ec,t}$).

The second group of expenditures comprises only one summand. It stands for the expenditures for energy conversions, which are determined by multiplying the activity (or process) levels of the conversion processes $PL_{proc,t}$ by their specific costs $Cvar_{proc,t}$.

The final group of expenditures includes fixed expenditures related to the individual units. In particular, fixed operational expenditures ($Cap_{unit,t} \cdot Cfix_{unit,t}$) and investments in new capacities ($CapNew_{unit,t} \cdot Cinv_{unit,t}$) are considered. In addition, load change costs are taken into account. They are calculated as a product of the absolute value of load changes and the specific load change costs of the units $((LVup_{unit,seas-1,seas,t} + LVdown_{unit,seas-1,seas,t}) \cdot Cload_{unit,t})$.

The minimization of all system relevant expenditures as target function implies a certain market understanding (perfect market), which is discussed in detail in chapter 8.

$$min \sum_{t \in T} \alpha_t \cdot \left[\begin{array}{l} \left(\begin{array}{l} \sum\limits_{im \in IM} \sum\limits_{ec \in EC} \sum\limits_{pro \in PROD} FL_{im,prod,ec,t} \cdot Cfuel_{prod,ec,t} \\ + \sum\limits_{prod \in PROD} \sum\limits_{ec \in EC} \sum\limits_{prod' \in PROD'} (FL_{prod,prod',ec,t} \cdot \\ \qquad Cvar_{prod,prod',ec,t}) \\ + \sum\limits_{ex \in EX} \sum\limits_{ec \in EC} \sum\limits_{prod \in Prod_{ex,ec}} (FL_{prod,ex,ec,t} \cdot Cvar_{prod,ex,ec,t}) \end{array} \right) \\ + \sum\limits_{proc \in GENPROC} (PL_{proc,t} \cdot Cvar_{proc,t}) \\ + \sum\limits_{unit \in UNIT} \left(\begin{array}{l} (Cap_{unit,t} \cdot Cfix_{unit,t}) \\ + (CapNew_{unit,t} \cdot Cinv_{unit,t}) \\ + \sum\limits_{seas \in SEAS} \left(\begin{array}{l} (LVup_{unit,seas-1,seas,t} \\ + LVdown_{unit,seas-1,seas,t}) \\ \cdot \; Cload_{unit,t} \end{array} \right) \end{array} \right) \end{array} \right] \tag{5.1}$$

5.3.3. System of equations for power generation

In the following section, the technical and economical constraints of the optimization problem concerning power generation will be described.

5.3.3.1. Energy and material flow balances

Satisfaction of the demand The driving force of the model PERSEUS-NET is the exogenously given demand for energy carriers. Therefore, inequation 5.2 assures that the export flow of an energy carrier *ec* is in any region reg at any point in time $t,\ seas$ greater than or equal to the exogenously given, regionally differentiated demand $D_{reg,ec,t,seas}$.

$$FL_{prod,ex,ec,t,seas} \geq D_{reg,ec,t,seas}$$
$$\forall\ prod \in PROD; \forall\ ec \in EC; \forall\ t \in T; \forall\ seas \in SEAS \tag{5.2}$$

Energy and material flow balances The energy and material flows of energy systems are subject to physical constraints. Not to respect them correctly in energy models will lead to erroneous results. Therefore, in energy models like PERSEUS-NET, the energy and material flow balances are of utmost importance. They guarantee that the sum of the inflows of an energy carrier or other material *ec* into a node *prod* of the network complies with the outflows from the node. Consequently, as a general rule, storage of energy carriers is not allowed (The only exception to this rule is the special case of pumped storage power plants).

Equation (5.3) describes the yearly energy and material flow balance of PERSEUS-NET. Its left hand side includes all the inflows from the sources of the graph $FL_{im,prod,ec,t}$ as well as all the flows $FL_{prod',prod,ec,t}$ from all neighboring nodes into a producer node. The generation inside a node of the digraph is included, by multiplying the activity level $PL_{proc,t}$ of the generation process ($proc \in GENPROC$) by the share of energy carrier in the total input or output of the process $\lambda_{proc,ec}$.

The right hand side of the equation includes transmissions of energy carriers and other materials from the considered producer to other producers $prod' \in PROD'_{prod,ec}$ as well as to the sinks of the digraph $ex \in EX$. Furthermore, the consumptions of the producer nodes, which typically result from conversions of energy carriers to other energy forms, are taken into account. In the model they are determined as the quotient of the activity level $PL_{proc,t}$ of a demand process ($proc \in DEMPROC$) and its efficiency $\eta_{proc,ec}$. The model parameter $\lambda_{proc,ec}$ stands for the share related to the total input or output of the process and $f_{proc,t,seas}$ for the load profile of the demand process.

$$
\begin{aligned}
&\sum_{im \in IM} FL_{im,prod,ec,t} + \sum_{prod' \in PROD_{prod,ec}} FL_{prod',prod,ec,t} \\
&+ \sum_{proc \in GENPROC_{prod,ec}} PL_{proc,t} \cdot \lambda_{proc,ec} \\
&= \sum_{ex \in EX} FL_{prod,ex,ec,t} + \sum_{prod' \in PROD_{prod,ec}} FL_{prod,prod'ec,t} \\
&+ \sum_{proc \in DEMPROC_{proc,ec}} PL_{proc,t} \cdot \frac{\lambda_{proc,ec}}{\eta_{proc,ec}} \cdot f_{proc,t,seas} \\
&\forall\ t \in T;\ \forall\ prod \in PROD;\ \forall\ ec \in EC; \forall\ seas \in SEAS
\end{aligned}
\tag{5.3}
$$

In addition to the annual balances, seasonal energy and material flows $FL_{prod,ec,ex,t,seas}$ satisfying the seasonal demands for electricity and heat are considered. The corresponding equation is assembled analogously to the annual balance. Equations 5.4 and 5.5. ensure that the sums of the seasonal values of the energy flows and of the process utilization correspond to the annual values.

$$
\begin{aligned}
&\sum_{seas \in SEAS} FL_{prod,prod',ec,t,seas} = FL_{prod,prod',ec,t} \\
&\forall\ t \in T; \forall\ prod \in PROD; \forall\ prod' \in PROD'; \forall\ ec \in EC
\end{aligned}
\tag{5.4}
$$

$$
\begin{aligned}
&\sum_{seas \in SEAS} PL_{proc,t,seas} = PL_{proc,t} \\
&\forall\ t \in T; \forall\ proc \in PROC
\end{aligned}
\tag{5.5}
$$

5.3.3.2. Energy and material flow constraints

In the model PERSEUS-NET, all energy and material flows can be limited to upper and lower bounds. In addition, constant flow levels can be defined. They are modeled as restrictions of the flow levels ($FLMIN_{prod,prod'ec,t}$ $FLMAX_{prod,prod',ec,t}$) or binding energy flow levels ($FLLEV_{prod,prod',ec,t}$).

5.3.3.3. Generating capacity restrictions

The evolution of the conversion capacities in the power plan portfolio is part of the optimization. Therefore, the capacity stock and expansion options are distinguished. The residual capacity $CapRes_{unit,t}$ sets the level of the remaining capacity, which is available in a specific period t without additional investment. It complies with the capacity which was installed before the base year minus the capacity that is decommissioned. Thus, the sum of the residual capacity of a unit in a period t and the sum of all capacities expansions $CapNew_{unit,t}$ realized since the base year equals the value of capacity, which is installed in t (see Equation 5.6).

$$
\begin{aligned}
&Cap_{unit,t} = CapRes_{unit,t} + \sum_{t'=(t-LT_{unit})} CapNew_{unit,t'} \\
&\forall\ unit \in UNIT; \forall\ t \in T
\end{aligned}
\tag{5.6}
$$

Upper ($CapMax_{unit,t}$) and lower ($CapMin_{unit,t}$) limits for each period can be specified for each unit capacity. In case the residual capacity is equal to the maximum capacity, capacity expansion is precluded. However, in case $CapRes_{unit,t} \leq CapMax_{unit,t}$ capacity up to the amount of ($Cap_{unit,t} = CapMax_{unit,t} - CapRes_{unit,t}$) can be constructed. Moreover, the maximum amount of capacity that can be added to a unit in period t is limited to $MaxAdd_{unit,t}$.

5.3.3.4. Restrictions of process utilization

Besides power flow levels and capacity evolution, the activity levels of the processes of each unit are part of the optimization and can therefore be restricted.

Capacities and availabilities First of all, the activity levels of a process $PL_{proc,t}$ are restricted by the installed unit capacity $Cap_{unit,t}$ and its availability $Avai_{unit,t}$. In Equation (5.8) this is realized for processes with seasonal specifications. Processes without seasonal specification are restricted in the same way (see Equation 5.7).

The parameter h_t (h_{seas}) stands for the number of hours of the year t (season $seas$), the power production equivalent $\omega_{proc,t}$ represents the share of the electricity output.

$$Cap_{unit,t} \cdot Avai_{unit,t} \cdot h_{year} \geq \sum_{proc \in PROC_{unit}} (PL_{proc,t} \cdot \omega_{proc,t})$$
$$\forall\ t \in T; \forall\ unit \in UNIT \tag{5.7}$$

$$Cap_{unit,t} \cdot Avai_{unit,t} \cdot h_{seas} \geq \sum_{proc \in PROC_{unit}} (PL_{proc,t,seas} \cdot \omega_{proc,t})$$
$$\forall\ t \in T; \forall\ unit \in UNIT\ \forall\ seas \in SEAS \tag{5.8}$$

Full load hours In addition, minimum ($VlhMin_{proc,t}$) and maximum ($VlhMax_{proc,t}$) full load hours, which limit the production of a process, can be set (see Equations 5.9 and 5.10).

$$\frac{VlhMax_{proc,t}}{h_{year}} \cdot Cap_{unit_{proc},t} \geq PL_{proc,t} \cdot \omega_{proc,t}$$
$$\forall\ proc \in PROC; \forall\ t \in T \tag{5.9}$$

$$\frac{VlhMin_{proc,t}}{h_{year}} \cdot Cap_{unit_{proc},t} \leq PL_{proc,t} \cdot \omega_{proc,t}$$
$$\forall\ proc \in PROC; \forall\ t \in T \tag{5.10}$$

Load variation Since the capabilities for load variation differ largely between the technologies for power and heat generation, they are commonly categorized into base (e.g. lignite power plants), intermediate (e.g. coal power plants), and peak load technologies (e.g. gas turbines). In PERSEUS-NET this is realized by using load change costs for the different conversion technologies[5], which are multiplied by the accumulated load changes of a specific unit ($LVup_{unit,seas-1,seas,t} - LVdown_{unit,seas-1,seas,t}$) and are thus taken into account in the objective function (see section 5.3.2). Therefore, in Equation 5.11 the load changes between two time slots are recorded and weighted by the number of transitions between those two time slots $No_{seas-1,seas}$ to derive the accumulated load change. Positive variables are used instead of free variables to account for the absolute value of the load change for each unit.

[5] Another way to consider load change rate limitations is introduced in [Fichtner 1999 p. 75].

$$LVup_{unit,seas-1,seas,t} - LVdown_{unit,seas-1,seas,t} =$$

$$No_{seas-1,seas} \cdot \left(\sum_{proc \in PROC_{unit}} \left(\left(\frac{PL_{proc,seas,t}}{h_{seas}} - \frac{PL_{proc,seas-1,t}}{h_{seas-1}} \right) \cdot \frac{1}{\eta_{proc,t}} \right) \right) \tag{5.11}$$

$$\forall\ t \in T;\ \forall\ seas \in SEAS;\ \forall\ unit \in UNIT$$

Pumped storage power plants In energy systems, pumped storage power plants play a double role. On the one hand, in turbine operation mode, they act as power suppliers. On the other hand, in pump operation mode, they consume electric energy to transport water from a lower to a higher level. These roles of power generators as suppliers and consumers (sources and sinks) of electrical energy are directly linked to their storage function. In general, pumped storage power generators are operated in pump mode when abundant base load capacities are available. By contrast, the flexible and quickly controllable plants are generally operated in turbine mode to either provide peak load or ancillary services such as balancing power. Thus, pumped storage power plants are used to convert low-priced base load power into higher-priced peak load or balancing power.

In PERSEUS-NET pumped storage power plants are modeled according to their roles as two different producers, which are mapped via the so-called pump map ($PMAP$). Equation 5.12 assures that during one year, the amount of water drained from the storage capacity equals the amount of water pumped to the storage facility.

$$\sum_{ex \in EX} FL_{prod',ex,to-storage,t} = \sum_{im \in IM} FL_{im,prod,from-storage,t}$$
$$\forall\ t \in T; \forall\ (prod; prod') \in PMAP_{PROD,PROD'} \tag{5.12}$$

Heat extraction Like power generation, heat production of a generation unit is limited due to technological restrictions. Hence, the maximum heat extraction of a specific unit or technology class is defined in the model. Based on historical data, the average heat extraction of the technology is expressed in terms of maximum full load hours of process operation. Different heat types can be distinguished, such as high temperature process heat and low temperature heat for space heating (see Equation 5.13).

$$
\begin{aligned}
&\sum_{proc \in HEATPROC_{unit,heattype}} \left(\frac{VlhMax_{proc,t}}{h_{year}} \cdot Cap_{unit,t} \cdot \frac{\lambda_{proc,heattype}}{\omega_{proc,t}} \right) \\
&\leq \sum_{proc \in HEATPROC_{unit,heattype}} (PL_{proc,t} \cdot \lambda_{proc,heattype}) \qquad (5.13) \\
&\forall\ unit \in UNIT; t \in T
\end{aligned}
$$

Furthermore it has to be assured, that the heat demand of a sub-region is met.[6] Thus the accumulated heat production of a certain subtype within a sub-region has to correspond to the heat profile of that heat subtype in the sub-region $HGF_{unit,t,seas,heattype}$ (see Equation 5.14).

$$
\begin{aligned}
&\sum_{proc \in HEATPROC_{unit,heattype}} (PL_{proc,t,seas} \cdot \lambda_{proc,heattype}) = \\
&\sum_{proc \in GENPROC_{unit,heattype}} (PL_{proc,t} \cdot \lambda_{proc,heattype}) \cdot HGF_{unit,t,seas,heattype} \\
&\forall\ unit \in UNIT; \forall\ t \in T; \forall\ seas \in SEAS; \forall\ heattype \in HEAT \qquad (5.14) \\
&with: \\
&HGF_{uni,t,seas,heattype} = \frac{\sum_{proc \in DEMPROC_{reg_{unit},heattype}} (PL_{proc,t,seas} \cdot \lambda_{proc,heattype})}{\sum_{proc \in DEMPROC_{reg_{unit},heattype}} (PL_{proc,t} \cdot \lambda_{proc,heattype})}
\end{aligned}
$$

5.3.3.5. Reserve capacity requirements

The installed capacity in a power supply system must always be sufficient to cover the maximum peak load. Besides, imbalances between supply and demand which might occur due to e.g. power plant failures, fluctuating resources or forecasting errors have to be balanced. To avoid imbalances or even grid failures, sufficient positive and negative reserve capacity[7], the so-called balancing reserve, has to be provided at any time. In the ENTSO-E grid, balancing power is provided using a three-stage procedure and therefore separated into primary, secondary, and minute reserve. The three stages differ

6 No heat exchanges between subregions are allowed.

7 Capacities which provide electrical energy in case of load shortages are called positive reserve, whereas capacities providing negative power in case of load excess, such as consumer loads or power plants reducing their production, are referred to as negative reserve.

concerning ramping time and duration of operation. The primary reserve automatically provides stabilizing balancing power in a matter of seconds, whereas the secondary reserve balances the power exchanges between the different control areas. The minute reserve replaces primary and secondary reserve after 15 minutes at the latest and is used to balance load failures. In general, primary and secondary reserve are provided by already operating conventional steam power stations and minute reserve by gas-turbine, gas-steam or pumped storage power plants that are started up. In the synchronous UCTE grid 3000 MW of primary reserve currently have to be held back. Concerning the secondary reserve, the ENTSO-E recommends a minimum reserve capacity of $R = \sqrt{10MW \cdot L_{max} + (150MW)^2} - 150MW$ which should be kept by each transmission system operator.[8] The amount of minute reserve which has to be held back, should at least amount to the size of the largest generating unit in the control area. However, the increasing number of wind energy plants in the future is expected to result in a higher demand for minute reserve (cf. ENTSO-E [2009]).

In energy system models availability limitations can be used to ensure that enough capacity is held back to balance fluctuations or power plant failures. Often, an availability factor less than one is set, meaning that more capacity for peak load covering is needed. This reserve factor represents all capacities not available, e.g. due to revisions, outages or reserve holding.[9] However, this also implies that the production capacities can never run at maximum load and thus wrong marginal expenditures may result. Alternatively, a factor can be included stating by which percentage the installed capacity[10] has to exceed the maximum peak load.

In PERSEUS-NET both factors are included in inequation 5.15. It states that the used production capacity on the left side of the equation, increased by the reserve factor *Reserve*, has to be equal or less than the sum of the capacities of all units times the availability factor $Avai_{unit,t}$.

$$
\begin{aligned}
&\tfrac{(1+Reserve)}{h_{seas}} \cdot \left(\sum_{proc \in DEMPROC_reg,electr} PL_{proc,seas,t} \right) \\
&\leq \sum_{unit \in GENUNIT} (Cap_{unit,} \cdot Avai_{unit,t}) \\
&\forall\ seas \in SEAS; \forall\ t \in T; \forall\ reg \in REG
\end{aligned}
\tag{5.15}
$$

Furthermore, the balancing reserves can be considered in PERSEUS using restriction 5.16. It ensures that in each region, the power capacity available for each reserve type

8 L_{max} corresponds to the maximum anticipated consumer load of the control area.

9 An approximation of the availabilities of different conversion capacity types is published in Vandezande et al. [2008].

10 If desired production capacities using fluctuating resources can be excluded.

$Rcap_{(pr/sr)tr,unit,seas,t}$ is equal to or exceeds the reserve requirements $Rdem_{(pr/sr)tr,unit,seas,t}$ of the ENTSO-E.

However, due to computing time restrictions as well as due to the limited temporal resolution of the model primary and secondary reserve are set aside and thus only minute reserve is considered in PERSEUS-NET.

$$\sum_{unit \in UNIT_{reg}} Rcap_{(pr/sr)tr,unit,seas,t} \geq Rdem_{(pr/sr),tr,re,seas,t}$$
$$\forall\ seas \in SEAS; \forall\ t \in T; \forall\ reg \in REG \tag{5.16}$$

The capacity restriction 5.17 ensures, that for each unit, the installed capacity exceeds the total of production capacity and reserve capacity.

$$\frac{\sum_{proc \in PROC_{unit}} (PL_{proc,seas,t} \cdot \omega_{proc,t,})}{h_{seas}} + Rcap_{tot,unit,seas,t}$$
$$\leq Cap_{unit,t} \cdot Avai_{unit,t} \tag{5.17}$$
$$\forall\ seas \in SEAS; \forall\ t \in T; \forall\ unit \in UNIT$$

5.3.4. System of equations for power transmission

In addition to the constraints regarding power generation, equations modeling the DC power flow are integrated into the PERSEUS-NET source code. As described in section 4.3.2 the active power flow can be calculated as the product of line susceptances and phase angle difference. Written in matrix form this is

$$[P] = [B][\theta]. \tag{5.18}$$

Given a reactance X and a resistance R, the elements of the matrix [B] are equivalent to

$$B_l = \frac{-X_l}{R_l^2 + X_l^2}. \tag{5.19}$$

Since only active power flows are considered, matrix [B] is the admittance matrix of the power system network.[11] It is composed by the self (on-diagonal) and mutual (off-diagonal) admittances of the network buses. The on-diagonal elements equal the sum of the admittances in the column associated with the diagonal element. The off-diagonal elements correspond to the admittances of the power lines between the bus bars.[12]

5.3.4.1. Line flows

The line flow constraints integrated into PERSEUS-NET have to guarantee that the power flows in the model meet Equation (5.18). First, this has to be assured for power flows over a transmission line. Hence, the active power flow $FL_{ext,ext',elec,t,seas}$ over a transmission line *(ext,ext')* has to equal the product of the susceptance of the line $h_{ext,ext',ext'',t}$ and the phase angle differences $\theta_{ext'',t,seas}$ at grid node *ext"* at any time (see Equation (5.20)).

$$\begin{aligned} &FL_{ext,ext',elec,t,seas} = \sum_{ext'' \in EXT} h_{ext,ext',ext'',t} \cdot \theta_{ext'',t,seas} \\ &\forall\ ext, ext' \in EXT \subset PROD;\ \forall\ t \in T;\ \forall\ seas \in SEAS \end{aligned} \tag{5.20}$$

The matrix H with its elements $h_{ext,ext',ext'',t}$ is called the transfer admittance matrix. By contrast to the admittance matrix, the columns of the transfer admittance matrix correspond to the grid nodes of the system network, whereas the rows of the matrix refer to the lines of the system network. Since a flow as well as a line is described by its start and end nodes in PERSEUS-NET, the first two indices refer to the line and the third index refers to the grid node. Correspondingly, the element $h_{ext,ext',ext'',t}$ is the negative of the element $h_{ext',ext,ext'',t}$. In the model, the transfer admittance matrix is determined by multiplying the transpose of the vector of susceptances by the transpose of the incidence matrix[13] of the system network.

[11] It is also referred to as the self admittance or driving point admittance matrix.

[12] The employed approach is based on Schweppe et al. [1988] and Stigler and Todem [2004]. For a detailed derivation of the power flow equations see Schweppe et al. [1988] p. 313ff.

[13] The incidence matrix indicates the connections of a graph. The rows represent the vertices and the columns the edges of the graph. The elements $i_{v,e}$ of the matrix are 1 if the edge e is incident and directed away from vertex v, -1 if the edge e is incident and directed towards vertex v, and 0 if the edge e is not incident of the vertex.

The second power flow constraint describes the line flows as a function of network characteristics and bus injections. The sum of the net injections into a bus $NetIn_{ext,elec,t,seas}$ is equal to the the sum of the power flows towards and away from the node (see Equation 5.21). The power flows are the product of the elements of the admittance matrix $b_{ext,ext',t}$ and phase angle difference $\theta_{ext',t,seas}$. In the model, the admittance matrix is determined by multiplying the incidence matrix by the transpose of the transfer admittance matrix.

$$\sum_{ec \in EC} NetIn_{ext,elec,t,seas} = \sum_{ext' \in EXT} b_{ext,ext',t} \cdot \theta_{ext',t,seas} \qquad (5.21)$$
$$\forall\ ext \in EXT;\ \forall\ t \in T;\ \forall\ seas \in SEAS$$

5.3.4.2. Thermal limits of power lines

A special case of energy flow constraints are the thermal limits ($ThLimit_{ext,ext',t}$) of the transmission lines, which are specified in PERSEUS-NET as flow limitations over a specific line (see Equations 5.22 and 5.23). As reactive flows are not taken into account, the thermal limits are adapted average values for typical types of transmission lines.

$$FL_{ext,ext',elec,t,seas} \geq (-1) \cdot ThLimit_{ext,ext',t} \qquad (5.22)$$
$$\forall\ ext, ext' \in EXT \subset PROD;\ \forall\ t \in T;\ \forall\ seas \in SEAS$$

$$FL_{ext,ext',elec,t,seas} \leq THLim_{ext,ext',t} \qquad (5.23)$$
$$\forall\ ext, ext' \in EXT \subset PROD;\ \forall\ t \in T;\ \forall\ seas \in SEAS$$

5.3.4.3. Slack bus definition

Moreover, a slack bus has to be defined, in reference to which all voltages are measured. *"Balanced three-phase networks can be described by equivalent positive sequence elements with respect to neutral or ground point. An infinite conducting plane of zero impedances represents this ground plane, and all voltages and currents are measured with reference to this plane."* (Das [2002, p. 72]) The reference plane other than the ground plane with reference to which all the variables are measured is called slack or swing bus (cf.

Das [2002, p. 73]). In DC power flow modeling, this is realized by setting the phase angle difference of the slack node to zero.[14]

$$\theta_{ext,t,seas} \cdot Slack_{ext} = 0$$
$$\forall\ ext \in EXT,\ \forall\ t \in T;\ \forall\ seas \in SEAS \tag{5.24}$$
$$with\ Slack_{ext} = \begin{cases} 1, & if\ reference\ bus \\ 0, & otherwise \end{cases}$$

5.4. Summary

In this chapter, the model PERSEUS-NET has been described. Using PERSEUS-NET, the long-term development of the German power supply system can be analyzed. The main results of the energy system optimization with PERSEUS-NET are the optimal future power plant mix and the optimal topology of the power system. In the model, the main decision criteria for a geographically optimal power plant expansion are the spatially differentiated marginal costs of electricity supply, which are determined by calculating the optimal power flow. Aspects of an increasing decentralization of the power system are integrated in PERSEUS-NET using georeferenced data stored in a newly-created GIS database.

In the optimization, all system expenditures discounted to a base year are minimized on the condition that a predefined demand is satisfied. The system of equations for generation comprise energy and material flow balances and constraints, generating capacity restrictions, restrictions of the process utilization, and reserve requirements. To adequate consider the influence of grid constraints, a system of equations for power transmission has been added. They model the DC power flow in the system and restrict the capacity of power lines.

14 In power system analysis the slack bus acts additionally to supply losses and acts as a sink for excess demand (cf. e.g. Das [2002], p. 16).

6. Structure and data basis of the energy system model

In the following sections, the structural composition of the input data, which is used to analyze the development of the German power supply system, is specified. First, the time horizon and the temporal resolution is addressed. Then, in section 6.2, the geographical structure of the power system model and its implementation is presented. Section 6.3 addresses the technical specifications of the power grid model, followed by section 6.4 that presents the assumptions made regarding the level and regional distribution of the power demand. After that, the specifications of conventional power generation (section 6.5) and power generation based on RES (section 6.6) are addressed. The levels and temporal resolutions of the inter-regional power transfers are presented in section 6.7. In the last section assumptions regarding CO_2 emissions, EUA prices, and the discount rate are outlined.

6.1. Time horizon and temporal resolution

PERSEUS-NET is an inter-temporal multi-period optimization model, in which all time periods are analyzed simultaneously. A time horizon from 2007 to 2030 is chosen to analyze the long-term development of the German electricity supply system. For being able to calibrate the model with statistical data, the base year was settled to 2007, which is the only year for which a complete set of data is available. Due to computational restrictions, characteristic years are selected to model periods within the time horizon. The point in time and the number of characteristic years is optional. In this work, a time horizon of 5 years per characteristic year was chosen, beginning in 2010. Furthermore, characteristic days are used to model the annual load curves of the characteristic years. For this purpose, the year is divided into four seasons: spring, summer, autumn, and winter. For each season, typical working days and typical weekend days are considered. Due to the characteristic developments of the load curves, winter, autumn, and spring days are divided into up to 7 characteristic time slots, whereas summer days are divided into up to 6 characteristic time slots.[1] Thus 42 different time slots per year are modeled, providing a reasonably accurate representation of the load profiles. The temporal resolution is illustrated in Figure 6.1.

[1] The number of time slots per period have been derived from model calculations based on Eßer et al. [2006b,a].

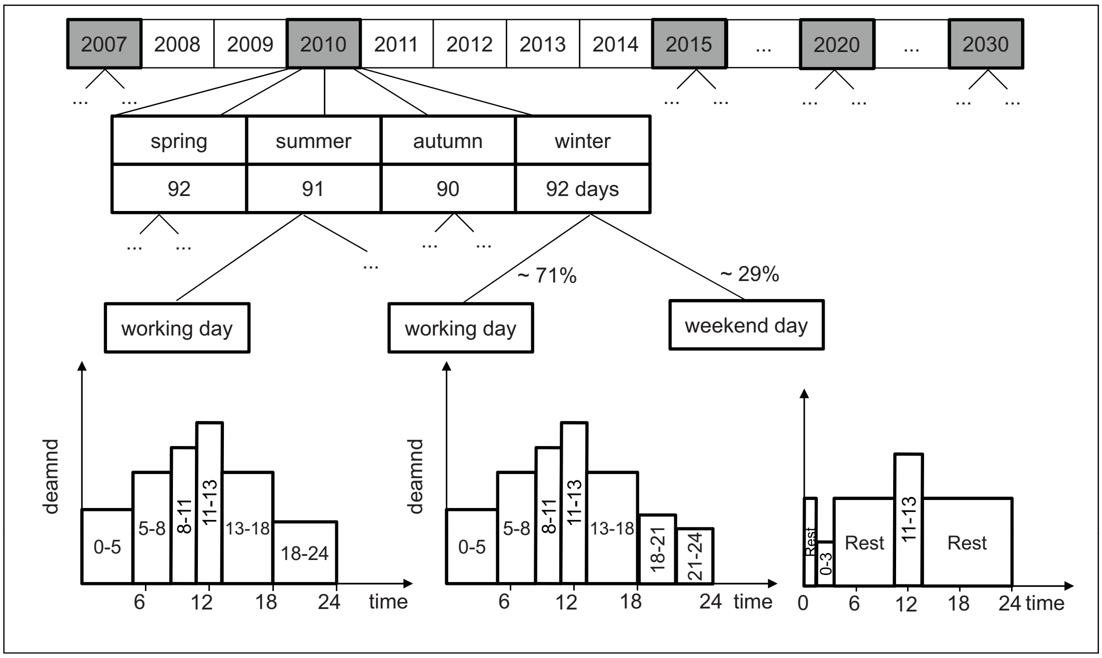

Figure 6.1.: Temporal resolution and time horizon (based on Möst [2006])

6.2. Geographic structure of the power system model

The objective of this work is to analyse the long-term development of Germany's power system, taking into account its regional characteristics including grid constraints. Therefore, special interest has to be paid to the mapping of the power grid. The German power transmission and distribution grid conduces to transfer electric energy from the power plants to the ultimate consumer. It is part of the integrated network of the European Network of Transmission System Operators for Electricity (ENTSO-E) that links up the national grids in Europe (see section 3.3.4).

As part of the ENTSO-E network, it is connected to the national Dutch, Belgian, Danish, French, Swiss, Austrian, Czech, and Polish transmission grids via AC-interconnection. In addition, DC-interconnection to the Swedish and East-Danish transmission grids exist.

In the following, first the representation of the German power grid in the PERSEUS-NET model is described. Then, the geographic mapping of power stations to the grid nodes of the PERSEUS-NET grid model is presented.

6.2.1. Modeling of the German power grid

Within this work, an aggregated network model of the German transmission grid comprising the extra high voltage levels 220 kV and 380 kV has been developed. Therefore, a geometric network, consisting of edge features to model the power lines and junction

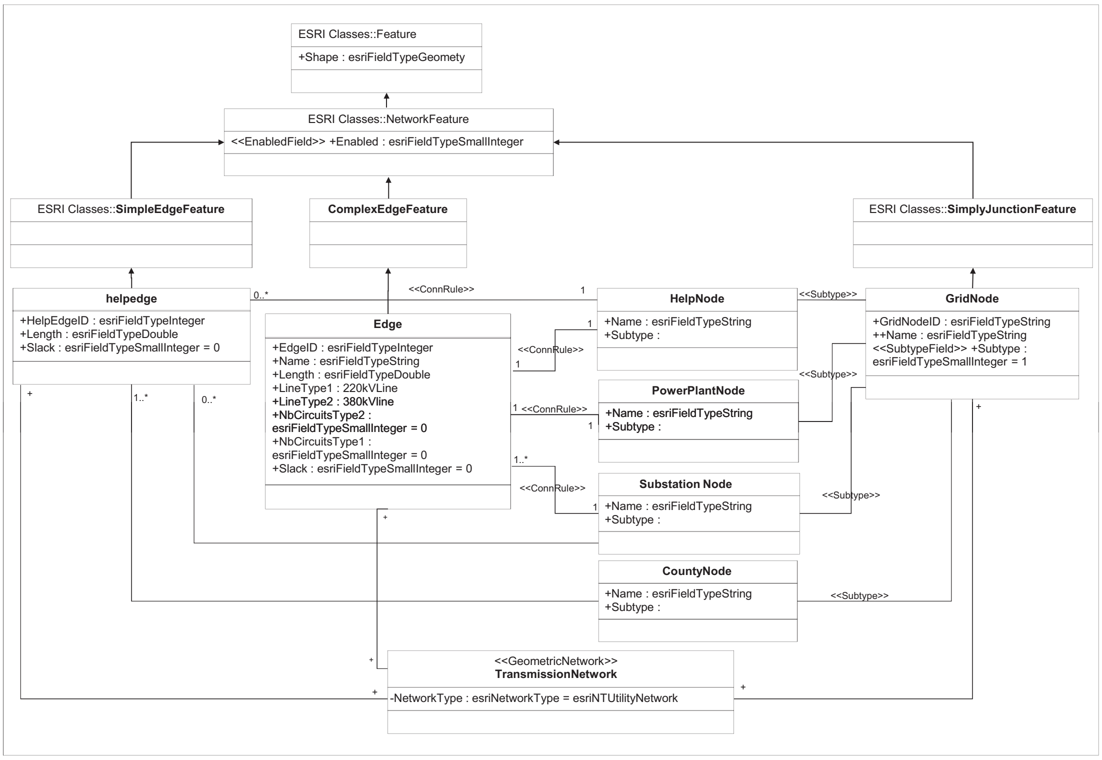

Figure 6.2.: UML diagram of the geometric network

features to model the grid nodes of the power system has been designed in UML and then imported in the commercial GIS software ArcGis™released ESRI©. The relevant data had to be taken from publicly available sources. Therefore, the model of the German transmission grid used in this work is an approximated model based on a printed map of the UCTE grid (UCTE [2008]). Figure 6.2 shows the UML diagram used to design the geometric network. The transmission lines are modeled as the edges of a geometric network, whereas multiple circuits in one corridor are merged in the model and considered as one single edge, with the attributes *"Number of 380 kV circuits in year XXX"* and *"Number of 220 kV circuits in year XXX"*. In total, 563 network edges, consisting of 739 380-kV and 520 220-kV circuits are stored in the geodatabase.

Three different types of grid nodes corresponding to the network buses of the German transmission grid are distinguished:

- Grid nodes to which large power plants are connected (PowerPlantNode),
- SubstationNodes, which represent the aggregation of lower voltage distribution systems, and
- auxiliary junctions that connect two transmission lines (HelpNodes).

While the transmission grid is modeled in a detailed way, the lower voltage levels are aggregated into a single network junction at the substation node. Furthermore, grid nodes representing the centers of the areas of the NUTS3-regions in Germany (CountyNodes) are considered in the geodatabase. Edge features called "helpedge" are used to connect these SubstationNodes to the closest SubstationNodes. The resulting geometric network of the German transmission system is shown in Figure 6.3. While power plant, substation, and auxiliary nodes compose the subregions in the optimization model, county nodes are needed to georeference the input data. In total 882 grid nodes are stored in the PERSEUS-NET geodatabase, of which 442 are subregions in the optimization model. They consist of 100 PowerPlantNodes, 265 SubstationNodes, 77 HelpNodes, and 440 CountyNodes.

As Germany holds a central part within the European interconnected power grid, power exchanges with bordering power systems play a significant role for the power flows within the German transmission system. Therefore, Germany's power imports and exports are considered in PERSEUS-NET. The bordering power systems are represented each by one single grid node, in which electricity is generated or consumed corresponding to the net exchanges between Germany and the respective bordering system. To connect the foreign grid nodes to the German transmission grid, the regional interconnectors of the ENTSO-E transmission grid and their ending grid node in the neighboring country are modeled. The end grid nodes of the interconnectors in the bordering countries are then connected to the single grid node of the country.

Regarding future grid expansions, the 24 projects named in the EnLAG [2009] are taken into account (see Table 6.1). They comprise the construction of new transmission lines as well as the commissioning of additional wires or the upgrade of 110 kV and 220 kV to 380 kV lines. The dates of commissioning assumed in the model calculations are based on Amprion [2010], transpower [2010], Niedersächsische Staatskanzlei [2010], and DEWI et al. [2005].

In the following, the way of allocating large power stations and regional power demands to the grid nodes is described.

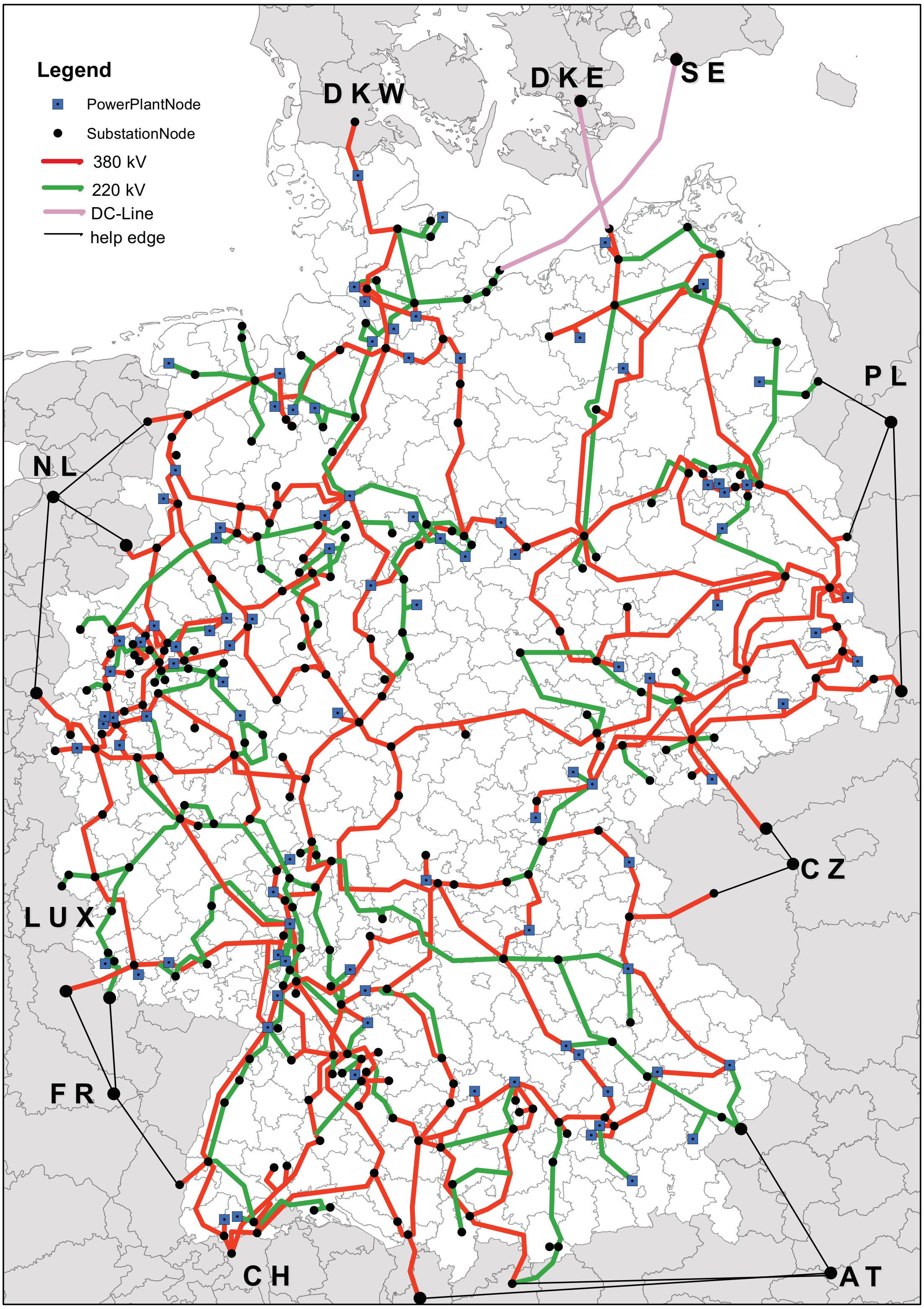

Figure 6.3.: Geographic scope of the model PERSEUS-NET

Table 6.1.: Transmission grid expansion projects according to EnLAG [2009]

No.	Type of project	Voltage level	Route	Year
1	New construction	380 kV	Kasso (DK) - Hamburg North - Dollern	2013
2	New construction	380 kV	Ganderkesee - Wehrendorf	2013
3	New construction	380 kV	Neuenhagen - Bertikow / Vierraden - Krajnik (PL)	2015
4	New construction	380 kV	Lauchstädt - Redwitz	2012
5	New construction	380 kV	Diele - Niederrhein	2015
6	New construction	380 kV	Wahle - Mecklar	2015
7	Additional wire	380 kV	Bergkamen - Gersteinwerk	2015
8	Additional wire	380 kV	Kriftel - Eschborn	2015
9	New construction	380 kV	Hamburg / Krümmel - Schwerin	2010
10	Upgrade	220 kV→380 kV	Redwitz - Grafenrheinfeld	2012
11	New construction	380 kV	Neuhagen - Wustermark	2015
12	New construction	380 kV	Eisenhüttenstadt - Baczyma (PL)	2010
13	New construction	380 kV	Niederrhein / Wesel - NL	2013
14	New construction	380 kV	Niederrhein - Utfort - Osterath	2017
15	New construction	380 kV	Osterrath - Weißenturm	2017
16	New construction	380 kV	Wehrendorf - Gütersloh	2017
17	New construction	380 kV	Gütersloh - Bechterdissen	2017
18	New construction	380 kV	Lüstringen - Westerkappeln	2017
19	New construction	380 kV	Kruckel - Dauersberg	2020
20	New construction	380 kV	Dauersberg - Hünfelden	2020
21	New construction	380 kV	Marxheim - Kelsterbach	2020
22	Upgrade	220 kV→380 kV	Weier - Villingen	2020
23	Upgrade	220 kV→380 kV	Neckarwestheim - Mühlhausen	2020
24a	New construction	380 kV	Bünzwangen - Lindach	2020
24b	Upgrade	110 kV→380 kV	Lindach - Goldshöfe	2020

6.2.2. Geographic mapping of power stations and power demand to the grid nodes of the transmission system

Large power stations, with unit block sizes larger than 100 MW, are assigned directly to the corresponding power plant nodes of the transmission grid model, based on publicly available thematic maps.

By contrast, for all other regional input data, such as distributed generating capacities or regional power demands, no information regarding the correct assignment to a network bus of the German transmission system is available. Therefore, they are assigned to the county nodes (NUTS3-regions), which are then related to the two closest substation nodes inversely proportional to the distance between the county node (NUTS3-region) and the substation node.

A detailed description of the way of georeferencing power demands and generating capacities is given in section 6.4 and section 6.6, respectively.

6.3. Technical specification of the power grid model

Regarding the technical specifications of overhead power lines, the maximum and minimum thermal limit power or current as well as the resistance and reactance are of importance. Today the individual conductors of an overhead power line are made of aluminum-clad steel (Al/St) composite cords. The thermal limits correspond to the maximum power line current at continuous operation. Increasing temperatures are related to increasing line losses as well as to a decreasing power line strength, which results in an increasing sag of the cables. To guarantee an adequate power line strength, overhead power lines are usually built for a maximum conductor temperature of up to 80 °C. The thermal limits for a 220 kV or 380 kV circuit assumed in this work amount to 490 MVA and 1700 MVA, respectively (Spring [2003, p. 153]). The (n-1)-criterion is considered in a simplified manner, by taking a reliability margin of 10% into account.

Since short overhead power lines of up to 100 km have a very low capacitance, they are sufficiently specified by a series impedance $\underline{Z} = R'l + jX'l$ (cf. Andersson [2009, p. 100]; Spring [2003, p. 151f.]). Therein *R'* stands for the line resistance per unit length, *X'* for the line inductive reactance per unit length, and l for the line length. The active resistance as well as the inductive reactance are proportional to the length of the overhead line. Further, the resistance is inversely proportional to the cross section of the power line. Regarding the parallel connection of circuits, the resistance of one circuit of a double circuit equals the resistance of a single circuit.

The inductive reactance of a power line is expressed by the angular frequency and its inductance that characterizes the changes in the electromagnetic field caused by changes in the current. If power lines are close together, the electromagnetic fields of the lines influence each other. The degree of influence depends on the distance between the lines. To avoid or at least reduce this effect the lines are generally transposed. Nevertheless, the inductive reactance of one circuit of a double line is fractionally greater than the reactance of a single circuit. Yet, to simplify matters and because no reliable data regarding the actual degree of influence is available, we assume that the resistance and reactance per unit length of one circuit of a double-circuit line equal the resistances and reactances per unit length of single-circuit power line.[2]

In Table 6.2 the electrical line parameters used in this work are shown. They correspond to typical overhead power lines used in Germany today. An aluminum-clad steel (Al/St) twin bundle has been chosen to represent the 220 kV and an aluminum-clad

[2] A complete decoupling of the two systems of a power double circuit can be achieved using β-transposition. Yet, since this is very costly, it is not used in Germany any more (cf. Oswald [p. 8f. 2005]).

Table 6.2.: Electrical parameters of 220 kV and 380 kV aluminum-clad steel power lines (cf. Spring [2003, p. 212])

Voltage level	220 kV	380 kV
Conductors Al/St (240/40)	2 x 240/40	4 x 240/40
Resistance per unit length $R_1^{'}$ [Ω/km]	0,062	0,031
Inductive reactance per unit length $X_1^{'}$ [Ω/km]	0,32	0,26

steel quadruple bundle has been chosen for 380 kV lines.[3] The resistances per unit length amount to 0,062 Ω/km for the 220 kV voltage level and to 0,31 Ω/km for the 380 kV voltage level. The reactances per unit length amount to 0,32 Ω/km and 0,26 Ω/km, respectively.[4] In the model, per unit values are used (cf. Spring [2003, p. 212]).

6.4. Electricity demand

In the PERSEUS model, the trend of electricity demand over the time horizon as well as the load profiles are modeled. To provide for a detailed representation, the power demand is determined for each NUTS3-region (CountyNode). Therefor, a bottom-up approach based on statistical data is used. The modeled load profiles are derived from data published by the transmission system operators,[5] by determining the averages for the load characteristics within the temporal structure described in section 6.1. In the base scenario, they are assumed to be unchanging over the time horizon and identical for all NUTS3-regions.

In the following, the method of deriving regional power demand is described. To validate the thus derived total power demand in Germany, it is compared to demand forecasts from other scientific studies.

6.4.1. Regional power demands

Figure 6.4 illustrates the way of deriving the regional power consumptions of the German counties. The total power consumption $D_{nuts3,electr,t,seas}$ in a NUTS3-region *nuts3* in time slot *(seas,t)* is composed of the annual power consumption of households and the annual power consumption of commerce and industries within the region, multiplied by the weight $f_{nuts3,t,seas}$ of the time slot *seas* related the total annual demand (see Eq. 6.1).

$$D_{nuts3,electr,t,seas} = (\delta^{CI}_{nuts3,electr,t} + \delta^{HH}_{nuts3,electr,t}) \cdot f_{nuts3,t,seas} \tag{6.1}$$

3 240 [m²] indicates the cross section of the aluminum and 40 [m²] the cross section of the steel core.
4 Similar electrical parameters are given in Kießling et al. [2003, p. 84] or Oswald [2005, p. 63])
5 (http://www.entsoe.eu)

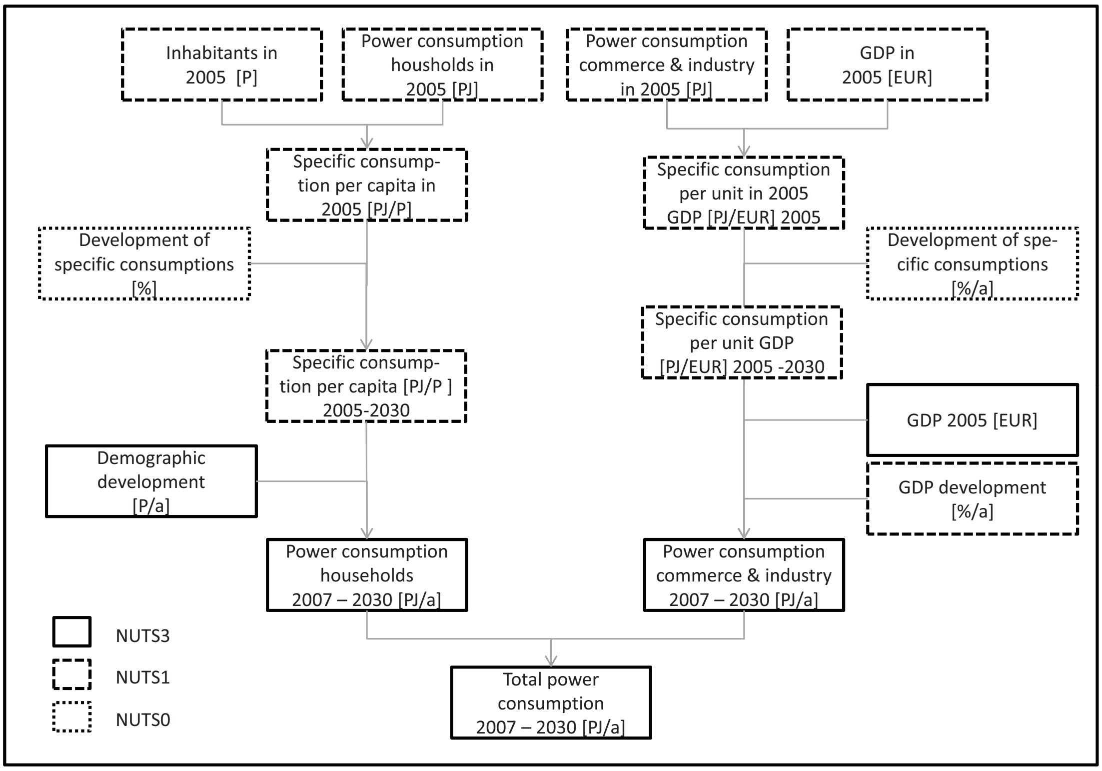

Figure 6.4.: Derivation of the regional power consumptions

Moreover, the assumption of proportionality between the number of inhabitants in a region and the households power demand of that region as well as between the GDP of a region and the power demand of commerce and industries within the region is made. Thus, the annual consumption of households is calculated out of the expected number of inhabitants $INH_{nuts3,t}$ in a NUTS3-region *nuts3* and the specific power consumption $\sigma^{HH}_{nuts1,t}$ of the corresponding NUTS1-region (see Eq. 6.2). Similarly, the annual consumptions of commerce and industries are determined by multiplying the expected $GDP_{nuts3,t}$ in t by the specific consumption $\sigma^{CI}_{nuts1,t}$ (see Eq. 6.3).

$$\delta^{HH}_{nuts3,electr,t} = \sigma^{HH}_{nuts1,t} \cdot INH_{nuts3,t} \tag{6.2}$$

$$\delta^{CI}_{nuts3,electr,t} = \sigma^{CI}_{nuts1,t} \cdot GDP_{nuts3,t} \tag{6.3}$$

Since in the case of specific power consumptions there is no data available on NUTS3-level, the specific consumptions of the NUTS1-levels are used, assuming identical specific consumptions of all NUTS3-regions within the same NUTS1-region. The specific consumptions of the NUTS1-regions in the base year are calculated by dividing the NUTS1-power consumption of household and commerce and industries, respectively, by the number of inhabitants and the GDP of the NUTS1-region. Their supposed trend

Table 6.3.: Development of specific power consumptions (based on EWI and Prognos [2005], Prognos [2009])

	2010	2015	2020	2025	2030
Change in household's specific power consumption	1,04%	0,32%	0,16%	0,00%	-0,12%
Change in industries's specific power consumption	-1,82%	-1,25%	-1,73%	-1,90%	-0,92%

is based on EWI and Prognos [2005], Prognos [2009] (see Table 6.3). Because no more detailed data was available, identical developments are taken for all NUTS3-regions within a NUTS1-region.

The number of inhabitants in the NUTS3-regions is taken from BBR [2008], whereas the regional GDP levels are calculated based on the NUTS3-GDP in 2005 (DESTATIS [2006]) and the expected increases of GDP in the Federal States (NUTS1) (Prognos [2009], cited in Schlesinger [2006]). Hence, identical GDP developments are assumed for each NUTS3-region in the same NUTS1-region. The regional distribution of GDP and the demographic development are illustrated in the appendix (see Figures B.1 and B.2).

Figure 6.5 shows the resulting regional distributions of power demand. A shift in demand from rural to urban regions can be noted. The relative increases or decreases in power demand between 2007 and 2030 shown in Figure B.3 in the appendix.

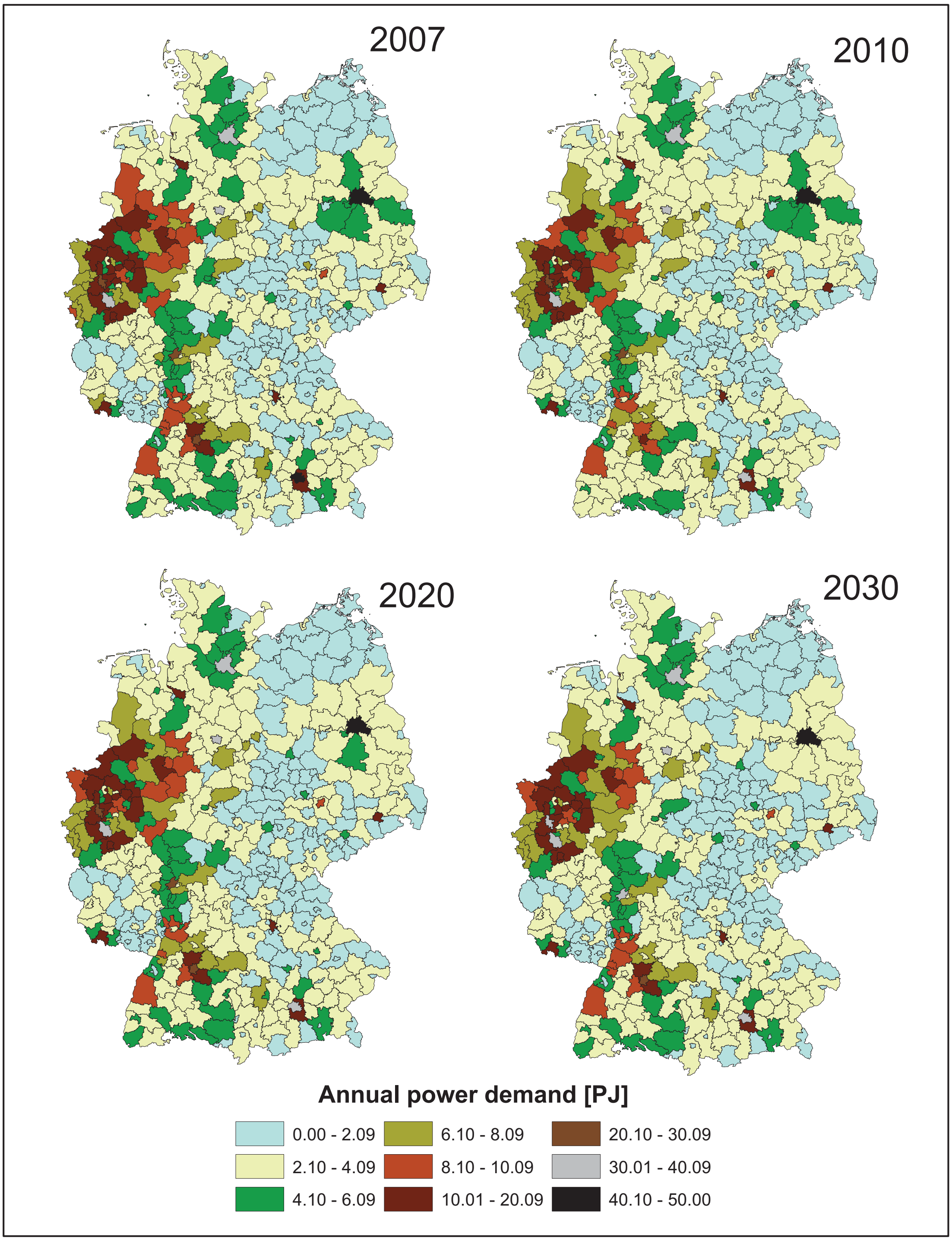

Figure 6.5.: Development of power demand between 2007 and 2030

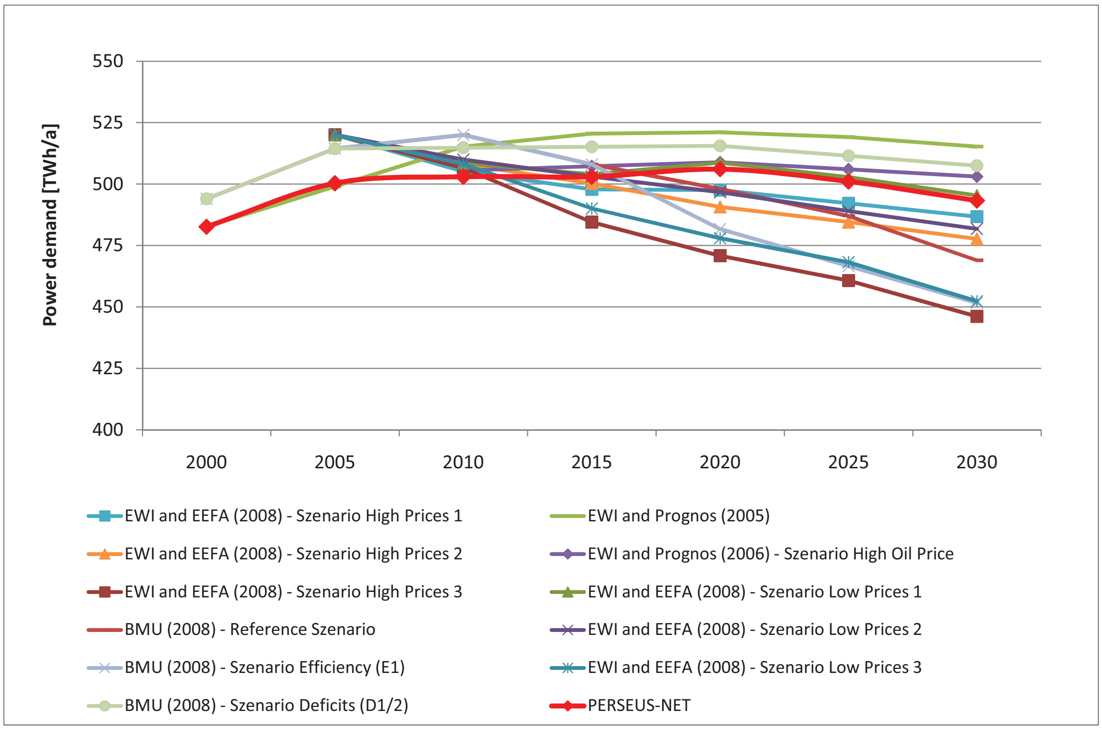

Figure 6.6.: Projections of the demand development in Germany (EWI and EEFA [2008], EWI and Prognos [2005, 2006], TREN [2008], BMU [2008])

6.4.2. Comparison with other studies

In PERSEUS-NET, the total power demand in the model region Germany corresponds to the sum pf the power demands in the NUTS3-regions:

$$D_{reg,electr,t,seas} = \sum_{nuts3 \varepsilon NUTS3} D_{nuts3,electr,ec,t,seas} \tag{6.4}$$

As described in the previous section, the demands of the NUTS3-regions are determined using a bottom-up approach. Regarding the trend of total power demand in Germany, a slight increase is expected until 2020. Following this, demand decreases until 2030, because of an overall rise in energy efficiency. This expectancy is in line with other studies, such as EWI and EEFA [2008], EWI and Prognos [2005, 2006], BMU [2008] (see Figure 6.6). Compared to the afore mentioned studies, a medium developing is assumed in this work for both, the trend of demand and the development of energy efficiency.

Table 6.4.: Techno-economic parameters of the modeled power stations (based on Rosen [2007, p. 138])

<table>
<tr><th rowspan="2"></th><th colspan="2" rowspan="2">Technical data</th><th colspan="2">Economical data</th><th rowspan="2">Ecological data</th></tr>
<tr><th>Parameters</th><th>Restrictions</th></tr>
<tr><td rowspan="3">Unit</td><td colspan="2">Installed capacity</td><td>Investments</td><td rowspan="2">Free commissioning</td><td rowspan="3"></td></tr>
<tr><td colspan="2">Availability</td><td>Fixed expenditures</td></tr>
<tr><td colspan="2">Technical lifetime</td><td>Economic lifetime</td><td>Predetermined commissioning</td></tr>
<tr><td rowspan="7">Process</td><td>Input 1</td><td rowspan="3">Respective share of total input</td><td rowspan="3">Other variable costs (excl. fuel)</td><td rowspan="3">Restriction to base-/peakload operation</td><td rowspan="7">Emission factors (specific CO_2 emissions)</td></tr>
<tr><td>Input 2</td></tr>
<tr><td>Input 3</td></tr>
<tr><td>Output 1</td><td rowspan="3">Respective share of total output</td><td rowspan="4">Load change costs</td><td rowspan="3">Fixed output share of operating modes</td></tr>
<tr><td>Output 2</td></tr>
<tr><td>Output 3</td></tr>
<tr><td colspan="2">Efficiency</td><td>Full load hours</td></tr>
</table>

6.5. Conventional electricity generation

This section addresses the modeled conventional power stations and expansion options, paying special attention to the techno-economic parameters that characterize the units as well as to the siting of new power stations. To obtain feasible results, all relevant techno-economic and ecological data of the power generating units has to be considered in the model.

In this work, large conventional generating units with unit sizes greater than 100 MW are modeled individually. By contrast smaller conventional units as well as units using RES are aggregated for each grid node. Regarding the technical characteristics of the aggregated units as well as of expansion options a technology class approach is used. Each generating unit or technology class is characterized by the techno-economic and ecological parameters presented in Table 6.4. The parameters include, amongst others, installed capacities, availabilities, lifetimes, investments, and expenditures. Furthermore, the inputs and outputs of the generating processes, emission factors, as well as further economical data such as load change costs or maximum or minimum full load hours are defined. For the technology classes and for power stations, for which no individual data could be obtained, average values are used.

In the following, the fuel supply options at the grid nodes as well as the modeling of conventional power stations will be described, giving special attention to the siting of the generating units.

6.5.1. Fuel supply options and fuel prices

Since fuel costs account for a considerable share in electricity generation costs, special interest has to be given to the constitution of fuel prices today and in the future. For this purpose regular energy market scenarios and price projections are published by various institutions. Among the most prominent forecast rank:

- the World Energy Outlook of the International Energy Agency (IEA [2008]),
- the International Energy Outlook of the Energy Information Administration of the US Department of Energy (EIA [2010]), and
- the World Energy Technology Outlook of the European Commission (EC [2010]).

Yet, the fuel price projections can differ considerably, both from one another as well as from one volume to the next volume of the same forecast series.[6]

In Germany, mainly hard coal, lignite, uranium, natural gas, and fuel oil are deployed in conventional electricity generation. Table 6.5 contains the world market price developments of fuel oil, nature gas, and hard coal that are assumed in the base scenario of this work. They are based on the World Energy Outlook of 2008 (IEA [2008]). While significant price increases of 2.42 $\text{Cent}_{2007}/\text{kWh}_{therm}$ and 1.31 $\text{Cent}_{2007}/\text{kWh}_{therm}$ are expected for fuel oil and natural gas between 2007 and 2030, coal prices are expected to stay at a constant level of approximately 1 $\text{Cent}_{2007}/\text{kWh}_{therm}$. Aside from the market prices, additional fuel costs that comprise transport costs as well as taxes are considered for fuel oil, hard coal, and natural gas. They rank from 0.08 $\text{Cent}_{2007}/\text{kWh}_{therm}$ for coal to 1.1 $\text{Cent}_{2007}/\text{kWh}_{therm}$ for fuel oil.

Regarding uranium, the cost of the fuel accounts for only about 5% of the total costs of nuclear power production (IEA [2008, p. 158]). Furthermore, the uranium costs only account for 20% to 30% of nuclear fuel costs, whereas the remaining 70% to 80% are made up by conversion, enrichment, fuel fabrication, and final processing. Therefore, increases in uranium prices as they have been encountered over the last years affect the costs of nuclear fuel only to a lesser extent. As a consequence, the price of uranium is set to a constant level of 0.6 $\text{Cent}_{2007}/\text{kWh}_{therm}$ in the model calculations (cf. IEA and NEA [2010]). It comprises fuel costs as well as costs for the enrichment of fuel elements.

Due to a lower energy density compared to other primary energy carriers, it is inefficient to transport lignite over longer distances. Therefore, lignite-fired power stations are normally constructed close to lignite mining sites. The most important German lignite deposits are in Rhineland, Lusatia, and Central Germany. Furthermore, as lignite is not traded on the market, but rather used on-site, in company owned power station or sold in long-term contracts few information regarding lignite prices is available. In this work, a constant lignite price of 0.4 $\text{Cent}_{2007}/\text{kWh}_{therm}$ is assumed.

Primary energy carrier prices of RES are considered to be zero. They are integrated in the model calculations using the variable generation costs.

To pay regard to the increasing importance of natural gas in electricity generation as well as to deal with significant uncertainties regarding its price development, gas prices will be varied in a scenario analysis.

[6] Enzensberger [2003] deals with the problem by proposing a price corridor for fuel oil, natural gas, and hard coal.

Table 6.5.: World market prices for fossil fuels [$\text{Cent}_{2007}/\text{kWh}_{therm}$] (cf. IEA [2008])

Fuel	2007	2010	2015	2020	2025	2030
Fuel oil	3.20	4.61	4.61	5.07	5.35	5.62
Natural gas	2.18	2.77	2.86	3.16	3.35	3.53
Hard coal	0.76	1.08	1.08	1.05	1.02	0.99

6.5.2. Modeling existing power stations

6.5.2.1. Large power stations

In PERSEUS-NET, all power generating units of the German power system with a unit size larger than 100 MW are modeled individually (see section 6.2). If available, their characteristics, such as their electrical and thermal capacities, unit technologies, construction years, fuels, and efficiencies are considered. The data is based i.a. on Platts [2005], BMWi [2010], UBA [2007], the web page "www.kraftwerke-online.de", on the web pages of power station operators, as well as on estimates by specialists from the industries. Moreover, unit availabilities as well as the economical data, such as variable and capacity costs (see Table 6.4) are based on technology type and age-specific average values taken from the IIP technology database. To pay regard to the decommissioning of power stations, each unit is modeled with a technical lifetime, at the expiry of which the power station is shut down.

As outlined in section 6.2, the large power stations are directly allocated to the grid nodes of the transmission system. The resulting geographic distribution of the power system is shown in Figure 6.7. A list of all power generating units modeled individually in PERSEUS-NET can be found in annex C.

6.5.2.2. Small power stations

In addition to the large generating units, 1613 generating units with a unit size of less than 100 MW are considered in the model. As described in section 6.2 they are assigned to the NUTS3-regions based on the location information given in Platts [2005].[7] The overall capacity developing of these distributed conventional power stations is shown in Table 6.6 by fuel type. It is calculated based on the first year of operation of the power stations and corresponding average operational lifetimes.

7 Mostly due to incomplete information, approximately 130 MW of small conventional capacities could not be assigned to a NUTS3-regions.

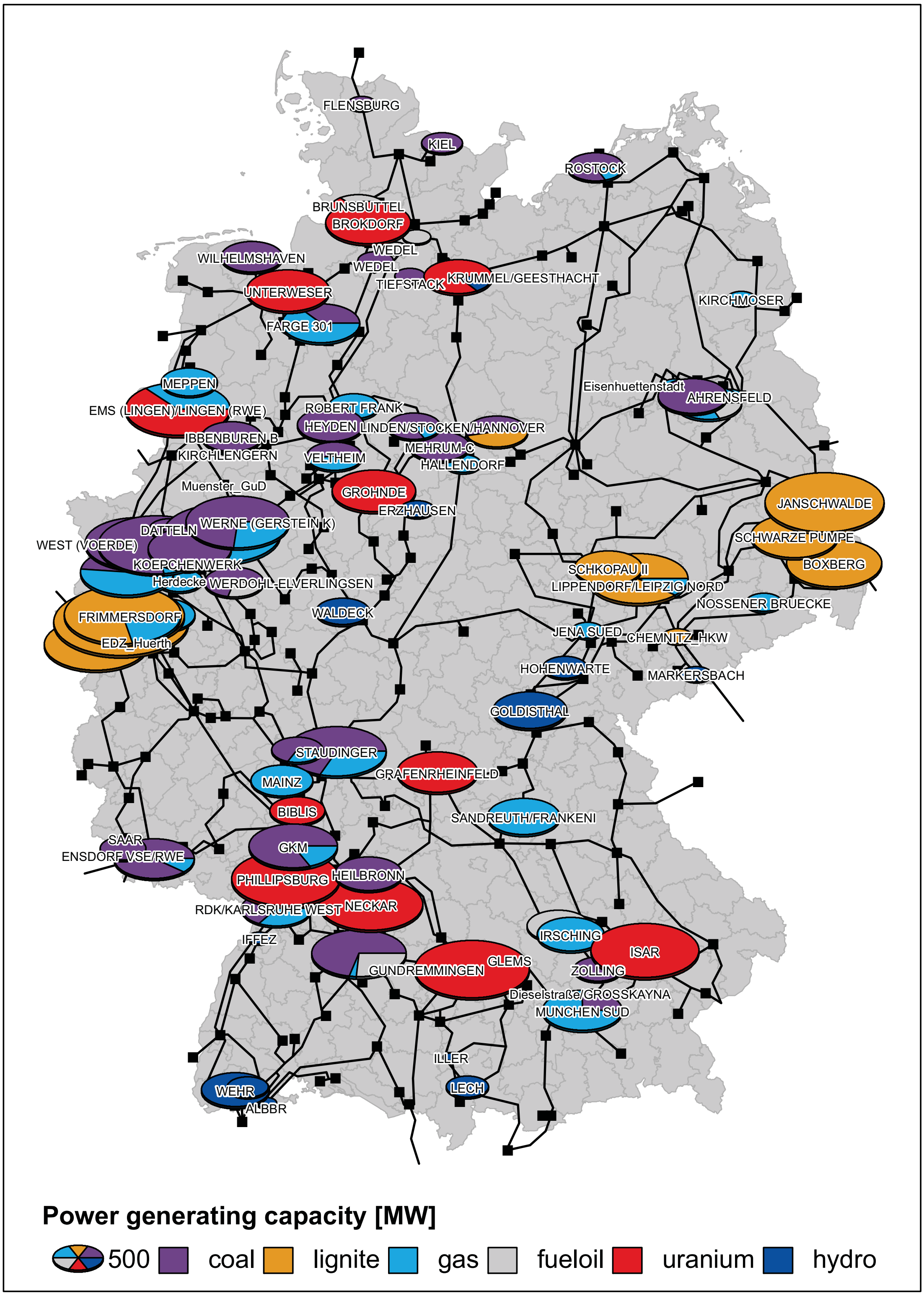

Figure 6.7.: Regional distribution of large power stations in Germany in the year 2007

Table 6.6.: Development of small conventional generating capacities [MW] (based on Platts [2005])

	2007	2010	2015	2020	2025	2030
Hard coal	2224	2184	1820	1627	1571	1362
Fuel oil	2310	2239	2211	1432	1064	707
Natural gas	5210	5169	5099	4708	4530	4297
Total	9745	9592	9129	7766	7166	6366

6.5.3. Techno-economic characteristics and feasible sites of investment options

In addition to the existing conventional power stations, the model takes into account all relevant technology options of future capacity expansion, which are modeled using technology classes. Table 6.7 contains the most relevant technological data describing the conventional expansion options. Technological progress is taken into account by means of higher efficiencies and (partially) lower investments in later periods. The availability of different technology options as well as their efficiencies and costs are based on different sources, such as Enquete-Kommission [2002], Enzensberger [2003], Jopp [2008], and the IIP technology database.

When optimizing the development of the German power system, the solver chooses the optimal technology options to meet the future capacity demand as well as the optimal location of the expansion capacity. The siting of power stations in the model is subject to two preconditions:

1. The fuel supply at the potential site has to be ensured.
2. Sufficient transport capacity of the power grid has to be available.

In real life, additional preconditions such as environmental restrictions or the availability of cooling water have to be satisfied (cf. e.g. Cremer [2005], p. 80), which are however not covered in PERSEUS-NET.

While the availability of sufficient grid capacity is ensured by the consideration of the transmission grid, it is inefficient to transport lignite over longer distances, lignite-fired power stations are normally located close to lignite mining sites. Therefore, in PERSEUS-NET new lignite-fired power stations can only be constructed at grid nodes at which mining capacity and resources are available on long-term. The most important German lignite deposits are in Rhineland, Lusatia and Central Germany. In the model, it is assumed that the lignite supply will increase from 1600 PJ/a in 2007 to 2000 PJ/a in 2015. After 2015, it will remain on the same level. The distribution of the mining capacities among the different districts maintains the same ratio as in the base year 2007. Since hard coal is increasingly imported on the costs of domestically produced coal (cf. CONSENTEC et al. [2008]), new hard coal-fired power stations will predominantly rely on imported coal. Therefore, in particular the availability of waterway transport plays a decisive role in site selection. To simplify matters in PERSEUS-NET, the assumption was made that new coal-fired power stations can only be erected at grid nodes where coal supply is already ensured. Likewise, gas-fired power stations can be commissioned at all grid nodes where natural gas is available today.

Table 6.7.: Conventional expansion options (based on the IIP technology database)

Technology	Fuel	Year	Block size [$MW_{install}$]	Net efficiency [%]	Specific investments [€/$kW_{install}$]	Fixed costs [€/kW/a]	Additional variable costs [Cent/kWh_{el}]
Combined cycle	Natural gas	2010	650	59.0	800	14	0.30
		2020	650	63.0	800	14	0.30
Gas turbine		2010	150	36.0	350	6	0.15
		2025	150	39.0	350	6	0.15
Pulverized super-critical steam generator	hard coal	2010	700	46.5	1400	20	0.30
		2020	700	50.0	1400	20	0.30
	lignite	2010	900	45.0	1700	20	0.40
		2020	900	47.5	1700	20	0.40
Integrated gasification combined cycle	hard coal	2010	650	52.0	2240	95	0.15
		2020	650	57.0	2000	95	0.15
	lignite	2010	650	47.5	2548	102	0.20
		2020	650	52.3	2450	102	0.20
Integrated gasification combined cycle CCS	hard coal	2020	275	50.0	2417	124	1.06
		2030	275	53.5	2115	124	1.06
	lignite	2020	300	44.5	2867	133	0.80
		2030	300	46.5	2767	133	0.80

6.6. Electricity generation using renewable energy sources

Electricity generation from RES will play a decisive role in Germany's future power system. Since the potentials, in particular of wind and solar energy are inhomogeneously distributed, a detailed modeling of the regional distribution of existing units as well as of the regional development of RES-E generation is necessary.

6.6.1. Modeling existing RES-E capacities

According to art. 52.1 (EEG [2008]) transmission system operators have to publish the data of RES-E generating units connected to their system. This data published in EnBW [2009], E.ON [2009], Vattenfall [2009], RWE [2009] has been standardized and related to the corresponding NUTS3-region. For 2007, RES-E units with a total installed capacity of 30,761 MW are considered in PERSEUS-NET. The sum of the total RES-E capacities by unit type is presented in Table 6.8.

Table 6.8.: Installed capacities of existing RES-E units considered in PERSEUS-NET by energy carrier (based on EnBW [2009], E.ON [2009], Vattenfall [2009], RWE [2009])

Energy carrier	Installed capacity
Biomass	2,854.0 MW
Geothermal energy	0.3 MW
Solar	4,212.6 MW_{peak}
Water	774.7 MW
Wind	22,919.3 MW
Total	30,760.8 MW

To allow for a regional differentiation of onshore wind and solar power potentials, full load hours, which are based on historical data are distinguished by NUTS1-region (cf. Staiß [2007]). While the highest full load hours of onshore wind turbines have been measured in Schleswig-Holstein, the lowest have been measured in Baden-Wuerttemberg. Thus the full load hours of onshore wind show a north-south divide. By contrast, the highest full load hours of PV installations have been achieved in Southern Germany. Regarding offshore wind farms 4000 full load hours per year are assumed. The full load hours of existing RES-E units are also applied for newly built generating capacities.

Since the model focus lies on the long-term development of the German power system, a highly detailed temporal resolution of RES-E feed-in cannot be taken into account. The availabilities of biomass, wind, run-of-river, and geothermal energy are rather considered as being uniformly distributed over the 42 time slots. By contrast PV is only considered to be available during daylight hours. While this is feasible for power generation in geothermal biomass and run-of-river power stations, the (stochastic) course of PV and wind power generation, which causes significant peaks and valleys in RES-E availability, is neglected. For a detailed discussion of the reasons for this choice of assumption as well as its flaws, please refer to the critical reflection in chapter 8.

6.6.2. Modeling additional RES-E capacities installed between 2007 and 2030

In this work, the development of RES-E generation capacities is preset and not part of the optimization. On the one hand, this is done because, at present, there is no sufficiently detailed regional data available, for example regarding the regional cost-potentials of RES-E generation within Germany. On the other hand, making the expansion of RES-E part of the optimization would disproportionately increase computing time. The assumptions regarding the overall development of RES-E generating capacities in Germany are based on the lead scenario of the 2008 German lead study (BMU [2008]). In the lead scenario, the authors evaluate, how Germany's targets of reaching a share of RES in electricity generation of at least 20% by 2020 could be met. Accordingly, the overall RES-E generating capacity is expected to rise to approximately 90 GW by 2030. The largest growth rates are expected for offshore wind power and photovoltaic.

While the capacity of offshore wind farms is expected to rise to 23 GW by 2030, the PV capacity is expected to reach 24 GW_{peak} by 2030. Moreover, the total capacity of onshore wind turbines is considered to increase by 62% to almost 30 GW by 2030. As for biomass use, the authors of the lead study assume an increase in installed capacity from 2.6 GW in 2005 to 7.9 GW by 2030. Since the potential of renewable hydro power is almost exhausted, its use is expected to increase by only 0.5 GW and thus to stay at an almost constant level of approximately 5 GW. Finally, the installed capacity of power stations using geothermal energy is expected to not exceed 1 GW (BMU [2008, Annex, p. 79]). In the following, the regional allocation of additional RES-E generating capacities will be described.

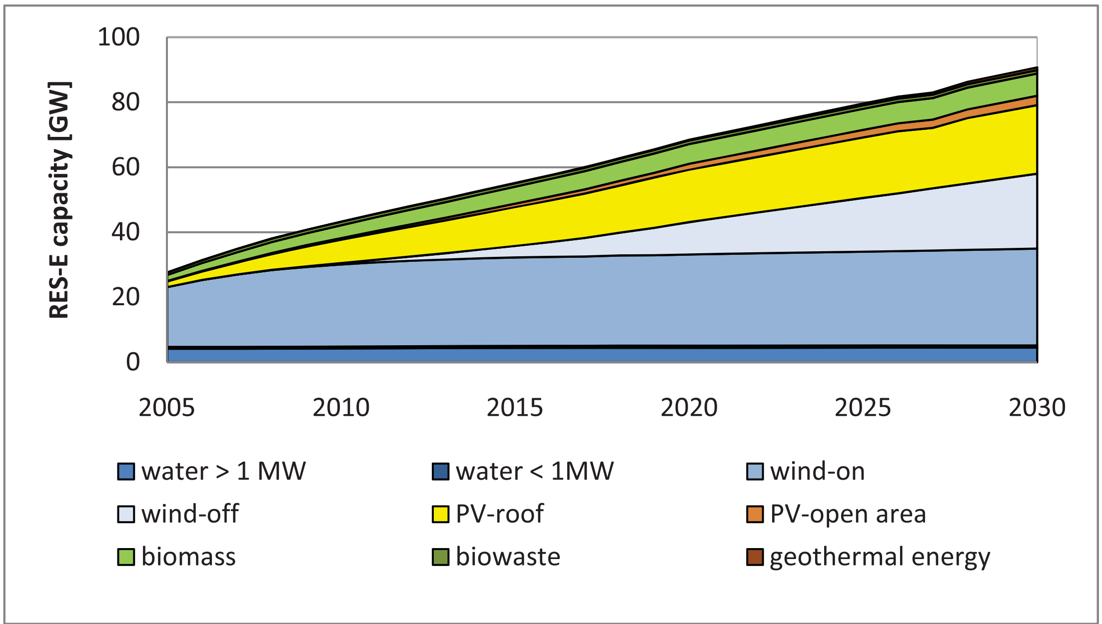

Figure 6.8.: Development of RES-E capacities in Germany based on the lead scenario of the German lead study 2008 (BMU [2008])

6.6.2.1. Offshore wind energy use

Like large conventional power stations, offshore wind farms are modeled individually. By September 2010, the first German offshore wind turbines have been commissioned in the North Sea. Two single test turbines turbines near Emden and Wilhelmshaven, the first test wind farm Alpha Ventus has been connected to the grid. Until 2030 the capacity of offshore wind farms is expected to rise to 23 GW (BMU [2008]). The wind farms considered in PERSEUS-NET are listed in Table 6.9. Insofar as the expected date of the first grid connection is known, it has been considered in the model. In the further development of offshore wind parks, the erection of wind turbines complies with the development path fixed by the lead scenario (BMU [2008]), in consistence with the targeted maximum capacity of the wind farms. Regarding the regional distribution, 19.2 GW are expected to be erected in the North Sea and 3.8 GW in the Baltic Sea. This assumption is based on the regional distribution of the projects published at present.

Table 6.9.: Offshore wind parks considered in PERSEUS-NET (DENA [2010b])

Name	Year of commissioning (phase 1)	Capacity phase 1 [MW]	Capacity in the final expansion phase [MW]	Location
Emden	2008	4.5	4.5	North Sea
Alpha Ventus	2009	60	1,040	North Sea
Wilhelmshaven	2009	4.5	4.5	North Sea
Borkum Riffgrund West	2010	280	1,603	North Sea
Nordergruende	2011	90	125	North Sea
Baltic I	2011	48.3	48.3	Baltic Sea
Borkum West II	2011	360	400	North Sea
Butendiek	2012	300	300	North Sea
GEOFReE	2012	25	25	Baltic Sea
Noerdlicher Grund	2012	320	2,010	North Sea
Nordsee Ost I	2012	288	1,250	North Sea
Nordsee Ost II	2012	400	1,005	North Sea
Bard I	2013	200	1,600	North Sea
Dan Tysk I	2013	200	1,500	North Sea
Global Tech I	2013	400	1,600	North Sea
Gode Wind I	2014	400	1,120	North Sea
MEG I	2014	400	400	North Sea
Delta Nordsee	2015	216	1,255	North Sea
Meerwind	2015	288	1,350	North Sea
Arkona	2016	400	1,005	Baltic Sea
Sandbank	2016	480	4,720	Baltic Sea
Kriegers Flak	2017	330	330	Baltic Sea
Amrumbank W	2018	400	400	North Sea
Borkum Riff II	2018	231	540	North Sea
He Dreiht	2018	400	400	North Sea
Nordsee	2018	400	2,540	North Sea
Sum	-	6,856.3	26,575.3	-

Maps with the regional distribution of the offshore wind projects in the North Sea and Baltic Sea, which also show their connecting points to the power grid are illustrated in the Figures 6.9 and 6.10. The offshore wind parks in the North Sea are connected to the power grid at Brunsbüttel and near Norden. Since near Norden the wind parks are connected to the 110 kV grid, which is not part of the modeled transmission system, these offshore wind parks are modeled in PERSEUS-NET as if they were directly connected to the SubstationNode Diele. In the Baltic Sea the offshore wind parks are connected to the on shore grid at Rostock, Lubmin, and Herrenwyk.

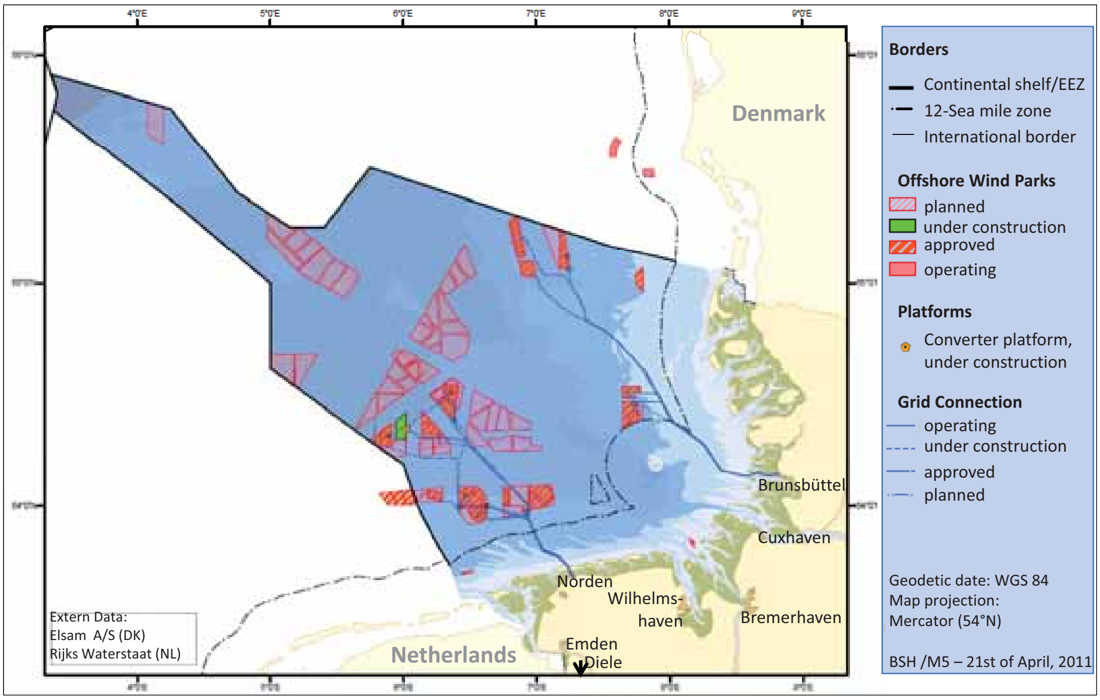

Figure 6.9.: Offshore wind parks in the North Sea (based on BSH [2011a])

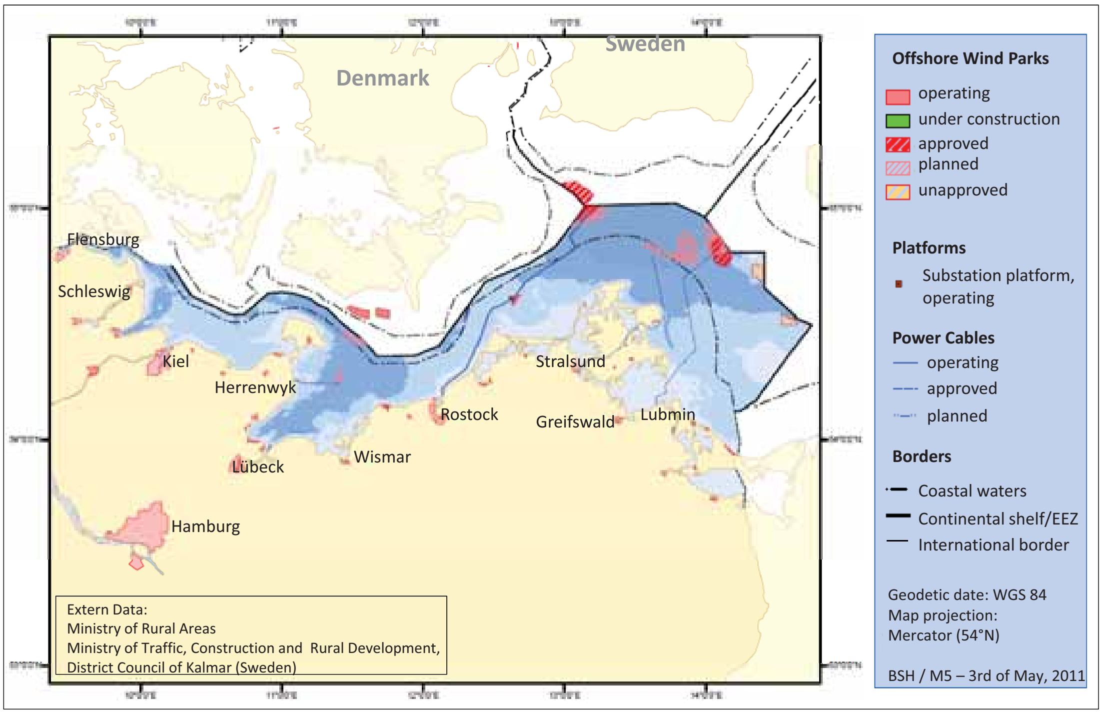

Figure 6.10.: Offshore wind parks in the Baltic Sea (based on BSH [2011b])

6.6.2.2. Onshore wind energy use

To correctly assign the potential for expansion of wind energy to the NUTS3-regions, a detailed regional analysis of the zones designated for onshore wind energy use that is based i.a. on land-use plans of territorial authorities would be necessary. Since it was not possible to conduct such a detailed analysis within this work, a simplified approach is used to locate the additional capacities based on publicly available data (see Figure 6.11).

First, the additional onshore wind energy capacities are assigned to the NUTS1-regions using the expansion and repowering potential for onshore wind energy use in the NUTS1-regions, which are published in the DENA study (DEWI et al. [2005, p. 11]).[8] The total remaining potentials of the NUTS1-regions add up to14,360 MW in 2007 (see Annex D). Thereof, the highest shares in total remaining capacity remain in North Rhine-Westphalia, Brandenburg, and Saxony-Anhalt. Based on this, the new onshore wind capacities $NewCap_{wind,nuts1,t}$ built in period t in a NUTS1-region *nuts1* are calculated out of shares of the NUTS1-regions in the total remaining German onshore wind potential $\beta_{wind,nuts1,nuts0}$ and the expected new wind capacities, which are constructed in period t according to the lead scenario (see Eq. 6.5).[9]

$$NewCap_{wind,nuts1,t} = \beta_{wind,nuts1,nuts0} \cdot NewCap_{wind,nuts0,t} \tag{6.5}$$

In the second step, the NUTS1-potentials are assigned to the NUTS3-regions using Corine land cover data (EEA [2007]).[10] Since repowering of wind farms often combines a restructuring of existing farms and the construction of new wind turbines in additional areas (DEWI et al. [2005, p. 16]), both the remaining as well as the repowering potential are allocated based on the Corine land cover data. Therefor, the dimensions of open areas within the NUTS3-regions, which are assumed to be potential wind farm sites, are determined, taking into account Corine land cover classes, which can totally or partly be considered, such as pastures, natural grasslands, non-irrigated arable land, annual crops associated with permanent crops, and land principally occupied by agriculture, with significant areas of natural vegetation.

Finally, the additional wind capacity $NewCap_{wind,nuts3,t}$ built in NUTS3-region in period t is determined using the ratio "open area within a NUTS3-region" $A_{wind,nut3}$ over "open area within the corresponding NUTS1-region" $A_{wind,nut1}$ (see Eq. 6.6).

$$NewCap_{wind,nuts3,t} = \frac{A_{wind,nuts3}}{A_{wind,nuts1}} \cdot NewCap_{wind,nuts1,t} \tag{6.6}$$

8 DEWI et al. [2005] determine the potential for wind power expansion based on the degree of utilization of zones designated for onshore wind energy use assuming land requirements of 7 ha/MW.

9 cf. BMU [2008, Annex, p. 79]

10 The Corine land cover database comprises the stock in Hectares for each of the land cover classes for each NUTS-region. The land cover classes comprise 15 types of artificial surfaces, 15 types of agricultural areas, 15 types forest and semi natural areas, as well as wetlands and water bodies.

Figure 6.12 (left) compares the resulting regional distribution of onshore wind turbine capacities in 2030 to the capacities already installed in 2007.

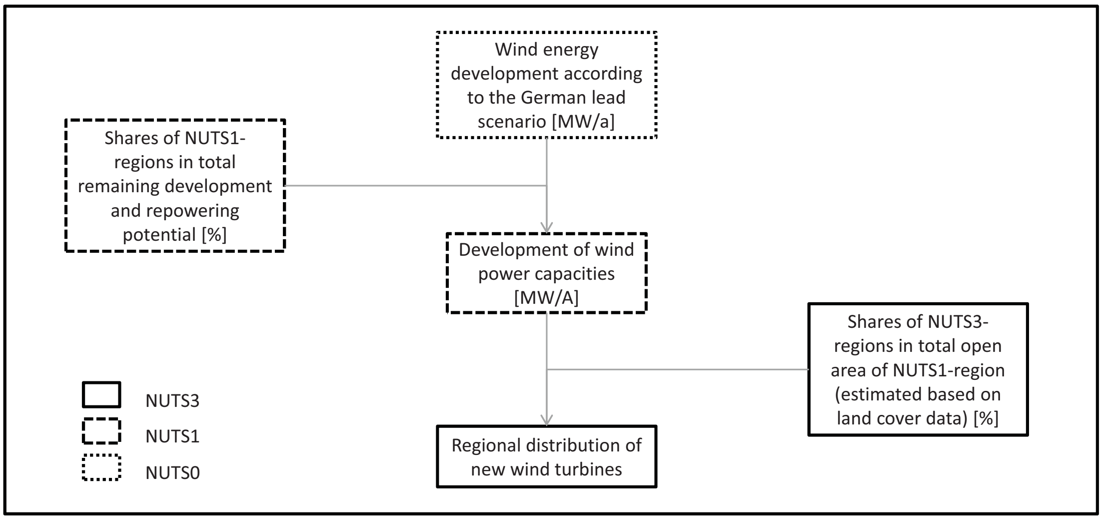

Figure 6.11.: Regional allocation of new onshore wind energy capacities

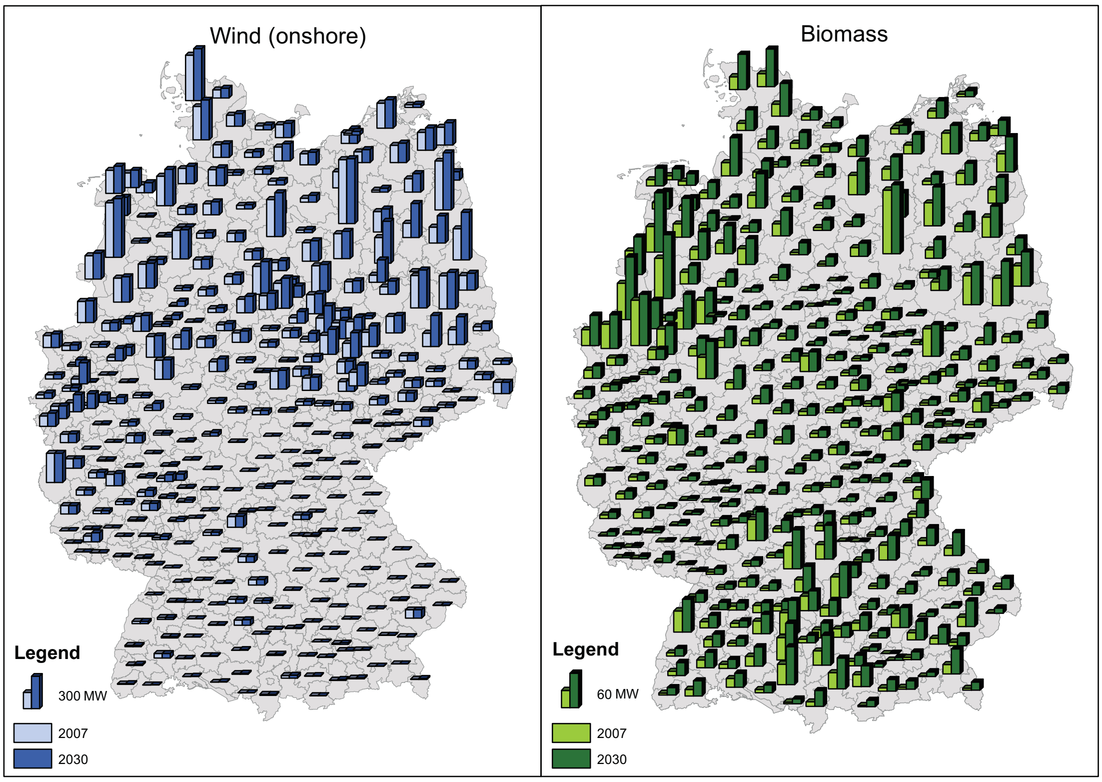

Figure 6.12.: Regional distribution of electricity generating capacities using onshore wind energy and biomass

6.6.2.3. Biomass use

By contrast to onshore wind capacities, new biomass units are directly allocated to the NUTS3-regions (see Figure 6.13). As in the German lead study of 2008, liquid and solid biomass types are distinguished. Regarding solid biomass, the forest wood residue outputs determined for each NUTS3-region by Brökeland [1998] are used to allocate the new solid biomass fired units to the NUTS3-regions. The total capacity of new solid biomass fired power stations in a NUTS3-region in period t is the product of the share of the NUTS3-region in the total German forest wood residue output $\beta_{bio_{solid},nuts3,nuts0}$ and the new solid biomass capacity $NewCap_{bio_{solid},nuts0,t}$ to be built in Germany in that period according to the lead study. In the same way, historical data regarding the amount of manure yielded by each NUTS3-region (cf. DESTATIS [2006]) and the NUTS3-region's straw outputs (cf. Brökeland [1998]) are used to assign the biogas units to the NUTS3-regions (see Eq. 6.7).

$$\begin{aligned} NewCap_{Bio,nuts3,t} &= \beta_{bio_{solid},nuts3,nuts0} \cdot NewCap_{bio_{solid},nuts0,t} \\ &\quad + \beta_{bio_{liquid},nuts1,nuts0} \cdot NewCap_{bio_{liquid},nuts1,t} \end{aligned} \tag{6.7}$$

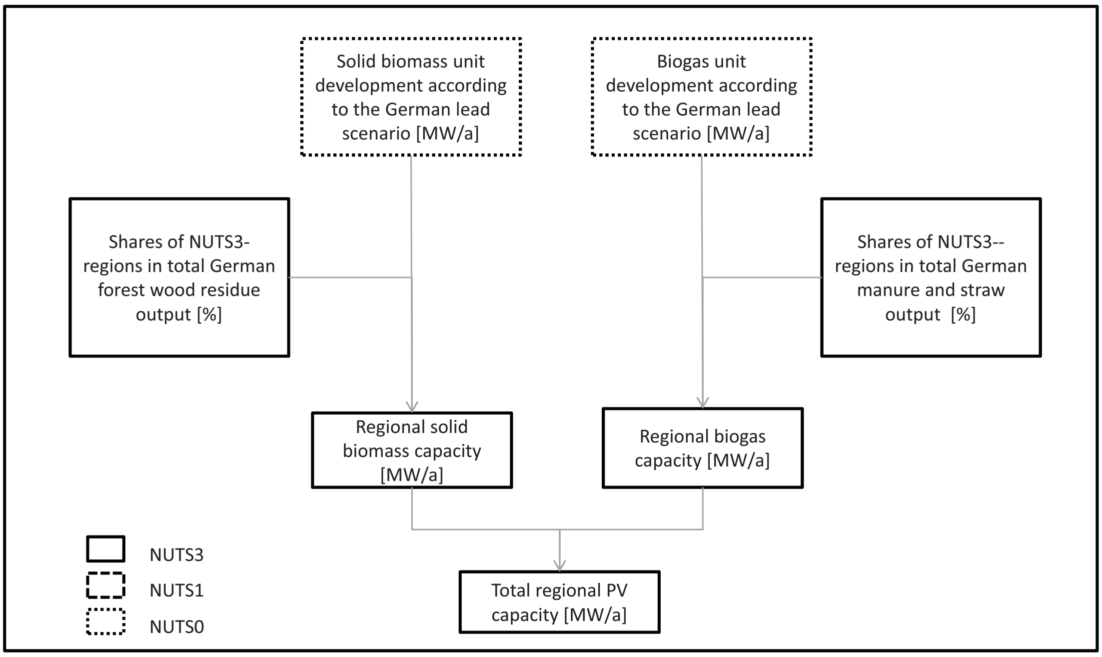

Figure 6.13.: Regional allocation of new biomass capacities

While the Northern Germany and Bavaria possess the highest manure and straw outputs, the Spreewald, Rothaargebirge, northern Brandenburg and the Ueckermuender

Heide, the Harz, and the Black Forest yield the highest amounts in forest wood residues. The proportion of the NUTS3-regions in solid biomass and biogas units is shown in Figure B.4 (see annex B). The regional distribution of biomass units between 2007 and 2030 is shown in Figure 6.12 (right).

6.6.2.4. Solar energy use

The overall German PV expansion capacities are allocated to the NUTS3-regions using a similar approach as used for onshore wind turbines (see Figure 6.14). First, the additional PV-capacities are allocated to the NUTS1-regions proportional to the NUTS1-region's shares in PV potential. The PV potential is divided into roof-top and open space installations (see Eq. 6.8 and Eq. 6.9). An overview of the assumed PV potentials of the NUTS1-regions, which are based on Staiß [2007], is given in Table D.2 in the annex.

$$NewCap_{PV_{roof},nuts1,t} = \beta_{PV_{roof},nuts1,nuts0} \cdot NewCap_{PV_{rroof},nuts0,t} \tag{6.8}$$

$$NewCap_{PV_{space},nuts1,t} = \beta_{PV_{space},nuts1,nuts0} \cdot NewCap_{PV_{space},nuts0,t} \tag{6.9}$$

Based on Staiß [2007] the allocation of roof-top capacities is based on the total roof area within the NUTS1-regions that is assumed to be usable for PV installation. The sizes of open areas that are potentially usable for PV are considered for open space installation. With 157 million m^2 (20%) and 127 million m^2 (16%) North Rhine Westphalia and Bavaria possess the highest potentials for roof-top PV units. As for open space installations, Bavaria (237 km^2) and the Lower Saxony (213 km^2) posses the highest potentials.

In the second step the PV-capacities are allocated to the NUTS3-regions using Corine land cover data (cf. EEA [2007]) (see Eq. 6.10).

$$\begin{aligned} NewCap_{PV,nuts3,t} \quad = \quad & \frac{A_{PV_{roof-top},nuts3}}{A_{PV_{roof-top},nuts1}} \cdot NewCap_{PV_{roof-top},nuts1,t} \\ & + \frac{A_{PV_{openspace},nuts3}}{A_{PV_{openspace},nuts1}} \cdot NewCap_{PV_{openspace},nuts1,t} \end{aligned} \tag{6.10}$$

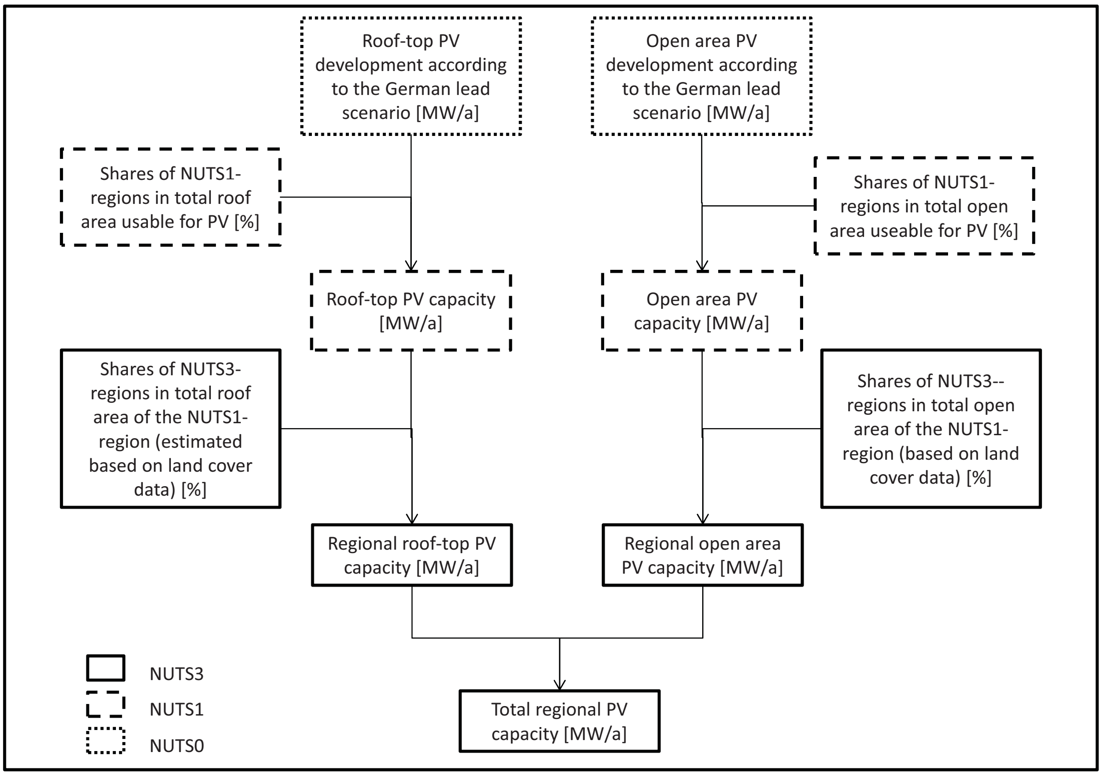

Figure 6.14.: Regional allocation of new photovoltaic capacities

Regarding open area PV the Corine land cover classes “pastures”, “dump sites”, and “sparsely vegetated areas” are considered. Concerning roof-top installations, the classes “continuous urban fabric”, “discontinuous urban fabric”, and “industrial or commercial units” are taken into account. The resulting distribution of PV units in 2007 and 2030 is exemplary shown in Figure 6.15 (left).

6.6.2.5. Geothermal energy

Regarding geothermal energy in power generation, an increase in installed capacity of 859 MW between 2007 and 2030 is expected. According to Rogge [2004], relevant technical potentials for using geothermic energy exist in the North-German Basin (216 GWa_{el}), the Upper Rhine (65.5 GWa_{el}), and in the North Alpine Molasse Basin (18.8 GWa_{el}). In Table 6.10 the existing and planned projects that are considered in PERSEUS-NET are presented. Using GIS, the remaining additional capacities are allocated to the NUTS3-regions proportionally to the part of the area of the NUTS3-region in the total area of the corresponding region with geothermal potential. The resulting allocation of geothermal power stations to the NUTS3-regions is shown in Figure 6.15 (right).

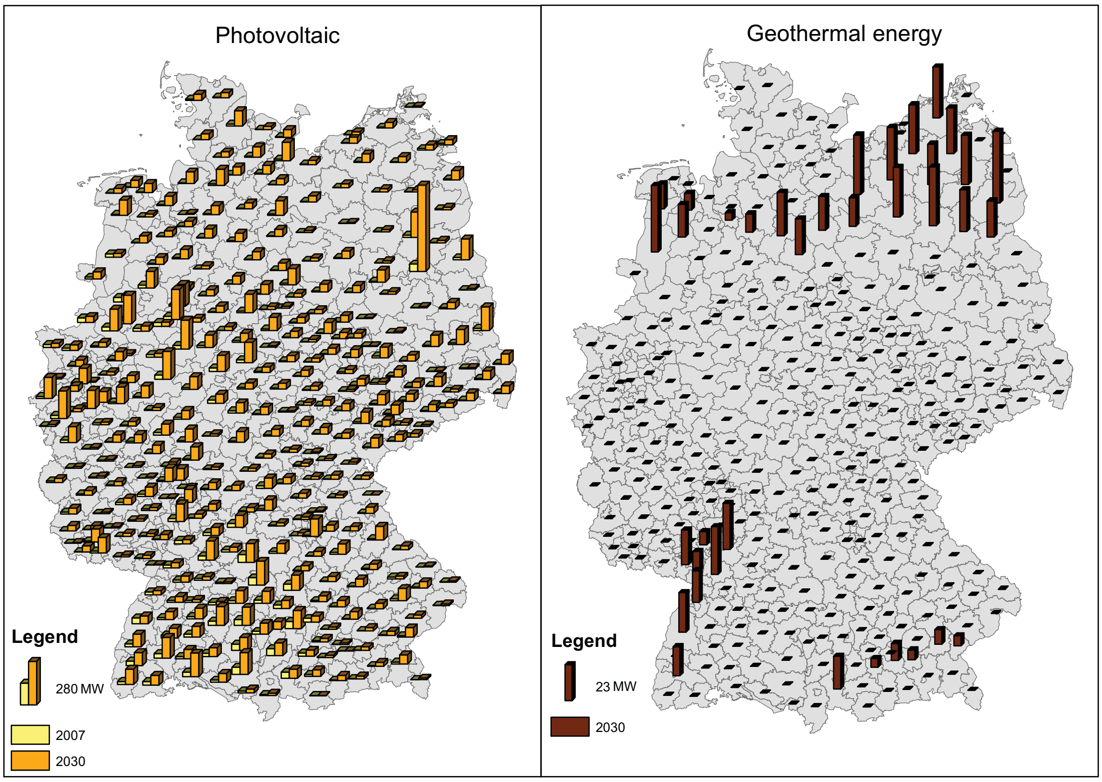

Figure 6.15.: Regional distribution of electricity generating capacities using photovoltaic and geothermal energy

Table 6.10.: Existing and planned geothermal power stations (GtV [2011])

Location	Region	Capacity [MW]	Year of realization
Landau	Upper Rhine	3.80	2007
Glewe	N.-German Basin	0.21	2007
Groß Schoenbeck	N.-German Basin	1.00	2007
Bruchsal	N.-German Basin	0.50	2008
Unterhaching	N. Alpine Molasse Basin	3.36	2008
Insheim	Upper Rhine	4.00	2010
Mauerstetten	N. Alpine Molasse Basin	5.00	2010
Sauerlach	N. Alpine Molasse Basin	8.00	2011

6.6.2.6. Renewable hydro power

BMU [2008] estimates an expansion of small renewable hydro stations ($<$ 1 MW) between 2007 and 2030 of 132 MW. Furthermore, an increase in large renewable hydro power capacity of 328 MW is expected between 2007 and 2030. In PERSEUS-NET the extension of the run-of-river power station in Rheinfelden, as well as additional capacities on the Danube, Lech, and on the High-Rhine (cf. Kaltschmitt et al. [2009]) are considered. The expansion of small hydro power capacities, however, is not taken into account, because of the high georeferencing effort in combination with its marginal level of influence on the results.

6.7. Inter-regional power exchanges

The German power system is connected to the neighboring systems via transmission lines and high voltage direct current (HVDC) sea cables. In 2007 the German power exports over these so-called interconnectors amounted to 63.4 TWh, imports to 44.3 TWh, which corresponds to 11% of the total German generation, and 8% of the total German consumption, respectively (cf. ENTSO-E [2008, p. 32ff.]). While the center of focus of this work is the German power system, to totally disregard the power exchanges with the bordering systems would lead to erroneous results. Therefore the bordering power systems are each represented in the model as one single network bus, which is connected to the German junctions of the corresponding interconnectors (cf. section 6.2). Furthermore, a seasonal flow is defined between these two network buses, which represents the net power import in between the two power systems.

The temporal resolution of power imports and exports has been deduced for the base year 2007 from data published by the German transmission system operators (EnBW [2008], E.ON [2008], RWE [2008], Vattenfall [2008]) and ENTSO-E (ENTSO-E [2008, p. 34]). This data has been aggregated by country and adapted to the temporal structure of the model. The resulting seasonal imports and exports are shown in Figure 6.16. In the model calculation the yearly flow levels and load curves are assumed to be unchanging, whereas different developments are analyzed in the scenario analysis.

6.8. Further input data

In the following, all relevant additional assumptions regarding EUA prices and the underlying discount rate are described.

6.8.1. Emission factors and EU Emission Allowance prices

The limitation of GHG emissions to the level of allowances allocated involves significant changes for the production planning of electricity generators and energy intensive industries. As a price evolves for scarce resources, the formerly free and unlimited resource CO_2 emission is now accounted for as a production factor. Independent of whether the emission allowances are allocated free of charge or not, the entity owning the emission allowance always has the choice either to use the allowance to cover its CO_2 emissions

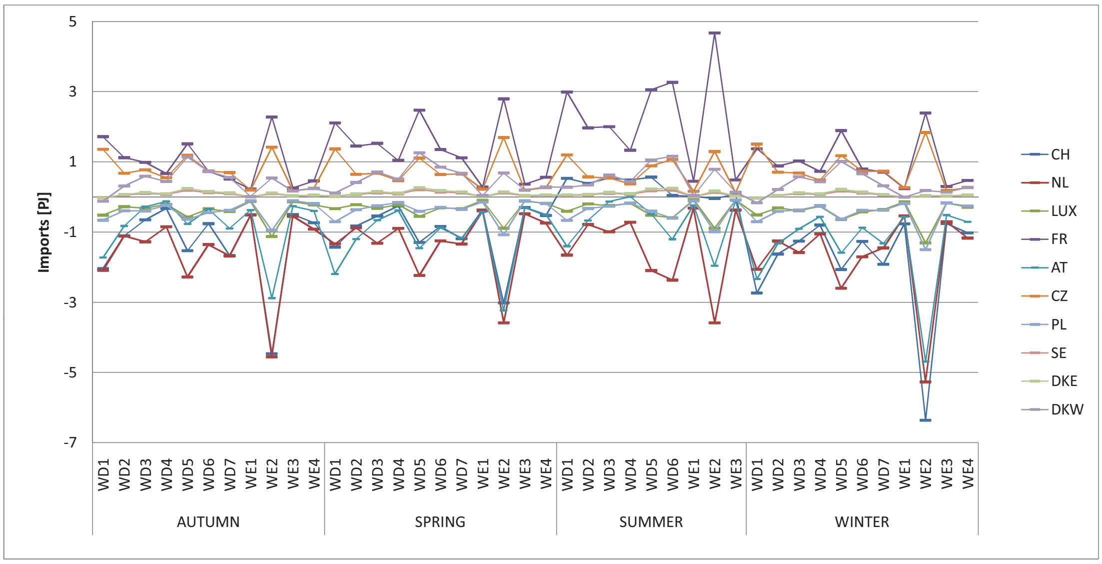

Figure 6.16.: Level and temporal resolution of Germany's electricity imports by exporting country (own calculations based on EnBW [2008], E.ON [2008], RWE [2008], Vattenfall [2008], and ENTSO-E [2008, p. 34])

or to sell it on the market. Therefore, the opportunity costs of the use of CO_2 emission allowances are included in the electricity generation costs. Furthermore, the EUA price signals whether or not it is economically reasonable to invest in emission reduction technologies.

The amount of CO_2 emitted within the process of power generation depends, on the one hand, on the efficiency of the power plant and, on the other hand, on the carbon content of the fuel. Because of different calorific values, fossil fuels possess different CO_2 emission factors. Thus, their combustion involves different levels of CO_2 emissions. The emission factors range from 56 ktCO_2/PJ for natural gas to up to 114 ktCO_2/PJ for lignite. The emission factors used in the model are summarized in Table 6.11. The specific emission of RES including biomass are assumed to be zero.

Table 6.11.: CO_2-emission factors in power generation

Fuel	Emission factors [ktCO_2/PJ_{th}]	Efficiency [%]	Specific Emissions [kt CO_2/TWh_{elec}]
Coal	98	42 - 46	767 - 840
Lignite	108 - 114	40 - 43.5	894 - 1026
Heavy fuel oil	78	41 - 44	640 - 685
Light fuel oil	74	52 - 54	495 - 510
Natural gas	56	56 - 59	342 - 360

Under the assumption that the cost of CO_2 emissions are accounted for as opportunity costs, the EUA price development is fixed and included in the electricity generation costs as an add-on to the fuel market prices. Due to the undeniable exigence to act against climate change, the EU Emission Trading will continue beyond the Kyoto trading period 2008 - 2012 (cf. EC [2009c]). The CO_2 prices used within the model calculation are based on historical data (see section 2.1.3) as well as on the results of studies analyzing the development of future CO_2 price (cf. e.g. Möst and Fichtner [2010], EWI and EEFA [2007], BMU [2010], Möst et al. [2008]). In these studies a wide range of future CO_2 price developments is presented, in which carbon prices by 2030 rank from 27 EUR/tCO_2 to up to 55 EUR/tCO_2. The CO_2 price development assumed in the base scenario calculations are shown in Table 6.12. The fuel specific emission are valued with 8.0 €/t$\mathrm{CO_2}$ in 2007 and 45.0 €/t$\mathrm{CO_2}$ in 2030, which can be considered as a medium price increase. Since provision is made for more stringent emission caps, the price for EUAs is expected to rise significantly till 2030 (cf. EC [2009c]).

Nevertheless, since the actual development of CO_2 prices is uncertain, the influence of different levels of EUA prices will be addressed in the scenario analysis.

Table 6.12.: CO_2 price development in the base scenario

	2007	2010	2015	2020	2025	2030
$\mathrm{CO_2}$ prices [€/t$\mathrm{CO_2}$]	8.0	11.25	22.5	27.0	33.0	45.0

6.8.2. Discount rate

Discounting means converting future amounts of money at different points in time into a comparable amount of money at a specific point in time. The choice of interest rate determines how future cash flows are weighted. In energy system analysis, a variety of opinions regarding the correct choice of discount rates exist. Correspondingly, a large spectrum of discount rates, ranging from 3% to 15%, is used.

Lower rates between 3% and 5% are generally used in policy consultation, in particular in state owned systems with a high degree of certainty regarding future cash flows. They correspond to returns of risk-free investments (cf. e.g. Dimson [1989], Le Dars and Loaec [2007]), such as index-linked state bonds.[11]

In liberalized energy markets such low discount rates can be considered as the minimum acceptable return on investment. Due to the introduction of competition as well as uncertain and volatile prices, actors willing to invest in generation capacity rather require higher risk premium. Moreover, privatized firms have to pay taxes and thus the pre-tax cash flows have to be discounted at higher rates (Dimson [1989], Le Dars and

[11] At present, the 10 year (30 year) German state bonds posses a fixed interest rate of 2.25% (4.75%) (cf. Finanzagentur [2010]).

Loaec [2007], Szabo et al. [2010]). Therefore discount rates of 8% - 12% are typically used in models of liberalized power markets that contain a detailed representation of the behavior of actors. As the uncertainties and price volatilities differ between the fuels and as different technologies feature different maturities, the level of the risk premium vary for different technology options (cf. Szabo et al. [2010, p. 3814]). Nevertheless, due to the unavailability of data which would allow for a correct technology specific differentiation, a constant, for all technologies identical discount rate of 10% is used in this work.

6.9. Implementation, database, and analysis options

The model PERSEUS-NET is implemented in GAMS (General Algebraic Modeling System). GAMS has been developed to model and solve large mathematical optimization problems. Among the advantages of GAMS is that the formulation of a problem in GAMS is very similar to its mathematical formulation. Furthermore, GAMS offers the possibility to select different types of solvers without the need to change the model formulation. For PERSEUS-NET the GAMS version 23.5 with the CPLEX version 12.2 is used. Moreover, for PERSEUS-NET the CPLEX lpmethod 4 (barrier optimizer) has been proven to be the fastest CPLEX optimizer that can be chosen.

The PERSEUS-NET input data is managed via a MS Access relational database. The corresponding PERSEUS-NET data management system (see figure 6.17) permits easy data handling. Moreover, a fully automated link to the GAMS model as well as to the geodatabase exists. Via the link to the geodatabase, a power network model edited in ArcGis can easily be loaded into the PERSEUS-NET database. Using GAMS data exchange (gdx), the model results are made available in MS Excel and MS Access format. Furthermore, charts are created automatically for the large number of output parameters. A link between the GIS and the MS Excel files permits a simple design of maps containing the regional model results.

The model PERSEUS-NET has been implemented as a PC version, but can only be run on commercial PCs with sufficient memory. When six optimization periods are considered, the PERSEUS-NET model for Germany with a time horizon from the year 2007 up to the year 2030 consists of approximately 2.6 million equations, 2.9 million variables, and 12.3 million non-zero elements. Depending on the model specifications, computing times range from several hours to more than a week. On a computer with four 3.07 GHz processors and 12.0 GB RAM, the basic version of the model can be solved in approximately 19 hours. Model versions, in which grid restrictions are tightened, take up to 43 hours to be solved, while when considering grid restriction and investments in cogeneration units in an integrated model run, solving the model takes more than 10 days.

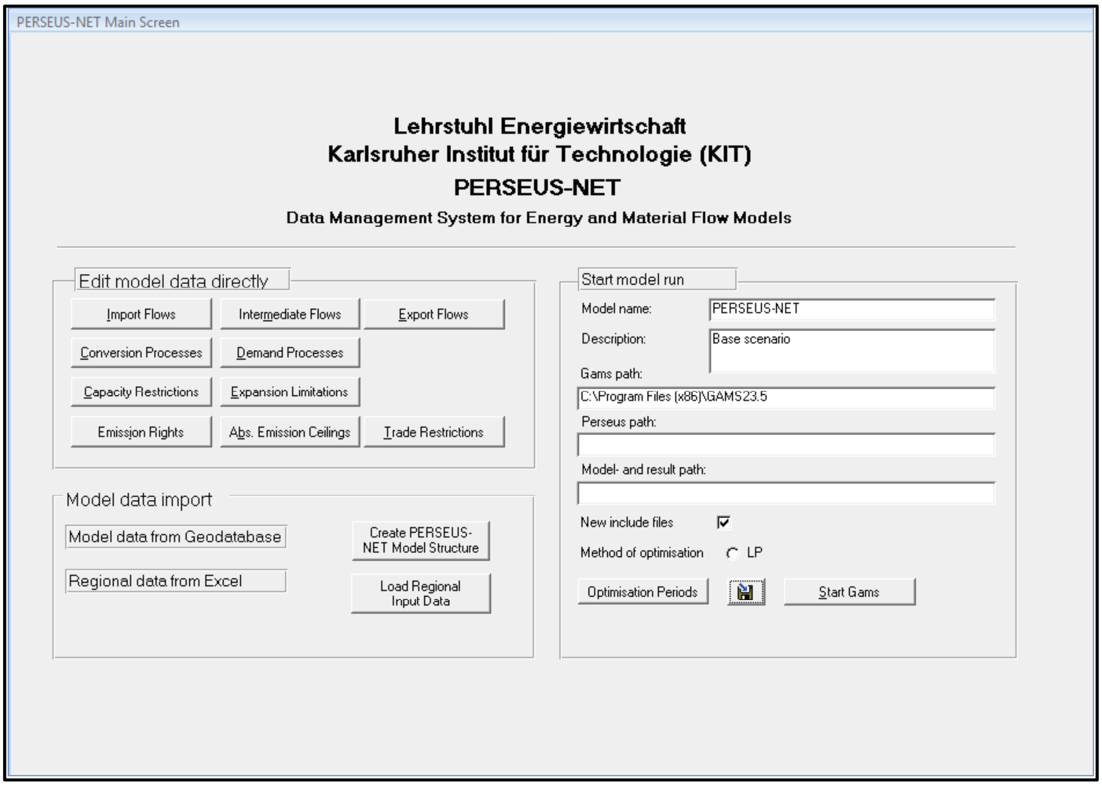

Figure 6.17.: PERSEUS-NET Data Management System

6.10. Summary

In this chapter, the data basis for the energy system model developed to analyse the long-term regional development of the German power system was presented. In particular the data describing the power stations, power grid capacities, and power demands are introduced. Regarding the infrastructure capacities, the most important technical and economical parameters are described. Moreover, special attention was given to how realistic regional allocations of the infrastructure capacities and demands have been derived. In particular the mapping of RES-E technologies and power demands has been described in detail.

In the following, the model PERSEUS-NET will be used to analyse the regional development of the German power system.

7. Model-based analysis of the regional development of the German power system till 2030

The nodal pricing based energy systems model described in the previous chapters is used to analyse the long-term development of the German power system. Special focus is given to the spatial distribution of power generation, power generating capacities, and the marginal cost of power supply. In this chapter, the results obtained are presented. First, the base scenario is studied, reflecting the most likely development of the framework condition. Then, the regional development of the German power system under alternative framework conditions such as delays in power grid expansion projects, an alternative development of power imports and exports, and increasing gas and CO_2 prices is presented. Based thereupon, the results from the scenario analysis are condensed and comprehensively discussed in chapter 9.

7.1. Definition of the base scenario

The following key assumptions regarding the future development of the German power system were made for the reference scenario, which will be called BASE scenario in the following:

- In PERSEUS-NET 250 large existing conventional thermal power stations as well as 9.7 GW of small conventional power stations with a capacity larger than 100 MW are modeled. They are considered to be decommissioned after a technical lifetime ranging from 25 to 45 years. Furthermore, the investment options described in table 6.7 are taken into account.
- The sizes and locations of existing RES-E units are considered as published by the transmission system operators. Expecting that Germany will reach its 2020 target, the overall development of RES-E capacities is based on the lead scenario of the German environment ministry (BMU [2008]). The assumptions regarding the regional distribution of additional RES-E capacities as well as their availabilities are described in section 6.6. Due to the rough temporal structure of the optimization model, the supply dependent RES-E generators are uniformly distributed over the time slots of the year.
- Regarding the phase-out of the German nuclear power stations the decision of the German government of June 2011 to shut down the last nuclear power station at the end of 2022 applies (see section 2.1.6).

- Thermal line limits and resistances of the considered high voltage grid are based on technical characteristics of typical overhead power lines used in Germany (see section 6.3). Moreover, a reliability margin of 10% is taken into account.
- Regarding future grid expansions, the projects named in EnLAG [2009] are considered.
- Fuel and CO_2 prices are expected to develop as presented in sections 6.5.1 and 6.8.1. They comprise world market prices as well as transport costs.
- Business as usual is assumed regarding the development of inter-regional power exchanges.

In the process of calculation, run-time has proven to be a critical factor. In particular test runs with an integrated optimization of power and heat generation in model calculations considering power grid constraints resulted in run-times of more than 20 days on conventional desktop computers, which could only slightly be reduced using more powerful computers. Therefore, a two-step approach that reduces computing time to an acceptable level is used to determine the development of co-generation plants. The construction of additional co-generation units is mainly determined by the location of the heat demand in combination with the location of dismantled co-generation plants rather than by possible restrictions in the power grid. In the model calculations, the new co-generation plants that are commissioned to replace old co-generation stations are therefore first determined in a model run neglecting the grid restrictions. In a further step, these co-generation plants are taken into account when calculating the optimal long-term power plant commitment and expansion using PERSEUS-NET.

7.2. Development of the German power system in the base scenario

In this section, the reference case scenario regarding the development of the German power system is analyzed using the nodal pricing-based energy system model developed in chapter 5. Firstly, the evolution of nodal prices and congestion, which are the basis for the optimal unit commitment and investment decisions, are described. Then, the average marginal cost of power supply is addressed. Based thereupon, the resulting overall development and regional distribution of the structure of the capacity mix and power generation in Germany are presented. In the last part of this section, the evolution of the CO_2-emissions is addressed.

7.2.1. Nodal prices and congestion

In PERSEUS-NET, nodal prices are used as price signals to plan an optimal, regional power station capacity expansion. As outlined in chapter 3, nodal price differences occur if the power system is congested. By contrast, if no bottleneck in the system exists, nodal prices are identical at all grid nodes.

In the following, the regional developments of power grid congestion and nodal prices are presented. Section 7.2.1.1 addresses the development of average annual nodal prices in Germany, while section 7.2.1.2 addresses the development of nodal prices and power generation in selected time slots. The latter aims to show the situation in the German transmission grid in situations of extreme system load. Finally, section 7.2.1.3 outlines the relationship between regional nodal prices and capacity expansion. It should be noted that due to the uniform temporal distribution of offshore wind power feed-in, situations with maximum wind power feed-in cannot be taken into account. Thus, the levels of congestion and nodal prices occurring in the real world are likely to be underestimated. This underestimation is intensified because only active power flows are considered.

7.2.1.1. Development of the average annual nodal prices and congestion

In the BASE scenario, the situation in the German transmission grid can be divided into two main time segments. In the first time segment, from 2007 to 2020, no structural bottlenecks exist. By contrast in 2025 and 2030, structural bottlenecks occur. As will be shown in the following, they have an influence on the development of nodal prices as well as on regional power generation and capacity expansion.

Figure 7.1 shows the development of congestion in the BASE scenario. The base year 2007 is not illustrated, because no binding line constraints exist in the German power system. Moreover, between 2010 and 2020 only local bottlenecks resulting from congested stub lines occur. Thus, since no structural bottlenecks occur in the German transmission grid between 2007 and 2020, nodal prices are identical at all or almost all grid nodes. Figure 7.2 shows the regional development of average annual nodal prices in the BASE scenario. The average annual nodal prices correspond to the yearly averages of the nodal prices in the individual time slots. Between 2010 and 2020 only minor variation in average annual nodal prices in Northern Germany exist, which result from the congested stub lines. The resulting nodal price difference is rather small, varying between 0.01 €/MWh in 2010 and 1.17 €/MWh in 2015.

From 2025 on, zones with differing nodal prices develop within Germany. In 2025, two price zones exist, which result from congestion on a line connecting Diele and Rhede in Northwest Germany (see Figure 7.1). Yet, the nodal price differential between the price zones is very small. While average annual nodal prices at the side of the bottleneck with a capacity surplus (surplus side), amount to 69.83 €/MWh, nodal prices at the side of the bottleneck with a capacity deficit (deficit side) total 69.87 €/MWh. The generation surplus in Northwest Germany results from high offshore wind power feed-in. Moreover, average annual nodal prices in the other German grid nodes amount to 69.85 €/MWh in 2025.

By 2030, there are pronounced nodal price differences between North and South as well as between East and West Germany, which are caused primarily by congestion in north-south direction in the Northwest. The power line connecting Diele and Rhede is congested during all time slots. Moreover, five adjacent lines are congested in 7 - 79% of the time slots. The nodal price difference in north-south direction are increased by congestion on a line near Frankfurt, which is congested during 31% of the time slots. In the North, the nodal prices are far below the 2025 minimum level. It is notable that in the Northeast at and close to the grid nodes with high offshore wind power feed-in, nodal prices drop to an annual average of 5.23 €/MWh. The highest average nodal prices (97.73 €/MWh) occur at the deficit side of the bottleneck Diele - Rhede. Moreover, in the East and South of Germany nodal prices increase slightly above 2025 level and range between 65 €/MWh and 75 €/MWh. The reason for the increasing nodal price differences is congestion in north-south direction.

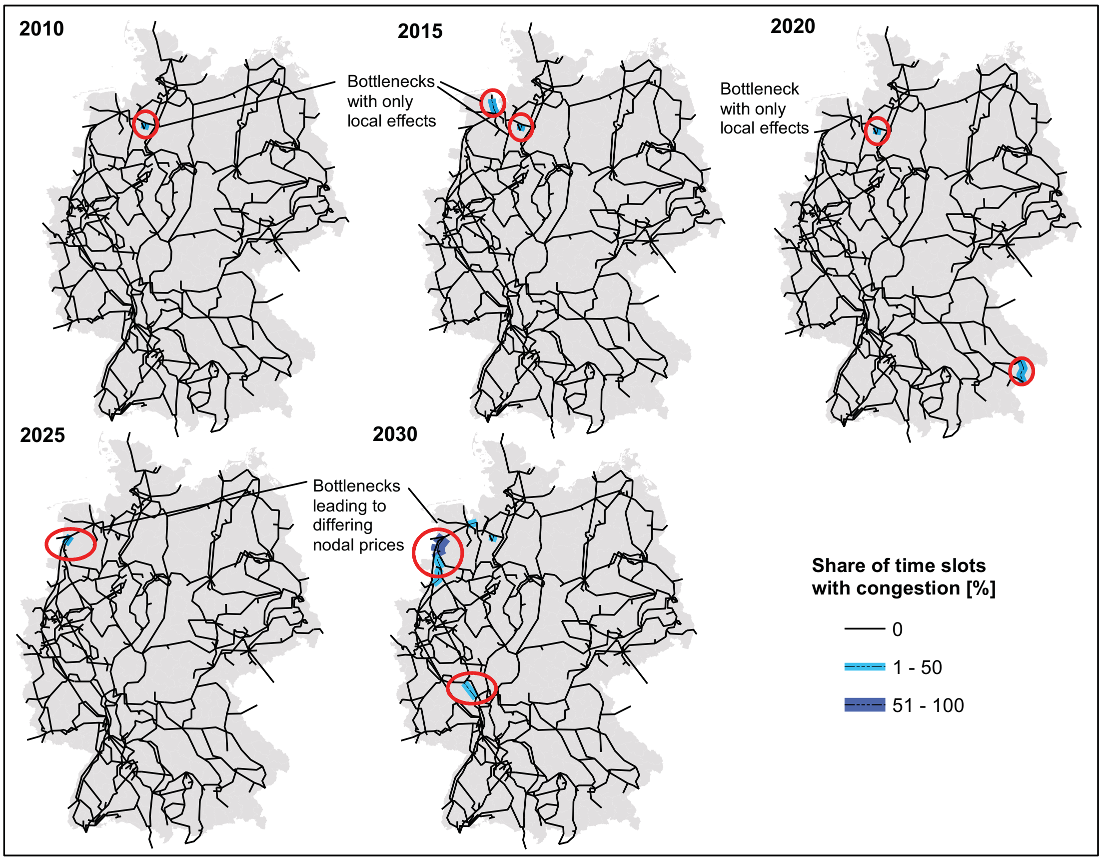

Figure 7.1.: Development of congestion in the BASE scenario

In the following nodal prices and grid congestion in selected time slots are analyzed to give a better understanding of the situation in the German transmission grid in different load situations. In doing so, the regional distribution of power generation during those situations will also be addressed. Thereafter, the influence of congestion and nodal prices on capacity expansion is discussed.

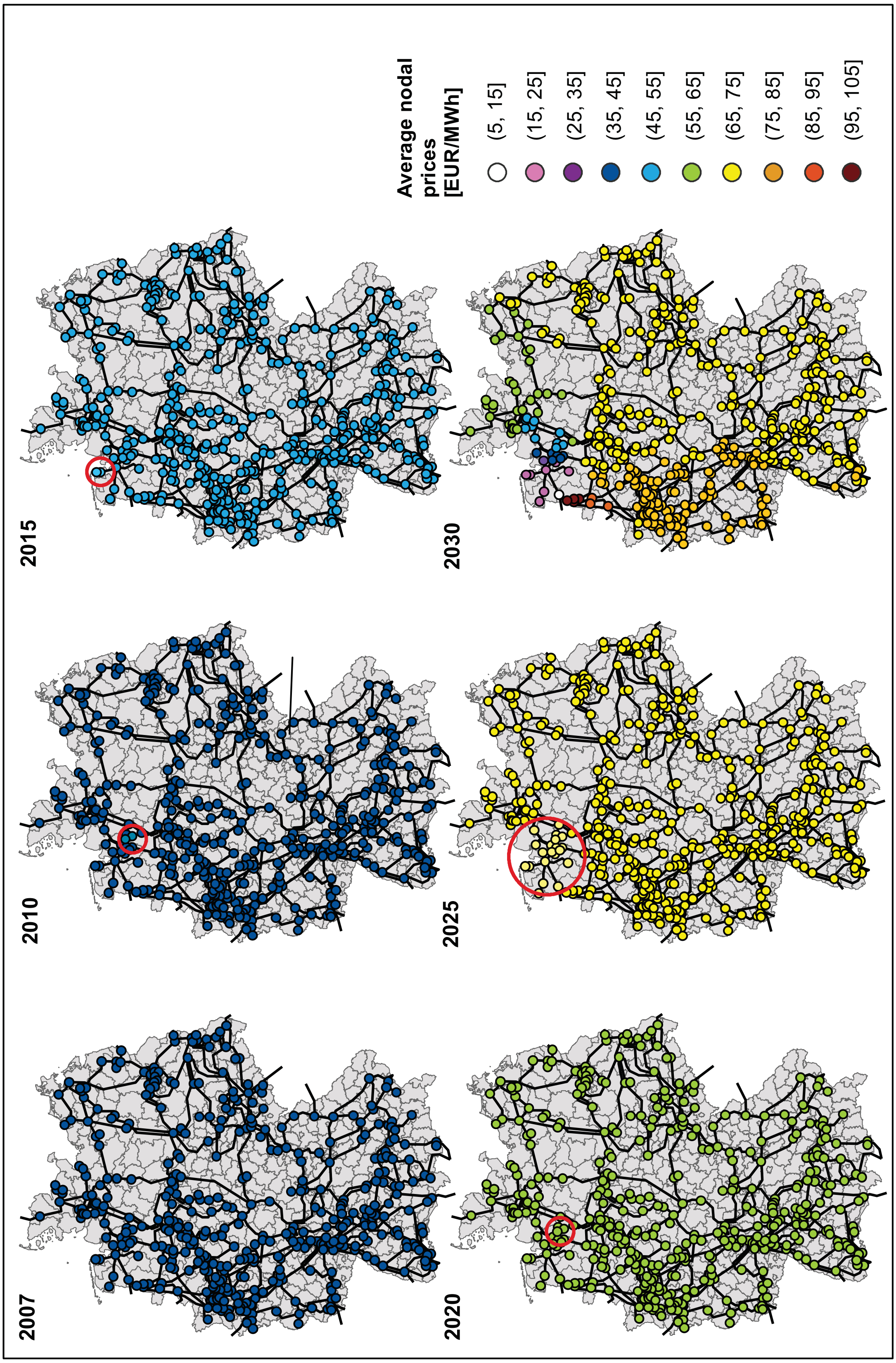

Figure 7.2.: Development of the average annual nodal prices between 2007 and 2030 in the BASE scenario

7.2.1.2. Nodal prices, congestion, and power generation in selected time slots

As described in chapter 3, differing nodal prices occur if there is congestion in the power grid. In the following, the situation in selected time slots in 2025 and 2030 is discussed. The periods 2007 - 2020 are not further discussed, because congestion in those periods has only local and negligible effects on nodal prices.

In 2025 congestion in the transmission system occurs on autumn and winter week-ends between 18:00 and 21:00. It is highest during autumn weekends. Figure 7.3 (left) shows the grid situation and the resulting nodal prices on autumn weekends in 2025 between 18:00 and 21:00, while Figure 7.3 (right) illustrates the regional distribution of power generation at that time. For reasons of clarity, only grid nodes with a power generation exceeding 1 GWh in the selected time slot are depicted. In the upper left corner, the congested corridor between Diele and Rhede that causes the differing nodal prices in the German transmission system in the first place is marked.

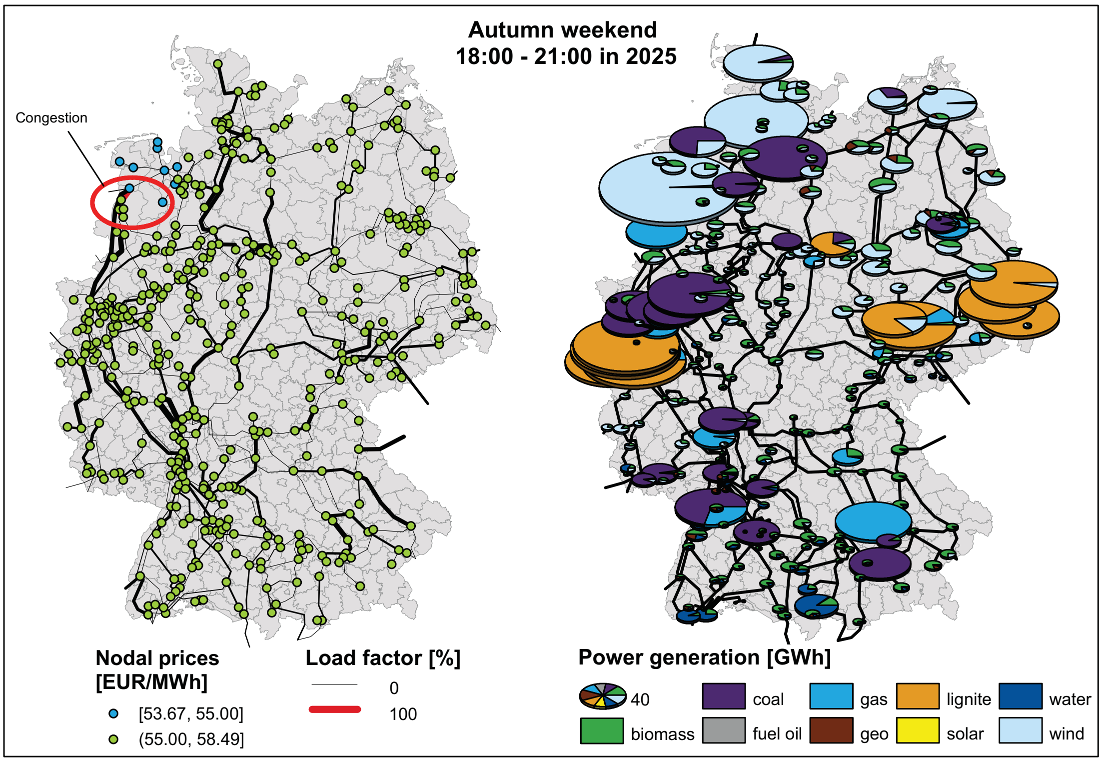

Figure 7.3.: Nodal prices, congestion, and generation on autumn weekend evenings in 2025 in the BASE scenario

Above all, congestion on that corridor is caused by offshore wind power feed-in from the North Sea of approximately 8.9 GWh/h, which cannot be used on the ground, but has to be transferred to the South. Furthermore, power injections by coal-fired thermal power stations in the same area (see Figure 7.3 (right)) that have to be used to meet the high demand in Germany intensifies the power flows in north-south direction, and, in particular, on the Diele - Rhede corridor.

By 2030, the power line between Diele and Rhede is congested during all time slots, because of the further increasing offshore wind power feed-in. Figures 7.4 and 7.5 show the spatial distributions of nodal prices and power generation at annual maximum and minimum system load, respectively. Like the average nodal prices in 2030 (see Figure 7.2), nodal prices in Northwest Germany, at the grid nodes or close to the grid nodes with high offshore wind power feed-in, are below 5 €/MWh at almost all time slots because of severe grid congestion. Nodal prices can drop below the marginal cost of the cheapest unit in the power system due to binding line flow constraints. Moreover, the ramping and opportunity cost of inflexible power stations can have a price reducing effect. The reasons for the low nodal prices in the region with high offshore wind power feed-in are, on the one hand that in PERSEUS-NET load change costs are considered for nuclear, lignite, and coal-fired power stations. The increasing wind power feed-in close to the North Sea causes the shutdowns of base load capacities in 2030 particularly in times of low demand. As shown in Figure 7.5 (right), the lignite-fired power stations are partly shut down in times of low system load. On the other hand, higher demand on the grid nodes with very low nodal prices would decrease the power flow on the lines connecting Conneforde and Diele.

Regarding the power generation at annual peak load, again, all large thermal power stations seem to be operating at full load. In addition to the power stations already existing in 2025, Figure 7.4 (right) shows a new gas-fired power station that is operating in Northern Germany at the left hand side of the congested Diele - Rhede corridor, whose power injections create a counter flow on the congested line. In the time slot of minimum annual system load (see Figure 7.5), the congested Diele - Rhede corridor persists. Nodal prices at the surplus side of the congested corridor amount to 4.65 €/MWh. At the other German grid nodes, nodal prices do not rise above 80.62 €/MWh. The highest nodal prices occur again at the left hand side of the congested corridor. Moreover, nodal prices are highest in the West of Germany.

The distribution of power flows is different in times of low system load than at high system load. The load factor on lines in east-west direction increases in times of low system load (see Figure 7.5). Regarding the power generation in times of low system load, on- and offshore wind turbines are the predominant power suppliers. Yet, to avoid system failure, which, in the optimization corresponds to model infeasibilities caused by binding line constraints, the offshore wind power feed-in at minimum load is slightly reduced by the optimizer. Lignite-fired power stations are the only remaining operational base load capacities, of which most are operated at part load. Furthermore, several gas-fired power stations operate in North and West Germany, on the one hand to create a counter flow and, on the other hand, to balance fluctuating wind power feed-in.

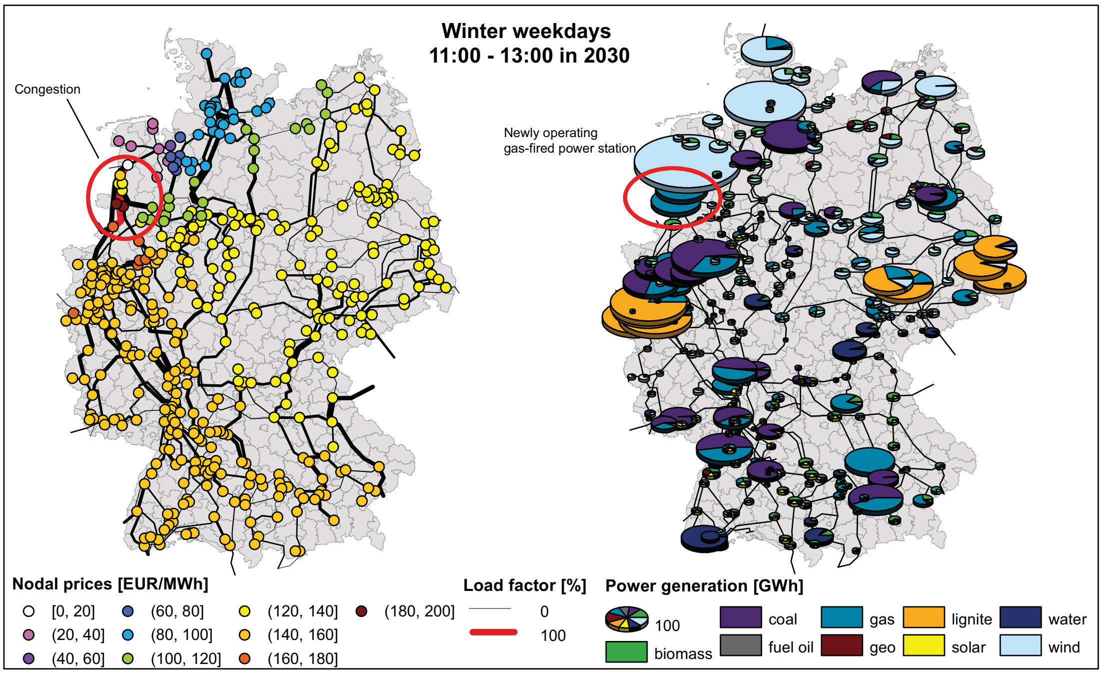

Figure 7.4.: Nodal prices, congestion, and generation at max. load in 2030

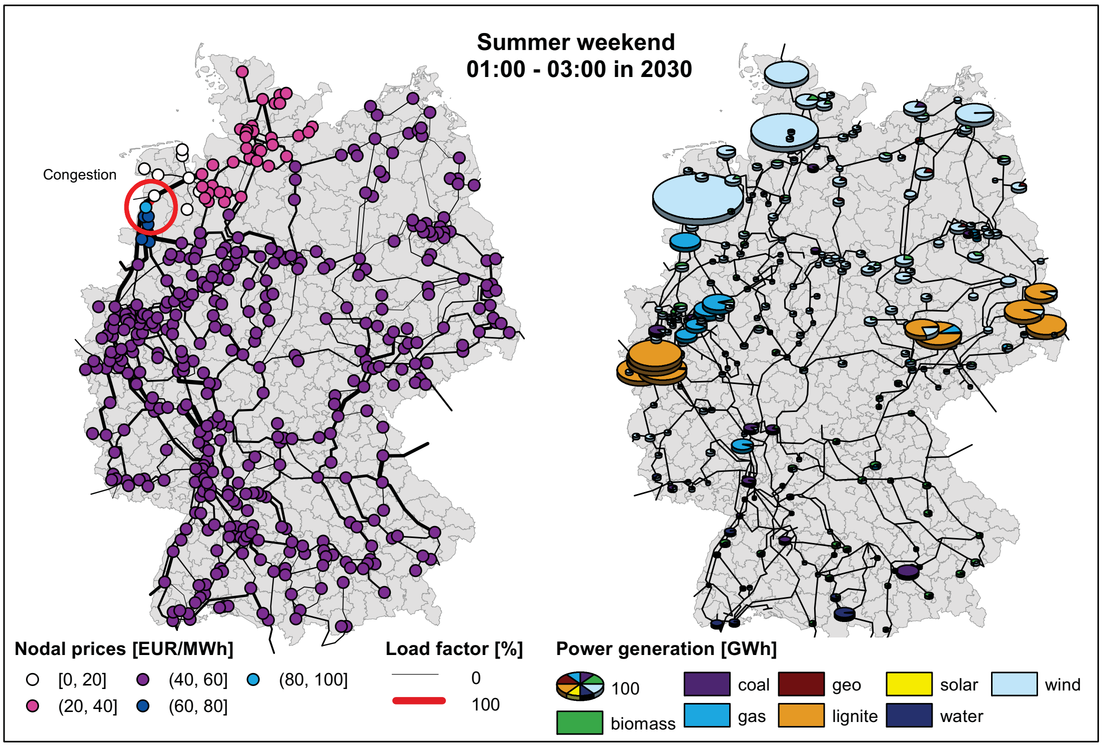

Figure 7.5.: Nodal prices, congestion, and generation at min. load in 2030

7.2.1.3. Nodal prices and capacity expansion

Concerning the regional distribution of additional generating capacities, the influence of grid congestion and hence differing nodal prices is obvious comparing 2025 and 2030 results. Figure 7.6 shows the regional distribution of new generating capacities in 2025 and 2030. Apart from the coal-fired heat and power stations, whose location is dependent on the regional heat demand, and the economically favorable lignite power stations that are located close to the lignite mining sites, a number of new gas-fired power stations is sited at locations that are favorable from a grid perspective by 2030. In 2025 all new power stations are situated outside the low price area in Northwest Germany. In particular new lignite-fired power station in the Rhenish lignite mining district are constructed (see Figure 7.6 (left)).

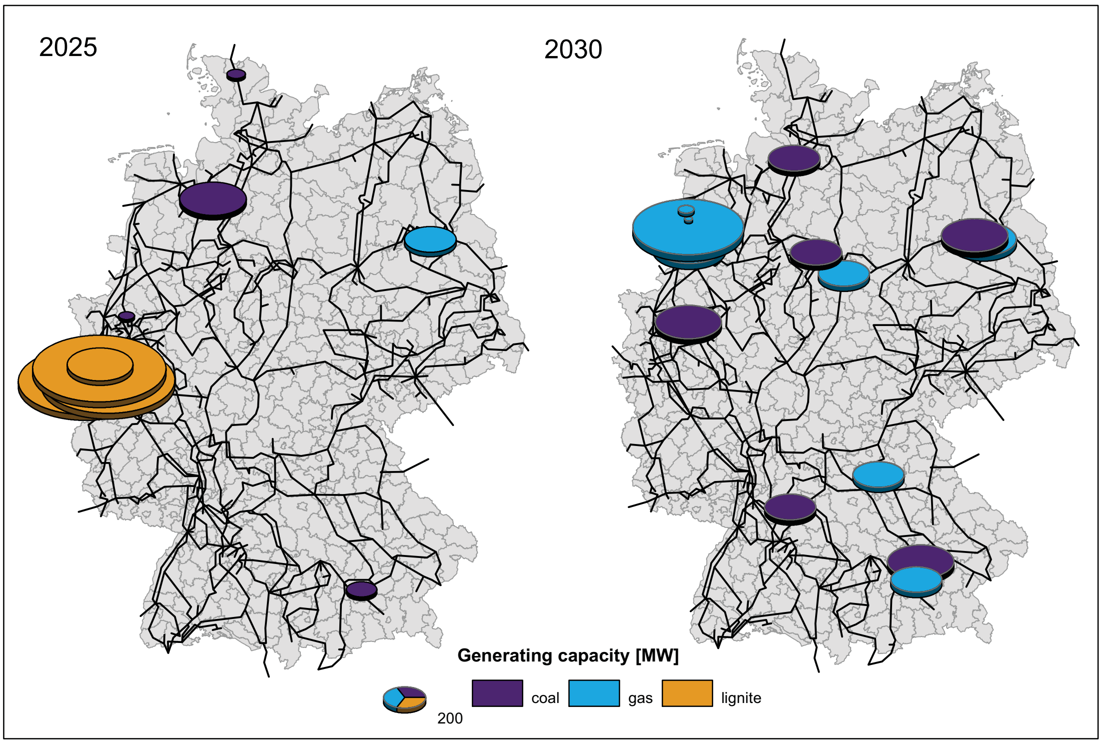

Figure 7.6.: Spatial distribution of additional generating capacity built in 2025 and 2030 in the BASE scenario

In 2030 two additional natural gas combined cycle (NGCC) and two pulverized coal combustion (PCC) stations are constructed in the south of Germany which remains short on generating capacity. The NGCC power stations are located on grid nodes with high nodal prices where only the comparatively expensive gas is available. Furthermore, a 1.5 GW and a 600 MW NGCC power station are built at the deficit side of the bottleneck, which is characterized by the highest nodal prices in Germany. In times of high system load, these power stations are used to create a counter flow at the bottleneck in Northern Germany.

7.2.2. Average annual marginal cost of power supply in Germany

In nodal pricing, differing nodal prices arise at the grid nodes if there is congestion in the power system. By contrast, if there is no congestion in the system, the nodal prices are identical at all grid nodes. Thus, if there is no congestion in the German power system during a year, the average annual nodal prices are identical to the average annual marginal cost (MC) of power supply in Germany. Otherwise, the average annual marginal cost of power supply corresponds to the yearly weighted averages of the nodal prices.

The average marginal cost of power supply increase in the BASE scenario from 38.50 €/MWh in 2007 to 70.15 €/MWh in 2030 (see Table 7.1). The rise is most pronounced between 2020 and 2025, when average annual marginal cost rise by 10.57 €/MWh. This is, induced by the shut-down of the last remaining nuclear power stations as well as by the increase in primary energy carrier prices. Moreover, fuel oil-fired power stations are more intensively used in times of peak load in 2025, which additionally increases the marginal cost of power generation in times of peak load in this period. The average peak load marginal cost increase from 57.18 €/MWh in 2007 to 98.10 €/MWh in 2025. By 2030 they decrease to 90.50 €/MWh, again, because of the less intensive use of fuel oil in the last period. Moreover, the marginal cost of base load power generation rise from 28.82 €/MWh in 2007 to 58.81 €/MWh in 2030.

Table 7.1.: Development of the average marginal cost in Germany from 2007 to 2030 in the BASE scenario

	2007	2010	2015	2020	2025	2030
Avg. MC [€/MWh]	38.50	41.32	50.43	59.28	69.85	70.15
Avg. MC peak [€/MWh]	57.18	58.71	66.26	77.15	98.10	90.50
Avg. MC off-peak [€/MWh]	28.82	31.58	43.47	50.15	55.64	58.81

7.2.3. Structure of the capacity mix

In the BASE scenario, significant changes in the structure of the capacity mix occur between 2007 and 2030. Figure 7.7 shows the overall development of generating capacity in Germany in the BASE scenario. Together with Figure 7.9, which illustrates the regional development of generation capacity, it gives an overview over the restructuring process of the German capacity mix within the covered time horizon of the optimization.

To avoid having too many categories, renewable energy carriers are totally or partly aggregated. RES in Figure 7.7 covers all renewable energy carriers specified in section 6.6. In Figure 7.9 the specification “wind” contains onshore wind turbines as well as offshore wind turbines. Similarly, “solar” covers roof-top PV installations as well as open-area installations. The “biomass” category comprises solid and gaseous biomass, which is specified in more detail in section 6.6. Moreover, “water” summarizes the run-over-river as well as storage and hydro pumped storage power stations (HPS). As a reference, the size of the pie in the legend of Figure 7.9 indicates the size of 5000 MW of power station capacity in the figure.

7.2.3.1. Overall development of the capacity mix

In the BASE scenario, the forecasts show an overall increase in total generating capacity between 2007 and 2030. Comparing the first and the last optimization periods, the installed capacity augments by 15%, increasing from 131.0 GW in 2007 to 150.4 GW in 2030. Between 2007 and 2015, total installed net capacity increases, while it decreases by 3% in 2020. Until 2015, installed capacity is in accordance with the development of the power demand (see Figure 6.6), while power demand and installed capacity move in opposite directions in the last optimization periods. This opposite effect of power demand and capacity development in the last optimization period indicates a less intensive utilization of generating capacity, which will be addressed in section 7.2.4 in more detail.

The changes in the capacity mix are strongly affected by the predetermined rise in RES-E capacities from 31.6 GW in 2007 to 86.5 GW in 2030 (for more detail see section 6.6). The generating units using RES have the highest share in totally installed capacity rising from 25% in 2007 to 58% in 2030. Furthermore, the phasing-out of nuclear power stations demands a replacement of existing base load capacities. Nuclear power stations are decommissioned as predefined partly in 2015 (7.5 GW) and 2020 (3.9 GW) and fully by 2025 (8.1 GW). The dismantled nuclear base load capacities are replaced to a large extent by the increase in RES-E capacity. The replacement of base load capacity by RES-E capacity is above all due to the assumption of uniformly distributed availability of RES-E feed-in (see section 6.6).[1]

The development of fossil-fueled generating capacities can be divided into two main time segments. The first segment ranges from 2007 to 2015. In the first time segment, the development of power generating capacities is strongly influenced by power stations whose commissioning is predefined, because they are already under construction or in an advanced phase of planning when the analysis was conducted. Until 2015 their capacity and the rise in RES-E generating capacities are sufficient to replace the phasing-out nuclear power stations as well as the decommissioned fossil-fueled capacities. By contrast, in the second time segment, which ranges from 2020 to 2030, the capacity development is strongly influenced by the optimization. Figure 7.8 shows the power station capacity expansion which result from the optimization.[2] In total, 7.4 GW of new lignite-fired pulverized coal combustion (PCC) power stations, 5.0 GW of new coal-fired PCC power stations, and 5.1 GW of NGCC power stations are commissioned

[1] The advantages and disadvantages of this way of modeling the RES-E feed-in will be further discussed in chapter 8.

[2] It comprises conventional power stations as well as co-generation units.

between 2010 and 2030. In the following, the development of the technologies in the capacity mix in the second time segment is described.

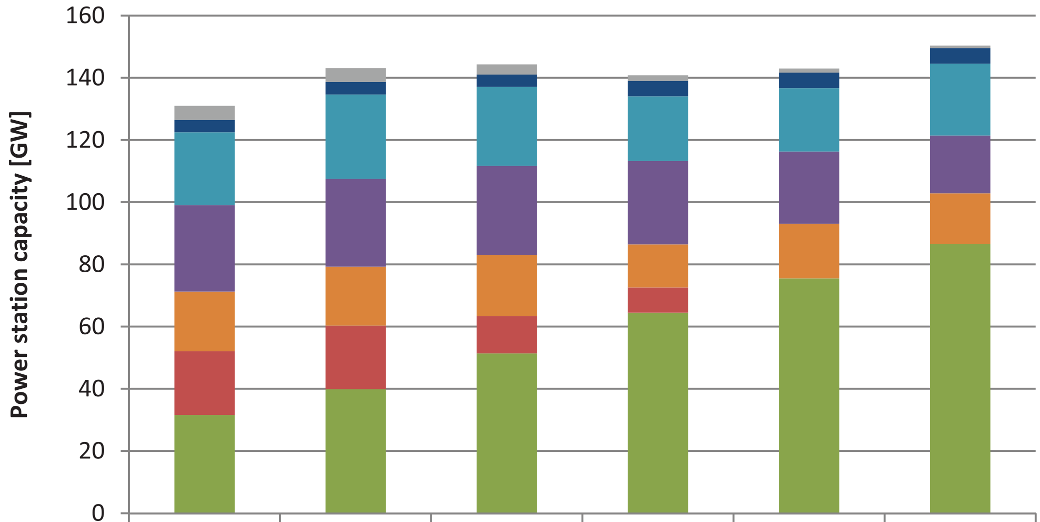

	2007	2010	2015	2020	2025	2030
fuel oil	4.5	4.5	3.3	1.8	1.3	0.8
HPS	4.0	4.0	4.0	5.0	5.0	5.0
gas	23.4	27.1	25.4	20.8	20.4	23.1
coal	27.8	28.3	28.7	26.8	23.2	18.6
lignite	19.2	18.9	19.6	13.8	17.6	16.3
nuclear	20.5	20.5	12.0	8.1	0.0	0.0
RES	31.6	39.9	51.4	64.5	75.5	86.5

Figure 7.7.: Overall development of the total power generating capacities in the BASE scenario

Most coal-fired power stations reaching the end of their (technical) lifetime are not replaced by modern coal-fired power stations. Between 2020 and 2030 total installed net coal-fired power station capacity decreases by 8 GW. Only 3 GW of old coal-fired power stations are replaced by modern, more efficient ones. The remaining decommissioned coal-fired power station capacity, is also replaced by the steep rise in RES-E capacity. By 2030, coal-fired power station capacity has a share of 12.4% in total net installed capacity.

The installed capacity of lignite-fired power stations between 2020 and 2030 is between 13.8 GW and 19.6 GW. In 2030 it amounts to 16.3 GW, which corresponds to 10.9% of the total installed capacity. The capacity gap is entirely filled up by capacities using RES, again. Neither new coal nor new lignite-fired power stations are built with CCS technology. Thus, the assumed EUA prices are too low to compensate the significantly higher investments of power stations with CCS compared to conventional PCC technologies.

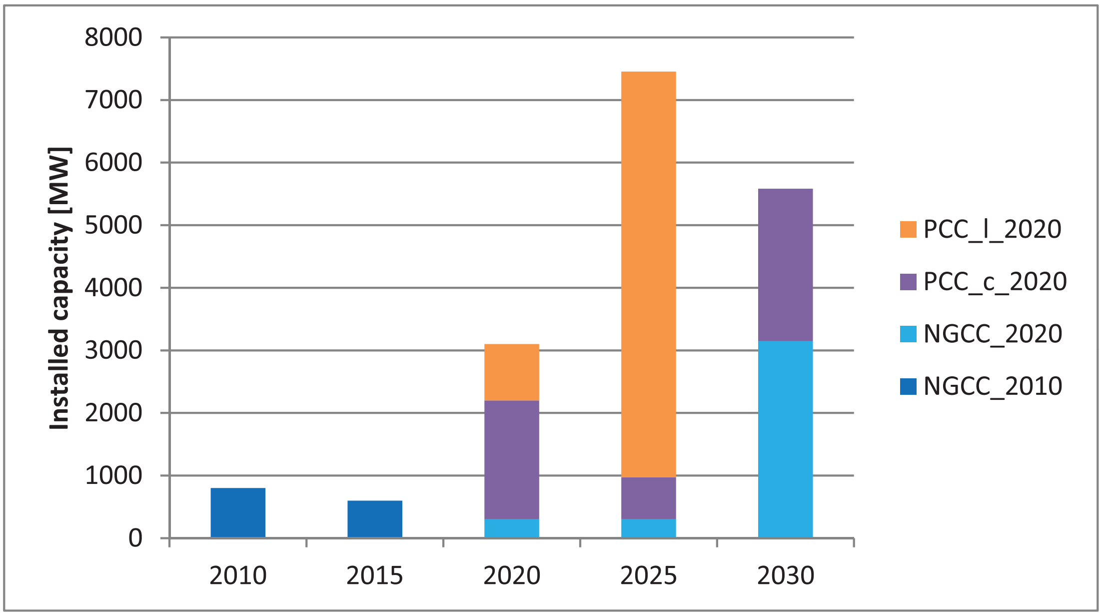

Figure 7.8.: Power station capacity commissioned in the BASE scenario

Regarding the installed capacity of gas-fired power stations, only small variations of up to 3 GW occur. In 2030 the share of gas-fired power stations accounts for 15.4% of the total installed capacity.

As predefined, the construction of the hydroelectric pumped storage power station in Atdorf increases the totally installed HPS capacity from 4 GW in 2007 to 5 GW in 2030. By contrast fuel oil capacity almost complete disappears by 2030.

Regarding the commissioning of new heat and power plants, total 8.9 GW of the capacity additionally commissioned between 2010 and 2030 are built as co-generation plants, which replace 11.9 GW of old decommissioned co-generation capacity. Approximately 50% of the additional co-generation capacity is realized as hard coal-fired PCC plants, while 36% are built as NGCC power stations. Furthermore, one lignite-fired co-generation station is built in 2020. Until 2015 gas-fired power stations are preferred over coal-fired stations. Because of increasing gas prices PCC plants are built at grid nodes at which coal is available, while at grid nodes without coal supply gas-fired power stations are built. Thus, the assumed CO_2-prices of 45 Euro/tCO_2 in 2030 is not high enough to trigger a fuel switch from carbon intensive fuels, such as lignite and coal, to the less carbon intensive gas, because the CO_2-price increase is overcompensated by increasing gas prices.

7.2.3.2. Regional development of power station capacities

As with the overall capacity development, the regional capacity development is strongly influenced by the development of power generation from renewable energy sources (see Figure 7.9). Over the time horizon of the optimization, especially offshore wind turbine capacity increases significantly in North Germany, while PV capacity rises in particular in the southern federal states as well as in the large metropolitan areas. Retiring conventional thermal power stations, in particular coal-fired and nuclear ones, are to a large extent not or only partly replaced by new conventional stations. In total, conventional power generating capacity decreases by 15.4 GW in Southern Germany (see Figure 7.9).

Installed capacity decreases by 0.6 GW near Bremen, by 1.3 GW near Saarbrucken, by 5.0 GW between Karlsruhe and Mannheim, and by 2.6 GW around Munich. In the area of Frankfurt power station capacity increases by 1.5 GW. In Berlin 0.8 GW coal and 1.0 GW of fuel oil-fired power stations are replaced by 0.8 GW of NGCC and 0.5 GW PCC power stations. Moreover, additional 1.8 GW coal-fired PCC capacity is built in Hamburg. In the highly industrialized and densely populated Ruhr district, the installed coal- and gas-fired power station capacity decreases by 1.6 GW comparing 2007 and 2030 levels.

Regarding lignite-fired power stations, the optimization results suggest that lignite-fired power stations near the Helmstedt lignite mining district disappear completely by 2030. Moreover, lignite-fired power station capacity in Lusatia increases by 0.7 GW in 2015 before it declines again by 2.8 GW until 2030. In the central German lignite mining district it remains at a constant level. Regarding the Rhenish districts, the installed capacity decreases between 2010 and 2020 by 7.7 GW and increases again by 6.5 GW in 2025.

In the following, initially the overall development and then the development of the regional structure of power generation in the BASE will be outlined.

7.2.4. Structure of power generation and capacity utilization

7.2.4.1. Overall development of power generation

Like power demand, the overall power generation in Germany increases by 2.2% over the covered time horizon. The following figures give an overview of the changes in the German power generation mix till 2030. While Figure 7.10 illustrates the overall development, Figures 7.11 and 7.12 show the unit load in the BASE scenario by time slot for the seasons winter and summer in 2007 and 2030, respectively.

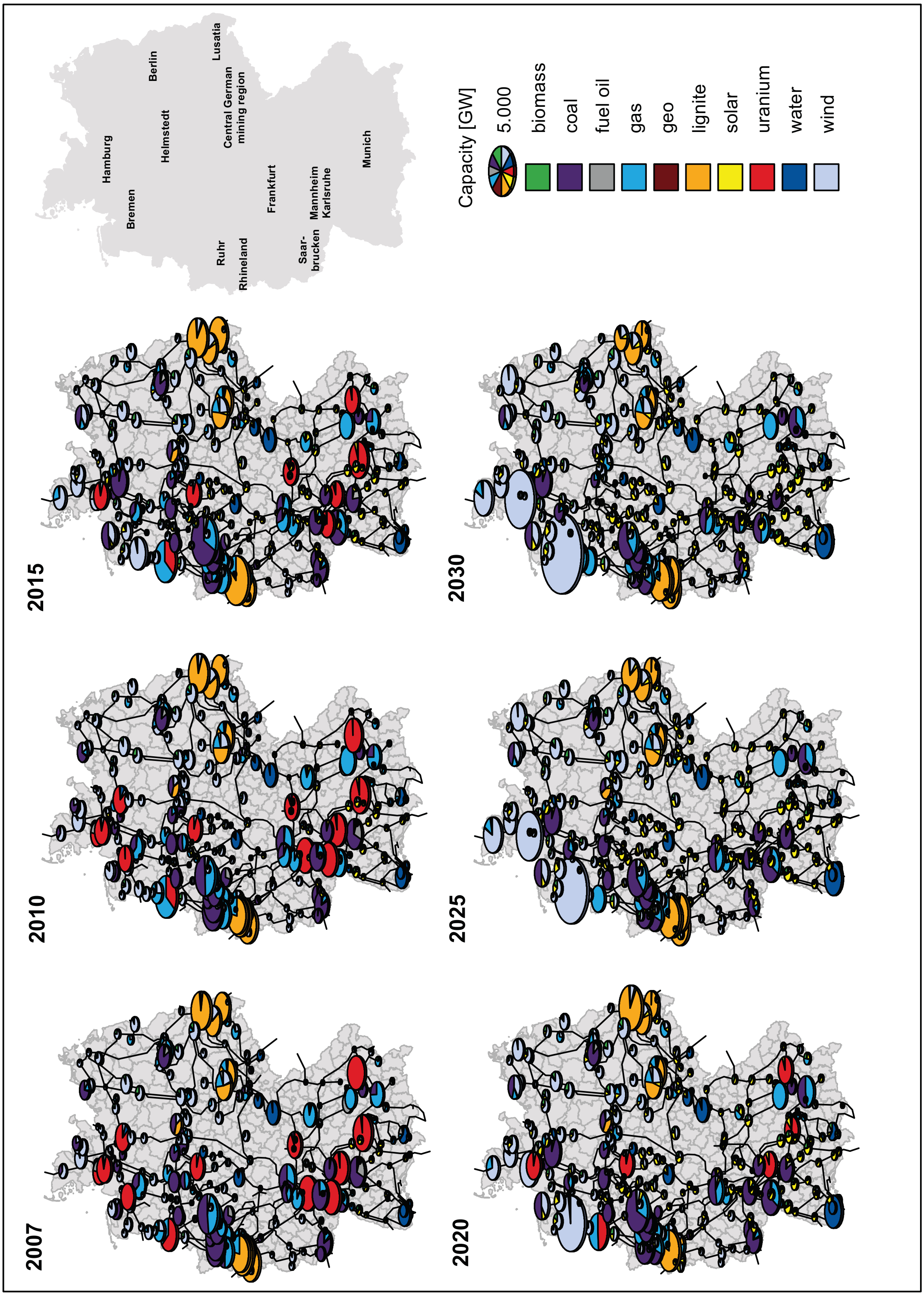

Figure 7.9.: Regional development of power generating capacity between 2007 and 2030 in the BASE scenario

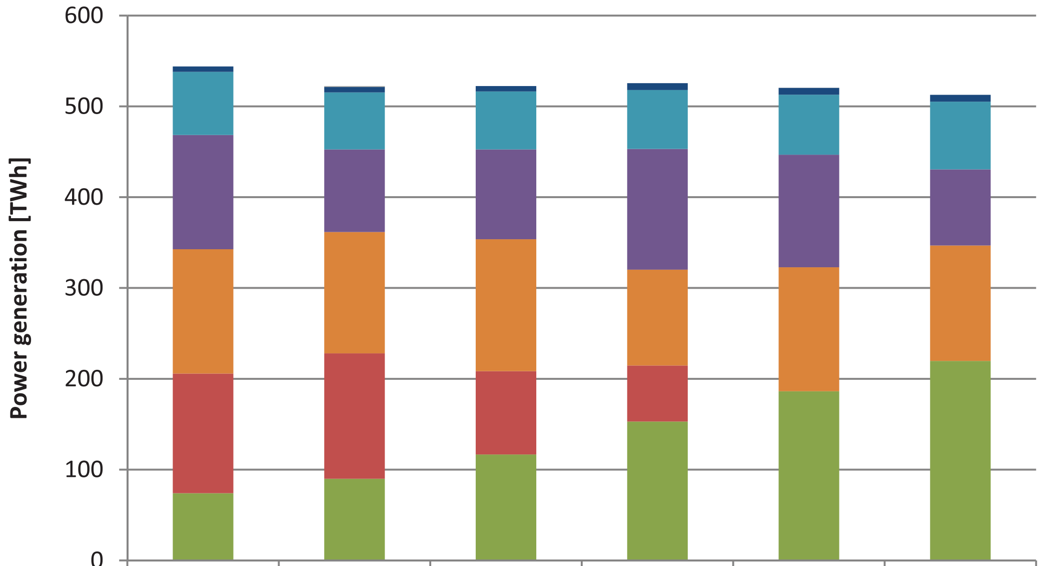

	2007	2010	2015	2020	2025	2030
fuel oil	0.0	1.0	0.0	0.0	0.1	0.0
HPS	6.0	6.0	6.0	7.5	7.5	7.5
gas	69.4	62.8	63.8	64.9	66.1	74.6
coal	125.8	91.0	99.0	133.0	123.9	83.7
lignite	137.0	133.6	145.2	105.4	136.5	127.2
nuclear	131.7	138.1	91.8	61.7	0.0	0.0
RES	74.0	89.9	116.7	153.0	186.3	219.7

Figure 7.10.: Overall development of power generation in the BASE scenario

As with the RES-E generating capacity, power generation from renewable sources increases significantly between 2007 and 2030. It rises from 74.0 TWh in 2007 to 219.7 TWh in 2030, which corresponds to a total share in power generation of 42.8% (see Figure 7.10). The fact that the share in power generation is significantly lower than the shares in totally installed capacity indicates that RES-E capacities have comparatively lower average full load hours than most conventional power stations. Due to the model assumptions, RES-E capacities are modeled with a uniform distribution over the time slots. Yet, to avoid grid-caused infeasibilities due to strongly increasing offshore wind power feed-in, the optimizer can turn down offshore wind production to a certain extent. Figure 7.12 shows that it makes use of this option in 2030 in the summer in times of low system load (0:00 - 4:00 am).

The development of carbon based electricity generation is strongly influenced by the predefined gap between increasing RES-E generation and decreasing generation from nuclear energy (see Figure 7.10). In 2007, lignite and uranium are used as base load technologies that are operated at full load around the year, while coal- and gas-fired power stations are operated as intermediate and peak load power plants (see Figure

7.11).

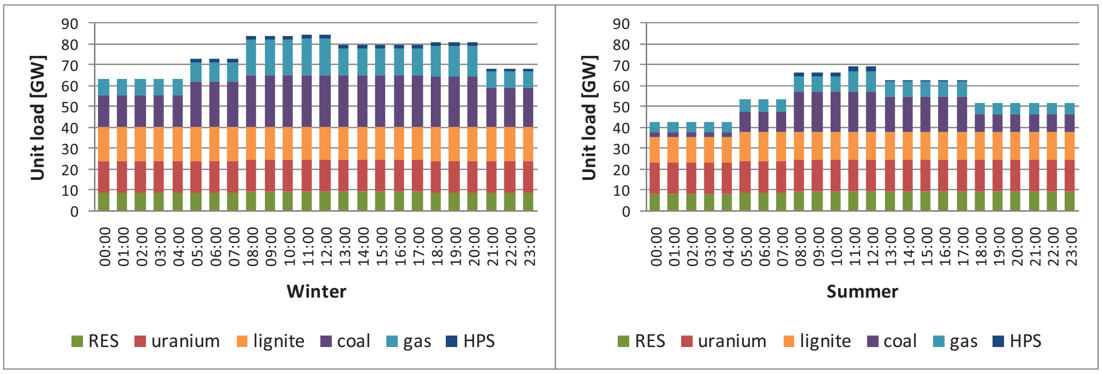

Figure 7.11.: Unit load in the BASE scenario 2007

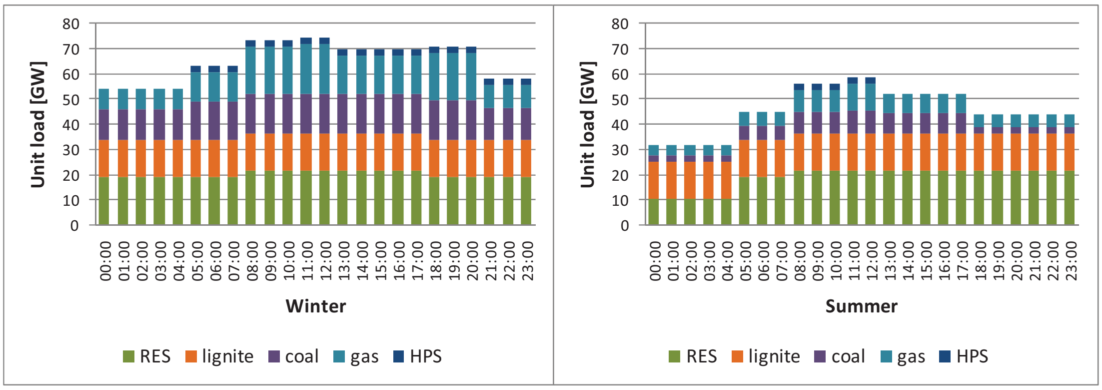

Figure 7.12.: Unit load in the BASE scenario 2030

In accordance with the results regarding the capacity mix, lignite power generation stays at a constantly high level between 133.6 TWh and 145.2 TWh until 2015 (see Figure 7.10). In 2020, power generation from lignite declines to 105.4 TWh, but increases again in 2025. By 2030 it decreases, again, and amounts to 127.2 TWh. Comparing the first and the last optimization period it remains the second most important fuel in power generation. In 2015 power generation from lignite replaces part of the decreasing nuclear production and reaches with 145.2 TWh the highest share in power generation. The full load hours of lignite-fired power stations increase from 7171 h/a in 2007 to 7726 h/a in 2030.

Coal-based power generation decreases between 2007 and 2010 from 125.8 TWh to 91.0 TWh. In the following periods it increases again and reaches a level of 133.0 TWh by 2020. Thus, it fills up part of the gap resulting from the phase-out of nuclear power stations and declining generation from lignite (see Figure 7.10). Since after 2020 offshore wind power becomes more and more important, it decreases again and reaches a level of 83.7 TWh in 2030. While the share of coal in power generation amounts to 23.1% in 2007, it decreases to 16.3% by 2030. Comparing the changes in installed capacity and electricity generation of coal-fired power stations shows that the generation increase in 2020 is not reached by installing additional capacities, but rather by a more intensive utilization of existing capacities. The average full load hours of coal-fired plants rise from 4634 h/a in 2007 to 5264 h/a in 2020. By 2030, they reach a level of 5327 h/a. The reduced relevance of coal-based power generation in 2030 becomes also obvious by comparing the unit loads in 2007 and 2030 illustrated in Figures 7.11 and 7.12.

Power generation in gas-fired power stations varies between 62.8 TWh and 74.6 TWh in the 2007-2030 period. By 2030 its share in total power generation is, with 14.6%, slightly higher than in 2007 (12.8%). Yet, the capacity utilization of gas power stations decreases by 896 h/a, which leads to the conclusion that gas-fired power stations are primarily used as peak load reserve and to counter grid congestion. Since they are required by the model assumptions as reserve to balance fluctuating RES-E feed-in, they are also used in times of low system load (see Figures 7.11 and 7.12). In 2010 and 2025, gas-fired power stations are backed up by power generation from fuel oil during peak load hours. Yet, the full load hours of the oil-fired power stations amount to less then 200 h/a.

Power generation in HPS power stations stays at a constant level of 6.0 TWh/a between 2007 and 2015 and increases to 7.5 TWh/a from 2020 onwards. In 2007 HPS power stations are used the winter between 5:00 and 24:00, while in the summer they are only used between 8:00 and 17:00. By contrast, during summertime in 2030 HPS power stations are only used between 8:00 and 12:00.

In the following the development of the regional structure of power generation will be addressed.

7.2.4.2. Regional development of power generation

Figure 7.13 shows the regional development of power generation in the BASE scenario. For reasons of clarity, the generation at the grid nodes is only depicted if it exceeds 200 GWh/a. As a reference, the size of the pie in the legend of Figure 7.13 indicates the size of 15 TWh of power generation in the figure. Like the spatial development of the power generating capacity, the regional distribution of power generation shifts from south to north until 2030. In particular offshore wind power generation increases significantly at the coasts. With the phase-out of nuclear power stations, the number of thermal power stations that remain operating in the South decreases. Comparing the first and the last optimization period, power generation in Southern Germany decreases by 66.0 TWh. Furthermore, power generation in lignite-fired stations partly shifts from Lusatia to the Rhineland, while gas and coal-fired power generation in the Ruhr district decreases by 10%.

Particularly in the last optimization period, a significant amount of power generated in newer fossil-fueled power stations in North Germany is replaced by offshore wind power

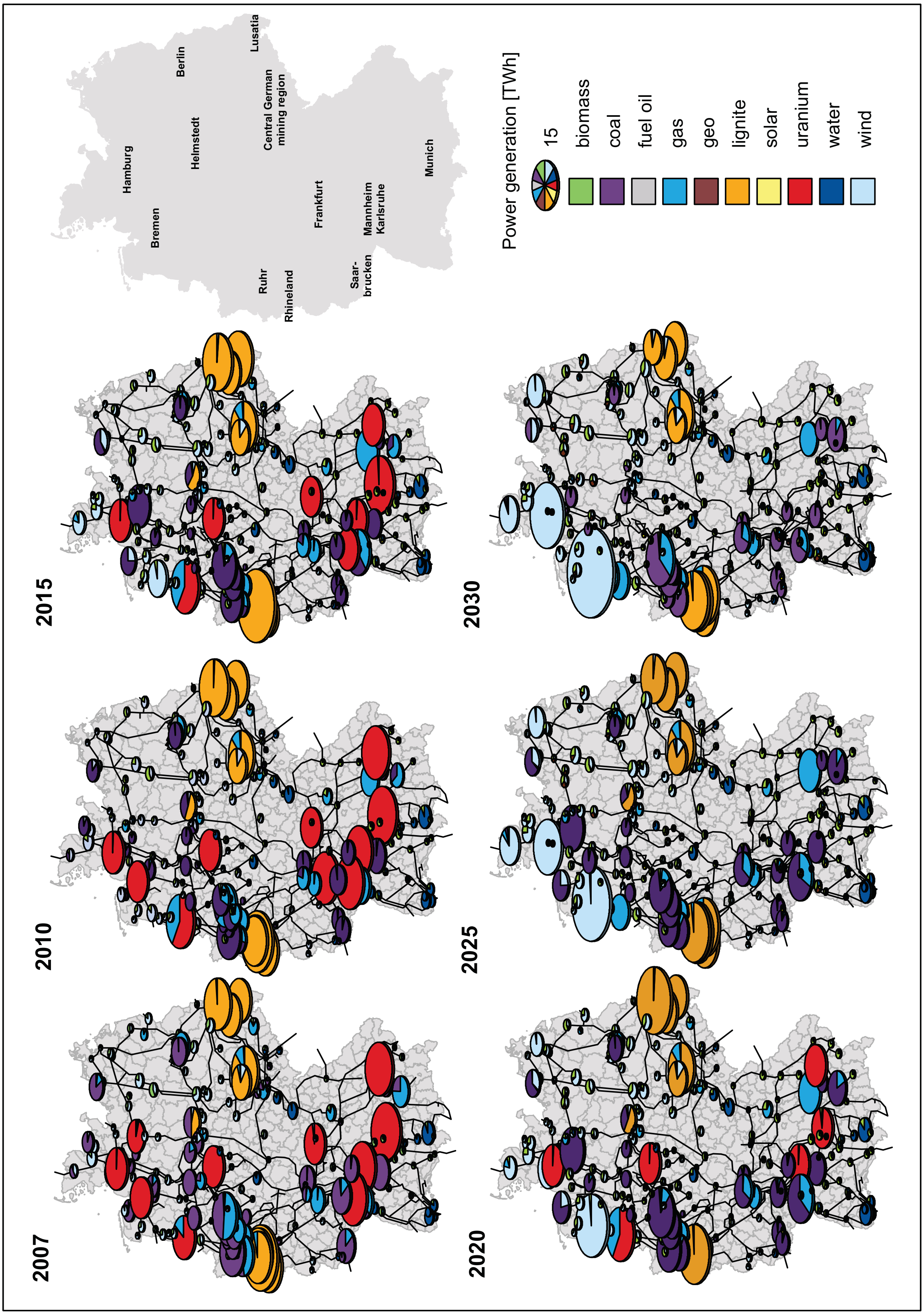

Figure 7.13.: Regional development of power generation from 2007 to 2030 in the BASE scenario

generation. While until 2025 power generation from coal plays an important role around Hamburg, Bremen, and north of the Ruhr area, it is to a large extent replaced by wind power by 2030, except for generation in heat and power stations, which continues to have a small share during the winter.

As predefined based on the lead study, the relevance of distributed RES-E generation increases significantly between 2007 and 2030. In Figure 7.13 this is illustrated by the significantly increased number of 2-5 TWh sized RES-E pies spread across Germany. While distributed generation based on biomass rises in the whole country, onshore wind power increases particularly in the north. Regarding PV, even though capacity increases significantly, solar power still plays a minor role in power generation.[3]

7.2.5. Carbon dioxide emissions

Despite of the phase-out of nuclear power stations, carbon dioxide emissions decrease within Germany from 287.5 Mt CO_2 in 2007 to 204.2 Mt CO_2 in 2030 (see Table 7.2). Yet, the reduction is to a large extent due to the predefined increase of power generation from RES. Carbon emissions from coal-fired power stations decrease by 44.0 Mt CO_2, because, on the one hand, the relevance of coal in power generation is reduced significantly over the covered time horizon. On the other hand, the newly built PCC power stations possess higher efficiencies than the replaced ones. Likewise, carbon emissions from lignite-fired power stations decrease by 37.9 Mt CO_2 comparing 2007 and 2030 levels.

Furthermore, increasing efficiencies of NGCC stations are the reason why carbon emissions of gas-fired power stations decrease by 2.7 Mt CO_2 between 2007 and 2030. Comparing the first and the last optimization period, carbon emissions from lignite decrease by 27.2 Mt CO_2. Above all this is due to higher efficiencies of modern technologies. Yet, no CCS technologies are installed, which would have led to a further decrease in carbon emissions.

Table 7.2.: Development of the CO_2-emissions in the base scenario by fuel type [Mt CO_2 / a]

	2007	2010	2015	2020	2025	2030
coal	106.8	76.3	77.5	103.0	95.3	62.8
gas	28.1	23.6	23.9	24.1	24.5	26.8
lignite	152.6	147.7	154.3	104.5	124.8	114.7
fuel oil	0.0	0.7	0.0	0.1	0.0	0.0
sum	287.5	248.4	255.7	231.5	244.5	204.2

[3] Power from geothermal energy is generated east of Hamburg, north of Berlin, as well as around Karlsruhe and Munich from 2025 onwards. By 2030, total power generation using geothermal energy amounts to 5.7 TWh.

7.2.6. Summary of the results of the BASE scenario

The results of the BASE scenario show that from 2025 onwards, structural bottlenecks occur in the German power grid that result in differing nodal prices in Germany. The most important bottleneck runs from Diele, a grid node with high offshore wind power feed-in, southwards. By 2030, the bottleneck in the Northwest causes average annual nodal price differences of 92.50 €/MWh. In times of system peak load, the nodal price differences rise up to almost 200 €/MWh. Nodal prices are lowest in the Northwest, at and close to the grid nodes with high offshore wind power feed-in, and highest at the deficit side of the bottleneck in the Northwest. Moreover, an overall nodal price differential between Northern and Southern Germany as well as between East and West Germany can be made out. The average annual marginal cost of power supply increases over the covered time horizon from 35.50 €/MWh in 2007 to 70.15 €/MWh in 2030.

Regarding the structure of the capacity mix, lignite and coal-fired power stations still play an important role in 2030. Moreover, the share of gas-fired power stations increases slightly. The regional development of installed power station capacity is, as expected, characterized by a shift from Southern to Northern Germany. Moreover, the optimization results indicate that by 2030 conventional thermal power stations should be located preferably in the Rhineland, Lusatia and the Ruhr area as well as close to the large metropolitan areas of Hamburg, Berlin, Frankfurt, Mannheim, Karlsruhe, Stuttgart, and Munich.

In the overall structure of the generation mix, lignite remains the most important fossil fuel in power generation. However, by 2030 the share of gas-fired power stations in electricity generation increases. The main reason for this increase is that by 2030 flexible power stations are needed to counteract congestion in the transmission grid. Regarding the regional distribution of power generation, a shift from South to North Germany takes place. The main centers of power generation are the lignite mining districts, the Ruhr district, as well as the industrialized areas around Frankfurt, Mannheim, Karlsruhe, Stuttgart, and Munich.

Finally, CO_2-emissions decrease in the BASE scenario from 287.5 Mt CO_2 per year to 204.2 Mt CO_2 per year. This corresponds to an emission reduction of 29%. Since no power stations using CCS are built, lignite-fired power stations remain the most important emitters of CO_2, followed by coal-fired power stations.

7.3. Scenario definitions

The assumptions made in the BASE scenario regarding the technical characteristics of the power system as well as regarding the political and economic framework of power generation are subject to uncertainties. To profoundly analyze the regional development of the German power system under alternative developments of system characteristics and framework conditions, a scenario analysis has been conducted. The scenarios are selected in a way to take the principal influencing factors with respect to the increasing relevance of line constraints and price uncertainties into account. Table 7.3 gives an overview of the selected scenarios.

Table 7.3.: Scenario definitions

Attribute	**Scenario**	**Description**	**Motivation**
Power grid extension	BASE	Power line capacities are assumed as stated in section 6.3. Grid extension is based on EnLAG [2009].	Analysis of the influence of the availability of additional grid capacity.
	GRID	Grid extension is delayed by 5 years compared to EnLAG [2009].	
Import balance	BASE	Power imports and exports are assumed to be unchanging over time (see Figure 6.16).	Analysis of the relevance of an alternative import balance.
	IMP+	Power imports linearly increase by 100% and exports decrease by 50% until 2030	
Gas price	BASE	Gas price development according to Table 6.5.	Analysis of the sensitivities of the results to varying gas prices.
	Gas + 20	Markup to the gas price 2007-2020: rising from 0 to 20% 2020-2030: constantly + 20%	
	Gas + 50	Markup to the gas price 2007-2020: rising from 0 to 50% 2020-2030: constantly + 50%	
EUA price	BASE	EUA price according to Table 6.12	Analysis of the sensitivities of the results to varying EUA prices.
	CO_2 + 50	Markup to the EUA price 2007-2015: rising from 0 to 50% 2015-2030: constantly + 50%	
	CO_2 + 100	Markup to the EUA price 2007-2015: rising from 0 to 100% 2015-2030: constantly + 100%	

In a first scenario, it is assumed that the grid extension is delayed compared to the BASE scenario. The power line expansions named in EnLAG [2009] are assumed to be built with a delay of five years.

In the second alternative scenario, the influence of changing imports and exports are accounted for. Since the German power system is part of the interconnected European system, its development is coupled to the developments of the surrounding systems. Yet, due to computational restrictions the surrounding systems are not modeled, which is why the exchanges between Germany and its neighbors are predefined and considered as unchanging in the BASE scenario. However, the German import balance is likely to change over the covered time horizon. Therefore, an alternative development of power imports and exports is analyzed.

In the last two scenarios the most relevant economical parameters that affect the choice in power station technology are varied, comprising variation of the gas (and fuel oil) as well as of the EUA prices.

7.4. Evolution of the German power system under alternative framework conditions

In the following sections, the results of the alternative scenario calculations outlined in Table 7.3 are presented.

7.4.1. Influence of delays in grid expansion

Due to long-lasting approval procedures the necessary extension of the German transmission grid is currently delayed by several years. Therefore, the influence of delays in grid extension on the long-term development of the German power supply are analyzed in this scenario, which is named GRID scenario. Compared to the dates of completion indicated in Table 6.1, a delay of five years is assumed for all projects that are not completed before 2010.

In the following, firstly the development of nodal prices and congestion in the GRID scenario will be discussed. Secondly, the development of the average marginal cost of power supply is described. Based thereupon, the influence of the additional grid constraints on the developments of installed generating capacity, power generation, and capacity utilization will be addressed. In the last part of this scenario result description, the resulting CO_2-emissions will presented.

7.4.1.1. Nodal prices and congestion

Due to the delays in grid extension, congestion in the German power grid increases in the GRID scenario. Figure 7.14 shows the development of congestion in the GRID scenario. The delays affect primarily the optimization periods 2015 and 2020. Among others, the delays concern the connection between Thuringia and Bavaria. In particular the upgrade of the corridor between Redwitz and Würgau will now be realized only in 2017. As a consequence, this grid constraint is binding in 95% of all times slots in 2015. The only exceptions are times of low system load in the summer. The bottleneck is resolved in 2020, because of the upgrade of the Redwitz - Würgau corridor. Furthermore, congestion in north-south direction occurs on several corridors in Northern Germany in times of high system load in 2015 and 2020 (see Figure 7.14). By 2025 congestion in the GRID scenario corresponds to the situation in the BASE scenario, again.

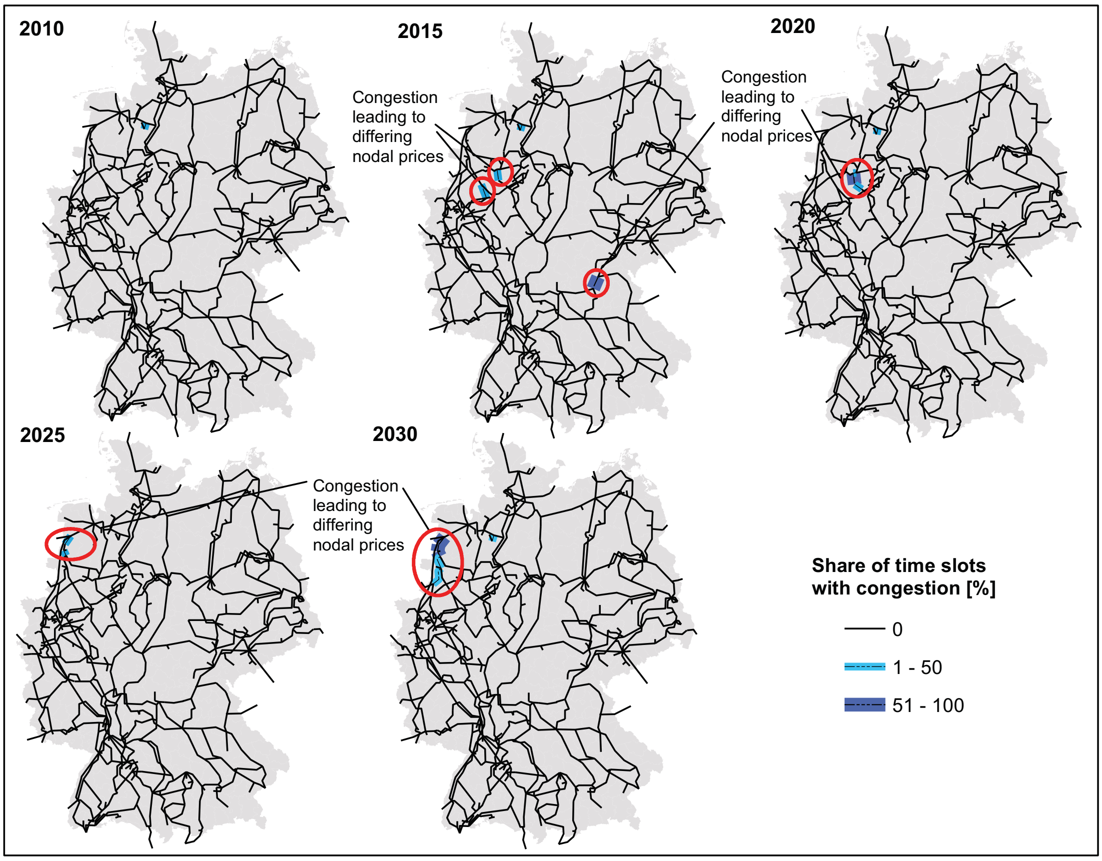

Figure 7.14.: Development of congestion in the GRID scenario

Figure 7.15 shows the development of the average annual nodal prices in the GRID scenario. Due to the additional congestion in 2015 and 2020, average nodal prices in these optimization periods in the GRID scenario differ significantly from those in the BASE scenario. While in the BASE scenario average annual nodal prices varied by less than 1.20 €/MWh in 2015 and 2020, in the GRID scenario nodal price differences of up to 56.09 €/MWh occur. In 2015, they are caused, above all, by the congested Redwitz - Würgau corridor in North Bavaria.

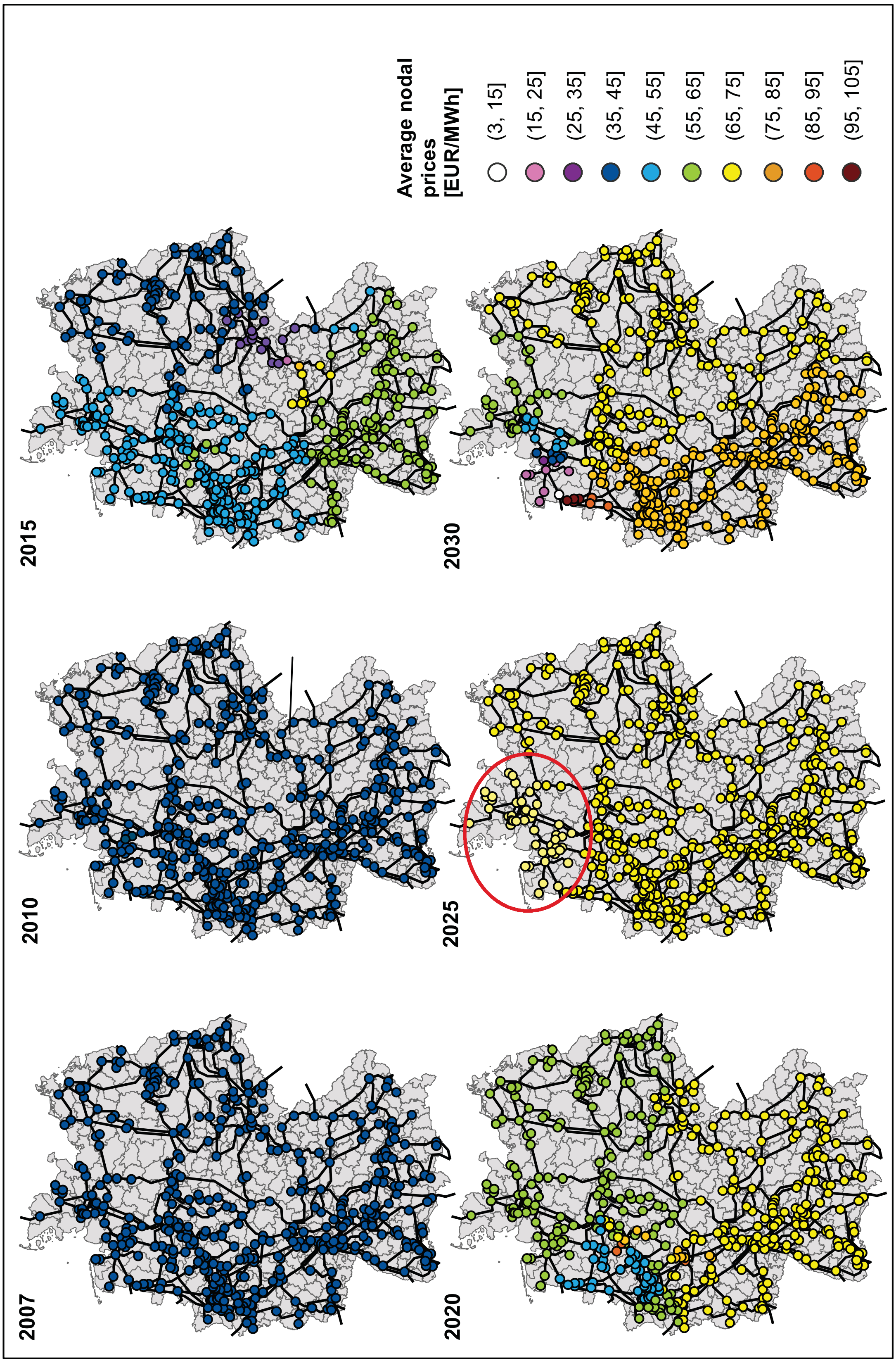

Figure 7.15.: Development of average annual nodal prices in the GRID scenario

Average annual nodal prices range from 20.62 €/MWh to 76.71 €/MWh. They are highest at the deficit side of the congested corridor in North Bavaria and lowest at the surplus side of this corridor. Altogether, nodal prices are lowest in East Germany, where they range from 20.62 €/MWh to 35.11 €/MWh, and highest in the South, where they are between 45.05 €/MWh and 67.71 €/MWh.

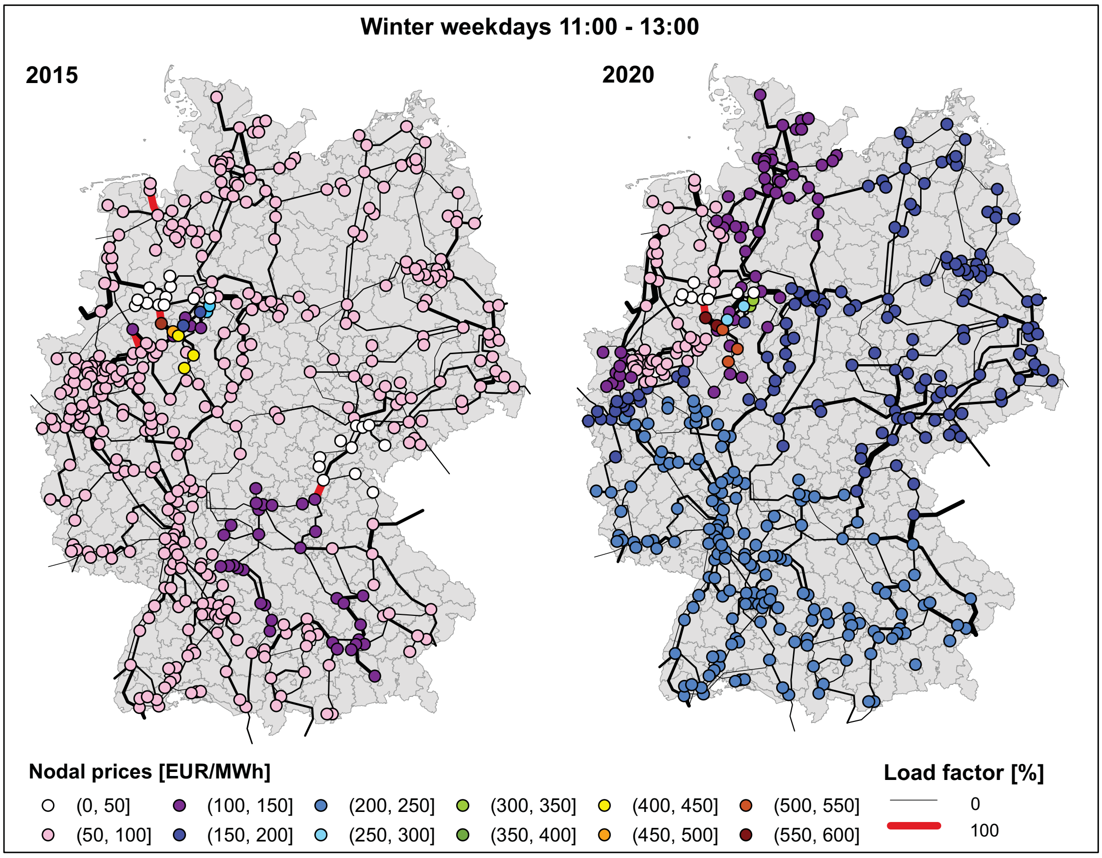

Figure 7.16.: Congestion and peak load nodal prices in 2015 and 2020 in the GRID scenario

At the time of annual peak load, that is on winter weekdays between 11:00 and 13:00, nodal prices range from 21.96 €/MWh to 459.7 €/MWh (see Figure 7.16 (left)). The lowest nodal prices during annual peak load occur at Redwitz, on the surplus side of the congested corridor in the Southeast, while the highest nodal prices occur at Hesseln at the deficit side of a congested corridor in North Westphalia. On winter and autumn weekday evenings, nodal prices at Redwitz in North Bavaria drop below zero and amount to -1.75 €/MWh and -0.21 €/MWh, respectively. Negative nodal prices arise due to the inflexibility of some types of thermal power stations, such as lignite or nuclear power stations. Above all, they are caused by their ramping and opportunity costs (cf. Genoese et al. [2010], EWI [2010]).[4] Furthermore, in LMP schemes nodal

[4] In Germany, negative market prices have been observed so far in case of low system load combined

prices can drop below the marginal cost of the cheapest unit in the power system due to binding line flow constraints. In that case, an increase in load at a node with a negative nodal price might decrease power flows on the congested lines and, in that way, reduce total system costs. The negative nodal prices then reflect the value of "counter flow" in the power system. In the GRID scenario, a combination of both factors is responsible for the negative nodal prices.

By 2020 congestion between Redwitz and Würgau on the Thuringia - Bavaria corridor is resolved by an upgrade from 220 kV to 380 kV. Yet, now further bottlenecks occur (see Figure 7.14). Among them counts the Luestringen - Hesseln corridor between the Lower Saxony and North Westphalia. It causes significant average nodal prices differences in Central West Germany, where nodal prices now vary between 44.36 €/MWh and 87.81 €/MWh (see Figure 7.15). Yet, the nodal price differences are not as pronounced as in 2015. Regarding the regional distribution of nodal prices, a north-south nodal price differential exists. During annual peak load on winter weekdays, nodal prices range from 25.33 €/MWh at Luestringen and 597.90 €/MWh at Hesseln in the northwest of Germany (see Figure 7.16 (right)).

In 2025, the low price zone in Northwest Germany has spread to the North, compared to the BASE scenario (see Figure 7.15). The nodal price difference amounts to 0.43 €/MWh at the most. Apart from that, 2025 results are almost identical to the results of the BASE scenario. Once more, the nodal price difference is caused by the bottleneck Diele - Rhede.

This bottleneck is, again, also responsible for regionally differing nodal prices in 2030. By 2030, the lowest annual average nodal price, which occurs at Diele, amounts to 3.86 €/MWh, while the highest annual average nodal price, which occurs at Rhede, amounts to 98.5 €/MWh (see Figure 7.15). Moreover, the orange colored 75 €/MWh - 85 €/MWh price zone has spread south. This slight increase in average annual nodal prices is caused by an increase in average annual nodal prices during off-peak hours. In times of annual peak load (see Figure 7.17), nodal prices at the deficit side of the congested corridor in the Northwest amount amount to 208.22 €/MWh, while the annual average nodal price at Diele, on the surplus side with high offshore wind power feed-in equals -0.17 €/MWh. The negative nodal price is caused by the bottleneck Diele - Rhede. Moreover, nodal prices in Southern Germany are by approximately 10 - 15 €/MWh lower than in the BASE scenario, while nodal prices in the Northeast are by 5 €/MWh - 10 €/MWh higher than in the BASE scenario. The average annual nodal prices in times of extremely low load, e.g. during summer nights, are almost identical to the development in the BASE scenario.

To summarize, it can be stated that the model, especially the nodal prices, reflect the dilemma of delayed transport capacity and congestion.

with moderate wind power feed-in or in case of moderate system load in combination with high wind power feed-in (cf. Genoese et al. [2010], EWI [2010]).

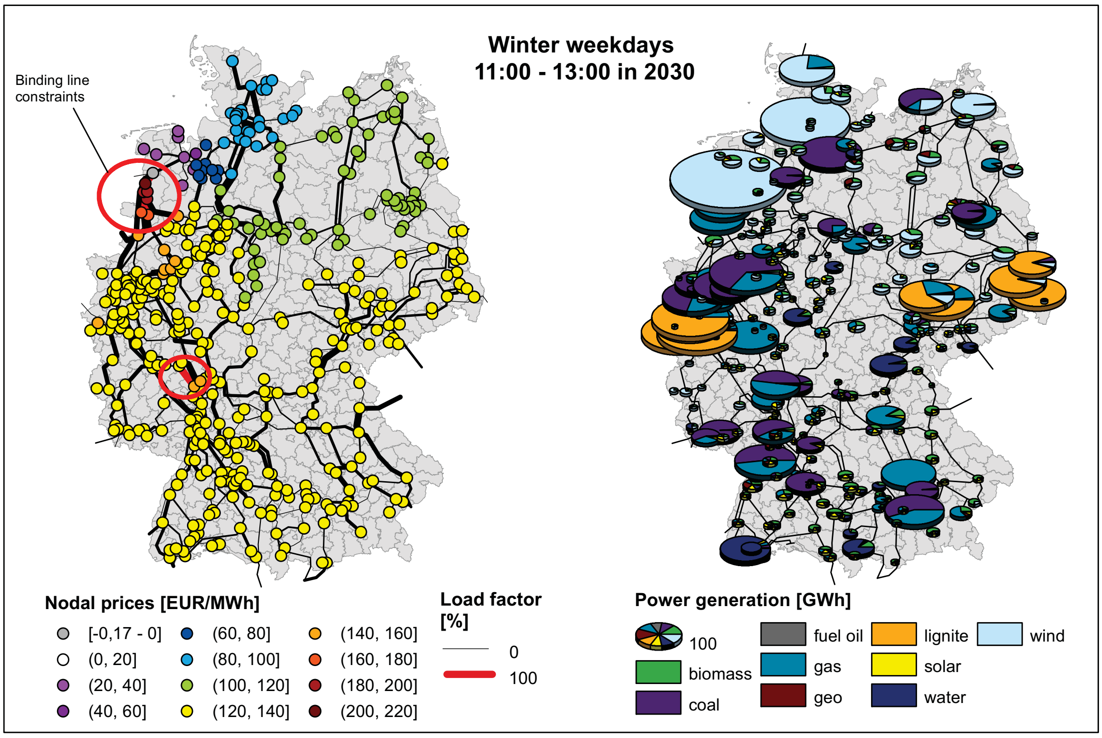

Figure 7.17.: Generation, congestion, and peak load nodal prices in 2030 in the GRID scenario

7.4.1.2. Average marginal cost of power supply

Between 2007 and 2030 the average annual marginal cost of power supply increases from 38.50 €/MWh to 71.03 €/MWh. Peak prices rise from 57.18 €/MWh in 2007 to 94.16 €/MWh in 2025. By 2030, it decreases again, to 60.72 €/MWh (see Table 7.5). From 2010 onwards, the average marginal cost of power supply in the GRID scenario differ from the marginal cost in the BASE scenario.

While in 2015, 2025, and 2030 the cost differences make up less than 1 €/MWh, the average marginal cost in the GRID scenario in 2020 are up to 5.19 €/MWh higher than in the BASE scenario. The high average marginal cost as well as the high average marginal cost in peak load hours in 2020 result from the increased use of fuel oil-fired power stations. It should be noted that in 2015 and 2025 average marginal cost are lower in the GRID scenario than in the BASE scenario. In 2025 this is due to significant lower prices e.g. on winter weekday afternoons, because in the GRID scenario more new gas-fired power station capacity with comparatively lower marginal cost is available. It replaces power generation in old fuel oil- and gas-fired power stations. In 2015 the average marginal cost in the BASE scenario amounts to 50.43 €/MWh, peak marginal cost to 66.26 €/MWh, and off-peak marginal cost of power supply to 43.47 €/MWh. The lower average marginal cost in the GRID scenario results from the nodal price reduction in most parts of Germany caused by congestion.

Table 7.5.: Development of average annual marginal cost in the GRID scenario

	2007	2010	2015	2020	2025	2030
Avg. MC [€/MWh]	38.50	43.85	49.80	64.47	69.08	71.03
Avg. MC peak [€/MWh]	57.18	61.71	65.87	91.12	94.16	89.48
Avg. MC off-peak [€/MWh]	28.82	33.43	42.76	50.44	56.61	60.72

7.4.1.3. Power generating capacity development

Additional congestion in the GRID scenario affects, above all, the optimization periods 2015 and 2020. However, since in the first three optimization periods most newly-commissioned power station capacity is predefined, the delays in grid extension have only a small influence on the choice of technology and on the point in time of capacity commissioning as well as on the grid node at which additional capacity is located. Figure 7.18 shows the overall capacity development in the GRID scenario.

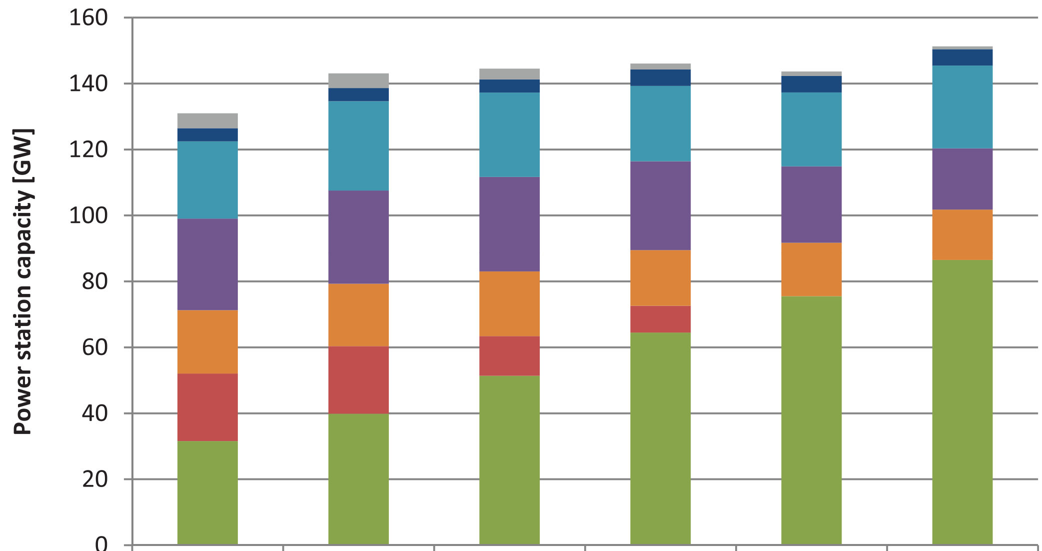

	2007	2010	2015	2020	2025	2030
fuel oil	4.5	4.5	3.3	1.8	1.3	0.8
HPS	4.0	4.0	4.0	5.0	5.0	5.0
gas	23.4	27.1	25.6	22.8	22.4	25.1
coal	27.8	28.3	28.7	26.9	23.2	18.6
lignite	19.2	18.9	19.6	16.9	16.2	15.3
nuclear	20.5	20.5	12.0	8.1	0.0	0.0
RES	31.6	39.9	51.4	64.5	75.5	86.5

Figure 7.18.: Overall development of power generating capacity in the GRID scenario

Even though the development resembles the development in the BASE scenario, small differences regarding gas and lignite capacity exist. In total, 5.0 GW of new coal-fired PCC power stations, 7.0 of new NGCC power stations, and 6.3 GW of new lignite-fired PCC power stations are erected in the GRID scenario.

By 2015, gas-fired power station capacity is by 190 MW higher than in the BASE scenario, while from 2020 on it is by approximately 2 GW higher than in the BASE scenario. Concerning the installed lignite capacity, 3 GW more of additional replacement capacity is built in 2020. In the last two optimization periods, there are 1.4 GW and 1.1 GW less installed lignite-fired power station capacity in the GRID scenario than in the BASE scenario. Thus, the delay in grid extension firstly results in the construction of more flexible gas-fired power station capacities. Secondly, it leads to the preference of an earlier replacement of decommissioned lignite capacities. Thirdly, it suggests a switch from lignite to gas in the last two optimization periods.

Figure 7.21 shows the regional development of power generating capacity. Therein, the grid nodes at which changes in installed capacity compared to the BASE scenario occur are circled. Like in the BASE scenario, a considerable shift of power station capacity from Southern to Northern Germany can be noted, which results, among other things, from the construction of large offshore wind farms at the coasts as well as from the shut down of nuclear power stations and old fossil fuel-fired power stations in the South.

The assumed delay in grid extension causes some changes in the regional development of power station capacity that affects in particular grid nodes with high or above average nodal prices. In 2015, additional gas-fired power stations are constructed at the deficit sides of the congested corridors in South Germany and north of the Ruhr. In 2020 NGCC power station capacities are commissioned at Dauersberg (west of the Rhineland) and, again, north of the Ruhr. Furthermore, the changes in lignite-fired power station capacity affect the Rhenish lignite mining district. At Weisweiler and Goldenberg, the construction of 1061 MW and 2000 MW, respectively, is shifted from 2025 to 2020, while at Niederaussem 900 MW less than in the BASE scenario are built in 2020.

7.4.1.4. Power generation and capacity utilization

In the following, the influence of the delays in grid extension on power generation and capacity utilization will be a analyzed. Figure 7.20 shows the overall development of power generation by fuel in Germany in the GRID scenario. As a whole, it resembles the development in the BASE scenario. Nevertheless, the delays in grid extension cause shifts in the generation mix between lignite, coal, and gas in the optimization periods 2010 - 2030. In 2010, power generation from gas increases by 1.3 TWh, while power generation from lignite increases by 0.5 TWh. By contrast, power generation in coal-fired power stations decreases by 0.7 TWh. In 2015, 0.9 TWh are shifted from lignite-fired power stations to gas-fired power stations. While in 2010 and 2015, the changes affect less than 1% of total generation, they become more pronounced in the later periods.

By 2020, lignite is the second most important fuel in power generation like in the BASE scenario. Lignite-based generation decreases by only 10.0% compared to 2015, while

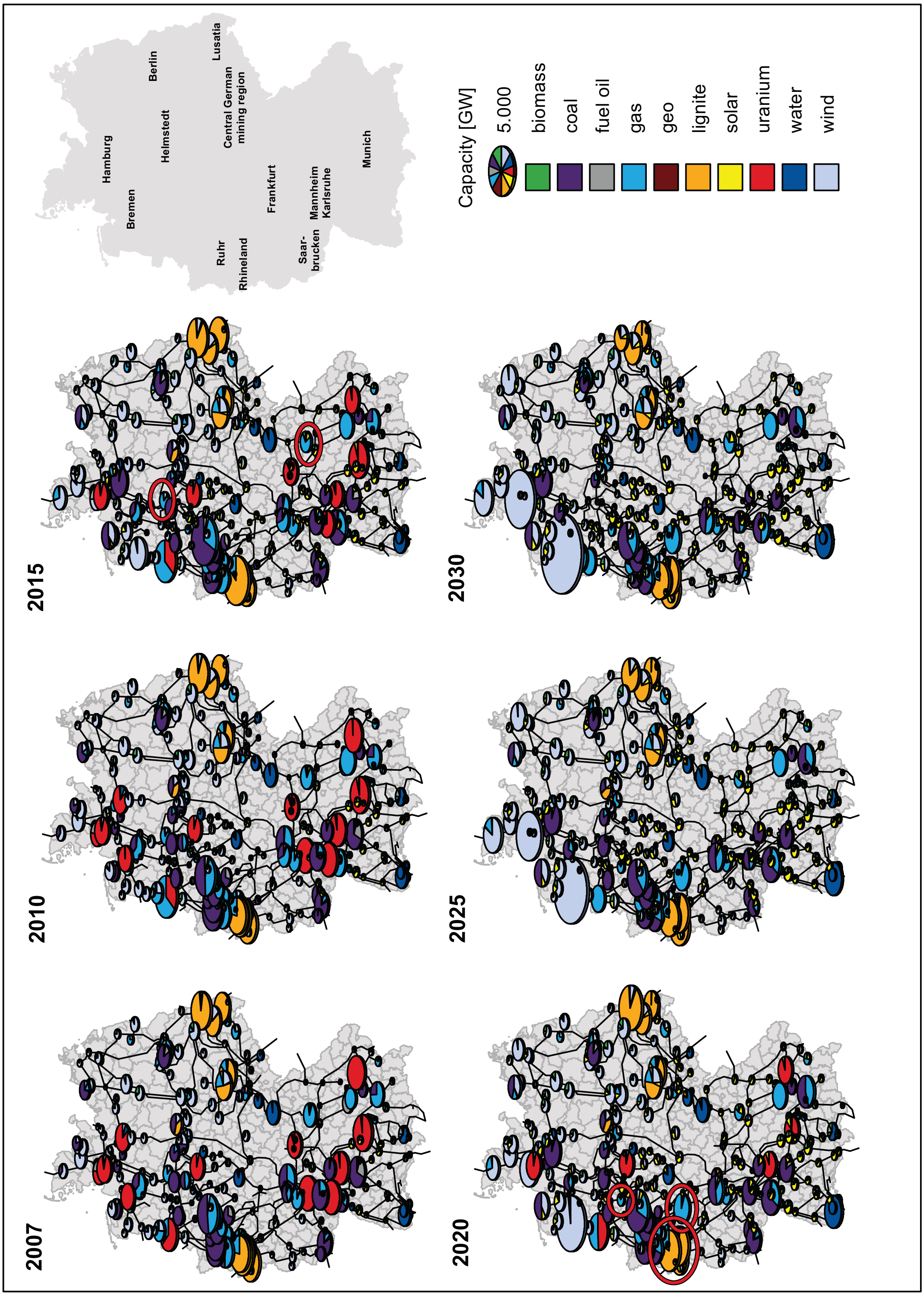

Figure 7.19.: Regional development of power generating capacity in the GRID scenario

coal-based generation increases by 7.9%. Compared to the BASE scenario, 26.3 TWh of generation from coal are replaced primarily by lignite (24.1 TWh) and gas (2.0 TWh). By contrast, in 2025 generation from coal increases by 24.1%, while lignite-bases generation decreases slightly by 3.1%. Thus, compared to the BASE scenario, a 11.1 TWh fuel switch from lignite to coal (8.6 TWh) and gas (2.5 TWh) occurs. Finally, in 2030 both coal and lignite-based generation decrease, while power generation from gas increases. As a result, coal-based generation has a share of 17.5%, generation from gas of 15.0%, and generation from lignite of 23.2% in total power generation, which, again, corresponds to a minor shift from lignite to coal and gas compared to the BASE scenario. The delay in grid extension results in the preference of more flexible power station capacities, which additionally can be sited more flexible.

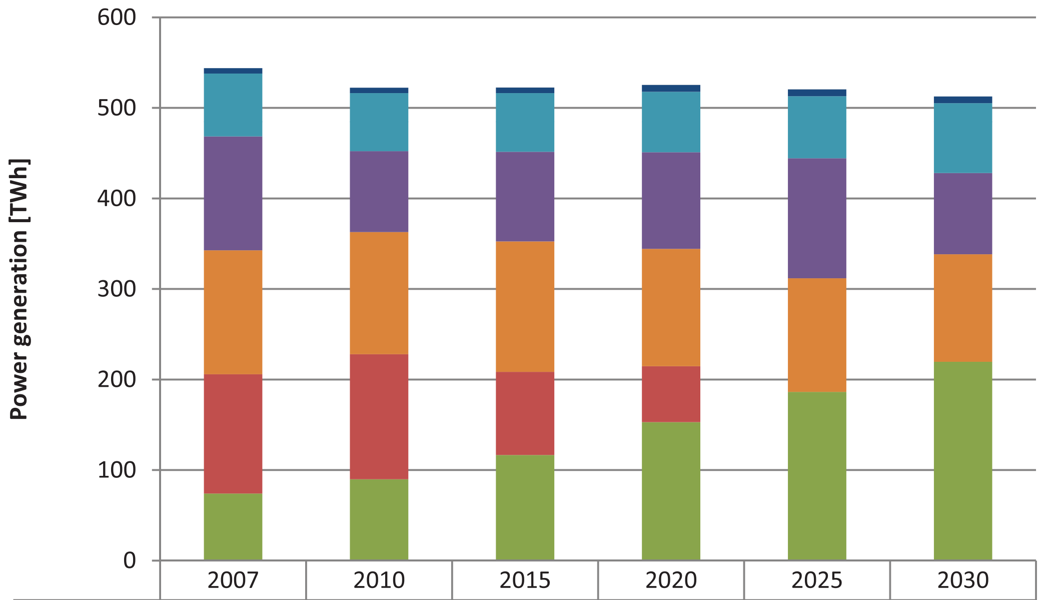

	2007	2010	2015	2020	2025	2030
oil	0.0	0.0	0.0	0.1	0.0	0.0
HPS	6.0	6.0	6.0	7.5	7.5	7.5
gas	69.4	64.1	64.9	66.8	68.6	77.1
coal	125.8	89.3	99.0	106.8	132.5	89.6
lignite	137.0	134.9	144.1	129.6	125.5	118.7
nuclear	131.7	138.1	91.8	61.7	0.0	0.0
renewable	74.0	89.9	116.7	153.0	186.3	219.7

Figure 7.20.: Overall development of power generation in the GRID scenario

In addition to those structural changes in the generation mix, more important changes in the regional development of power generation occur. Figure 7.21 illustrates the regional development of power generation in the six optimization periods. Like in Figure 7.13, only those grid nodes are depicted where power generation exceeds 200 GWh/a. Even though the regional development in the GRID scenario resembles the BASE scenario, several regional changes in particular in the optimization periods 2015 - 2030 can be made out.

In 2015, power generation in North and East Germany is replaced by generation in the South and particular in the West, compared to the BASE scenario. In particular, power generation at Hamburg (-5.6 TWh) and Berlin (-3.2 TWh) as well as in the Central German lignite district (-1.0) and in Lusatia (-0.8 TWh) decreases, while it increases in the region Karlsruhe - Mannheim - Heilbronn - Stuttgart (+9.4 TWh) and in the Southeast (+1.8 TWh). The spatial shift in power generation from East to West Germany results from congestion on the power line between Redwitz and Würgau, while the shift from Hamburg to the South is caused by congestion in north-south direction (see Figure 7.14).

By 2020, power generation from lignite in the Rhenish district is 27.0 TWh higher in the GRID than in the BASE scenario. Moreover, 3.6 TWh are generated in the additional NGCC station in Dauersberg, which is located west of the Rhineland. Additional 2.7 TWh are generated in the Karlsruhe - Mannheim region, and additional 2.0 TWh at Munich. Above all, they participate in replacing 34,7 TWh of generation from coal and gas in the Ruhr district as well as 5.2 TWh in Northwest Germany. Power generation in those areas is reduced because of the bottleneck between the Lower Saxony and North Westphalia.

In the last two optimization periods, the differences in power generation between the GRID and the BASE can be explained by the locational differences in installed capacity. On the one hand power generation at Niederaussem (Rhenish district) is by 7.2 TWh in 2025 and 4.6 TWh in 2030 lower than in the BASE scenario. On the other hand, the additionally built NGCC power station partly contributes to fill the gap (2025: 5.6 TWh; 2030: 2.5 TWh). The remainder is primarily covered by existing coal-fired power stations in the Ruhr district.

The changes in the development of generating capacity and power generation have an influence on the average full load hours of power stations. The average full load hours of lignite-fired power stations range from 6964 h/a in 2010 to 7670 h/a in 2030 and thus are almost equal to the full load hours in the BASE scenario. Similarly, the average full load hours of the nuclear power stations are identical to those in the BASE scenario. By contrast, there are changes in the average full load hours of coal and gas-fired power stations. The average full load hours of coal-fired power stations increase from 3577 h/a in 2010 to 5481 h/a in 2030. While in 2015, 2025, and 2030 they are 189 h/a, 327 h/a, and 153 h/a higher than in the BASE scenario, they are 602 h/a lower than in the BASE scenario by 2020. This is in line with the developments of power generation and installed capacity. The average full load hours of gas-fired power stations decrease over the covered time horizon and amount to 2972 h/a by 2030. In the last two optimization periods, they are 357 h/a and 207 h/a lower than in the BASE scenario. Thus, the construction of additional capacity in deficit areas induce a lower average utilization of gas-fired power stations.

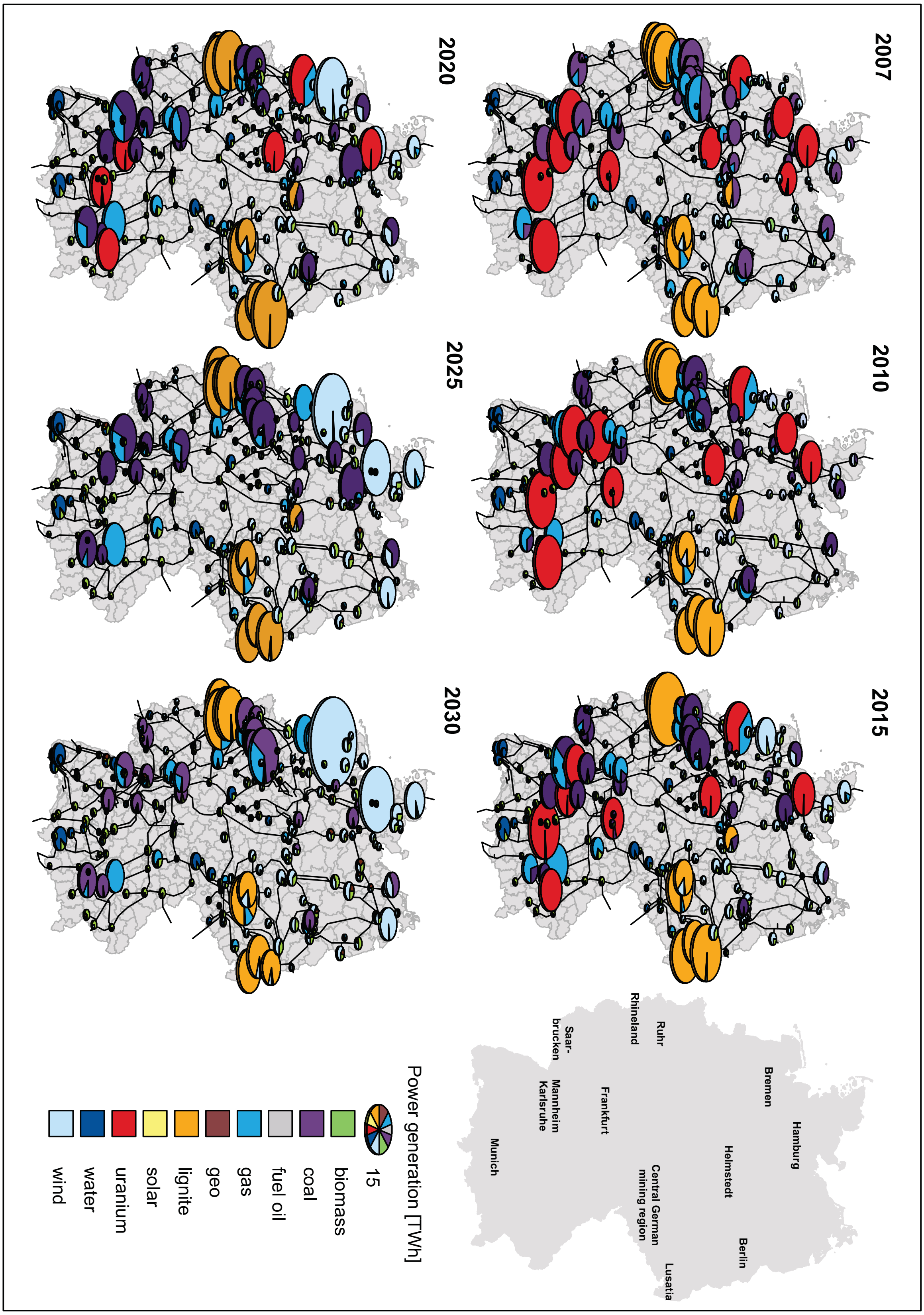

Figure 7.21.: Regional development of power generation in the GRID scenario

7.4.1.5. Carbon dioxide emissions

In the GRID scenario carbon dioxide emissions decrease by 29.6% from 287.5 Mt CO_2 in 2007 to 202.4 Mt CO_2 in 2030. The emissions by fuel as well as the total CO_2-emissions are presented in Table 7.6. Like in the BASE scenario, the most important emitters are lignite-fired power stations. Between 2007 and 2015 they are on a constantly high level of approximately 150 Mt CO_2. Since the relevance of lignite-based generation decreases in the following periods and because the newly built lignite PCC power stations have higher efficiencies, they decrease to 107.6 Mt CO_2 in 2030. Carbon dioxide emissions from coal-fired generation decrease from 106.8 Mt CO_2 to 74.9 Mt CO_2 between 2007 and 2010. Until 2025, it increase, again, to 102.0 Mt CO_2. By 2030 they amount to only 67.3 Mt CO_2, above all, because of the reduction of power generation from coal. CO_2-emissions from gas rank between 24.3 Mt CO_2 and 28.1 Mt CO_2 in the covered time horizon. Compared to the BASE scenario, total emissions are higher in 2010, 2015, and 2025 and lower in 2020 and 2030. However, the differences are negligible small and range between 0.2% and 1.1%.

Table 7.6.: Development of the CO_2-emissions in the GRID scenario by fuel type [Mt CO_2 / a]

	2007	2010	2015	2020	2025	2030
coal	106.8	74.9	78.5	83.8	102.0	67.3
fuel oil	0.0	0.7	0.0	0.1	0.0	0.0
gas	28.1	24.3	24.5	25.0	25.2	27.5
lignite	152.6	149.5	153.0	124.8	115.5	107.6
sum	287.5	248.8	256.0	233.7	242.7	202.4

7.4.1.6. Summary of the results of the GRID scenario

In the GRID scenario, a five year delay in the construction of the grid extensions is assumed. As a result, structural bottlenecks now occur already in the optimization periods 2015 and 2020. In particular the connections between Thuringia and Bavaria as well as between the Lower Saxony and North Westphalia are affected. Consequently significantly differing nodal prices now occur in 2015 and 2020, too. In 2015, the maximum nodal price difference in average annual nodal prices amounts to 56.09 €/MWh. Moreover, a nodal price differential between East and South Germany develops. In several time slots at high system load negative nodal prices occur at the surplus side of the bottleneck on the corridor connecting Thuringia and Bavaria. By 2020, the bottleneck between the Lower Saxony and North Westphalia causes significant nodal price differences. In times of system peak load, they exceed 500 €/MWh. However, the differences in the average annual nodal prices are less pronounced than in 2015. In the last two optimization periods, the situation in the German power grid is almost identical to the BASE scenario, yet with slightly increased nodal prices.

Regarding the influence of the delays in grid extension on the capacity mix and its regional distribution, above all the construction of additional flexible gas-fired power stations in deficit areas, e.g. in the South and in North Westphalia, is notable. As a consequence, also a switch from lignite to gas in the last optimization periods occurs compared to the BASE scenario. This shift from lignite to gas also affects power generation. In 2015 as well as in the last two optimization periods, power generation from gas increases, while power generation from lignite decreases compared to the BASE scenario. By contrast, in 2020 power generation from lignite as well as power generation from gas increases compared to the BASE scenario, while power generation from coal decreases. The regional shifts in power generation compared to the BASE scenario are most pronounced in 2015 and 2020. In 2025, in particular power generation in the South increases, while power generation in the northern parts of Germany decreases. By 2020, the bottleneck between the Lower Saxony and North Westphalia causes a shift of power generation from coal in the Ruhr district to gas and lignite-fired power stations in the Rhineland.

The reduction of power generation from lignite results in lower CO_2-emissions in 2030 compared to the BASE scenario. In the GRID scenario, CO_2-emissions in 2030 amount to 202.4 Mt CO_2, which corresponds to an emission reduction between 2007 and 2030 of 30%.

7.4.2. Influence of changes in power imports and exports

Using the model PERSEUS-NET, only the development of the German power system is optimized. The exchanges between Germany and its neighbors are predefined and considered as unchanging. However, in the future, changes in power imports and exports can be expected. This will also have a significant influence on power flows within the German transmission grid as well as on future structures of power generation and capacity mix. It is most likely that Germany will develop from a net exporter to a net importer over the next years (cf. e.g. Heinrichs et al. [2011]). In this scenario, abbreviated as IMP+, it is assumed that Germany's power imports will double between 2007 and 2030, while its exports will halve over the same time frame.

In the following, firstly the influence of the increasing imports on on nodal prices and congestion in the German transmission grid are presented. Secondly, the development of the average annual marginal cost of power supply in Germany is described. Then, the influence of the shrinking trade balance on the structures of capacity mix and power generation are analyzed. In the last paragraph of this section, the resulting carbon dioxide emissions are presented.

7.4.2.1. Average annual nodal prices and congestion

In the following, the development of grid congestion and average annual nodal prices will be addressed. Since there are only minor changes compared to the results of the BASE scenario until 2020, the focus will be on the last two optimization periods. Figure 7.22 shows the regional development of grid congestion in the IMP+ scenario, while Figure 7.23 illustrates the regional distribution of average annual nodal prices in 2025 and 2030.

Regarding the first four optimization periods, additional congestion compared to the BASE scenario appears on summer weekends north of Phillipsburg in Southwest Germany in 2010. Moreover, the bottleneck in 2020 in Southeast Germany is resolved. Yet, those changes have little effect on average annual nodal prices. Nodal price differences occur, if at all, in direct proximity to the bottlenecks and their level does not exceed 0.39 €/MWh. The overall nodal price level between 2010 and 2020 is slightly lower than in the BASE scenario (see also section 7.4.2.3).

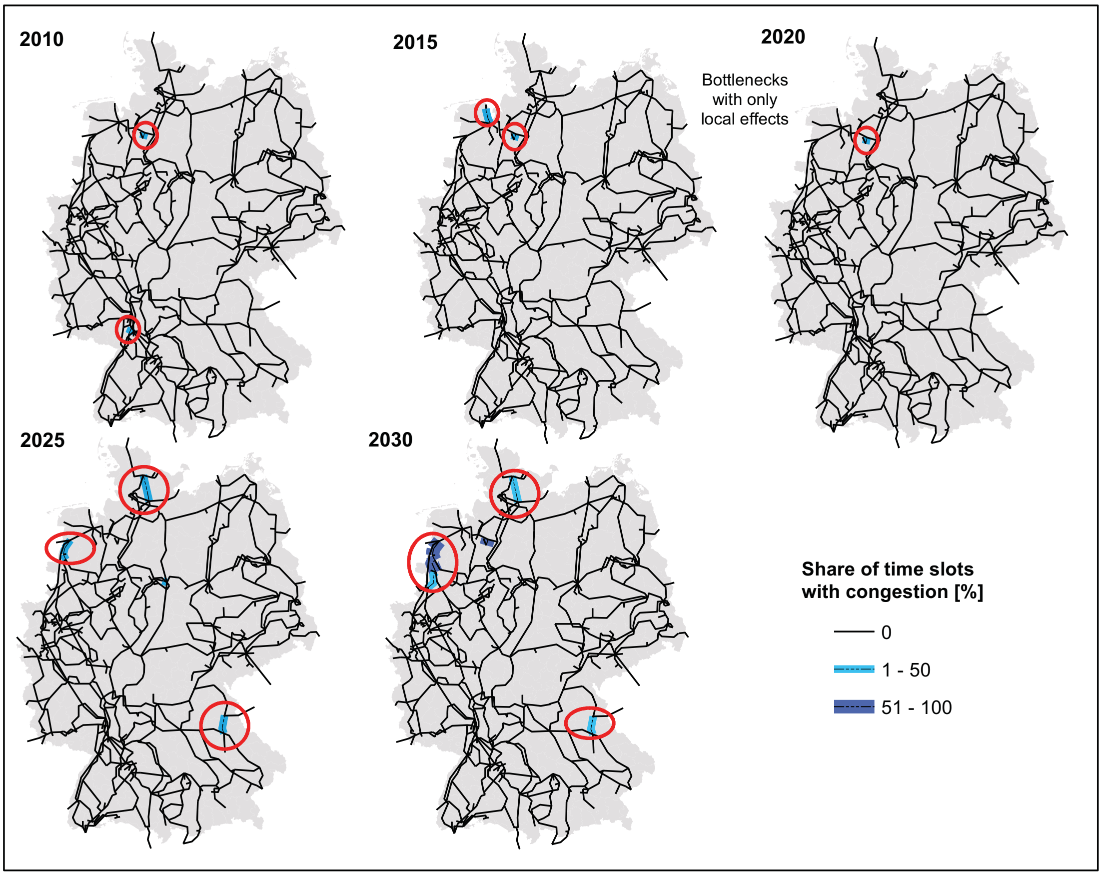

Figure 7.22.: Development of congestion in the IMP+ scenario

By 2025, the Diele - Rhede corridor is once more the most severe bottleneck in the German power system, which is congested during almost one third of the time. Moreover, two additional bottlenecks occur due to the changes in Germany's import balance.[5] On the one hand, the Hamburg Nord - Audorf corridor close to the Danish border, on the other hand, the Schwandorf - Etzenricht corridor in Bavaria close to the Czech border is congested. The congestion north of Hamburg is caused by the increasing imports from Denmark, while the congestion in Bavaria is stimulated by increasing imports from the

[5] A further bottleneck exists in central Germany, yet it has only local effects.

Czech Republic. In particular the bottlenecks in the Northwest and in the Southeast have a significant influence on the distribution of average nodal prices in Germany (see Figure 7.23). The average annual nodal prices in Germany range from 66.34 €/MWh in the northeast of Germany to 77.65 €/MWh in the Southeast. The nodal price difference between the surplus and deficit sides of the bottleneck Diele - Rhede amounts to 4.61 €/MWh, while the difference between Schwandorf and Etzenricht comes to 5.38 €/MWh. The nodal price difference caused by the bottleneck north of Hamburg amounts to 0.59 €/MWh.

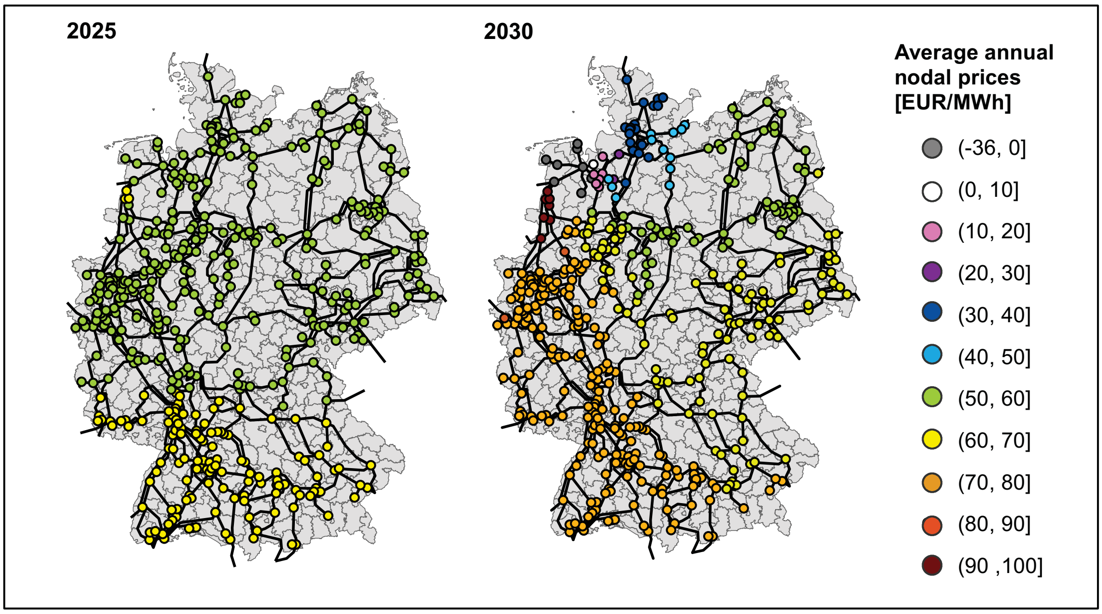

Figure 7.23.: Development of average annual nodal prices in 2025 and 2030 in the IMP+ scenario

In 2030, these three bottlenecks first occurring in 2025 become more severe. While the Diele - Rhede corridor is congested at all time, the bottlenecks Hamburg Nord - Audorf and Schwandorf - Etzenricht are congested during 24% and 19% of the time slots, respectively. Average annual nodal prices in 2030 in the IMP+ scenario range from -35.85 €/MWh to 99.18 €/MWh. They are lowest at the surplus side of the congested Diele - Rhede corridor and highest at the deficit side of this bottleneck. The nodal price differences between the grid nodes at the endings of the bottleneck Hamburg Nord - Audorf now amounts to 6.01 €/MWh, while the nodal price difference at the bottleneck Schwandorf - Etzenricht decreases to 1.62 €/MWh.

Like in the above described scenarios, a north south divide develops in the IMP+ scenario from 2025 onwards. Moreover, a east west divide exists. Yet, the changes in the import balance lead to more congestion in the German transmission grid and thus cause higher differences in average annual nodal prices in Germany. In particular the nodal price difference around the bottleneck Diele - Rhede as well as the north south divide becomes more pronounced.

In the following, the relationship between congestion and nodal prices in selected time slots is discussed.

7.4.2.2. Nodal prices, grid congestion, and power generation in selected time slots

The analysis of this section is limited to the optimization periods 2025 and 2030, since in those periods the increasing net imports have the most effect. Figure 7.24 shows the regional distribution of nodal prices and congestion in two selected time slots in 2025.

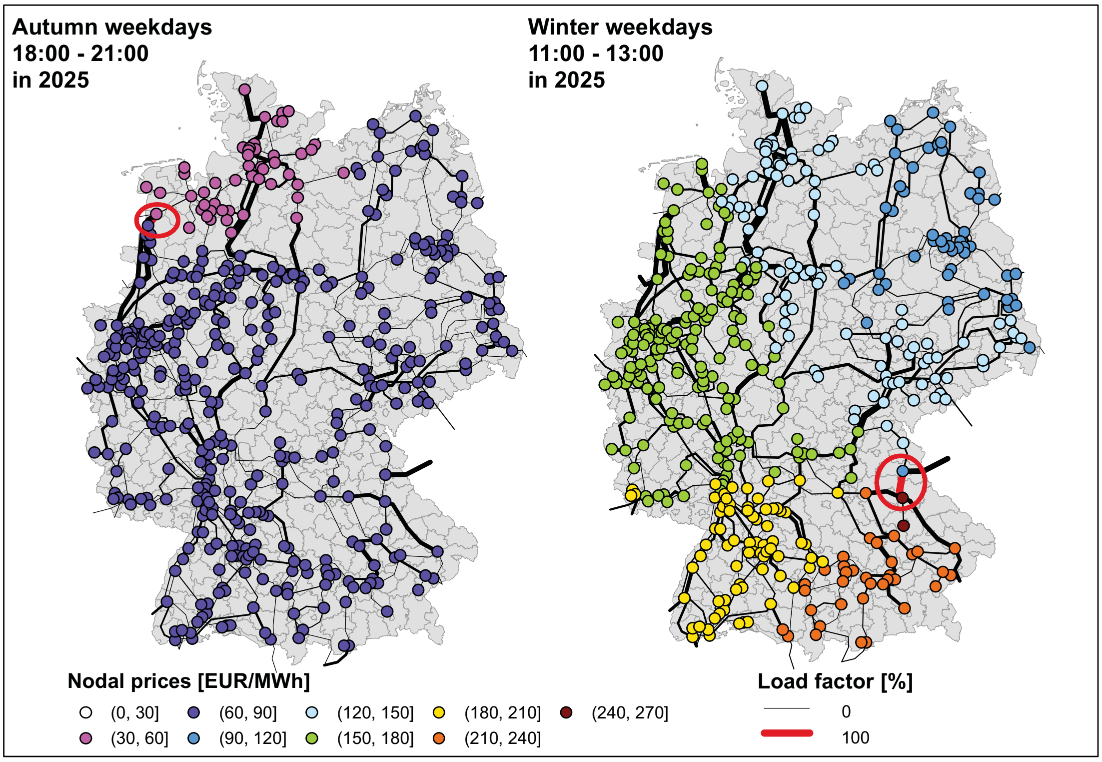

Figure 7.24.: Regional distribution of nodal prices and congestion in two selected time slots in the IMP+ scenario by 2025

While on autumn weekday evenings the bottleneck Diele - Rhede and thus the offshore wind power feed-in at the North Sea determines the regional distribution of nodal prices in Germany (see Figure 7.24 (left)), on winter weekdays it is determined by the bottleneck Schwandorf - Etzenricht that results from high imports from the Czech Republic (see Figure 7.24 (right)). As a result, on autumn weekday evenings nodal prices are lowest in the Northwest at the surplus side of the bottleneck, where they range between 45.11 €/MWh and 50.72 €/MWh. At Rhede on the deficit side, they amount

73.18 €/MWh, while in the rest of Germany they range between 52.94 €/MWh and 76.59 €/MWh. By contrast, on winter weekdays at noon nodal prices are lowest at Etzenricht, where they amount to 111.01 €/MWh, and highest at Schwandorf, where they amount to 259.21 €/MWh. Leaving apart those grid nodes in direct proximity of the congested corridor, nodal prices are lowest in central North and in Central East Germany and highest in the South.

By 2030, the bottleneck Diele - Rhede determines the regional distribution of nodal prices during all time slots. Figure 7.25 shows the regional distribution of congestion, nodal prices, and power generation in times of system peak load, while Figure 7.26 illustrates the situation in times of annual minimum load. While the nodal prices around the bottleneck are more extreme than in the BASE scenario, reduced nodal prices occur in most other parts of Germany. This nodal price decrease results from the increasing imports. Since imports increase compared to the BASE scenario, less of the power demand in Germany has to be met with power generation within Germany. Yet, the installed capacity does not decrease to the same extent. Thus, the intersection of the demand curve shifts left, which results in a decrease of the marginal cost of power supply. The more severe nodal price difference around the bottlenecks shows that congestion is more severe than in the BASE scenario.

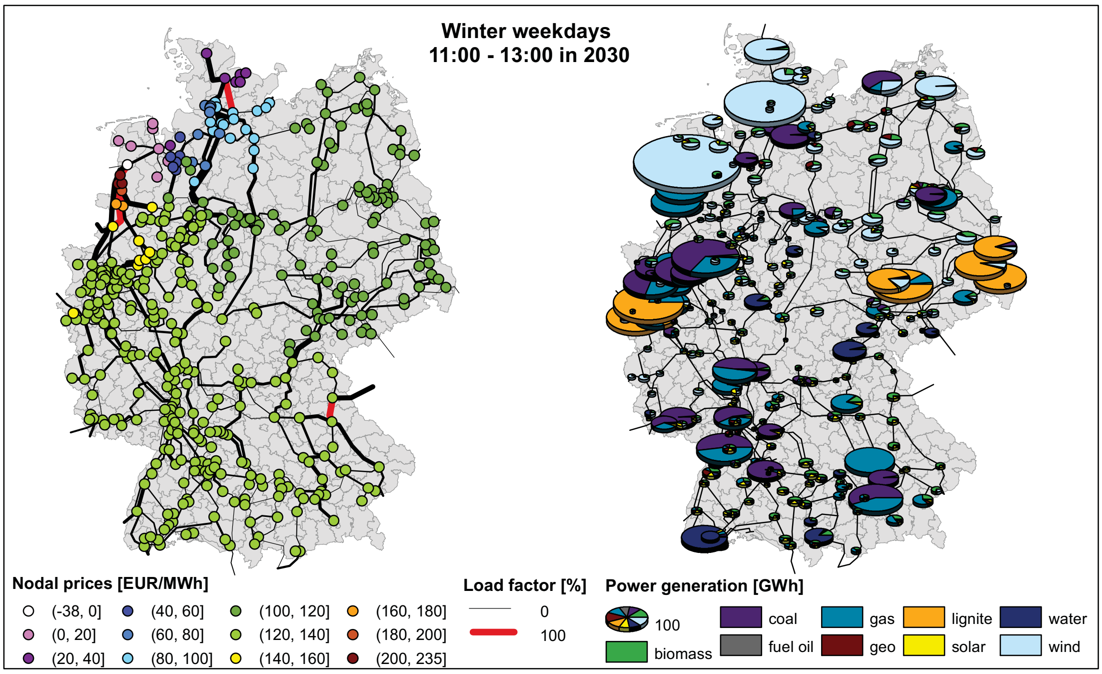

Figure 7.25.: Nodal prices, congestion, and power generation in times of annual peak load by 2030 in the IMP+ scenario

In times of annual peak load, nodal prices are approximately 20 €/MWh lower than in the BASE scenario. Regarding their regional distribution, nodal prices are again lower in the Northeast than in the South and West. Extreme positive and negative nodal price peaks occur, again, at the deficit and at the surplus side of the congested Diele - Rhede corridor. While nodal prices at Diele drop to -37.90 €/MWh, nodal prices at Rhede rise to 233.45 €/MWh. The negative nodal price reflects the value of "counterflow" in the power system, again. The congested Hamburg Nord - Audorf corridor causes nodal price differences between the Hamburg region and the far North of more than 77 Euros. While nodal prices at Audorf amount to 22.96 €/MWh, nodal prices at Hamburg rise up to 98.75 €/MWh during times of annual peak load.

By contrast, the nodal price difference between the deficit and the surplus side of the bottleneck Etzenricht - Schwandorf amounts to less than 2.00 €/MWh. Regarding power generation at annual peak load, the thermal power stations at the Rhineland and the Ruhr district as well as the offshore wind parks at the North Sea are the main centers of power generation. Yet, also the large conventional power stations in the Southwest, near Munich, Berlin, and Hamburg as well as the lignite-fired power stations in Eastern Germany run at full load. Again, the NGCC power stations at the deficit side of the bottleneck Diele - Rhede are used to create a counterflow.

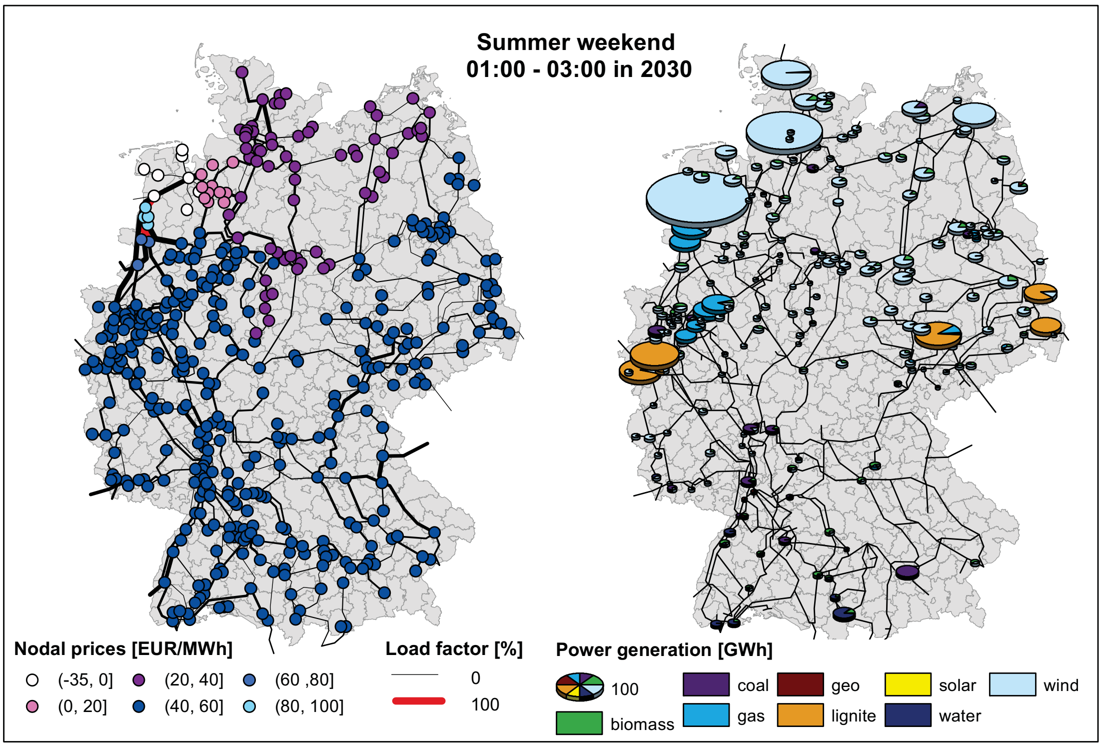

Figure 7.26.: Nodal prices, congestion, and power generation in times of minimum system load by 2030 in the IMP+ scenario

A somewhat different situation occurs in times of annual minimum grid load on summer weekends between 01:00 and 03:00, where nodal prices in most parts of Germany, except for the North, range between 40.02 €/MWh and 55.78 €/MWh. The only bottleneck in times of minimum grid load occurs in Northwest Germany. The highest (83.66 €/MWh) and lowest (-34.06 €/MWh) nodal prices can be found on the deficit and on the surplus side of this bottleneck. Moreover, during times of minimum grid load, seven grid nodes with negative nodal prices exist in the Northwest (see Figure 7.26 (left)). The main reason for this is that in addition to the binding line constraint the high wind power feed-in Northwest Germany causes lignite power stations either to run on part load or to entirely shut down (see. Figures 7.25 (right) and 7.26 (right)). In addition to the lignite-fired power stations, almost all coal-fired power stations are shut down. Since according to the model assumptions to balance fluctuations of wind power feed-in, some gas-fired power stations in the Ruhr district and in the East remain operating. Moreover, the NGCC power stations creating the counterflow are operating at part load.

7.4.2.3. Average marginal cost of power supply in Germany

In the IMP+ scenario, the average marginal cost of power supply increase from 38.50 €/MWh in 2007 to 68.83 €/MWh in 2025 (see Table 7.7). The increase is steepest between 2020 and 2025, which can be explained by the reduced relevance of lignite-fired power stations that are characterized by comparatively low marginal generating costs as well as with the increased use of comparatively expensive fuel oil-fired power stations during peak hours in 2025. In 2030, average marginal cost of power generation decreases to 64.16 €/MWh. This decrease in the average marginal cost of power generation in the last optimization period is primarily induced by the almost complete abandonment of the use of fuel oil in power generation in combination with the overall decrease in nodal prices induced by the increasing imports. Average marginal cost during peak times increases from 57.18 €/MWh in 2007 to 93.95 €/MWh in 2025. By 2030, they decrease to 83.84 €/MWh, again. Moreover, average marginal cost during off-peak hours increases from 28.82 €/MWh in 2007 to 55.67 €/MWh in 2025 and amount to 53.55 €/MWh in 2030.

Table 7.7.: Development of the average annual marginal cost in the IMP+ scenario

	2007	2010	2015	2020	2025	2030
Avg. MC [€/MWh]	38.50	40.80	47.69	55.56	68.83	64.16
Avg. MC peak [€/MWh]	57.18	58.47	62.77	72.19	93.95	83.84
Avg. MC off-peak [€/MWh]	28.82	31.11	42.03	47.77	55.67	53.55

In the whole, the average marginal cost of power generation in the IMP+ scenario is lower than in the BASE scenario. The reason for this is that due to the reduction of power generation in all types of conventional thermal power stations, now power stations with lower marginal costs are price setting. For instance, in the IMP+ scenario, fuel oil-fired power stations are more used than in the BASE scenario. The only exception to the lower marginal cost are off-peak marginal cost in 2025, where BASE scenario marginal cost are by 0.02 €/MWh lower. This can be explained by the existence of less lignite-base load capacities.

In the following, the influence of increasing imports and the different regional distribution of nodal prices on generating capacity and power generation will be addressed.

7.4.2.4. Structure of the capacity mix

In the IMP+ scenario, the total net installed capacity increases over the covered time horizon from 131.0 GW to 145.8 GW. Moreover, the two time segments (2007 - 2015 and 2020 - 2030) in the development of the capacity mix, which have been identified in the BASE scenario, are most obvious. Even though from 2015 on, Germany's trade balance is negative and thus power generation within Germany is significantly reduced, the development of the capacity mix in the IMP+ is identical to the development in the BASE scenario until 2020 (see Figure 7.27). The reason for this is that in the first time segment (2007 - 2015) the development of the capacity is almost entirely predetermined, because of the consideration of power stations under construction and in planning.

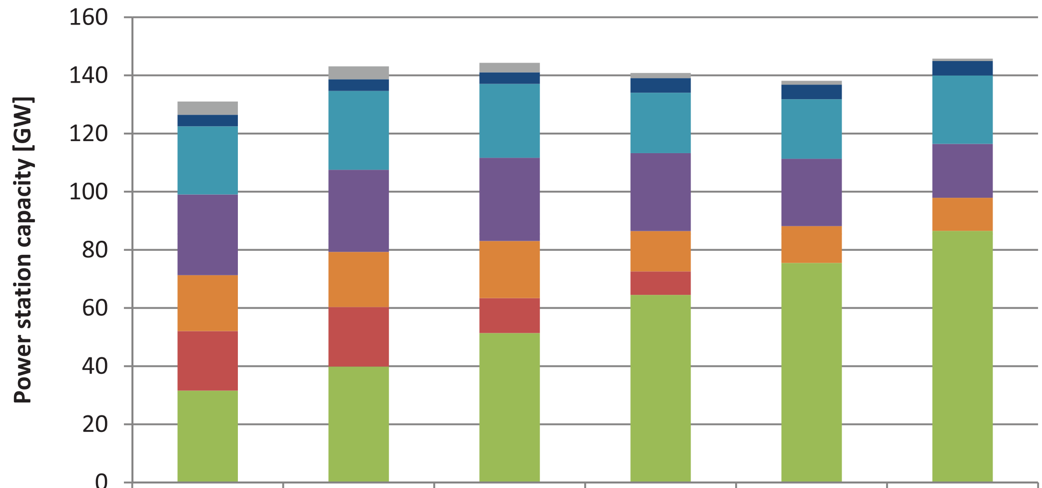

	2007	2010	2015	2020	2025	2030
fuel oil	4.5	4.5	3.3	1.8	1.3	0.8
HPS	4.0	4.0	4.0	5.0	5.0	5.0
gas	23.4	27.1	25.4	20.8	20.5	23.5
coal	27.8	28.3	28.7	26.8	23.2	18.5
lignite	19.2	18.9	19.6	13.8	12.7	11.4
nuclear	20.5	20.5	12.0	8.1	0.0	0.0
RES	31.6	39.9	51.4	64.5	75.5	86.5

Figure 7.27.: Overall development of power generating capacities in the IMP+ scenario

By 2025, when the exchange balance amounts to -19.9 TWh, the changing imports and exports have a visible influence on the structure of the capacity mix. Above all, the increasing imports reduce the installed capacity of lignite-fired power stations. In 2025 and 2030 4.9 GW less of lignite-fired power station capacity than in the BASE scenario are installed. As a result, the share of lignite-fired power stations in total net installed capacity decreases to 7.8% in 2030. Moreover, the net installed capacity of coal-fired power stations is reduced by 73 MW compared to the BASE scenario. By contrast, the net installed capacity of gas-fired power stations increases by 107 MW in 2025 and by 409 MW in 2030. The shares of coal and gas-fired capacities in total net installed capacity in 2030 amount to 12.7% and 16.1%, respectively. The share of RES-E capacities in total net installed capacity in Germany increases from 13.6% in 2007 to 59.4% in 2030. In total, 12.1 GW of new conventional thermal power station capacity is commissioned in the IMP+ scenario. Thereof, 107.3 MW gas turbines, 4.7 GW NGCC power stations, 4.9 GW coal-fired PCC power stations, and 2.4 GW lignite-fired PCC power stations are built.

Regarding the regional development of power generating capacities (see Figure 7.28), the model results correspond to the results of the BASE scenario until 2020. In 2025 and 2030, significant differences concerning the installed capacity in the Rhenish lignite district occur. In Figure 7.28, the grid nodes where the most important differences occur are encircled. By contrast to the BASE scenario, no new lignite-fired PCC power stations are built at the grid nodes Goldenberg, Niederaussem, and Neurath. Moreover, the additionally installed capacity at Weisweiler is by 0.5 GW lower than in the BASE scenario. By contrast, additional 300 MW NGCC capacity is built in 2030 in Northwest Germany, while additional gas turbines are constructed in Southeast Germany.

In the following the influences of the changes in Germany's import balance on the structure and regional distribution of power generation will be addressed.

7.4.2.5. Structure of power generation and capacity utilization

Due to increasing power imports in combination with decreasing exports, power generation in Germany decreases constantly from 543.9 TWh in 2007 to 462.4 TWh in 2030 (see Figure 7.29). By contrast to the development of the capacity mix, which can be considered as predetermined in the first three optimization periods, the narrowing export balance affects at first particularly power generation from coal. Between 2007 and 2015 power generation from coal decreases from 125.8 TWh to 85.6 TWh. Until 2025, it increases to 127.4 TWh, again. Compared to the BASE scenario, this corresponds to an increase of 3.5 TWh in 2025. By 2030, power generation from coal amounts to 77.4 TWh and remains with 16.7% the third most important fuel in power generation. Power generation from lignite varies between 132.7 TWh and 142.7 TWh in the first three optimization periods, which is slightly lower than in the BASE scenario. After 2015, it decreases significantly and amounts to 84.0 TWh by 2030, which is 18.2% of total power generation. Thus, in 2025 and 2030 the increasing power imports result in a reduction of lignite-based power generation of 39.0 TWh and 43.2 TWh compared to the BASE scenario. Moreover, while gas-based power generation decreases from 69.4 TWh in 2007 to 59.0 TWh in 2020, it increases in the last two optimization periods, again, and amounts to 73.9 TWh by 2030. Thus, the differences in power imports- and export

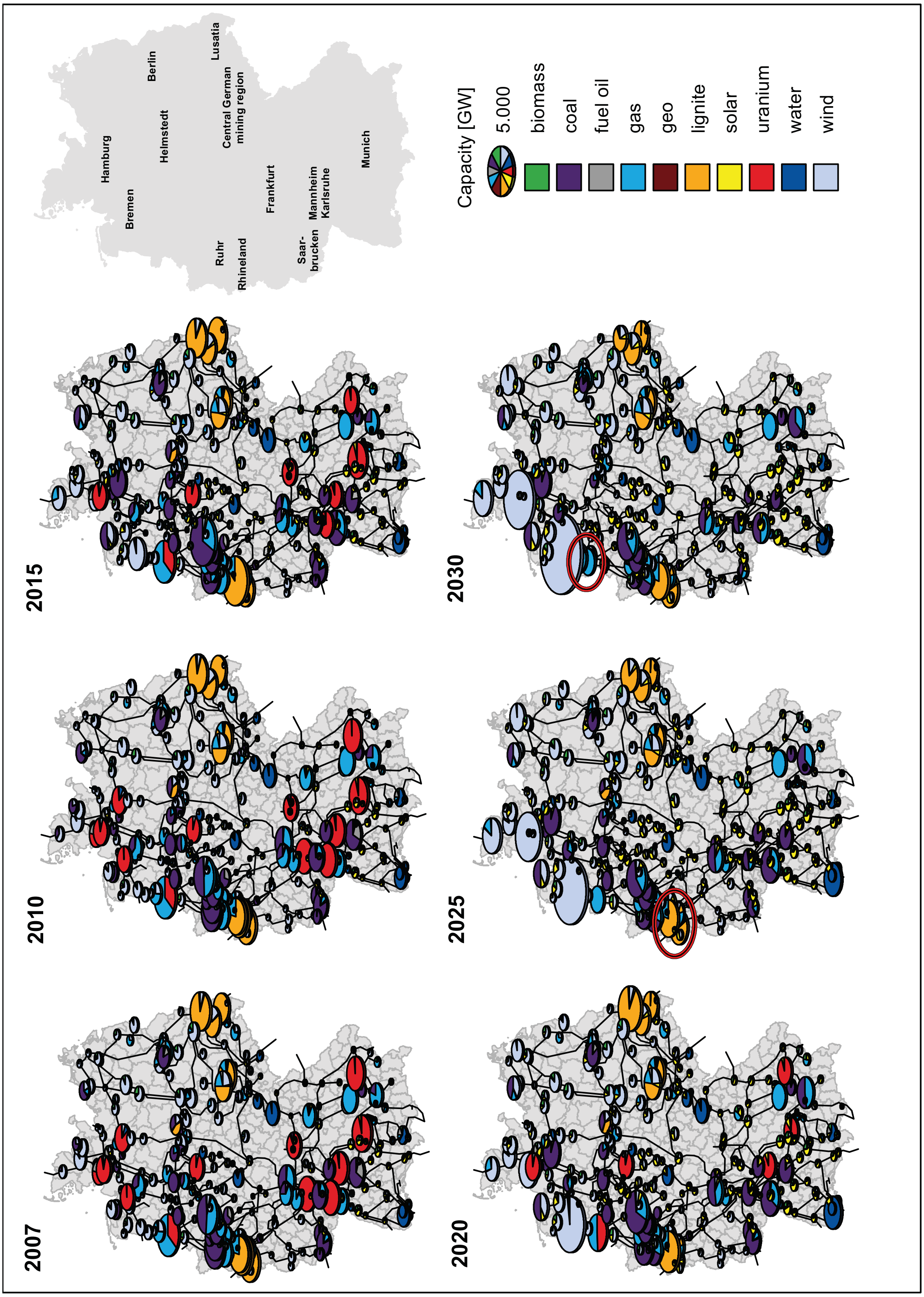

Figure 7.28.: Regional development of power generating capacity in the IMP+ scenario

have almost no effect on the level of power generation from gas. In 2030, it has a share of 16.0% in total power generation in Germany. Furthermore, by 2030 RES-E has a share of 47.5% and HPS of 1.6% in total power generation. Fuel oil-fired power stations are used in 2010, 2025, and 2030 in times of high system load.

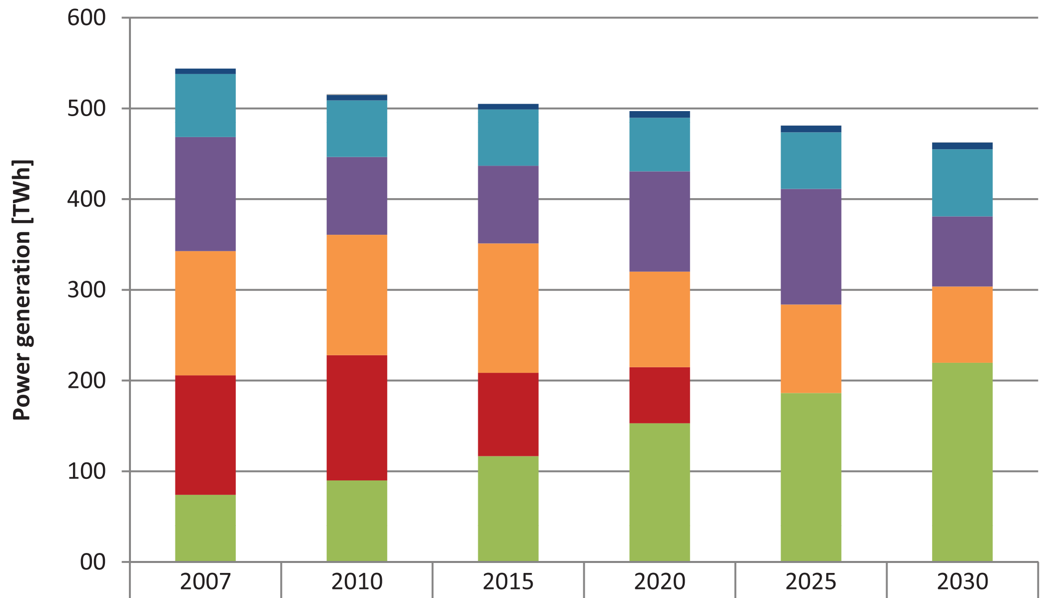

	2007	2010	2015	2020	2025	2030
fuel oil	0.0	1.0	0.0	0.0	0.1	0.0
HPS	6.0	6.0	6.0	7.5	7.5	7.5
gas	69.4	62.4	62.1	59.0	62.3	73.9
coal	125.8	85.8	85.6	110.5	127.4	77.4
lignite	137.0	132.7	142.7	105.4	97.5	84.0
nuclear	131.7	138.1	91.8	61.7	0.0	0.0
RES	74.0	89.9	116.7	153.0	186.3	219.7

Figure 7.29.: Overall development of power generation in the IMP+ scenario

To subsume, until 2020, above generation in medium load power stations is replaced by the increasing net power imports, because power generation in coal-fired power stations is comparatively more expensive than power generation in existing lignite-fired power stations. Since a certain share of gas in total power generation is demanded by the model assumptions as reserve to balance fluctuating RES-E feed-in, power generation from gas remains almost unaffected. In 2025, additional lignite capacity would have to be built to keep the high level of lignite-base generation of the BASE scenario. Since lignite-fired power stations have the highest specific investments of the considered investment options, the construction of additional capacity is renounced in favor of increasing imports and more flexible gas-based generation. Therefore, in the last two optimization periods, the changes in the import balance mainly have an influence on base load power generation technologies. Moreover, the relevance of gas-fired power stations increases.

Since the increasing net power imports result in the construction of less generating capacity on the long term, only minor changes in the average full load hours of power stations occur in the last optimization periods. While in 2030 the average full load hours of power stations in the IMP+ are (almost) identical to the full load hours in the BASE scenario, more significant changes occur between 2015 and 2025. Above all, they affect coal- and gas-fired power stations. The average full load hours of coal-fired power stations amount to 4763 h/a in 2020 and increase to 6116 h/a in 2025, which is in 2020 500 h/a lower and in 2025 275 h/a higher than in the BASE scenario. By contrast, the average full load hours of gas-fired power stations amount to 3421 h/a in 2020 and 3340 h/a in 2025. Compared to the BASE scenario this corresponds to a by 104 h/a increased capacity utilization in 2020 and a slightly decreased capacity utilization in 2025.

The regional development of power generation is illustrated in Figure 7.30. Until 2020, the decrease in power generation in Germany that is induced by the changing imports- and exports is reached by reducing the capacity utilization of existing power stations in the Ruhr district, at and around Karlsruhe and at Hamburg. In 2015, the reduction in coal-based generation affects above all the Ruhr district (-3.5 TWh). By 2020, 4.8 TWh less than in the BASE scenario are generated in coal-fired power stations in the Ruhr district, while 1.2 TWh and 1.5 TWh less are produced at Heyden in North Westphalia and at Hamburg. Moreover, power generation at Karlsruhe and Heilbronn is reduced by 2.2 TWh. Since in 2025 significantly less new lignite-fired generating capacity is built in the IMP+ scenario, the changes in the export balance affect, above all, lignite-based power generation in the Rhineland. In 2025 as well as in 2030 power generation in Rhenish lignite-fired PCC power stations is reduced by 39.0 TWh compared to the BASE scenario. Regarding the Ruhr district, the changes in power imports- and exports have little effect on the capacity utilization in the last two optimization periods. Moreover, in 2030 power generation in old lignite-fired power stations at Schwarze Pumpe in East Germany decreases by 3.3 TWh, while gas-based generation at Irsching (Southeast Germany) is reduced by 3.5 TWh. By contrast, additional 4.7 TWh are generated in the new NGCC power stations in Northwest Germany (see section 7.4.2.1). This shows that due to increasing power flows in the German transmission system, additional power generation from gas is used to counteract congestion.

Since the regional changes in power generation affect primarily Central and South Germany, the shift from Southern to Northern Germany becomes even more pronounced than in the BASE scenario.

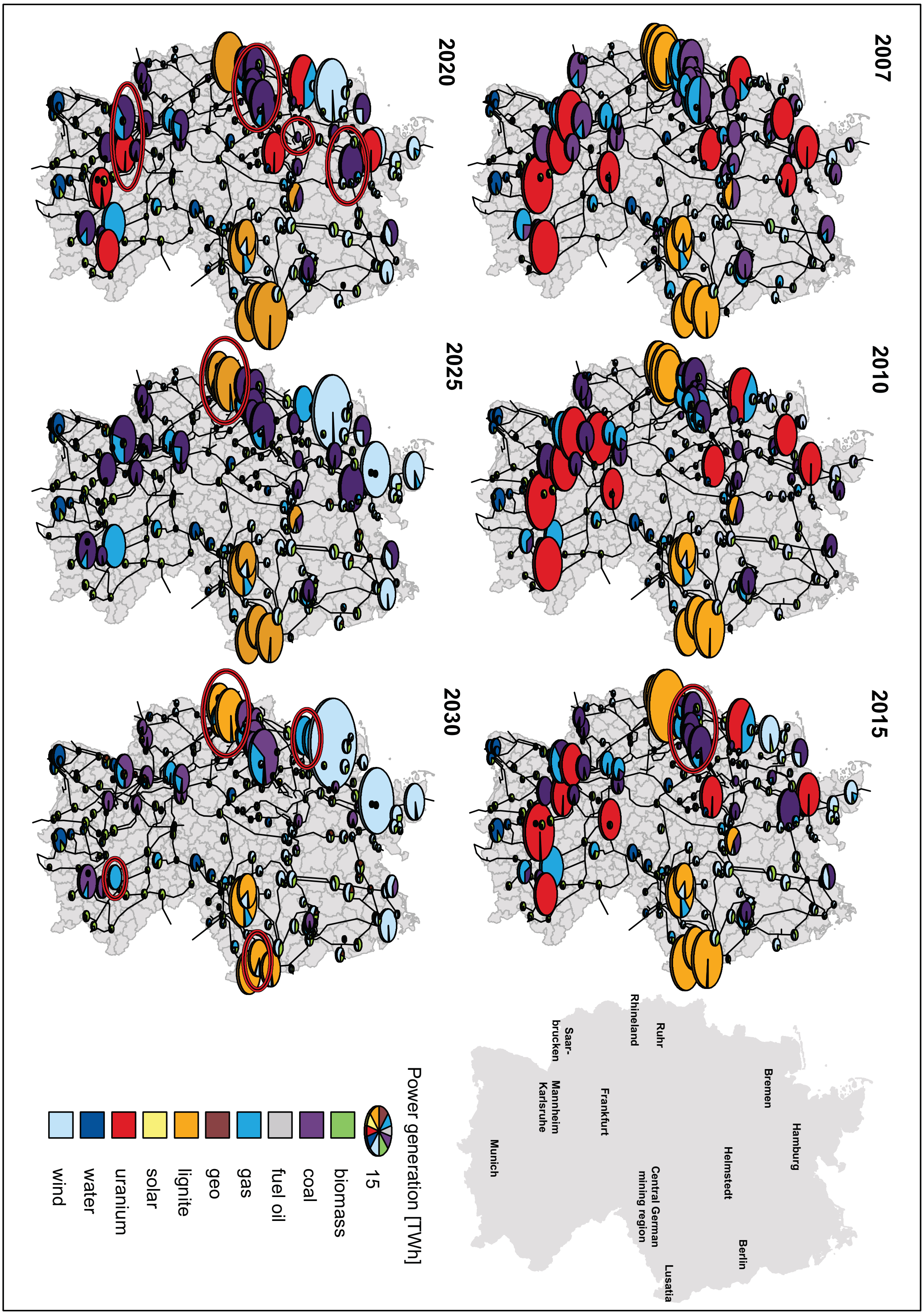

Figure 7.30.: Regional development of power generation in the IMP+ scenario

7.4.2.6. Carbon dioxide emissions

In the IMP+ scenario, the carbon dioxide emissions decrease by 43.6% from 287.5 Mt CO_2 in 2007 to 162.2 Mt CO_2 in 2030 (see Table 7.8). Since the power generation in lignite-fired power stations is significantly reduced, CO_2-emissions of lignite-fired power stations decrease by 49.1% from 152.6 Mt CO_2 to 77.7 Mt CO_2. The CO_2-emissions of gas and fuel oil based power generation remain on a similar level as in the BASE scenario. Since in Table 7.8 only total emissions in Germany are accounted for, while the emissions associated with the inter-regional exchanges are not taken into account, it is useful to also consider the emission per TWh generated within Germany. Due to the increase in RES-E generation and higher efficiencies of new conventional technologies, they decrease by 8.3% from 481.6 kt CO_2/TWh in 2007 to 441.7 kt CO_2/TWh in 2030 in the BASE scenario. In the IMP+ scenario they amount to 350.7 kt CO_2/TWh by 2030, which corresponds to a decrease by 27.2%. Thus, the reduced relevance of carbon intensive lignite-based power generation, leads to significant lower specific CO_2-emissions than in the BASE scenario.

Table 7.8.: Development of the CO_2-emissions in Germany in the IMP+ scenario by fuel type [Mt CO_2 / a]

	2007	2010	2015	2020	2025	2030
coal	106.8	71.8	67.0	85.3	97.9	58.1
gas	28.1	23.5	23.3	21.7	23.0	26.4
lignite	152.6	146.7	151.2	104.5	91.9	77.7
fuel oil	0.0	0.7	0.0	0.0	0.1	0.0
sum	287.5	242.8	241.4	212.4	212.9	162.2

7.4.2.7. Summary of the results of the IMP+ scenario

In the IMP+ scenario, power imports have been assumed to double between 2007 and 2030, while power exports have been assumed to halve. As a result, power generation within Germany decreases, while the power flows in some areas of the German transmission system increase considerably. As a consequence, two additional bottlenecks occur by 2025. One is located north of Hamburg, the other one in Bavaria close to the Czech border. They result from increasing imports from Denmark and the Czech Republic. As a consequence, the distribution of differing nodal prices becomes more heterogeneous. In 2025, in particular an increased nodal price differential between North and South Germany results. In 2030, congestion in the German power grid becomes more severe, which results in higher nodal price differences around the bottlenecks. In the area with high offshore wind power feed-in in the Northwest, prices are partly significantly negative, depending on the time slot. In the other parts of Germany, nodal prices decrease compared to the BASE scenario, because due to the increase in imports, now power stations with lower marginal costs are price setting for power generation in Germany. Therefore, also the average marginal cost of power supply in Germany is lower than in the BASE scenario.

Regarding the structure of the capacity mix, a significant influence of the increasing imports does not show before 2025. In the last two optimization periods, the installed capacity of lignite-fired power stations in the Rhineland is reduced compared to the BASE scenario. However, additional NGCC power stations are built at the deficit side of the bottleneck in the Northwest as a result of the increasing congestion. Regarding power generation, until 2020 in particular power generation from coal in the Ruhr district and in the Southwest is reduced. From 2025 on, power generation at the lignite mining sites in the Rhineland and in Lusatia decreases. The most significant increase in regional power generation compared to the BASE scenario occurs at the deficit side of the bottleneck in the Northwest, where the additional NGCC power stations are used to counteract congestion.

Concerning the development of the CO_2-emissions, the significant reduction of power generation from lignite in the last optimization periods has a positive effect.

7.4.3. Carbon price variations

In the following, the influence of alternative EUA price developments will be analyzed. In the CO2+50 scenario, EUA prices will increase from 8 €/t_{CO_2} in 2007 to 67.5 €/t_{CO_2} by 2030. In the CO2+100 scenario EUA prices will rise to 90 €/t_{CO_2} in 2030. The development of EUA prices in the scenarios is illustrated in Table 7.9.

In the following, firstly the influence of the EUA price variations on the structures and regional developments of the capacity and generation mix will be presented. Then, the effects on congestion and nodal prices as well as on the average marginal cost of power supply will be described. Finally, it will be addressed to which extent higher EUA prices contribute to lower CO_2-emissions.

Table 7.9.: Development of EUA prices in the carbon price variation scenarios [€/t CO_2]

	2007	2010	2015	2020	2025	2030
BASE	8.00	11.25	22.50	27.00	33.00	45.00
CO2+50	8.00	13.36	33.75	40.50	49.50	67.50
CO2+100	8.00	15.47	45.00	54.00	66.00	90.00

7.4.3.1. Structure of the capacity mix

The development of the capacity mix in the CO2+50 scenario resembles the development in the BASE scenario very much (see Figure 7.31). Regarding the development of carbon-fueled technologies, there is an overall decrease in installed capacities. In the CO2+50 scenario, the installed capacity rises from 131.0 GW in 2007 to 150 GW in 2030. The installed capacity of coal-fired power stations decreases over the covered time horizon from 27.8 GW to 18.5 GW, while the installed capacity of lignite-fired power stations drops from 19.2 GW to 16.5 GW. Moreover, gas-fired power station capacities decrease from 23.4 GW to 22.6 GW. Furthermore, 0.6 GW of lignite-fired and 0.7 GW of coal-fired power station capacity are constructed only in 2025, that is one period later than in the BASE scenario. Due to the increase in EUA prices, in 2030 0.7 GW of new coal-fired power stations are realized as with carbon capture and storage (CCS).

Regarding the regional development of the capacity mix, the results of the CO2+50 scenario are very similar to those of the BASE scenario. By 2020, 300 MW of additional NGCC power station capacity are constructed at Berlin, which are not built before 2025 in the BASE scenario. At Munich 700 MW of coal-fired power station capacity are constructed in 2025 instead of in 2020. Moreover, in 2030 an additional 698 MW of coal-fired power station with CCS technology is installed in the Ruhr district (see Figure 7.32). Compared to the BASE scenario, it replaces conventional thermal power station capacity in the same area.

By contrast, the more significant increase of EUA prices in the CO2+100 scenario has considerable influence on the structure of the capacity mix in the later optimization periods (see Figure 7.33). In the CO2+100 scenario, installed capacity amounts to 157.0 GW by 2030, which corresponds to an increase of 4.4% compared to the BASE scenario. Moreover, the mark-up of 100% to the EUA price in the CO2+100 scenario results in a strong increase of coal-fired power station capacities compared to the BASE scenario. This is due to the construction of coal-fired power stations with CCS.

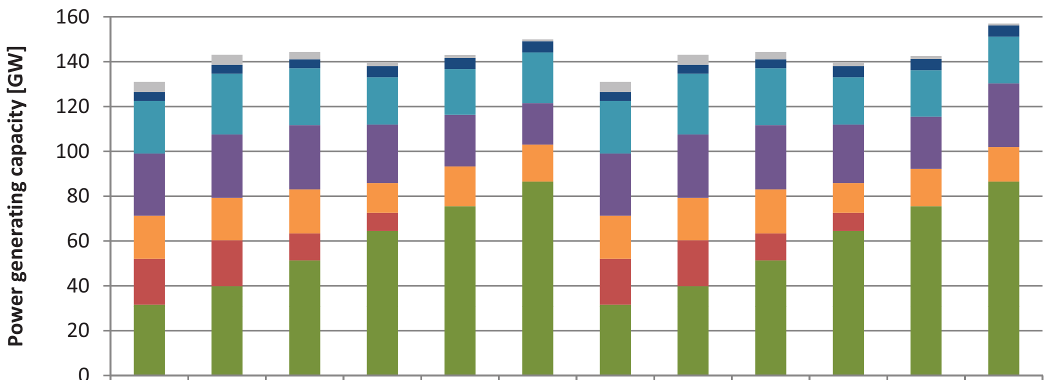

	CO2+50 2007	CO2+50 2010	CO2+50 2015	CO2+50 2020	CO2+50 2025	CO2+50 2030	CO2+100 2007	CO2+100 2010	CO2+100 2015	CO2+100 2020	CO2+100 2025	CO2+100 2030
fuel oil	4.5	4.5	3.3	1.8	1.3	0.8	4.5	4.5	3.3	1.8	1.3	0.8
HPS	4.0	4.0	4.0	5.0	5.0	5.0	4.0	4.0	4.0	5.0	5.0	5.0
gas	23.4	27.1	25.4	21.1	20.4	22.6	23.4	27.1	25.4	21.1	20.7	20.9
coal	27.8	28.3	28.7	26.1	23.1	18.5	27.8	28.3	28.7	26.1	23.3	28.4
lignite	19.2	18.9	19.6	13.2	17.7	16.5	19.2	18.9	19.6	13.2	16.7	15.4
nuclear	20.5	20.5	12.0	8.1	0.0	0.0	20.5	20.5	12.0	8.1	0.0	0.0
RES	31.6	39.9	51.4	64.5	75.5	86.5	31.6	39.9	51.4	64.5	75.5	86.5

Figure 7.31.: Overall development of the capacity mix in the EUA price variation scenarios

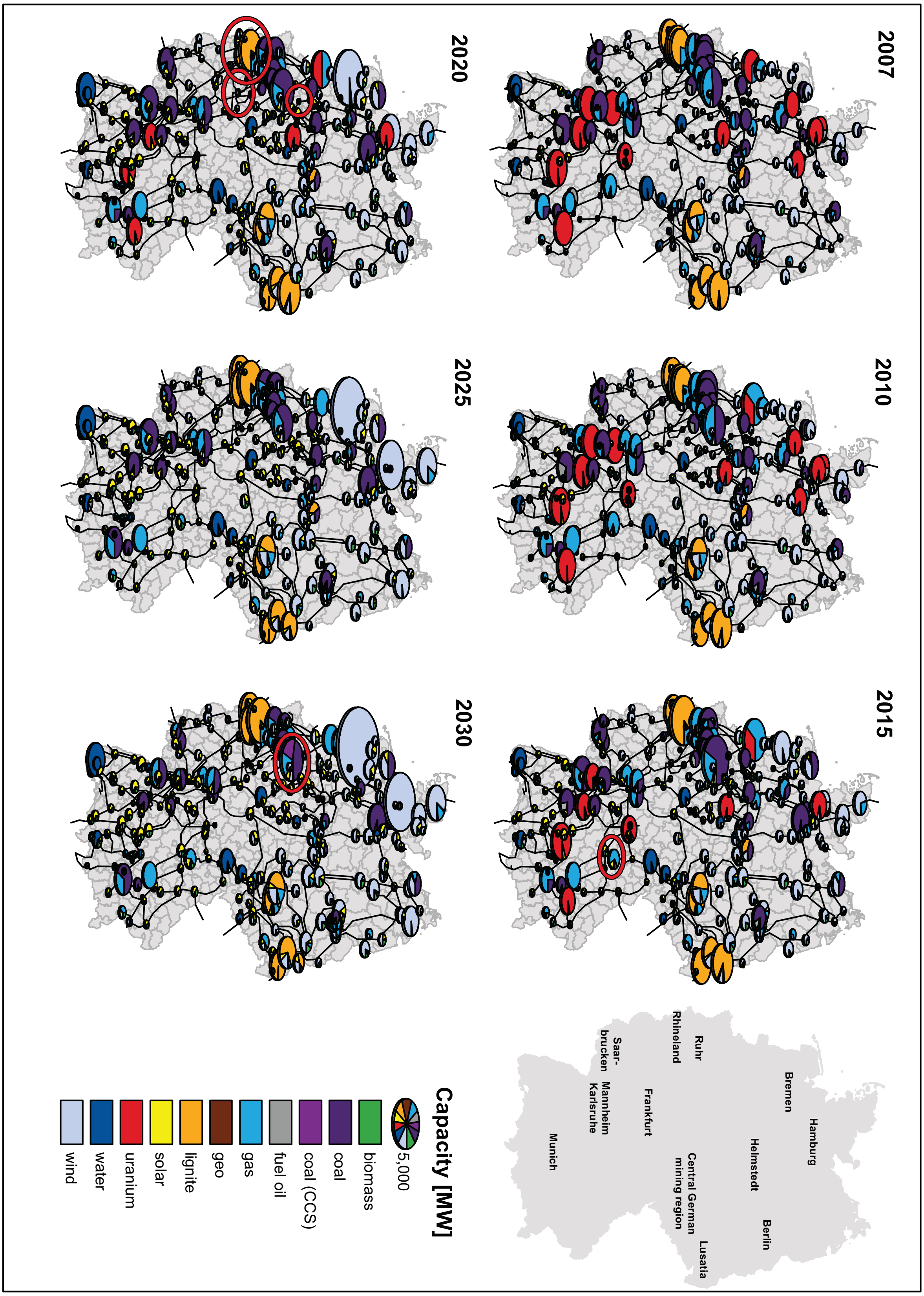

Figure 7.32.: Regional development of generating capacity in the CO2+50 scenario

Over the time horizon covered by the optimization, coal capacities now increases from 27.8 GW to 28.4 GW. The highest growth rate is realized between 2025 and 2030, when the net installed capacity of coal-fired power stations increases by 18%. In the last optimization period, 10.6 GW coal-fired power stations are realized as coal-fired power stations with CCS technology in 2030. At the same time, the installed capacity of gas-fired power stations decreases from 23.4 GW to 20.9 GW, while the installed lignite power station capacity decreases from 19.2 GW in 2007 to 15.4 GW in 2030. Thus, compared to the BASE scenario, the installed capacity of gas- and lignite-fired power stations decrease by 2.2 GW and 0.9 GW, respectively. In 2030, coal capacities rise by 9.8 GW compared to the BASE scenario, which results in a rise of the share of coal in total generation capacity from 12.4% to 18.1%. At the same time the share of lignite capacities falls from 10.9% to 9.8%. However, the price induced shift from lignite to coal takes only place in the last optimization period. In fact, in 2020 coal and lignite capacity each decrease by 0.3 GW compared to the BASE scenario, while gas capacities increase by 0.4 GW compared to the BASE scenario. In the CO2+100 scenario, all new gas-fired power stations are built as NGCC power stations.

Figure 7.33 shows the regional development of power generation in the CO2+100 scenario. Most striking is the considerable amount of new coal-fired power stations with CCS in the Ruhr area. Additional coal-fired power stations with CCS are built near Frankfurt and near Saarbrucken. Moreover, the installed capacity of gas-fired power stations in the Northwest decreases by approximately 2 GW by 2030.

7.4.3.2. Structure of power generation and capacity utilization

In the CO2+50 scenario, the EUA price increases have almost no effect on power generation compared to the BASE scenario. The increasing EUA prices show most in 2020, when power generation from lignite decreases by 4.7 TWh, while power generation from gas and coal increases by 3.1 TWh and 1.7 TWh, respectively. Nevertheless, lignite stays the second most important fuel in power generation, even though power generation from lignite decreases from 137.0 TWh in 2007 to 128.3 TWh in 2030 (see Figure 7.34). Compared to the BASE scenario this corresponds to an increase in lignite-based power generation of 1.1 TWh in 2030. Meanwhile, power generation from coal amounts to 82.1 TWh in 2030, which is 1.6 TWh lower than in the BASE scenario. Comparing the first and the last optimization period, power generation from gas increases by 5.7 TWh and reaches a level of 75.1 TWh by 2030, which is 0.5 TWh higher than in the BASE scenario. These variations in the structure of power generation correspond to a shift of 0.3% in coal's share in total generation to lignite and gas. This seemingly paradox reaction to higher EUA prices can be explained with more efficient new lignite-fired power stations replacing less efficient old coal-fired power stations, resulting in slightly decreasing total emissions from power generation within Germany compared to the BASE scenario (see section 7.4.3.6).

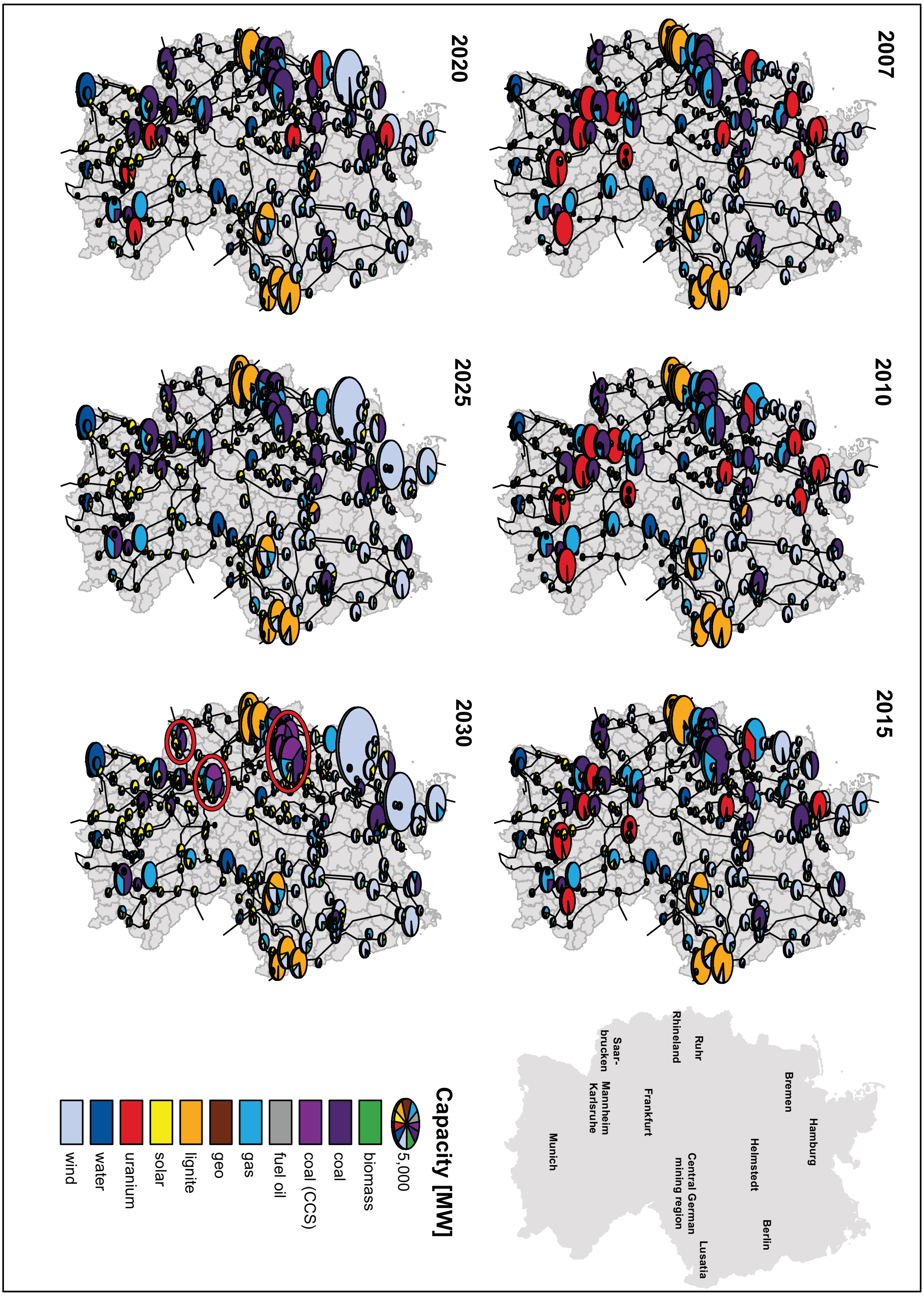

Figure 7.33.: Regional development of generating capacity in the CO2+100 scenario

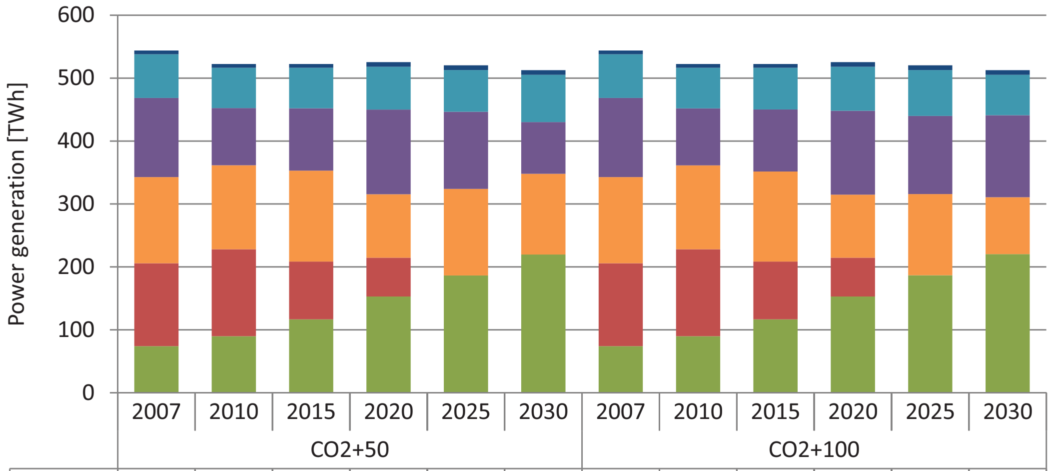

	CO2+50						CO2+100					
	2007	2010	2015	2020	2025	2030	2007	2010	2015	2020	2025	2030
fuel oil	0.0	0.0	0.0	0.0	0.1	0.0	0.0	0.0	0.0	0.0	0.1	0.0
HPS	6.0	6.0	6.0	7.5	7.5	7.5	6.0	6.0	6.0	7.5	7.5	7.5
gas	69.4	64.0	64.3	67.9	66.3	75.1	69.4	64.4	66.2	69.8	72.9	64.1
coal	125.8	90.8	99.1	134.7	122.6	82.1	125.8	90.7	98.7	133.3	124.2	130.3
lignite	137.0	133.5	144.5	100.7	137.6	128.3	137.0	133.3	143.0	100.2	129.1	90.5
nuclear	131.7	138.1	91.8	61.7	0.0	0.0	131.7	138.1	91.8	61.7	0.0	0.0
RES	74.0	89.9	116.7	153.0	186.3	219.7	74.0	89.9	116.7	153.0	186.7	220.3

Figure 7.34.: Overall development of power generation in the EUA price variation scenarios

Regarding the utilization of power stations in the CO2+50 scenario, also only minor changes in comparison with the BASE scenario can be made out. By 2020, the average full load hours of coal-fired power stations amount to 5415 h/a and thus increase by 150 h/a compared to the BASE scenario, while the average full load hours of lignite-fired power stations amount to 7442 h/a, which corresponds to a decrease of 104 h/a compared to the BASE scenario. In 2030 the average full load hours of the new coal-fired power stations with CCS technology amount to 7884 h/a. Moreover, the average full load hours of conventional coal-fired power stations total 5174 h/a and of lignite-fired power stations 7465 h/a. This corresponds to a decrease by 154 h/a and 261 h/a in comparison with the BASE scenario. The lower average full load hours of lignite-fired power stations result from the construction of more lignite-fired power station capacity than in the BASE scenario. The average full load hours of gas-fired power stations are approximately at the same level as in the BASE scenario.

By contrast to the CO2+50 scenario, the doubling of EUA prices in the CO2+100 scenario has a significant influence on the structure of power generation in Germany. In the CO2+100 scenario, power generation from lignite decreases more strongly between 2007 and 2030 and reaches a level of 90.45 TWh by 2030 (see Figure 7.34). Even though generation from coal still decreases between 2020 and 2025, it increases from 125.8 TWh to 130.3 TWh comparing the first and the last optimization period. Thus, by 2030 lignite is replaced by coal as the second most important fuel in power generation, which also results from the use of in coal-fired power stations with CCS. Compared to the BASE scenario this corresponds to an increase of 46.6 TWh, while power generation from lignite decreases by 36.7 TWh. Moreover, power generation in gas-fired power stations increases from 64.4 TWh in 2010 to 72.9 TWh in 2025. Yet, due to the installation of the new coal-fired power stations with CCS it decreases, again, to 64.1 TWh in 2030. By 2030, the share of coal in power generation amounts to 25.4% and the share of lignite to 17.6%.

Amounting to 12.5%, the share of gas remains almost at the same level as in 2007. In the last two optimization periods, RES-E is slightly higher than in the BASE scenario. Due to the shifts in regional power generation, offshore wind power has to be shut down to a smaller extent in times of low system load, which results in higher average full load hours and a marginally increased RES-E generation. In both scenarios, power generation from fuel oil remains at a level below 1 TWh, while power generation in HPS stations increases from 5.98 TWh in 2007 to 7.48 TWh in 2030.

Like in the BASE scenario, the average full load hours of large coal-fired power stations rise far above 5000 h/a in 2020 and 2025. Yet, when coal-fired power stations with CCS-technology start operating in 2030, the average full load hours of conventional coal-fired power stations without CCS decrease to 3414 h/a. By contrast, the new coal-fired power stations with CCS are operated at average full load hours of 7884 h/a. Furthermore, the average full load hours of lignite-fired power stations are above 7000 h/a until 2025. Due to the high EUA prices, power generation based on lignite becomes comparatively expensive in 2030. Correspondingly, the average full load hours of lignite-fired power stations decrease to 5332 h/a. The average full load hours of large gas-fired power stations stay at a level between 3100 h/a and 3400 h/a between 2020 and 2030.

The Figures 7.35 and 7.36 show the regional development of power generation in the CO2+50 and CO2+100 scenario. In the optimization periods 2007 - 2015 the regional distribution of power generation is almost the same as in the BASE scenarios.

In the CO2+50 scenario, part of the power generation in lignite-fired power stations in Lusatia as well as in coal-fired power stations at Munich is shifted to the Rhineland and the Ruhr district in 2020 and 2025. Otherwise, the regional distribution of power generation in the CO2+50 scenario strongly reassembles the BASE scenario until 2025. By 2030 5.5 TWh of conventional power generation are replaced by generation in coal-fired power stations with CCS located in the Ruhr district. It replaces in particular lignite-based generation in the Rhineland and power generation from coal in the Ruhr district.

In the CO2+100 scenario (see Figure 7.36), the most significant changes in comparison with the BASE scenario also occur in 2030, when the coal-fired power stations with CCS facilities start operating. By 2030, power generation in coal-fired power stations with CCS in the Ruhr district amounts to 71.2 TWh, while power generation in the coal-fired power stations with CCS near Frankfurt and Saarbrucken totals 5.8 TWh and 6.7 TWh. Compared to the BASE scenario, it replaces 39.6 TWh of coal and gas-based power generation in the Ruhr district, 23.8 TWh of power generation from lignite in the Rhineland, 13.5 TWh of lignite base generation in Lusatia, and 4.6 TWh of gas- and coal-based generation in South Germany. Moreover, a new coal-fired power station with CCS near Frankfurt replaces 8.8 TWh of power generated in conventional coal-fired power stations in the southwest of Germany. In the Southeast, NGCC power stations are the predominant generators by 2030. Yet, near Munich power generation in conventional coal-fired PCC stations persists. Power generation in the NGCC power station in the Northwest is 9.6 TWh lower in the CO2+100 scenarios than in the BASE scenario in 2030.

7.4.3.3. Average nodal prices and congestion

Due to the increases in EUA prices, the average marginal costs of power supply are higher in the CO2+50 and CO2+100 scenario than in the BASE scenario. Figure 7.37 illustrates the regional distribution of average nodal prices in 2030 in the EUA price variation scenarios.

In the CO2+50 scenario, congestion in the German power grid corresponds to the situation in the BASE scenario (see Figure 7.1). Therefore, until 2020 the only differences to the nodal prices in the BASE scenario is their increased level, which is caused by the increase in EUA prices. From 2015 on, nodal prices are almost 10 €/MWh higher than in the BASE scenario. On most grid nodes they amount to 59.31 €/MWh. An exception are grid nodes at the end of the congested stub lines in Northern Germany. In 2020, nodal prices lie between 70.49 €/MWh and 70.98 €/MWh. As in the BASE scenario the Diele - Rhede corridor is congested by 2025. Yet, since it is only binding during one time slot and since the cost of the constraint is still almost zero, no differences in average annual nodal price occur. In 2030 the bottleneck Diele - Rhede is more severe than in 2025 and causes differing nodal prices (see Figure 7.37). The nodal price difference between the surplus and the deficit side of the bottleneck amounts to 62.62 €/MWh. Average annual nodal prices at Diele are 40.01 €/MWh, while at Rhede they amount to 102.63 €/MWh. Regarding the nodal prices in the rest of Germany, their distribution resembles the distribution in the BASE scenario, yet with a price mark-up of approximately 15 €/MWh caused by higher EUA prices.

In the CO2+100 scenario, congestion in the optimization periods 2010 - 2020 resembles the situation in the BASE scenario (see Figure 7.38). However, in 2010, an additional bottleneck in the Southeast occurs during one time slot. Yet, it has no measurable effect on average annual nodal prices. The EUA price induced increase of average nodal prices from 2015 on, is more distinct than in the CO2+50 scenario. As in the previously described scenarios, nodal prices vary only marginally in 2015, ranging from 67.64 €/MWh at two grid nodes with wind power feed-in close to the North Sea to 68.93 €/MWh in the rest of Germany.

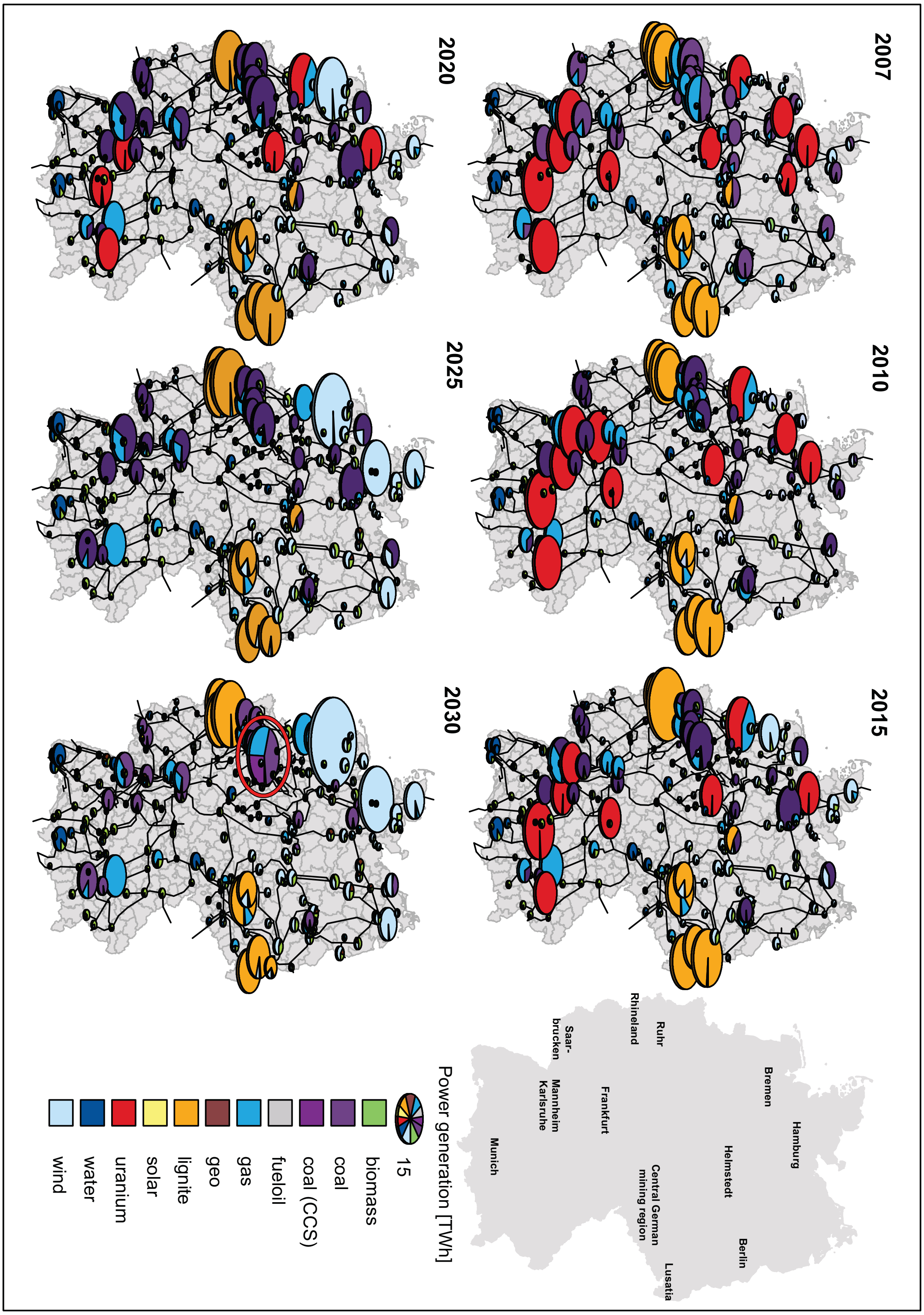

Figure 7.35.: Regional development of power generation in the CO2+50 scenario

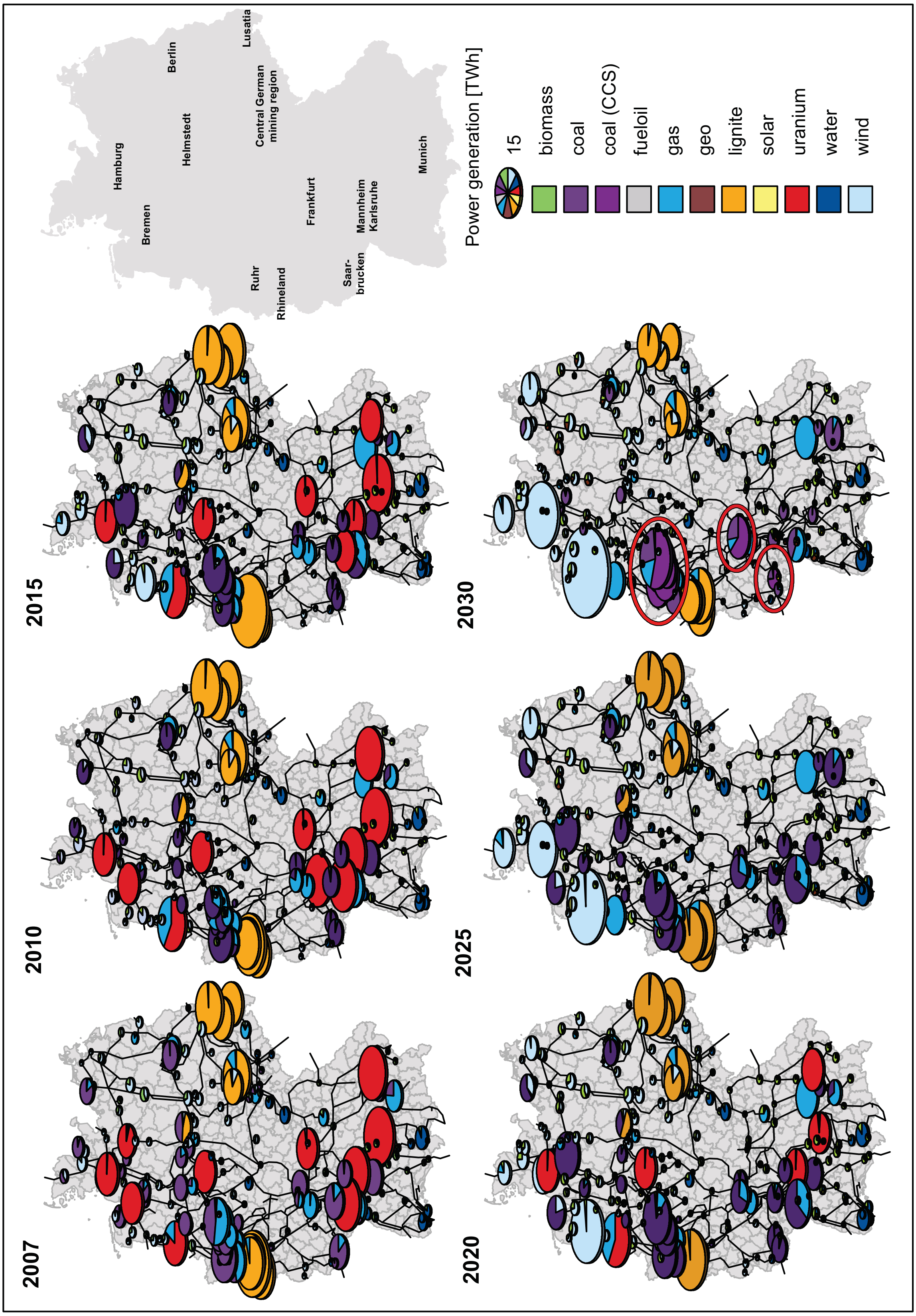

Figure 7.36.: Regional development of power generation in the CO_2+100 scenario

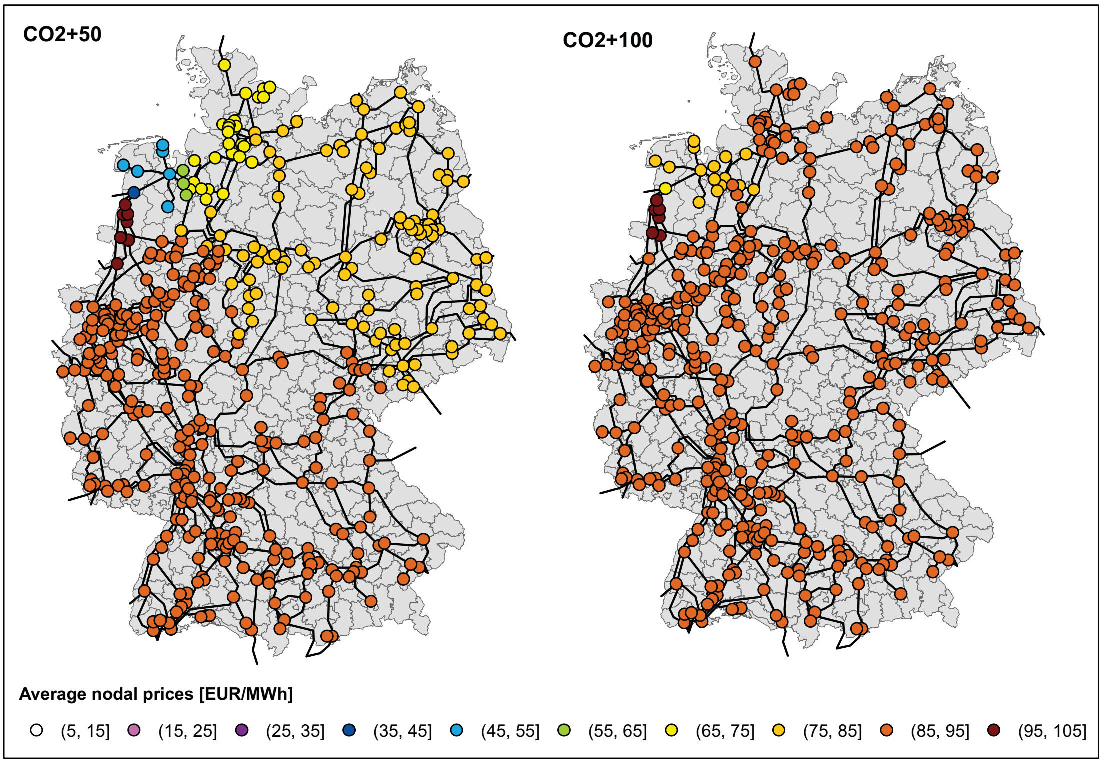

Figure 7.37.: Average nodal prices in 2030 in the EUA price variation scenarios

Like in the other scenarios, the thermal constraint of the bottleneck in the Northwest becomes binding in 2025. Yet, by contrast to the BASE and the CO2+50 scenario, a second bottleneck develops in Southeast Germany. This bottleneck causes nodal price differences of 2.96 €/MWh between Schwandorf and Etzenricht and has an influence on the regional distribution of nodal prices. Nodal prices are highest in the Southeast (approximately 96 €/MWh) and comparatively lower in the East (approximately 95 €/MWh). In the western Germany they amount to approximately 95.5 €/MWh.

Figure 7.37 (right) shows that in 2030 the differences in average annual nodal prices are much less pronounced in the CO2+100 scenario than in the previously described scenarios. The most important bottleneck is still Diele - Rhede, yet its significance is reduced in comparison with the BASE scenario. The main reason for this is that the relevance of congestion on the power lines between Conneforde and Diele decreases, which is caused by a further shift of generation from the lignite mining sites in Lusatia and in the Rhineland to the Ruhr area. Moreover, the reduced significance of lignite-fired power stations, which posses comparatively high load variation costs, results in less lower nodal prices at the surplus side of the bottleneck. While the average annual nodal prices at Diele amount to 70.26 €/MWh, they total 101.56 €/MWh at Rhede. Average annual nodal prices in the rest of Germany range between 70.26 €/MWh and 101.56 €/MWh with a nodal price divide between North and South as well as between East and West Germany.

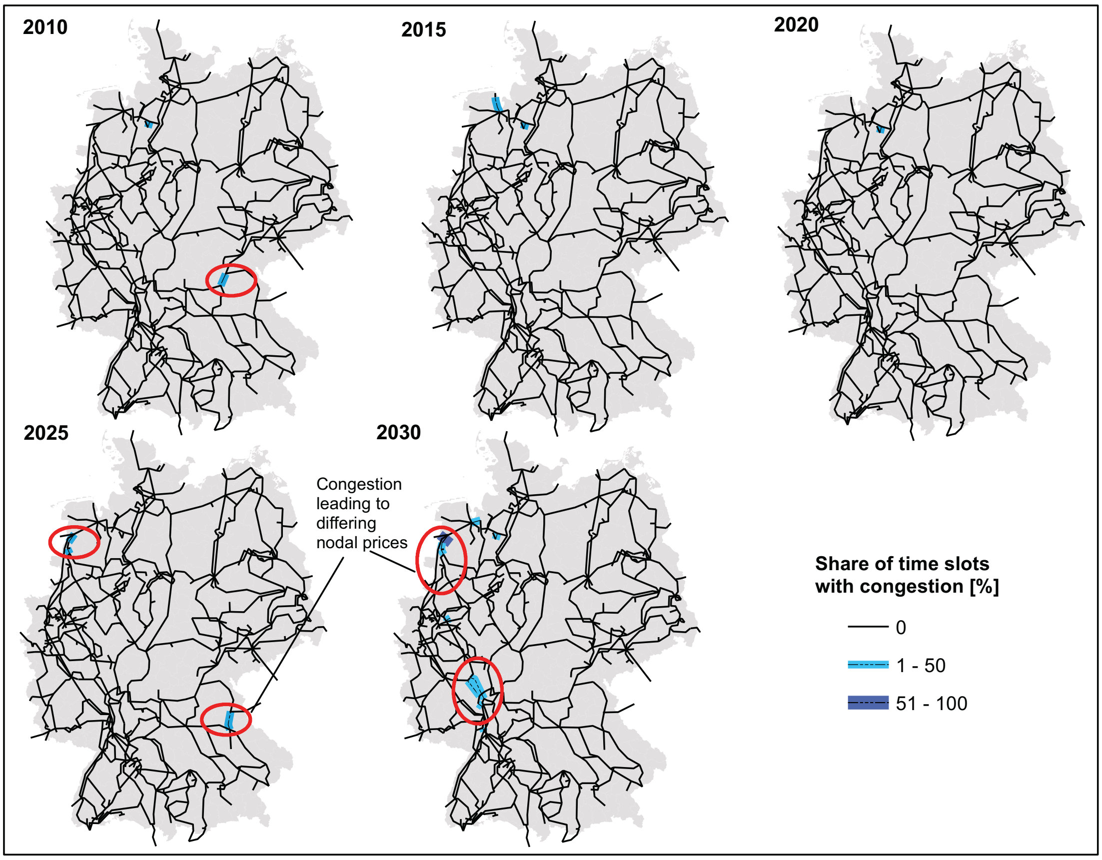

Figure 7.38.: Congestion in the CO2+100 scenario

7.4.3.4. Nodal prices, power generation, and congestion in selected time slots

Nodal prices, congestion, and power generation in situations of extreme system load in 2030 for the CO2+50 scenario are shown in the Figures 7.39 and 7.40. In times of system peak load, nodal prices show almost the same distribution as in the BASE scenario. However an increase in overall nodal prices occurs, which is most pronounced at and close to grid nodes with high offshore wind power feed-in. It is induced by a decrease in the value of the "counterflow" on the Diele - Rhede corridor, which is caused by the shift in generation from the lignite mining sites in Lusatia to the coal-fired power station with CCS in the Ruhr district (see Figure 7.39 (right)). Moreover, the higher EUA prices add to the overall nodal price increase. The second congested corridor near Frankfurt has only minor influence on nodal prices.

In times of low system load, the increase in EUA prices, which affects in particular the more CO_2-intensive base load power stations, such as lignite-fired power stations, leads to an increase in nodal prices in the western part of Germany. The only bottleneck remains the Diele - Rhede corridor. Except for a shift in generation from the lignite

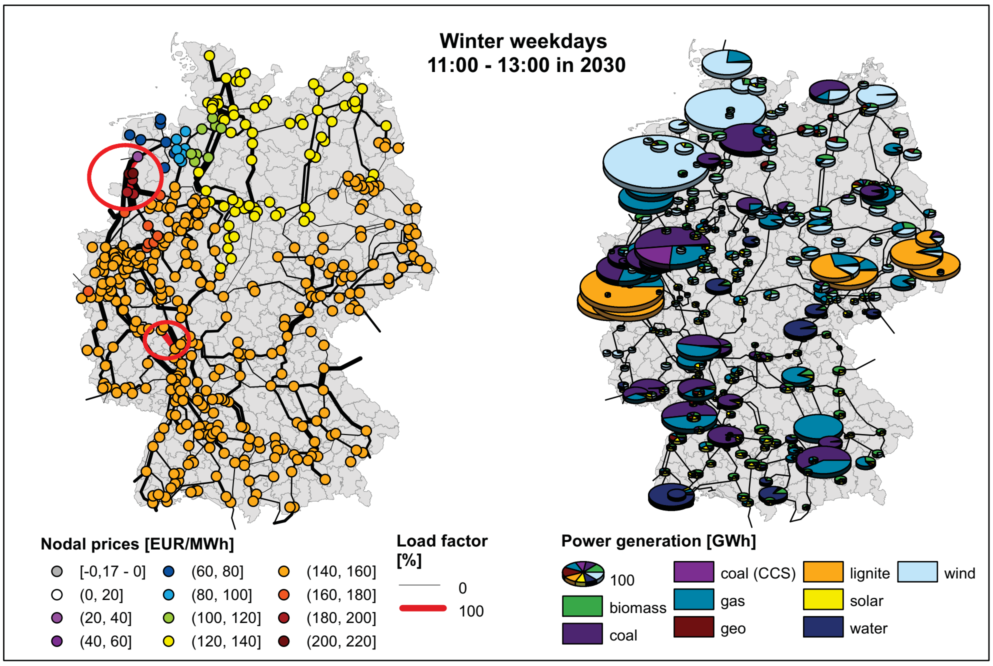

Figure 7.39.: Regional distribution of nodal prices, congestion, and power generation in times of high system load in 2030 in the CO2+50 scenario

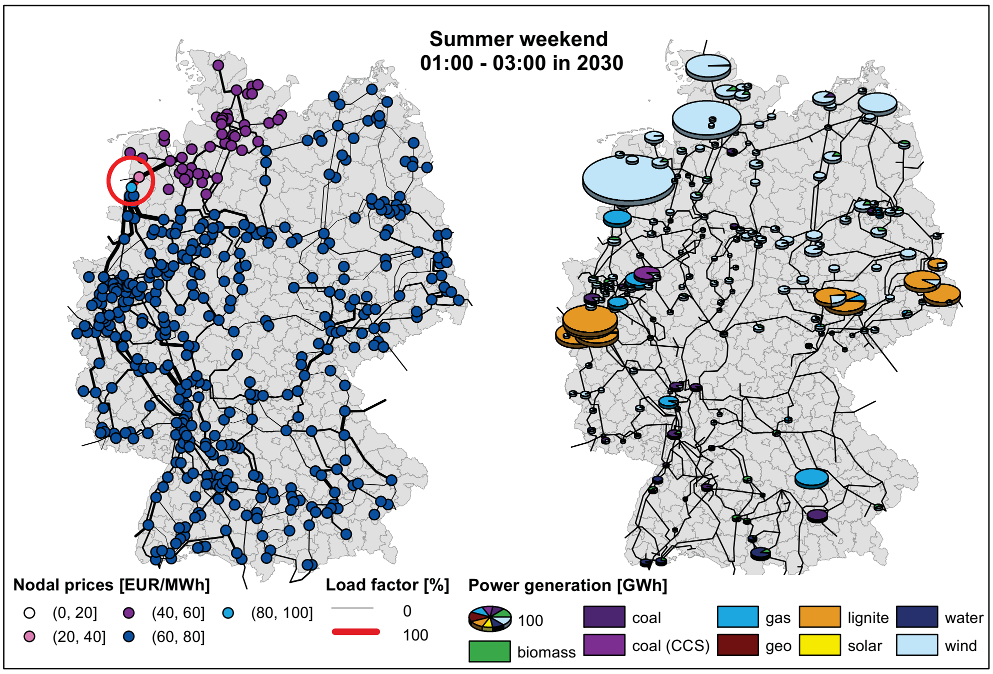

Figure 7.40.: Regional distribution of nodal prices, congestion, and power generation in times of minimum system load in 2030 in the CO2+50 scenario

mining district in Lusatia to Ingolstadt and a fuel switch from gas to coal in the Ruhr district, the regional distribution of power generation resembles the BASE scenario.

By contrast to the strong increase in EUA prices, nodal prices at system peak load in 2030 are in general lower in the CO2+100 scenario than in the CO2+50 or BASE scenario (see Figure 7.42 (left)). While nodal prices are comparatively lower in most parts of Germany, they are comparatively higher at the surplus side of the congested corridor and in the Northwest. This seemingly contradictory effect is due to the reduced relevance of the binding line constraint between Diele and Rhede. In general, the influence of the binding line constraint on nodal prices is highest in times of high system load. Since in the CO2+100 scenario the price rising effect of the bottleneck is much lower than in the CO2+50 scenario, nodal prices in times of system peak load are lower in the CO2+100 than in the CO2+50 scenario. Maximum nodal prices, which occur at Rhede amount to 176.11 €/MWh, while minimum nodal prices at Diele are equal to 68.83 €/MWh. Again, nodal prices close to the North Sea remain positive. Figure 7.42 (right) shows the regional distribution of power generation in times of maximum system load. The increased generation in coal-fired power stations with CCS is of significance again, since it results in a considerable regional shift in generation. In addition to replacing lignite power stations, the generation in coal-fired stations with CCS also leads to a decrease in power generation close to the Dutch border and in Hamburg.

Likewise, in times of minimum system load (see Figure 7.42 (right)) coal-fired power stations with CCS become the most prominent conventional base load power stations. This reflects that due to the mark-up to EUA prices, the relation of the different technologies in terms of marginal cost changes, which also has an influence on the merit order of the technologies. In Southern Germany, the change in marginal cost results in the utilization of an NGCC power station as base-load technology. Regarding the nodal prices in the CO2+100 scenario in 2030 in times of minimum load (see Figure 7.42 (left)), nodal prices are the same at all grid nodes of the power system. They amount to 72.14 €/MWh. The reason for this is that even though the Diele - Rhede corridor is utilized to a level that the bottleneck just persists, its cost are so low that in this scenario it does not show in the nodal prices any more. Again, this can be explained by the changes in the regional distribution of power generation.

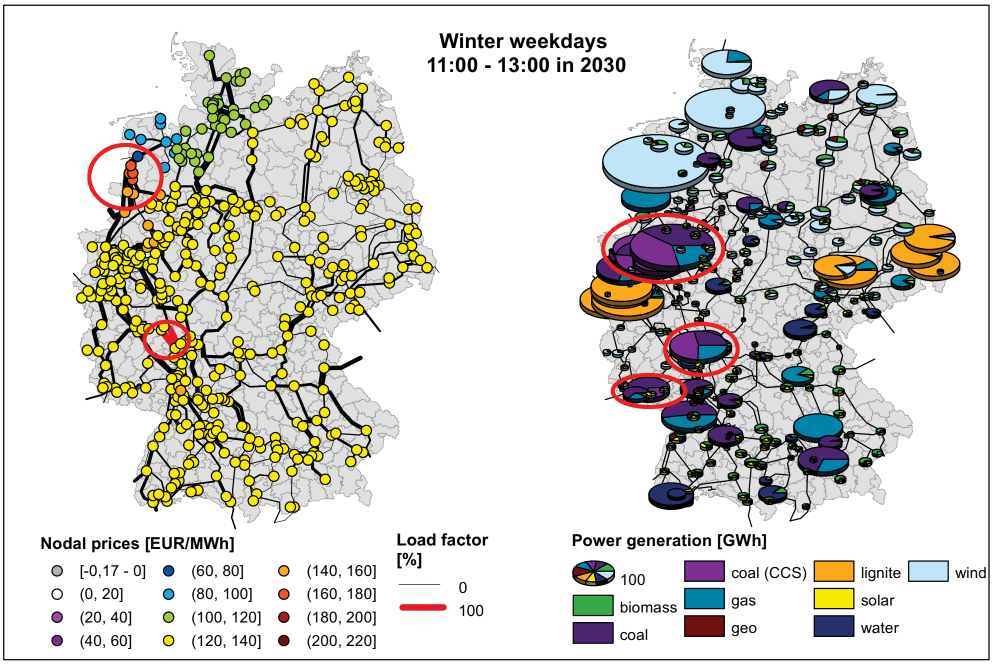

Figure 7.41.: Regional distribution of nodal prices, congestion, and power generation in times of system peak load in 2030 in the CO2+100 scenario

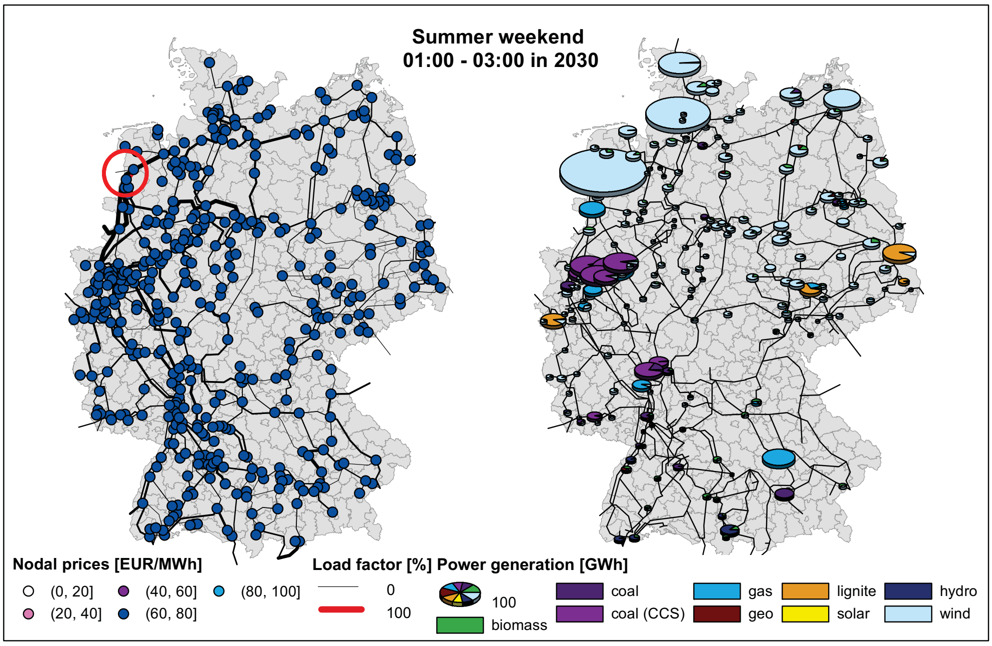

Figure 7.42.: Nodal prices, peak load, and power generation in 2030 in times of minimum system load in the CO2+100 scenario

7.4.3.5. Overall marginal cost of power generation

In both scenarios, the marginal cost of power supply rise due to the mark-ups to the EUA prices (see Table 7.10). In the CO2+50 scenario, the average marginal cost of power supply in Germany increase from 38.50 €/MWh in 2007 to 85.31 €/MWh in 2030. Meanwhile, the average marginal cost of power supply in peak hours rise to 109.63 €/MWh in 2025 and decrease again to 104.17 €/MWh in 2030. The average marginal cost of power supply during off-peak hours continuously rise from 28.82 €/MWh to 74.84 €/MWh. Like in the BASE scenario, the average marginal cost of power supply during peak hours are extremely high in 2025 due to the use of fuel oil-fired power stations and decrease in the last period when the use of fuel oil is abandoned.

In the CO2+100 scenario average marginal cost rises from 38.50 €/MWh in 2007 to 95.55 €/MWh in 2025 and decreases by 5.3% in the last optimization period to 90.47 €/MWh. Moreover, peak load prices rise to 125.65 €/MWh in 2025 and drop to 105.68 €/MWh in 2030. Like the decrease in nodal prices in the last period, this is due to the decreasing relevance of the congestion in the North as well as to the abandonment of power generation from fuel oil. The average marginal cost of power supply during off-peak hours rises from 28.82 €/MWh in 2007 to 84.02 €/MWh in 2030. The marginal cost during off-peak hours rises significantly in both scenarios due to the increasing costs of base load power generation, in particular of lignite-fired power stations.

Table 7.10.: Marginal cost of power supply in the EUA price variation scenarios [€/MWh]

Scenario	Prices	2007	2010	2015	2020	2025	2030
CO2+50	Avg. MC	38.50	43.33	59.31	70.50	81.82	85.31
	Avg. MC - peak	51.18	60.97	74.09	88.65	109.63	104.17
	Avg MC - off-peak	28.82	33.37	52.42	60.93	66.96	74.84
CO2+100	Avg. MC	38.50	44.94	68.16	80.57	95.55	90.47
	Avg. MC - peak	57.34	62.75	83.15	98.60	125.65	105.68
	Avg. MC - off-peak	38.50	34.91	60.66	70.78	79.32	84.02

7.4.3.6. Carbon dioxide emissions

The development of CO_2-emissions by fuel type are shown in Figure 7.43. Due to the mark-up in EUA prices, less carbon intensive technologies become favorable in the CO2+50 and CO2+100 scenario. Moreover, CCS becomes economically beneficial. Therefore, the CO_2-emissions are reduced compared to the BASE scenario. In the CO2+50 scenario, CO_2-emissions decrease from 287.5 Mt CO_2/a in 2007 to 200.3 Mt CO_2/a in 2030. In the CO2+100 scenario, CO_2-emissions are reduced to 144.3 Mt CO_2/a in 2030. Compared to the BASE scenario this corresponds to a reduction of 30%. In both EUA price scenarios, lignite-fired power stations remain the most important CO_2 emitters, followed by coal and gas. However, in particular in the CO2+100 scenario, the difference between coal and gas-fired power stations in terms of CO_2-emission is reduced in the last optimization period due to the increased use of coal-fired power stations with CCS technology.

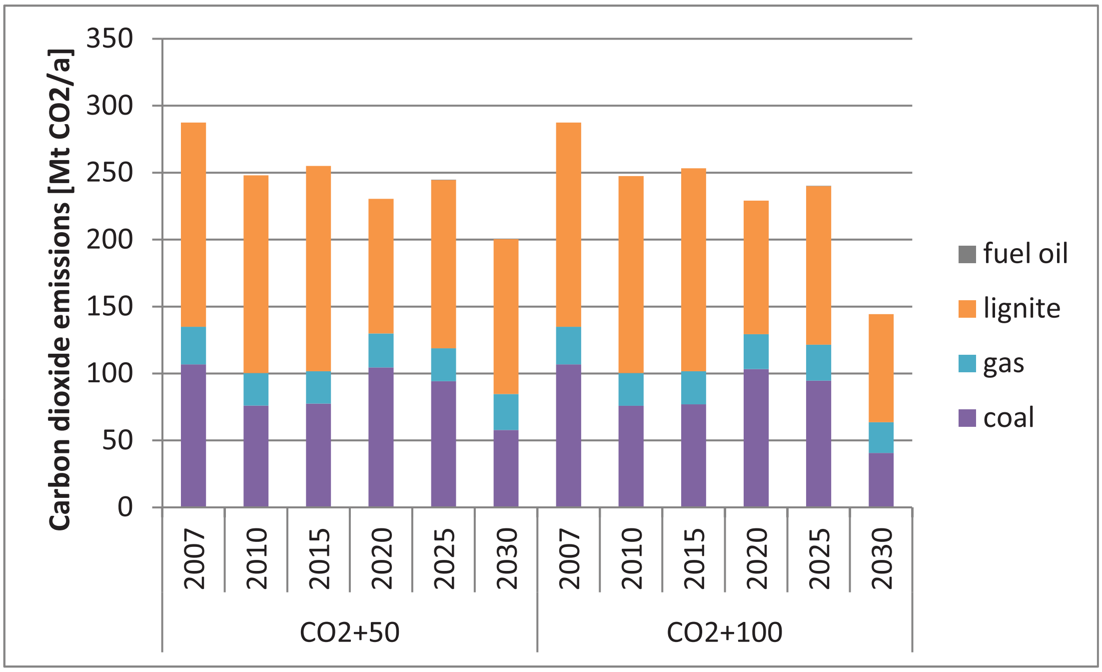

Figure 7.43.: Carbon dioxide emissions in the EUA price variation scenarios

7.4.3.7. Summary of the results of the carbon price variations

In the EUA price variation scenarios, mark-ups to the EUA price of 50% (CO2+50 scenario) and 100% (CO2+100 scenario) are assumed. The mark-up of 50% to the CO_2 price has only little effect on the structures of the capacity mix and power generation. Only one coal-fired power station with CCS is installed in the Ruhr district. It replaces lignite-fire capacities in the Rhineland. Moreover, slight shifts from coal to lignite and gas occur. Regarding the marginal cost of power supply, the additional rise in EUA prices causes an overall rise in nodal prices as well as in the average marginal cost of power supply in Germany.

By contrast to the mark-up of 50%, the mark-up of 100% to the EUA price has significant effects on the structures of the capacity mix and power generation. In particular, a strong increase in coal-fired power station capacity with CCS results. In 2030, 20.6 GW of coal-fired power stations are installed in the Ruhr district, near Frankfurt, and near Saarbruecken. Compared to the BASE scenario, they replace coal-fired capacities without CCS as well as lignite-fired capacities. Consequently power generation from coal in 2030 is by 47 TWh higher than in the BASE scenario. It replaces power generation from lignite and gas.

Since most power stations with CCS are located in the Ruhr, a considerable regional shift of power generation from the lignite mining districts to the Ruhr district occurs. As a result, congestion on the bottleneck in the Northwest is less severe than in the BASE scenario and the nodal price difference around the bottleneck is less pronounced. Moreover, annual average nodal prices as well as the annual average marginal cost of power supply in Germany are higher than in the BASE scenario due to the mark-up to the EUA price. However, reduced congestion in the power grid results in lower nodal prices in times of high system load. By 2030, the average annual marginal cost of power supply amounts to 90.47 €/MWh in the CO2+100 scenario.

Regarding the development of CO_2-emissions, the use of CCS results in a considerable reduction of CO_2-emissions by 2030. Over the time horizon covered by the optimization, CO_2-emissions are reduced by almost 50%.

7.4.4. Gas price variations

In this section two scenarios regarding the development of the gas (and fuel oil) prices are evaluated. In the Gas+20 scenario a mark-up to the gas and fuel oil price of 20% is assumed, while in the Gas+50 scenario a mark-up of 50% is considered.[6]

In the following, the influences of the gas price variations on the structures of the capacity and generation mix will be described. Then, the effect on nodal prices and congestion will be presented, followed by a description of the development of the average marginal cost of power supply in Germany. Finally, the influence of the gas price variations on CO_2-emissions will be presented.

7.4.4.1. Structure of the capacity mix

The development of the capacity mix in the gas price variation scenarios is very similar to the development in the BASE scenario (see Figure 7.44). Yet, in the gas price variation scenarios minor shifts compared to the BASE scenario occur, in particular from gas to lignite and coal. The model results show a slight decrease in the share of gas-fired power stations from 2010 on compared to the BASE scenario. In both scenarios, the installed capacity of gas-fired power stations between 2010 and 2020 is 200 MW lower than in the BASE scenario. In the Gas+20 scenario, the installed capacity of gas-fired power stations is 0.5 GW and 1.0 GW lower in 2025 and 2030 than in the BASE scenario.

In the Gas+50 scenario, the installed capacity of gas-fired power stations is reduced by 2.3 GW compared to the BASE scenario. As a result in 2030 gas-fired power stations have a share of 14.7% in the Gas+20 and of 13.5% in the Gas+50 scenario.

Moreover, in the Gas+20 scenario the increase of gas prices results in an increase in coal (367 MW) and lignite (900 MW) power station capacities in 2020. By 2030 the installed capacity of lignite-fired power stations is 1.8 GW higher than in the BASE scenario.

6 For an overview of the original development of the gas as well as of the other fuel prices see section 6.5.1.

The installed capacity of coal-fired power stations, however, decreases after 2020 and reaches a level of 17.8 GW in 2030, which is 755 MW lower than in the BASE scenario. Thus, due to the construction of more lignite fired power station capacity, not only gas-fired, but also coal-fired power stations are replaced compared to the BASE scenario. In the Gas+50 scenario, the decrease in gas-fired power station capacity compared to the BASE scenario is also compensated by an increase in coal- and lignite-fired power station capacities. Yet, it is more pronounced than in the Gas+20 scenario. In 2020, the installed capacity of coal- and lignite-fired power stations is 1.1 GW and 0.9 MW higher than in the BASE scenario. By 2030, lignite power station capacity reaches a level of 20.0 GW, which exceeds the lignite-fired power station capacity installed in the BASE scenario by 3.7 GW. Coal-fired power station capacity is 2.1 GW higher than in the BASE scenario.

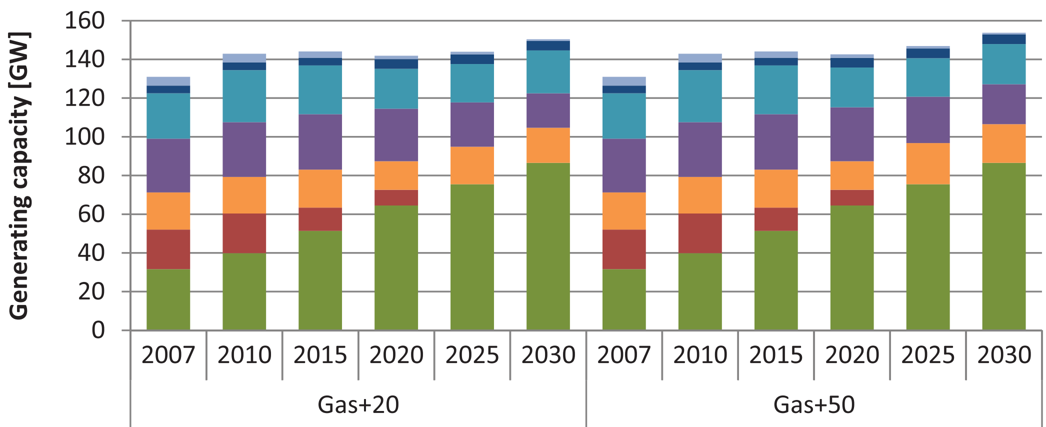

	Gas+20 2007	Gas+20 2010	Gas+20 2015	Gas+20 2020	Gas+20 2025	Gas+20 2030	Gas+50 2007	Gas+50 2010	Gas+50 2015	Gas+50 2020	Gas+50 2025	Gas+50 2030
fuel oil	4.5	4.5	3.3	1.8	1.3	0.8	4.5	4.5	3.3	1.8	1.3	0.8
HPS	4.0	4.0	4.0	5.0	5.0	5.0	4.0	4.0	4.0	5.0	5.0	5.0
gas	23.4	26.9	25.2	20.6	19.9	22.1	23.4	26.9	25.2	20.6	19.9	20.8
coal	27.8	28.3	28.7	27.2	22.9	17.8	27.8	28.3	28.7	27.9	23.9	20.7
lignite	19.2	18.9	19.6	14.7	19.3	18.1	19.2	18.9	19.6	14.7	21.3	20.0
nuclear	20.5	20.5	12.0	8.1	0.0	0.0	20.5	20.5	12.0	8.1	0.0	0.0
RES	31.6	39.9	51.4	64.5	75.5	86.5	31.6	39.9	51.4	64.5	75.5	86.5

Figure 7.44.: Overall power generating capacity development in the gas price variation scenarios

The regional development of the capacity mix is very similar to the development in the BASE scenario. The increase in lignite-fired capacity is in both scenarios more pronounced in the Rhineland than in Lusatia. Furthermore, coal-fired power station capacity is shifted within the Ruhr district. In both scenarios, the reduction in NGCC capacity affects above all Ingolstadt, Berlin, and Northwest Germany. Figures 7.45 and 7.46 show the regional developments of the capacity mix in the Gas+20 and Gas+50 scenario.

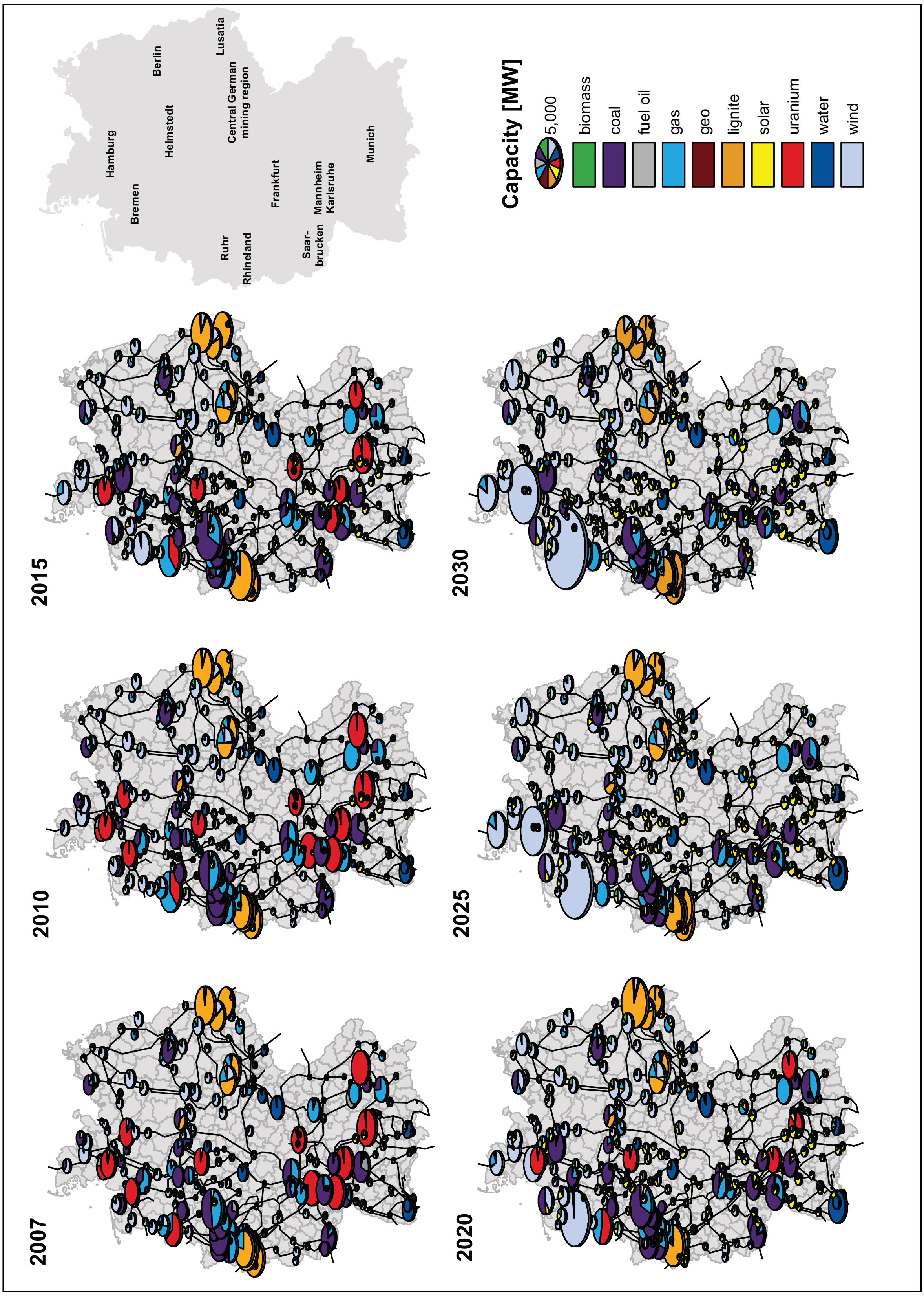

Figure 7.45.: Regional development of generating capacity in the Gas+20 scenario

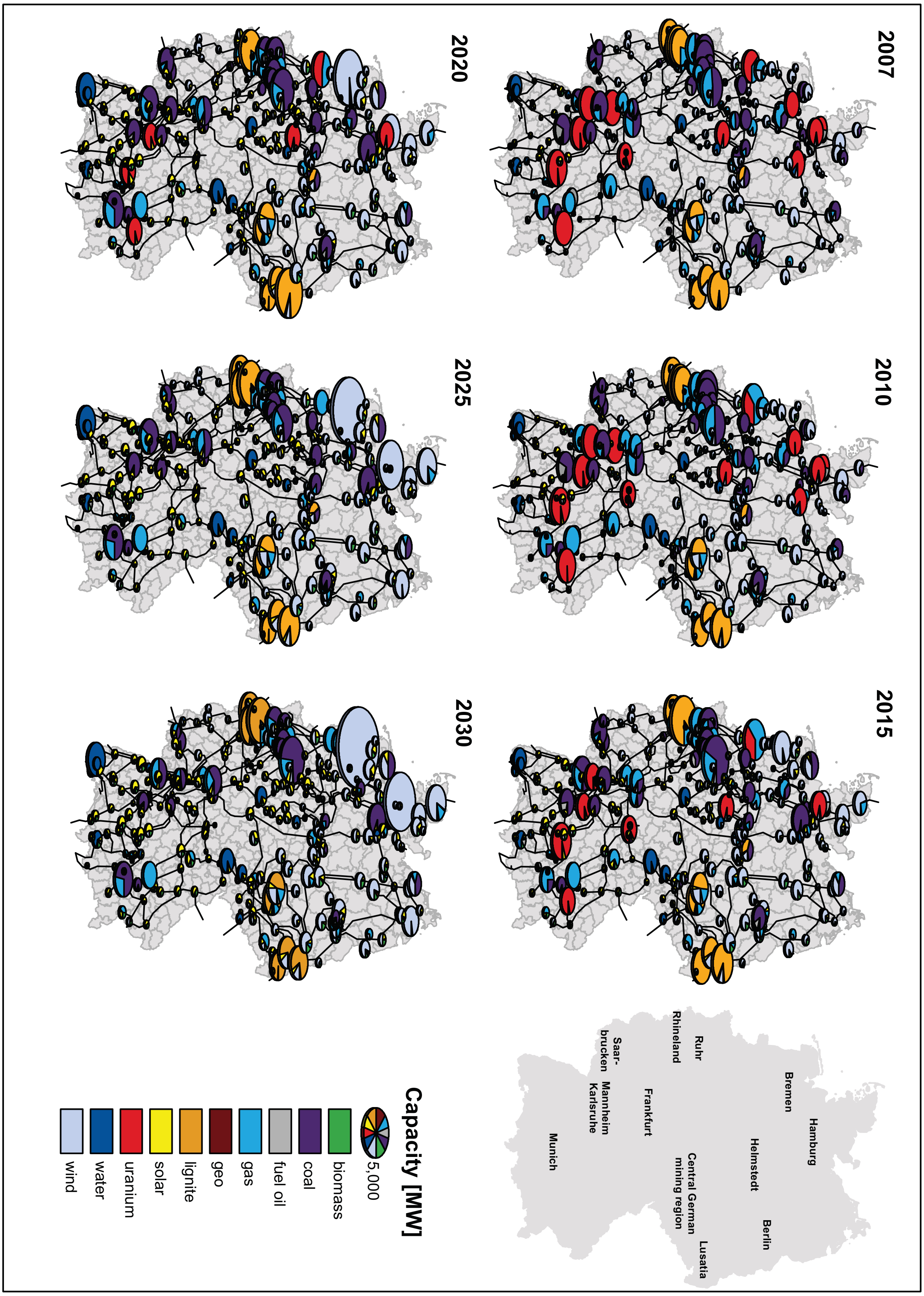

Figure 7.46.: Regional development of generating capacity in the Gas+50 scenario

7.4.4.2. Power generation and capacity utilization

The structure of power generation in the Gas+20 and Gas+50 scenarios (see Figure 7.47) also resembles the development in the BASE scenario. However, like generating capacity, power generation in gas-fired power stations is lower in than in the BASE scenario. Nevertheless, in the Gas+20 scenario, power generation from gas increases from 69.4 TWh in 2007 to 71.2 TWh in 2030, which is 3.4 TWh lower than in the BASE scenario. By contrast, in the Gas+50 scenario power generation from gas decreases to 59.4 TWh by 2030. This corresponds to a 3.0% decline compared to the BASE scenario. By 2030, power generation in gas-fired power stations accounts for 13.9% of total power generation in the Gas+20 scenario and for 11.6% in the Gas+50 scenario. The comparatively low decrease of power generation from gas can be explained, on the one hand, by the model requirement to install a certain percentage of flexible power stations to balance fluctuating RES-E feed-in. On the other hand, alternative technologies possess high load change cost, which is why gas-fired power stations are still the cheapest available alternative in the peak load segment. In both scenarios, power generation from fuel oil decreases compared to the BASE scenario. In the Gas+20 scenario, it amounts to 12.9 GWh in 2025 and 0.8 GWh in 2030, while in the Gas+50 scenario the use of fuel oil in power generation is completely abandoned.

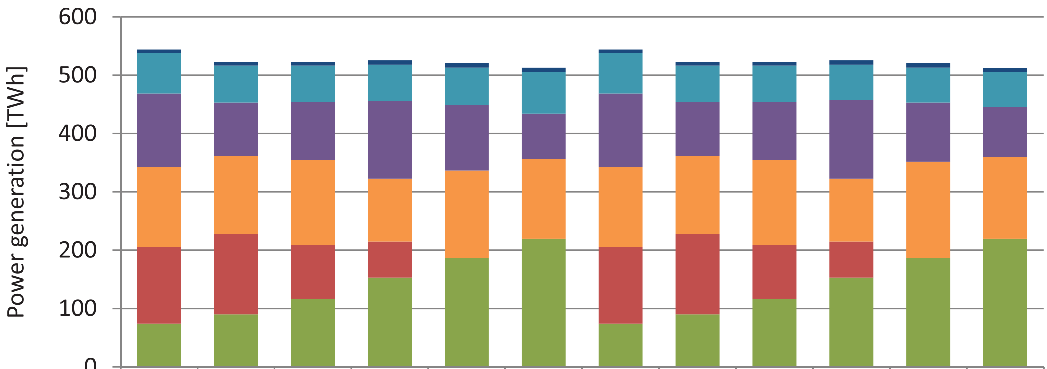

	Gas+20						Gas+50					
	2007	2010	2015	2020	2025	2030	2007	2010	2015	2020	2025	2030
fuel oil	0.0	0.0	0.0	0.0	0.0	0.0	0.0	0.0	0.0	0.0	0.0	0.0
HPS	6.0	6.0	6.0	7.5	7.5	7.5	6.0	6.0	6.0	7.5	7.5	7.5
gas	69.4	63.3	62.9	62.1	63.7	71.2	69.4	62.8	62.2	61.0	60.0	59.4
coal	125.8	91.6	99.1	133.3	112.8	77.3	125.8	92.1	99.8	134.4	101.3	86.3
lignite	137.0	133.5	146.0	107.8	150.2	137.0	137.0	133.5	146.0	107.8	165.4	139.8
nuclear	131.7	138.1	91.8	61.7	0.0	0.0	131.7	138.1	91.8	61.7	0.0	0.0
RES	74.0	89.9	116.7	153.0	186.3	219.7	74.0	89.9	116.7	153.0	186.3	219.7

Figure 7.47.: Overall development of power generation in the gas price variation scenarios

In the Gas+50 scenario, the decrease in power generation from gas is compensated by coal and lignite-based generation till 2020. In 2025, it is entirely compensated by power generation in lignite-fired power stations, which increases to 65.4 TWh in the Gas+50 scenario. Due to the availability of more lignite capacity, not only gas-based generation, but also additional 22.6 TWh coal-based generation is replaced by lignite in 2025. By 2030 it amounts to 139.8 TWh and accounts for 27.3% of total power generation.

In the Gas+20 scenario, the decline in gas-based generation is even less pronounced than in the Gas+50 scenario. In 2025 and 2030, 2.5 TWh and 3.4 TWh are replaced by power generation from lignite in comparison with the BASE scenario. Like in the Gas+50 scenario, not only power generation from gas but also power generation from coal is replaced by lignite from 2025 on (2025: 11.1 TWh; 2030: 6.4 TWh). By 2030 power generation from coal amounts to 77.3 TWh, while power generation from lignite amounts to 137.0 TWh. Thus, in the Gas+20 scenario the share of power generation from lignite in total power generation amounts to 26.7% and the share of coal to 15.1%.

In both scenarios power generation in coal-fired power stations increases in 2010, 2015, and 2020, which is partly realized by a higher capacity utilization of coal-fired power stations. However, in 2025 and 2030, the capacity utilization of coal-fired power stations decreases compared to the BASE scenario. In 2030, the average full load hours of large coal-fired power stations are 4989 h/a in the Gas+20 scenario and 4402 h/a in the Gas+50 scenario, which corresponds to an decrease of 338 h/a and 925 h/a compared to the BASE scenario. Likewise, the average full load hours of lignite power stations decrease from 2020 on compared to the BASE scenario. By 2030 they amount to 7289 h/a in the Gas+20 and 6462 h/a in the Gas+50 scenario. In the Gas+20 scenario, the full load hours of gas-fired power stations stay almost at the same level (3100 h/a) as in the BASE scenario, while they decrease in the Gas+50 scenario by 215 h/a to 2964 h/a. Combined with the shift from gas to lignite-base generation, this leads to the conclusion that due to the increase in gas prices the up and down regulation of lignite-fired power station is preferred over the use of gas in some time slots.

Assuming a sharper increase in gas prices, also the regional distribution of power generation changes. Figures 7.48 and 7.49 show the developments of the regional distribution of power generation in the gas price variation scenarios.

In the Gas+20 scenario, power generation from lignite increases mainly in the Rhineland and Lusatia. In 2030 it is 5.6 TWh and 3.4 TWh higher than in the BASE scenario. The decrease in power generation from gas affects all regions of Germany. In Northern Germany, in particular power generation in the NGCC power station that creates a counter flow on the congested power line in the BASE scenario is reduced by 1.0 TWh. Power generation in three NGCC power stations in Bavaria is reduced by 1.0 TWh, while power generation in gas-fired power stations in Berlin is reduced by 0.7 TWh. Due to the increase in lignite-based power generation in the Rhineland, generation from coal in the Ruhr district is reduced by 4.0 TWh.

In the Gas+50 scenario the increase of power generation in lignite-fired PCC power stations in the Rhineland is even more pronounced. By 2025 it is 21.9 TWh higher and by 2030 it is 19.7 TWh higher than in the BASE scenario. It replaces, gas and coal-based generation in the Rhineland and in the Ruhr district, as well as the completely

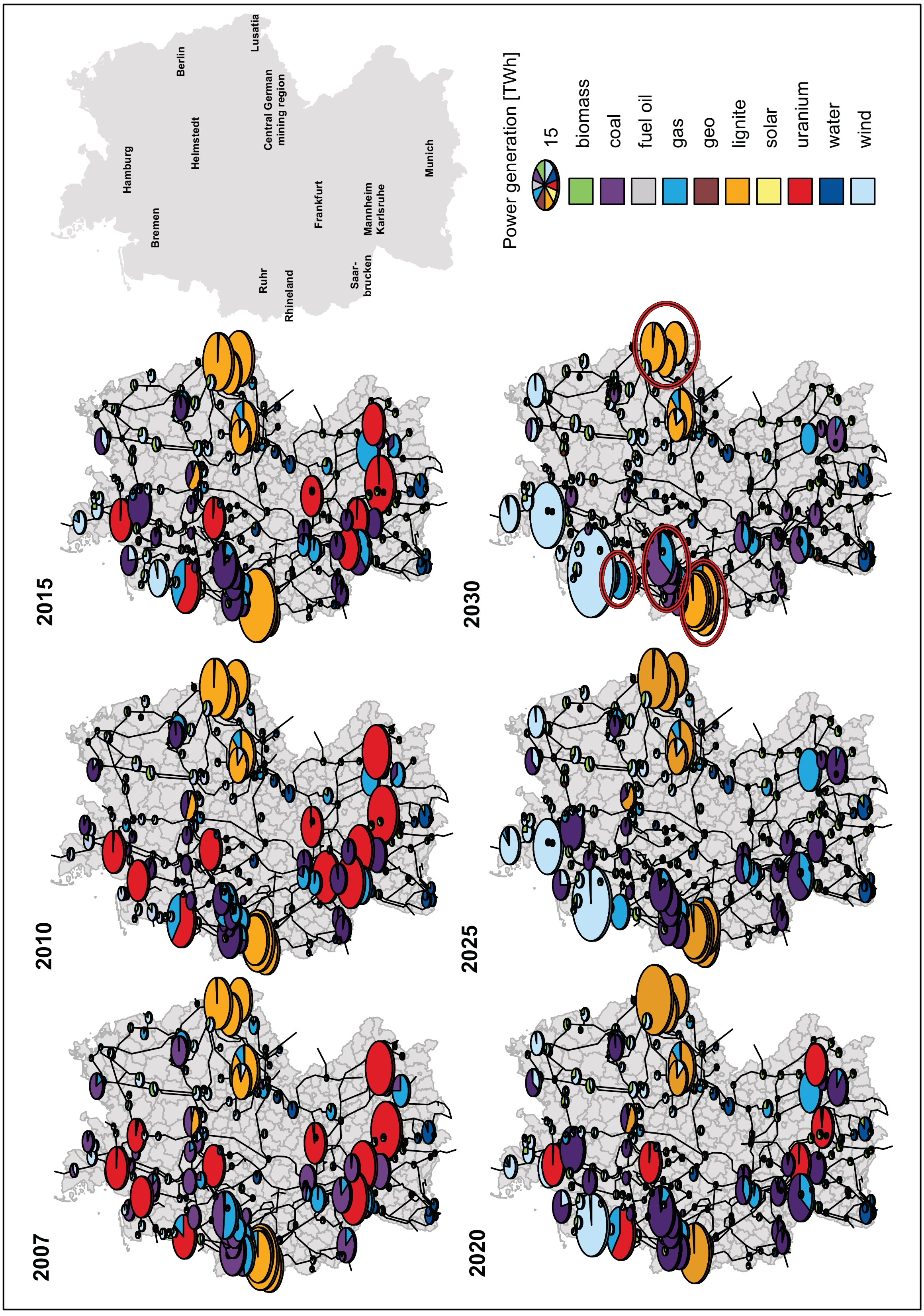

Figure 7.48.: Regional development of power generation in the Gas+20 scenario

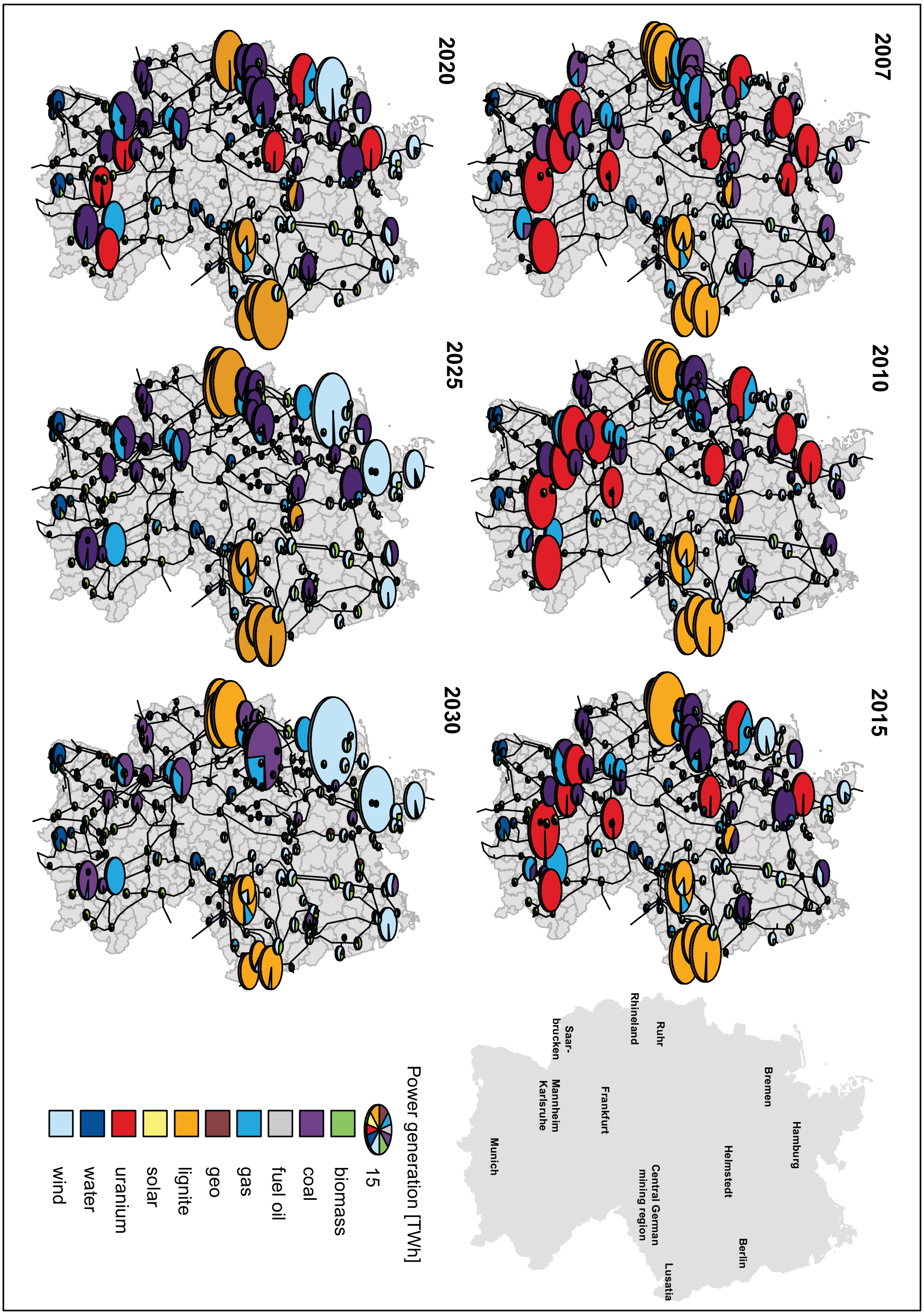

Figure 7.49.: Regional development of power generation in the Gas+50 scenario

disappearing NGCC power stations in Northwest Germany and Berlin. By contrast, lignite-based power generation in East Germany decreases by 8.4 TWh compared to the BASE scenario. It is also mainly replaced by the increase in generation in the Rhineland as well as by an increase in power generation in the Frankfurt area. The remaining decrease in coal and gas-based power generation evenly spreads over Germany. Thus, it can be concluded that the mark-up of 50% to the gas price results in a shift from power generation from the North and East to power generation in the Rhineland and near the load centers around Frankfurt.

7.4.4.3. Average nodal prices and congestion

In the following, the developments of congestion and average annual nodal prices in the Gas+20 and Gas+50 scenario are presented. Figures 7.50 and 7.51 illustrate the development of congestion in the gas price variation scenarios, while Figure 7.52 shows average annual nodal prices in 2030 in the two scenarios. The average annual nodal prices in the optimization periods 2007-2025 are not illustrated, because they only differ in the nodal price level, but not in the regional distribution from the results of the BASE scenario.

In 2010 and 2015 congestion occurs in both gas price scenarios on the same corridors as in the BASE scenario. The nodal price differences resulting therefrom have only local effects and do not exceed 1.67 €/MWh in 2015 the Gas+20 and 2.59 €/MWh in 2015 in the Gas+50 scenario. By 2020, there is no congestion in the German power grid, neither in the Gas+20 nor in the Gas+50 scenario. Correspondingly, there are no differences in nodal prices. By contrast, from 2025 on, congestion is more pronounced in the gas price variation scenarios than in the BASE scenario. In the Gas+20 scenario, an additional bottleneck in East Germany occurs near Eula in Saxony, while in the Gas+50 scenario there is an additional bottleneck near Frankfurt. Yet, the increasing congestion has almost no effect on average nodal prices. Like in the BASE scenario, there is a second price zone in Northwest Germany in the Gas+20 scenario. Yet, the nodal price difference amounts to only 0.01 €/MWh. In the Gas+50 scenario, only local price differences resulting from congested stub lines exist in 2025.

By 2030, congestion at the bottleneck in Northwest Germany is more severe than in the BASE scenario. In the Gas+20 scenario, the bottleneck near Eula in Saxony persists, while an additional bottleneck between Schwandorf and Etzenricht occurs. By contrast to the BASE scenario, there is no bottleneck in the Frankfurt region. Regarding the Gas+50 scenario, there is a bottleneck in north - south direction near Frankfurt, which is congested in 83% of all time slots. Moreover, the bottleneck in Northwest Germany persists. The Diele - Rhede corridor is congested at all times, while the grid adjacent in southerly direction is congested in 55% of all time slots, in particular in times of medium and low system load.

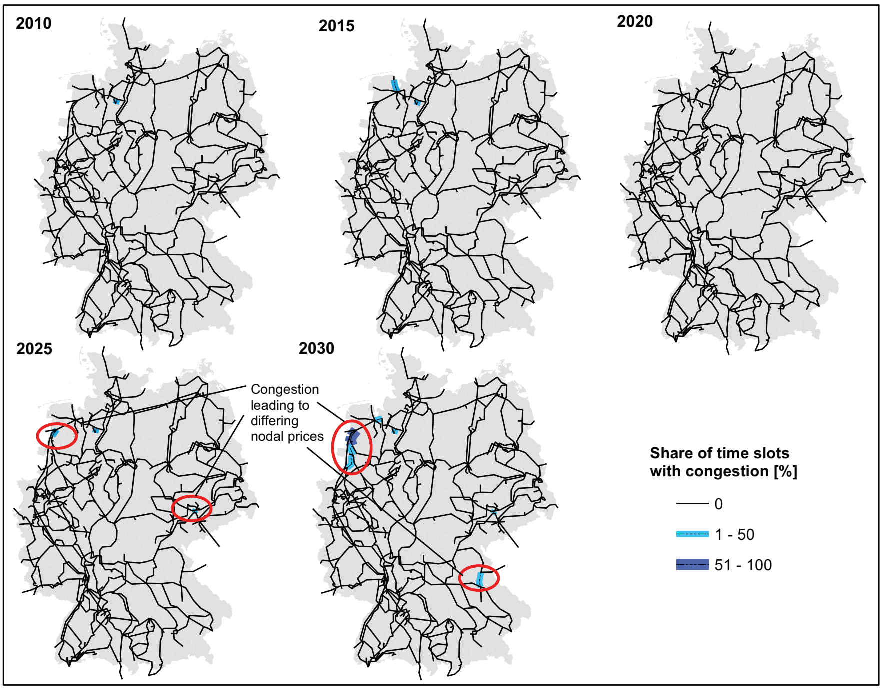

Figure 7.50.: Development of congestion in the Gas+20 scenario

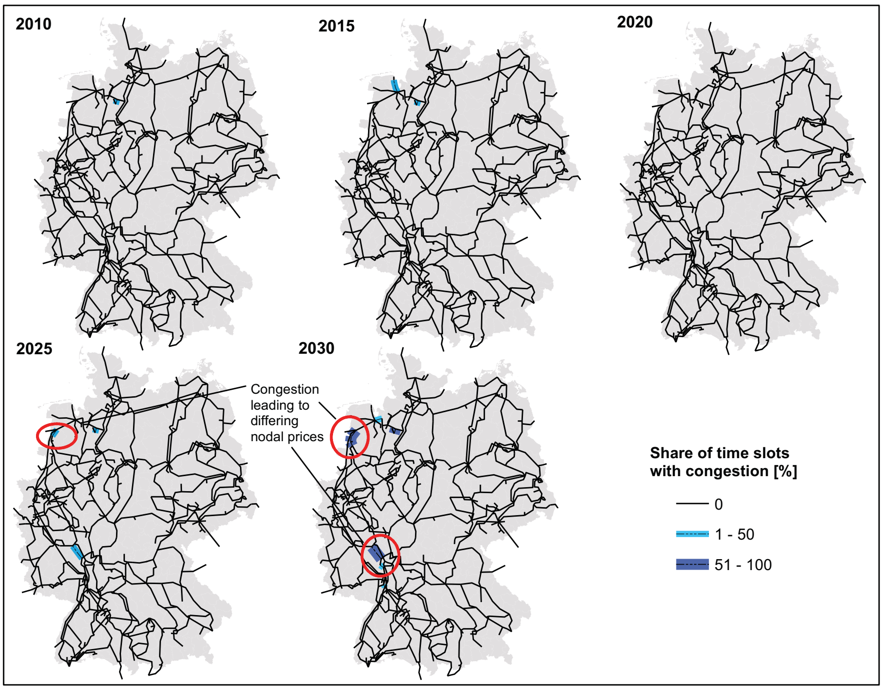

Figure 7.51.: Development of congestion in the Gas+50 scenario

Nodal prices in the Gas+20 scenario are slightly higher than in the BASE scenario and show a similar regional distribution until 2025. By 2030, more significant differences in average annual nodal prices occur. Average annual nodal prices range from -31.22 €/MWh at Diele to 111.52 €/MWh at Rhede. The negative nodal prices are caused by congestion between Diele and Rhede. Since the marginal cost of congestion on this power line increase, the negative nodal prices in the Northwest are lower than in the BASE scenario. The increase in congestion is due to the reduced generation in the NGCC power station at the deficit side of the bottleneck as well as to reduced power generation in the Ruhr district. Like in the BASE scenario, average annual nodal prices are lower in the Northeast than in the Southwest. This is also the reason for which more additional lignite capacity is built in the Rhineland than in Lusatia.

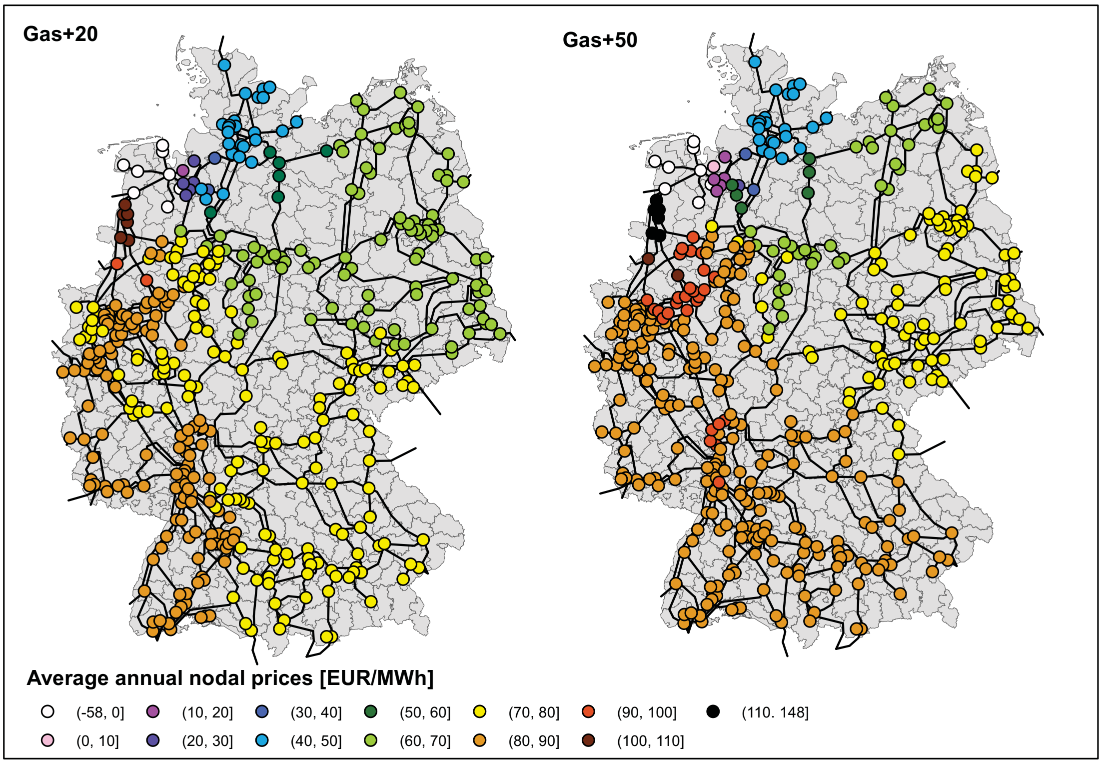

Figure 7.52.: Average annual nodal prices in 2030 in the gas price variation scenarios

Due to the mark-up to the gas price, nodal prices are significantly higher in the Gas+50 than in the BASE scenario (see Figure 7.52 (right)). Moreover, the increased difference in average annual nodal prices between the surplus and deficit side of the bottleneck in the Northeast is even larger than in the Gas+20 scenario. In 2030 average nodal prices range from -57.96 €/MWh to 147.61 €/MWh. The distribution of nodal prices is again similar to the BASE scenario. The negative nodal prices are lower than in the Gas+20, because firstly, the higher gas prices lead to the construction of more power stations with comparatively high load change cost. Secondly, the value of the counterflow increases because of less power generation in NGCC power stations at the deficit side of the bottleneck Diele - Rhede. Furthermore, additional congestion occurs in the transmission grid by 2030. Again, the grid constraint is also the reason for a shift of power station capacity from Lusatia to the western parts of Germany.

7.4.4.4. Nodal prices, congestion, and power generation in selected time slots

Figures 7.53 and 7.54 show the regional distribution of nodal prices, congestion, and power generation in times of system peak load and in times of minimum system load in the Gas+20 scenario. Regarding system peak load, the nodal prices show almost the same distribution as in the BASE scenario, again. Yet, in most parts of Germany, the nodal price level is by approximately 30 €/MWh higher. Above all, this is due to the increase in gas prices. By contrast, a stronger nodal price increase and decrease, respectively, compared to the BASE scenario can be found at the deficit and the surplus side of the bottleneck in the Northwest. The nodal price at Diele amounts to -40.04 €/MWh, while the nodal price at Rhede totals 268.21 €/MWh. The reasons for the more extreme nodal prices are the increased cost of the marginal grid constraint, which results from a shift in the mix and regional distribution of power generation. In addition to the bottleneck Diele - Rhede, the bottleneck Schwandorf - Etzenricht in Southeast Germany causes a nodal price difference of 69.10 €/MWh. While the nodal price at Schwandorf amounts to 204.61 €/MWh, the nodal price at Etzenricht amounts to 135.51 €/MWh. Concerning the nodal price differences in times of minimum system load, they are in most parts of Germany only 2 - 3 €/MWh higher than in the BASE scenario. The only exception is the zone in the Northwest, again. The nodal price at Diele is -34.73 €/MWh, while the nodal price at Rhede amounts to 88.02 €/MWh.

Regarding nodal prices at maximum system load in the Gas+50 scenario (see Figure 7.55) significantly higher nodal prices, compared to the BASE scenario, occur in most parts of Germany as a result of the mark-up to the gas price. Moreover, the marginal cost of the line constraint between Diele and Conneforde increases. As a result, nodal prices at the side with a generation surplus decrease to -70.99 €/MWh, while nodal prices on the other side of the congestion rise to 404.56 €/MWh. The marginal cost of the line constraint is higher than in the BASE scenario mainly because part of the NGCC power station which created a counterflow in the BASE scenario is no longer part of the optimal solution, and thus the counterflow on the lines is lower. Furthermore, the regional shift in generation can be expected to increase the net power flow at the Diele - Rhede corridor.

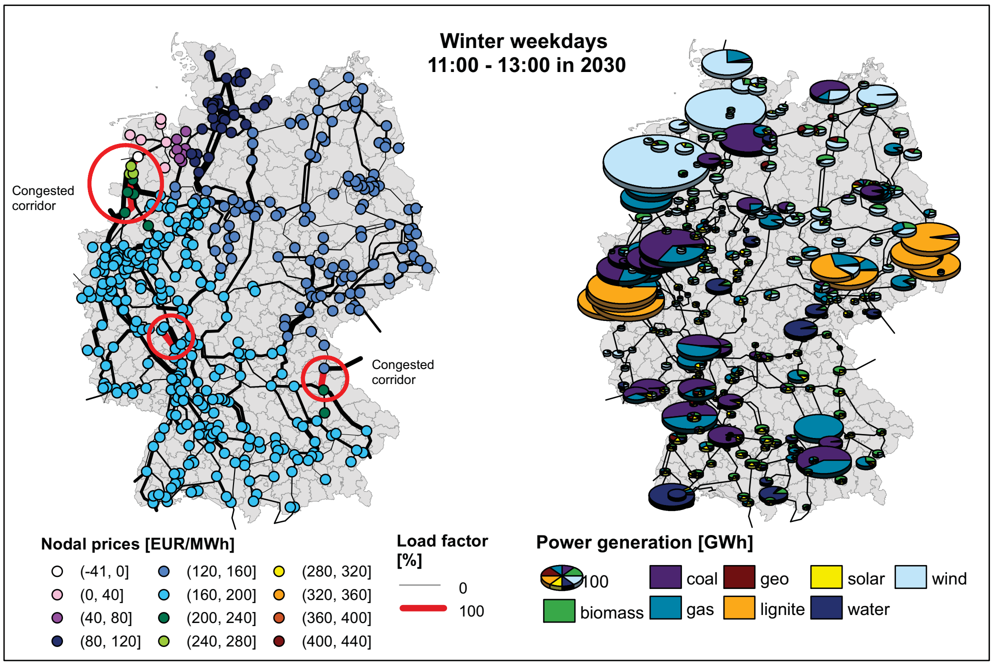

Figure 7.53.: Nodal prices, congestion, and power generation in 2030 at system peak load in the Gas+20 scenario

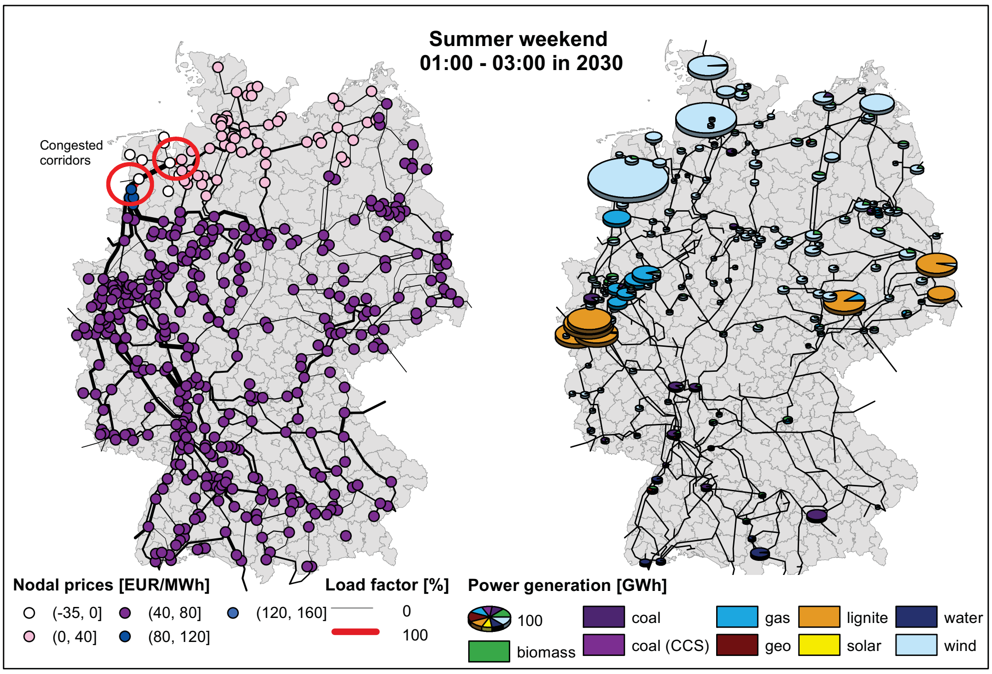

Figure 7.54.: Nodal prices, congestion, and power generation in 2030 at minimum system load in the Gas+20 scenario

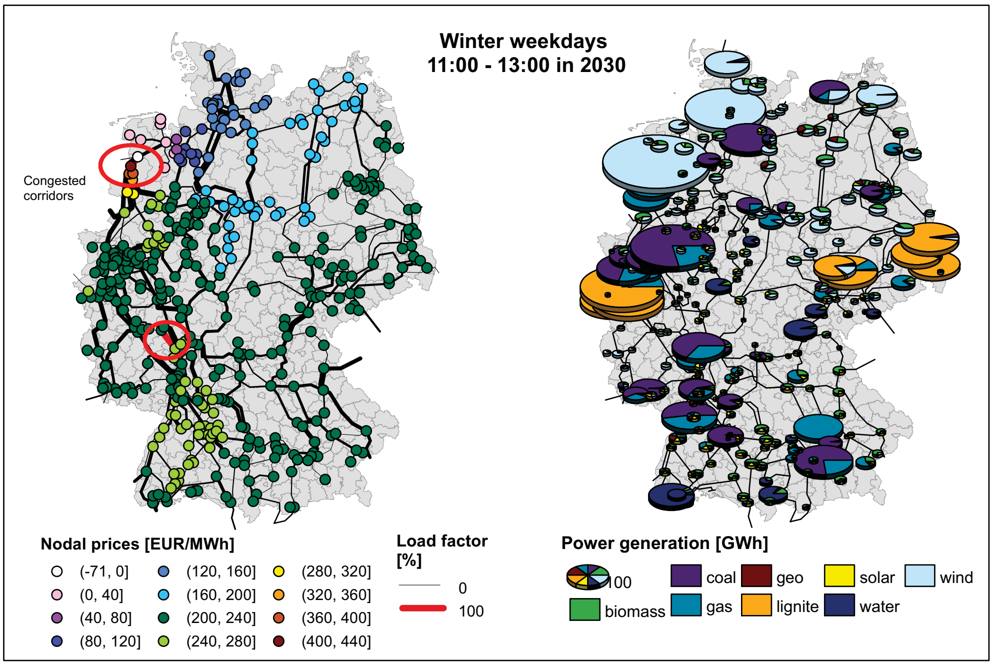

Figure 7.55.: Nodal prices, congestion, and power generation in 2030 at system peak load in the Gas+50 scenario

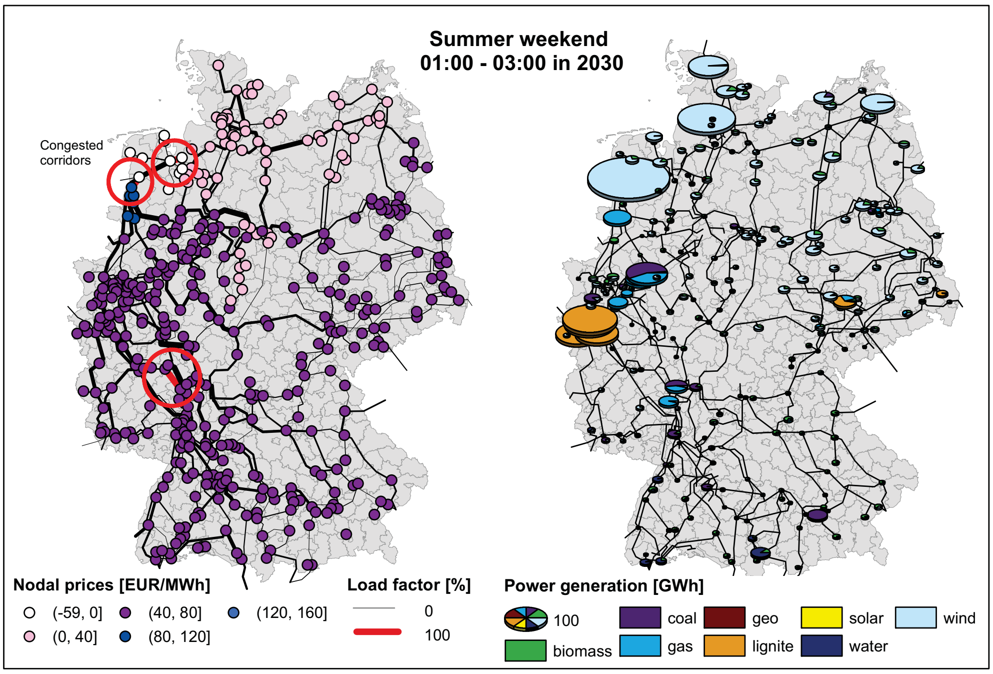

Figure 7.56.: Nodal prices, congestion, and power generation in 2030 at minimum system load in the Gas+50 scenario

Moreover, the bottleneck near Frankfurt causes higher nodal prices in Baden-Wuerttemberg. It is a consequence from increased power flows in north-south direction in the western parts of Germany, which result from the east west shift in power generation.

Due to the increased gas price, nodal prices are also higher in times of low system load, compared to the BASE scenario (see Figure 7.56). Yet, since the role of gas-fired power stations is of reduced importance in times of low system load and because the share of gas-based generation is further reduced in the Gas+50 scenario, the nodal price increase compared to the BASE scenario only totals approximately 5 €/MWh. Moreover, the gas price increase results in a regional shift in power generation from East to West Germany in times of minimum system load. Most notably, the lignite power stations in the East are almost completely shut down in times of low system load.

7.4.4.5. Average annual marginal cost of power supply

Table 7.11 summarizes the developments of the average marginal cost as well as the average marginal cost in peak and off-peak time slots for the two gas price scenarios. The average marginal cost of power supply increases in the Gas+20 scenario from 38.50 €/MWh in 2007 to 71.89 €/MWh in 2030. Moreover, the average marginal cost during peak hours increases to 101.27 €/MWh in 2030, while average marginal cost during off-peak hours increases to 56.5 €/MWh in 2025 and then decrease, again, to 56.34 €/MWh in 2030. In 2030, marginal cost during peak load hours is significantly higher than in the BASE scenario, marginal cost during off-peak hours is lower than in the BASE scenario. The decrease of average marginal cost of power supply during off-peak hours in the last optimization period results from the significant lower prices in the German Northwest.

Table 7.11.: Development of marginal cost of power supply in the Gas+20 and Gas+50 scenario [€/MWh]

Scenario	Price	2007	2010	2015	2020	2025	2030
Gas+20	Avg. MC	38.50	41.69	51.79	61.76	71.11	71.89
	Avg. MC - peak	57.18	59.45	68.84	82.44	100.71	101.27
	Avg. MC - off-peak	28.82	32.29	44.93	51.26	56.50	56.34
Gas+50	Avg. MC	38.50	42.31	53.82	65.78	77.30	77.14
	Avg. MC - peak	57.18	60.58	72.95	91.05	112.67	113.26
	Avg. MC - off-peak	28.82	33.00	47.23	53.29	59.19	58.59

In the Gas+50 scenario, average annual marginal cost of power supply rises between 2007 and 2025 to 77.30 €/MWh and decrease thereafter to 77.14 €/MWh in 2030. Like in the Gas+20 scenario, off-peak average marginal cost is approximately at the same level as in the BASE scenario. Furthermore, they decrease slightly in 2030, because of the extremely low nodal prices in Northwest Germany. Due to the mark-ups to the gas price, the levels of the average marginal cost of power supply as well as of the average peak and off-peak marginal costs are in both gas price variation scenarios higher than in the BASE scenario. In percentage terms, the increase of average peak marginal cost is higher than the increase of average marginal cost or average off-peak marginal cost, because gas-fired power stations are generally used as peak load power stations.

7.4.4.6. Carbon dioxide emissions

Since in the gas variation scenarios, the less carbon intensive power generation from gas and coal is replace by power generation from lignite, CO_2-emissions increase compared to the BASE scenario (see Table 7.12). Yet, in total they still decline in both scenarios. In the Gas+20 scenario, CO_2-emissions decrease by 81.2 Mt CO_2 between 2007 and 2030 and reach 206.3 Mt CO_2 in 2030. This corresponds an increase of 1.0% compared to the BASE scenario.[7] In the Gas+50 scenario, they reach 209.1 Mt CO_2 in 2030, which represents an rise of 2.4% compared to the BASE scenario.

Table 7.12.: Carbon dioxide emissions in the gas price variation scenarios [Mt CO_2 / a]

Scenario	fuel	2007	2010	2015	2020	2025	2030
Gas+20	coal	106.8	76.8	77.7	103.0	86.8	58.3
	gas	28.1	24.0	23.5	22.9	23.6	25.7
	lignite	152.6	147.7	155.3	105.2	136.3	122.3
	sum	287.5	248.5	256.5	231.1	246.6	206.3
Gas+50	coal	106.8	77.4	78.3	103.2	77.1	63.9
	gas	28.1	23.8	23.3	22.4	22.0	21.6
	lignite	152.6	147.5	155.3	105.2	149.1	123.6
	sum	287.5	248.7	256.9	230.9	248.1	209.1

7.4.4.7. Summary of the results of the gas price variations

In this section, the results of two scenarios in which mark-ups of 20% (Gas+20 scenario) and 50% (Gas+50 scenario) to the gas and fuel oil prices of the BASE scenario have been assumed.

Regarding the capacity mix, the mark-up of 20% results in a decrease in installed capacity of gas-fired power stations of 500 MW and in the installed capacity of coal-fired power stations of 755 MW compared to the BASE scenario by 2030. By contrast, lignite-fired power station capacity is 1.8 GW higher than in the BASE scenario. Likewise, 3.5 TWh power generation from gas and 6.4 TWh of power generation from coal are replaced by power generation from lignite. Concerning the regional distribution, power generation in the Rhineland increases.

In the Gas+50 scenario, the shift from gas to lignite is more pronounced. However, by contrast to the Gas+20 scenario, coal-fired power station capacity increases, too. Due to the mark-up to the gas price of 50%, 15.23 TWh of power generation from gas are

[7] The CO_2-emissions from fuel oil-based power generation in the Gas+20 scenario amount to only 10.1 kt CO_2 in 2025 and 0.64 kt CO_2 in 2030 and are therefore not considered in Table 7.12.

replaced by power generation from lignite and coal in 2030. Regarding the regional distribution, power generation in the Rhineland increases. Moreover, power generation in the gas-fired power stations at the deficit side of the bottleneck in the Northwest decreases.

As a consequence to the regional shifts in power generation, congestion in the German power system increases in the gas price variation scenarios. As a result, the nodal price differences in particular at the bottleneck in the Northwest are much more pronounced. Moreover, the additional rise in the gas prices results in higher nodal prices and average marginal cost of power supply in Germany. In the Gas+20 scenario, the average marginal cost of power supply amounts to 71.89 €/MWh in 2030, while in the Gas+50 scenario, they amount to 77.14 €/MWh in 2030.

Regarding the CO_2-emissions, the mark-ups to the gas price and the resulting shift of power generation from gas to lignite lead to higher CO_2-emissions in 2030 than in the BASE scenario. In the Gas+20 scenario, CO_2-emissions in 2030 amount to 206.3 Mt CO_2, while in the Gas+50 scenario, they amount to 209.1 Mt CO_2 in 2030.

8. Critical reflection of the chosen modeling approach

In this work, the optimizing bottom-up energy system model PERSEUS-NET is used to analyze the development of the German power system between 2007 and 2030. The model depicts the German power system at a high spatial resolution. Special attention is payed to the correct modeling of the techno-economic characteristics of regional power supply. Large power stations with block unit sizes larger than 100 MW are considered individually. Moreover, the complete German transmission system is represented in PERSEUS-NET and a DC optimal power flow approach is used in order to respect the technical restrictions of the power transmission grid. The main results of the model are the cost minimizing long-term unit dispatch and power station capacity expansion as well as the nodal prices of power supply.

However, in modeling the German power market and system, some major assumptions with respect to the chosen modeling approach, as well as regarding the parametrization of the input data had to be made. In order to be able to judge the significance of the model results, the chosen modeling approach as well as the assumptions regarding data representation will be critically reflected, including assumptions regarding the underlying market understanding and the behavior of market players, the price elasticity of power demand, the investment decisions in the model, the modeling of RES, the power flow model, and the modeling of uncertainties.

8.1. Underlying market understanding and behavior of market players

The objective of the introduced optimizing energy system model is to satisfy a given demand at minimum system relevant cost. The underlying market understanding implies that all market players follow the same strategy without any strategic behavior, i.e. demand satisfaction at minimal costs. Thus, a cost-based bidding strategy in a perfect, anonymous, non-discriminating market is assumed. This implies a considerable simplification compared to reality, in which a large number of different bidding strategies of market players, such as profit maximization or exercising market power, exist. Individual, diverse decision rules are replaced by a subordinate target function based on which a benevolent social planner configures the system development. Therefore, such a market understanding is disputable for short-term energy models, such as power market simulations (Möst [2006, p. 138f.]). An overview of models combining a detailed representation of the technical constraints of power systems and form's behavior is given in Ventosa et al. [2005]. In particular equilibrium models or, in case of high complexity of the modeled system, simulation models are used to model strategic behavior in imperfect markets (cf. Weigt [2009], Ventosa et al. [2005]).

However, not least because of the increasing liberalization of Europe's energy systems, the PERSEUS-NET underlying market understanding is passable for an optimizing energy model with a focus on the accurate and detailed representation of existing techno-economic restrictions. Möst and Genoese [2009], for example, found that the exertion of market power in the German power market cannot be confirmed in general for the years 2004 - 2006. They suspect that the discovered (rather low) price mark-ups are more likely caused by the *"rise of scarce capacity in the market"* (Möst and Genoese [2009], p. 69) stimulating new investments. Yet, in hours with a low residual supply index, the exertion of market power could not be ruled out (cf. Möst and Genoese [2009], p. 70). In the case of PERSEUS-NET, the potential of the used optimizing energy system model to consider in detail the technical and economic restrictions of the power system supports the modeling of the techno-economic characteristics of every individual (large) power station as well as an adequate representation of the transmission grid. Moreover, since the aim of this work is to analyze optimal future development paths under different framework conditions, the normative approach of the optimizing bottom-up energy system model, which supports the analysis and evaluation of (policy induced) developments from a sectoral perspective, is better suited than simulation models, such as agent-based or system dynamic approaches (cf. Rosen [2007, p. 126]).

8.2. Modeling of supply dependent renewable energy

The focus of PERSEUS-NET is on the analysis of optimum pathways from Germany's power system today to a RES-E dominated power system by 2030. Due to the increasing relevance of grid congestion, a DC power flow model has been integrated into an energy system model. However, the long-term perspective as well as the modeling of DC power flows both require longer computing times. Thus, a trade-off between computation time and the level of detail in the modeling of energy flows and conversions had to be found. Therefore, in PERSEUS-NET a temporal resolution based on representative years has been chosen. Each year is represented by 42 sample periods, each comprising between two and twenty hours that represent typical load segments of weekdays and weekend days in each of the four seasons (see section 6.1). This rather rough temporal structure allows for computing times of a maximum of a few days.

However, it does not allow for an adequate consideration of the fluctuating regional availabilities of wind and solar energy. Conolly et al. [2009] give an overview of modeling approaches used to analyze the integration of renewable energy into various energy systems. In comparing different modeling approaches, they find that to evaluate the long-term pathway of RES-E development, models with a low temporal resolution are to be chosen, while if the focus is on the consideration of the RES-E fluctuations, time steps of an hour or less are required (Conolly et al. [2009]).

Since fluctuations cannot be modeled with the selected temporal structure an equal distribution has been chosen to model the supply dependent renewable energy availabilities. In PERSEUS-NET the full load hours and availabilities are chosen in a way that a uniform perennial distribution of power feed-in from wind mills and biomass, renewable hydro, and geothermal energy units are achieved. Moreover, a uniform temporal distribution during daylight hours of PV feed-in is modeled. As a consequence, it is not possible to model situations of extreme system load. In particular, neither the influence of maximum wind power feed-in nor an entire lack of wind power feed-in in several areas can be modeled.

The simplified modeling of RES-E is typical for techno-economic models with a long-term perspective. To still capture the restriction arising from the fluctuating character of RES-E, often additional requirements regarding capacity reserve are integrated in such models. Rosen [2007] addresses the problem of additional system requirements due to a high wind power penetration in the German power system. He developed a two-part modeling approach consisting of a short-term simulation model Aeolius and the long term optimizing energy system model PERSEUS-RES-E. Using Aeolius he determined additional restrictions of power station operation which he fed into the optimizing energy system model. In particular he calculated necessary levels of secured capacity and available reserve requirements. Moreover, he determined efficiency losses caused by more frequent start-ups of conventional power stations.

Based on the findings of Rosen [2007], additional reserve capacity requirements have been considered in PERSEUS-NET. To guarantee the availability of sufficient reserve capacity in PERSEUS-NET to balance extreme fluctuations of the residual load, a capacity reserve of 15% has to be kept available at all times. Moreover, a minimum usage level of flexible, rapidly available power stations of 10% has been defined. Regarding the availability of sufficient grid capacity, a reliability margin of 10% has been taken into account.

Nevertheless, it should be noted that the results regarding grid load, congestion, and nodal prices that have been obtained using PERSEUS-NET represent only a moderate picture of reality. The full dimension of congestion and regional nodal price differences cannot be captured.[1] In the real world more situations in which congestion occurs as well as more extreme price peaks and more differences in nodal prices are likely. Regarding the siting of power stations additional small, flexible power stations in deficit area seems most likely.

Yet, due to the necessity to make a trade-off between computation time and level of detail the simplification seems inevitable. An outlook on a more advanced modeling approach that would remedy the shortcomings, but necessitates new methods to solve the mathematical problem, is given in section 10.3.

[1] In this context, also the use of typical days can be considered as a critical aspect. Due to their rather rough temporal structure, they induce an averaging of fluctuating input data, such as RES-E feed-in or load. Thus, they do not allow us to capture combinations of situation with extreme load and RES-E feed-in. In order to analyze the effects of extreme situations on grid load, nodal prices, etc. more detailed power flow models with a higher temporal resolution have to be used. However, since the focus of this work is on the long-term perspective, the chosen approach based on typical days is a necessary trade off to guarantee for an acceptable runtime of the model.

8.3. Modeling of the optimal power flow

In this work, a DC approach is used to calculate the power flows in the German transmission system. The main advantage of DC models is their rapid calculation time (cf. Powell [2004]). Therefore, they are primarily used for large systems, such as large energy system models.[2] However, DC models only give approximations of the actual power flows in a network. Therefore, the validity of their application in power system analysis has been questioned.

Overbye et al. [2004] analyzed the effect of the simplifications taking as an example a 13,965 bus model of the Midwest U.S. transmission grid. They found, that the power flow calculated with a DC model is normally a good approximation of the power flow calculated with an AC model. The only exception are lines with a high reactive and a low active power flow. Differences mainly occur in cases of high locational marginal prices, where the DC model underestimates the AC locational marginal prices. Additionally, Purchala et al. argue that if certain network criteria are met, a DC power flow approximation is justified for techno-economic analysis (cf. Purchala et al. [2005b]).

In accordance with Overbye's (Overbye et al. [2004]) findings Murillo-Sánchez and Thomas [2001] state that since the MVA loading of a transformer as well as line limit currents depend on their orthogonal active and reactive components, a *"DC-flow model can only predict (and even then, only for relatively small angle deviations and under a nominal voltage assumption) the active component, and therefore it is easy to find a situation in which it does a poor job of modeling important constraints"* (Murillo-Sánchez and Thomas [2001], p. 18), in particular, if the reactive component is large. In addition Powell observes that DC models *"become inaccurate if used to approximate thermal limits over broad ranges of voltage and reactive and active injections, ..."* (Murillo-Sánchez and Thomas [2001], p. 78). Using a 68 bus model of the CWE region Waniek et al. [2010] found that from a technical point of view, the *"liberation of the AC load flow equation leads to a comparatively low deviation"* from the optimal AC SC-OPF solution.

In general, the choice of the modeling approach depends on the application. Whenever the consideration of only active power flows is sufficient for the analysis, the DC approach should be chosen. When a power line or a network system has to be analyzed in detail and reactive power flows are relevant, the AC approach has to be used. Since the focus of this work is on analyzing the long-term development of the German power system, trade-offs between an adequate level of detail and exactitude and computing time have to be found. Therefore, the choice of a DC approach is passable for this work.

8.4. Investment decisions in the model

The underlying market understanding implies that (dis)investment decisions are made based on minimum expenditures. Yet, in the real world power markets, there are further

[2] In addition to its application in the (economic) analysis of large energy system, DC power flow models are also used to derive starting values for AC power flow calculations (cf. e.g. Powell [2004]).

factors contributing to the investment decisions of firms. Among them count portfolio management decisions. Firms generally try to diversify their generation portfolio to spread the risk of investments, political and legal targets and framework conditions, such as binding emission limits or the phase-out of nuclear power stations, or technological restrictions. To create a model of the power sector which is as realistic as possible, all these influencing factors have to be considered in the target function and side conditions of the optimization problem or by an adequate adaptation of the model parameters. An overview of alternative modeling approaches, e.g. with a focus on strategic investment decision, can be found in Weigt [2009, p. 30 f.].

Another critical point concerning the investment decisions in linear optimizing energy models is the so-called bang-bang (or penny switching) effect. The bang-bang effect means that small changes of input parameters can lead to important changes in the model output and occurs due to the strict cost minimizing decision-making of the optimizer. It is of particular significance for substitutable technologies with similar generation costs, where small changes in energy carrier prices, for example, may lead to a switch in the optimization results from one technology to another. In PERSEUS-NET this problem is met by a very detailed representation of individual power station block units and generation processes that allows for a detailed modeling of fixed and variable generation costs as well as load change costs. As a result, the technologies considered as investment options in the model can be assigned to specific load intervals (base / medium / peak load) and can thus only partially be considered as substitutes. Moreover, the technical restrictions of the power grid in combination with regional availabilities of primary energy carriers restricts the substitutability of investment options. Thus, in PERSEUS-NET, the problem is reduced to nearly insignificance.[3]

8.5. Price information based on locational marginal system expenditures

Due to chosen the modeling approach, price information is based on the opportunity costs (shadow prices) of the regional power demand. Thus, perfect competition without any strategic behavior is assumed, again. Following the nodal spot pricing concept developed by Schweppe et al. [1988], these locational marginal costs of the regional power demand are calculated. The locational marginal prices comprise a generation component as well as a transmission congestion component. The determination of the generation component in the model is in line with the theory of electricity peak load pricing in a deterministic case published by Boiteux [1960] according to which energy is priced with the marginal generation costs and, in case of peak load and scarce capacity, with an additional capacity mark-up (incl. investments). In the latter case, in which the construction of additional power generation capacity is necessary, extreme price peaks

[3] For a similar discussion of the critical points regarding investment decisions in bottom-up energy system models (of the PERSEUS model family) the interested reader may refer to Möst [2006] or Rosen [2007].

occur that are considerably higher than the prices in other time slots.[4]

In LMP schemes nodal prices can drop below the marginal costs of the cheapest unit in the power system or exceed the marginal costs of the most expensive unit due to binding line flow constraints. There is an ongoing debate on the efficiency of locational marginal pricing and whether locational marginal pricing gives correct price signals for network use and investments. An overview of the debate is given in Brunekreeft et al. [2005] and Brunekreeft et al. [2007]. Regarding the short-term, there is an agreement that locational marginal pricing sends signals for an efficient congestion management. By contrast, locational marginal price signals are considered to be insufficient to guide investments in generation capacity (Brunekreeft et al. [2007, p. 22]), because LMP does not recover all network costs (Brunekreeft et al. [2005, p. 75ff.]). This is the case if generation capacity investments lead to the necessity of transmission upgrades whose costs are not reflected by the LMP. Brunekreeft et al. [2007] conclude that LMP signals are the correct direction for investments, but that the magnitude of the price signals is too low. Yet, if generation capacity investments do not necessitate a transmission upgrade or if the investment *"would make an existing transmission "redundant" (...) the nodal prices would effectively set efficient investment signals."* (Brunekreeft et al. [2007, p. 23]).[5]

In PERSEUS-NET, the decision to invest in generation capacity is taken by a benevolent planner which considers the transmission grid as fixed. Grid extensions are considered according to EnLAG [2009] (which already considers the extensions that are considered as necessary for offshore wind power integration). An additional expansion of the grid is no option to serve load. The assumption of a predefined grid is acceptable, because decisions regarding investments in grid infrastructure, in particular in additional power lines, are considerably influenced by non-economic and non-technical influencing factors, such as political and public opinion. Thus, regarding PERSEUS-NET, it can be assumed that under the assumption of a predefined grid infrastructure the determined locational marginal prices give correct signals to guide investments in power generation assets.[6] However, due to the use of typical days as well as the simplified modeling of RES-E feed-in, extreme price peaks cannot occur.

To subsume, assuming perfect competition, the derived locational marginal costs can be used as plausible economic price information

8.6. Modeling of uncertainties

Due to uncertainties regarding the future development of a wide range of framework conditions, investment decisions in the power sector are associated with risks. Schemm

4 For a further discussion of the temporal assignment of system expenditures please refer to Möst [2006].

5 Regarding investments in grid infrastructure, locational marginal pricing singals are poor (cf. Brunekreeft et al. [2007], p. 27 f.). Bushnell and Stoft [1996] give an example of a profitable yet inefficient investment.

6 For real world applications additional price signals such as deep connection charges are proposed (cf. Brunekreeft et al. [2007]).

[2011] distinguishes six different categories of risk factors for investments in power stations: technological risks, market price risks, volume risks, regulatory risks, cost risks, and organizational risks. Technological risks comprise the availability and operating life of power stations as well as the future technology development. While market price risks include uncertainties regarding the development of fuel and EUA prices as well as of power prices, volume risks concern future demand levels, power station capacities, or RES-E feed-in. Moreover, regulatory risks concern, among other things, modifications of law, environmental or market design regulations, or approvals by regulatory authorities. Cost risks include uncertainties regarding the future development of specific investment as well as variable and fix operational costs. Finally, organizational risks comprise risks associated with the operation of power station as well as with events of misconduct (Schemm [2011, p. 6]).

There are several possibilities how uncertainties associated with power system investments can be taken into account in power system modeling. Fundamental stochastic fluctuations such as price or demand fluctuations can be modeled fundamentally. Uncertainties associated with them can then be integrated in the analysis using Monte Carlo simulations (cf. Weber [2004, p. 39]). However, the necessary high number of simulation runs can be very time consuming. Uncertainties regarding the technology development, e.g. of CCS technology, can be taken into account with learning curves which identify their likely developments (cf. Weber [2004, p. 19]). Moreover, in optimizing power system models like PERSEUS-NET the diffusion of technology options is a result of the optimization. Uncertainties such as fluctuating prices of availabilities can be described using probability measures. Particularly the stochastics of price developments can be described with finance and econometric models. An overview of power market models describing the stochastics of various input parameter is given in Weber [2004].

In this work, a scenario analysis has been conducted to account for uncertainties regarding gas and EUA price developments, the availability of additional transmission capacity and increasing power imports. While within this work, only a limited range of uncertain framework conditions could be varied, further scenario analyses can be conducted in order to take additional uncertainties regarding the furture development of input data and framework conditions into account. Yet, not all kind of uncertainties can be adequately considered in PERSEUS-NET. Particularly short-term fluctuations such as volatile fuel prices, demand fluctuations or fluctuation in technology availablilites cannot be considered in PERSEUS-NET. Above all, this is due to the rough temporal resolution of the model. While these types of uncertainties have to be considered in short-term price predictions, its influence is limited on the long-term (cf. Weber [2004, p. 39]), Therefore the chosen modeling approach seems acceptable for the analysis of the long-term development of the German power system conducted in this work.

9. Discussion of the results of the scenario analysis

In chapter 7, the results of the BASE scenario as well as of six alternative scenarios have been presented. In order to be able to judge the significance of the model results, the chosen modeling approach as well as the assumptions regarding data representation have been critically reflected in chapter 8. In the following, the main findings of the scenario-based analysis will be condensed and discussed. In doing so, some points of the critical reflection, in particular regarding the modeling of the RES-E availabilities, will be taken into account. Firstly, the increasing congestion and nodal price differences that occur in the scenarios over time will be discussed. Then the development of the average marginal cost of power supply is addressed. In the third section, the main structural changes in the capacity and generation mix as well as in the regional distribution of power generation of the scenarios will be compared. Finally, the last part of this chapter deals with the development of the CO_2-emissions of power generation in Germany.

9.1. Increasing congestion and nodal price differences

In PERSEUS-NET a nodal pricing-based approach has been used to determine the marginal cost of power supply at each grid node. Since the DC power flows as well as the thermal limits of the power lines have been considered, the nodal prices comprise the marginal cost of power generation as well as the marginal cost of congestion. The application of the modeling approach to the case study of Germany has shown that until 2030, congestion will increase in the German power system. As a consequence, significant differences in the regional prices for electricity supply would develop, if a nodal pricing approach is assumed.

In the following, firstly, the development of congestion in the different scenarios will be discussed. Since the scenario results can be expected to underestimate the developments in the real world (see chapter 8), special focus will be on the comparison of the results to the ones of other renowned studies. Moreover, the implications of the results regarding the need for grid extension are addressed. In the second part of this section, the development of nodal prices in the scenarios will be discussed. In particular, the regional differences in nodal prices as well as the possibility to judge the need for grid extension using nodal prices are addressed.

9.1.1. Development of congestion in the scenarios

Due to the fact that situations e.g. with maximum offshore wind power feed-in are not modeled (see section 8.2), an underestimation of the degree of congestion in the power system can be expected. Figure 9.1 gives an overview of the bottlenecks, which result from the model results of the scenario calculations. To compare, the results from the base scenario of the second DENA study, in which the German TSO determined the degree of non-transmittable power in between predefined regions by 2020 are also shown.

It is obvious that in all scenarios the relevance of grid constraints increases over the covered time horizon. Except for the local bottlenecks, congestion occurs in particular in north - south direction and, in the CO2+100 and GRID scenario, in east - west direction. However, it is evident that until 2020 only local bottlenecks develop in most scenarios. Regarding these earlier optimization periods, significant structural congestion occurs only in the GRID scenario, in which the extension of the transmission grid is delayed. In all scenarios, an important bottleneck exists in Northwest Germany in the optimization periods 2025 and 2030. It is caused by high offshore wind power feed-in from wind parks at the North Frisian coast. Moreover, bottlenecks north of Frankfurt occur in most scenarios in 2025 and in part in 2030.

In the following, initially the results of the scenario analysis will be compared to the results of the second DENA study (DENA [2010b]), whose results can be considered as a reference regarding the necessity for grid expansion in Germany until 2020. Then, the necessity for additional regional power grid extensions will be discussed with reference to the results obtained in this work.

9.1.1.1. Comparison of the results of the scenario analysis with the second DENA study

Comparing the results of the optimization periods 2015 and 2020 with the results of the DENA study (DENA [2010b]) shows that only the results of the GRID scenario resemble those of the second DENA study (see Figure 9.1). This is not surprising, because in the DENA study, only the expected grid extension realized by 2015, including some of the projects named in EnLAG [2009], is considered for the power flow calculations (DENA [2010b, p. 267]). Thus, the topology of the grid considered for 2020 in the second DENA study corresponds best to the situation in the GRID scenario. In the GRID scenario, the results show bottlenecks at some of the locations that have been identified as region's border with non-transmittable power in DENA [2010b]. Yet, even in the GRID scenario not all bottlenecks identified in DENA [2010b] occur in the PERSEUS-NET model results.

Many congested corridors determined in the second DENA study for 2020 appear in the model results in 2025 and 2030. In particular, the power flows in east - west direction seem to be underestimated using PERSEUS-NET. On the one hand, this is due to the simplified modeling of RES-E generation in PERSEUS-NET (see section 8.2). On the other hand, the reliability margin assumed in DENA [2010b] amounts to 0.3 and is thus much higher than the reliability margin of 0.1 that is assumed in this work (see section 6.3). Moreover, if reasonable from an economic point of view, the PERSEUS-NET optimizer locates, operates, and constructs (new) power stations at location so that system load on the bottlenecks is reduced. Thus, some of the bottlenecks may not appear in the model results because of an adapted placement of new (gas-fired) power stations.

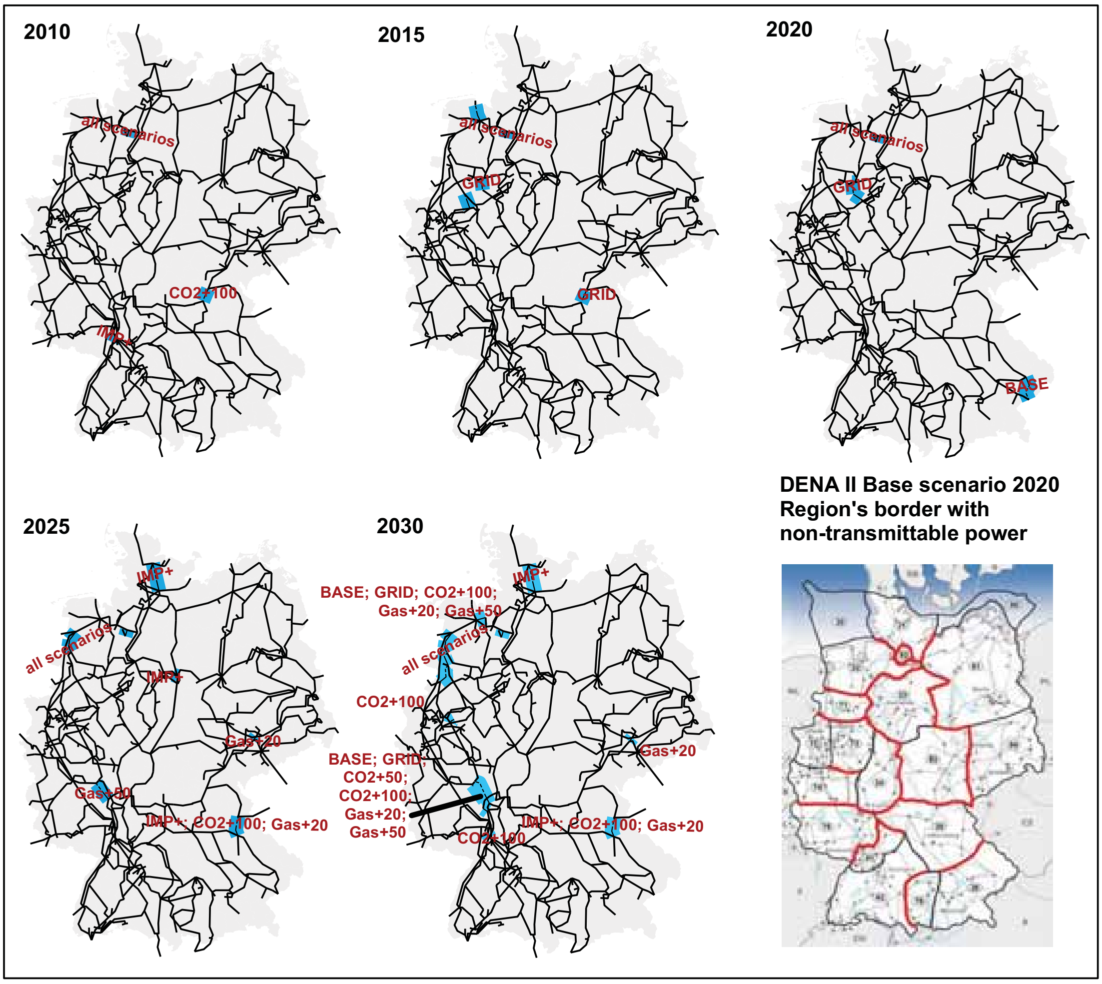

Figure 9.1.: Overview of bottlenecks in the scenario analysis compared to the results of the DENA II study (based on own calculations and DENA [2010a])

9.1.1.2. The need for power grid extensions

Regarding the necessity for additional grid extensions, it should be noted that since the grid extensions considered in the PERSEUS-NET model are based on EnLAG [2009], the last grid extensions are assumed to be realized in 2020. Thus, the results of the last two optimization periods can be used to identify regions or corridors where an expansion of the transmission grid might be useful. The model results suggest that to integrate the expected offshore wind power generation, extensions of the transmission grid should be realized in addition to the projects considered in EnLAG [2009]. In particular expansions of the corridors leading from Diele southwards seem to be necessary. In addition, the grid north of Frankfurt doesn't seem to be amply dimensioned to transmit the increasing power in north - south direction. If imports from Scandinavia increase significantly, as they are expected to, it might also be necessary to additionally expand the congested corridor north of Hamburg.

To identify which of the bottlenecks should be resolved first by an extension of the transmission grid, the nodal prices can be used. Their development and regional distribution will be discussed in the following section.

9.1.2. Regional price developments

Nodal prices indicate the locational marginal prices of power supply, comprising the cost of generation and congestion. If there is no congestion in the considered transmission grid, all nodal prices are identical. However, if congestion occurs, the nodal prices in the considered system might differ considerably. Thus, the nodal prices signal in which regions there is a generation surplus and in which a generation deficit. Thus, they function as price signals for an optimal regional expansion of power stations.

The development of nodal prices in the scenarios suggest a division into two time stages. The first one, which ranges from 2007 to 2020, is characterized by almost completely identical nodal prices in Germany in almost all scenarios. In the second stage, which comprises the optimization periods 2025 and 2030, differing nodal prices are to be expected.

In the following, the development of nodal prices in those two time stages will be discussed. Then the necessity of additional transmission grid extensions will be adressed, again, by analyzing local differences in nodal prices.

9.1.2.1. Nodal prices between 2007 and 2020

Regarding the development of the average annual nodal prices, the results of the scenario analysis show that, except for in the case of delayed grid extensions (GRID scenario), no regional nodal price differences will occur within Germany between 2007 and 2020. Either, only local bottlenecks on stub lines exist that result in only locally differing nodal prices or the cost of the bottlenecks are not high enough to have a measurable influence on nodal prices. The latter is the case in the CO2+100 scenario in 2010, for example, where there is a bottleneck between East and South Germany (see Figure 9.1), but the differences in the nodal prices do not even show in the post decimal positions.

By contrast, in the GRID scenario, the additional congestion in north - south and east - west directions leads to significant nodal price differences in 2015 and 2020. In 2015, the structural bottleneck between the lignite mining sites in the east of Germany and the southern load centers causes significantly differing average nodal prices (see Figure 7.15). The highest average annual nodal price differences amount to 56.09 €/MWh and occurs between Redwitz and Würgau on the corridor connecting Thuringia and Bavaria. Since the bottleneck separates the lignite mining sites in the East, where there is a surplus in power generation capacity, from the South, which has a capacity deficit, nodal prices are highest in the southern parts of Germany and lowest in East Germany. Moreover, two additional bottlenecks are located north of the Ruhr district. In times of system peak load, they cause nodal price differences of up to 550 €/MWh. All bottlenecks occur in particular in times of high system load.

By 2020, the bottleneck Redwitz - Würgau is resolved in the GRID scenario too, by an upgrade of the transmission line. Now congestion north of the Ruhr district determines the regional distribution of nodal prices. In particular during times of maximum system load, significant nodal price differences of more than 570 €/MWh result. Moreover, there is an average annual nodal price difference of approximately 10 €/MWh between the southern and northern parts of Germany. Yet, the average annual nodal price difference between North and South Germany is less pronounced than in 2015.

9.1.2.2. Nodal prices in 2025 and 2030

By 2025, congestion occurs in all scenarios. The most important bottleneck leads from Diele southwards. Except for the CO2+20 scenario, in which the congestion has no significant influence on nodal prices, this bottleneck causes differing nodal prices from 2025 onwards. A price zone with below average annual nodal prices develops in the Northwest at the deficit side of the bottleneck. Yet the nodal price differences caused by this bottleneck range between 0.05 €/MWh in the BASE scenario and 4.61 €/MWh in the IMP+ scenario.

In addition to the most important bottleneck in the Northwest, several other bottlenecks occur in Germany depending on the scenario, which partially have significant influence on nodal prices. Figure 9.1 shows that in the IMP+ scenario additional bottlenecks occur in north - south direction as a result of the increasing inter-regional power exchanges. They are both caused by increasing imports. As a result, the nodal price difference between North and South Germany increases. Moreover, additional bottlenecks, which result from regional shifts in power generation, appear by 2025 in the gas price variation scenarios as well as in the CO2+100 scenario (see section 9.3). Again, Southern Germany is therefore characterized by a capacity deficit, while North and East Germany have a surplus. In all scenarios, nodal price differences are highest in times of high system load, because the bottlenecks then are most severe.

By 2030, strongly differing nodal prices occur in all scenarios. Above all, the bottleneck in the Northwest has a significant influence on average annual nodal prices. Thus, in all scenarios, this results in a distribution of nodal prices that is characterized by very low nodal prices in the areas with high offshore wind power feed-in and higher nodal prices in Southern Germany. Moreover, nodal prices are generally lower in the east than in the west of Germany. Except for the deficit side of the bottleneck near Rhede, the highest nodal prices always occur in West and Southwest Germany. However, there are considerable differences in the level of nodal prices in the scenarios. The regional price differences are most pronounced in the IMP+ scenario, because of the higher regional power transmissions.

Of particular interest is the level of nodal prices at the surplus side of the bottleneck in the Northeast. In the IMP+ scenario as well as in the gas price variation scenarios, significantly negative nodal prices occur in the region with a high surplus of offshore wind power. They arise due to the inflexibility of some types of thermal power stations, such as lignite or nuclear power stations. Above all, they are caused by their ramping and opportunity costs (cf. Genoese et al. [2010], EWI [2010]).[1] Furthermore, they occur due to binding line flow constraints. In that case, an increase in load at a node with a negative nodal price might decrease power flows on the congested lines and, in that way, reduce total system costs. The negative nodal prices then reflect the value of "counter flow" in the power system. In the IMP+ scenario the negative nodal prices in the Northwest arise due to the increasing power flows from the Danish border to the south. In the gas price variation scenarios, in particular the abandonment of power generation from gas in the deficit area in the Northwest in combination with an increased use of technologies with high ramping costs cause nodal prices in the Northwest to decrease significantly. A different situation exists in the EUA price variation scenarios. The increased use of gas and coal instead of lignite, in combination with a shift of power generating capacities to the Ruhr district results in much higher nodal prices in the Northwest and less pronounced regional price differences.

9.1.2.3. Nodal prices as signals for grid extensions

Regarding possible extensions of the German power grid, the nodal prices suggest firstly that the projects considered in EnLAG [2009] should be realized as fast as possible to avoid considerable congestion and strongly differing nodal prices as they occur in the GRID scenario.

To select which additional extension projects should be realized before 2025 and 2030 respectively, the nodal prices can be used. Congestion can be considered as most severe where there are the highest differences in nodal prices. In all scenarios, this is true for the bottleneck in the Northwest, which is caused by the high wind power feed-in from wind parks in the North Sea. Thus, for being able to integrate the considerable amount of offshore wind power from wind parks at the East Frisian coast in the German transmission system, this bottleneck should be resolved first. If significantly higher power imports are expected, the power grid close to the Czech border as well as north of Hamburg should be upgraded, too. According to the level of nodal price differences, the upgrade of the grid close to the Czech border seems more important in 2025, while the upgrade of the grid north of Hamburg becomes more important in 2030. The upgrade of the grid north of Frankfurt seems less important than the other projects,

[1] In Germany, negative market prices have been observed so far in case of low system load combined with moderate wind power feed-in or in case of moderate system load in combination with high wind power feed-in (cf. Genoese et al. [2010], EWI [2010]).

since the nodal price differences caused by this bottleneck are comparably low. It has the most effect in the CO2+100 and in the Gas+50 scenario.

9.2. Development of the average marginal cost of power supply in Germany

The average marginal cost of power supply gives an indication on the average nodal price level. In case no congestion occurs, the average annual nodal prices equal the average marginal cost of power supply. Figure 9.2 shows the average marginal cost of power supply in the presented scenarios.[2] Comparing the first and last optimization period, a considerable increase in the average marginal cost of power supply can be observed. In the BASE scenario, the average marginal cost of power supply increases from 38.50 €/MWh in 2007 to 71.03 €/MWh in 2030. Above all, the increase in the average marginal cost of power supply is caused by the increases in primary energy carrier and EUA prices. Moreover, the replacement of nuclear power stations by technologies with higher marginal costs leads to an increase in the average marginal cost of power supply.

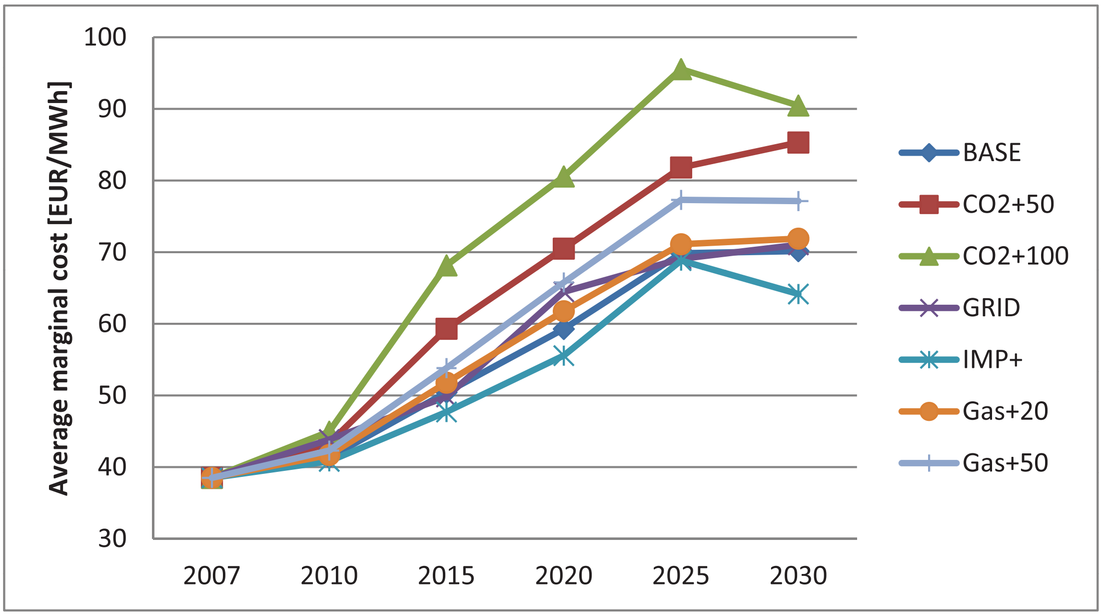

Figure 9.2.: Development of average marginal cost of power supply in the scenarios

Until 2025 the marginal cost of all scenarios shows a similar increasing trend, yet with different slopes. The marginal costs in the alternative scenarios, except for the IMP+ scenario, are at the same level or higher than in the BASE scenario. The gradient is

[2] In the scenario analysis in chapter 7 the marginal cost of peak and off-peak supply are also presented.

highest and thus the increase is most pronounced in the EUA price variation scenarios and in the scenario Gas+50. In the CO2+100 scenario, the average marginal cost of power supply rises to 95.55 €/MWh in 2025. By contrast, the marginal cost of power supply is lowest in the IMP+ scenario.

In the last optimization period, the developments of the marginal costs are different depending on the scenario. While in the BASE, GRID, and Gas+20 scenario there is only a minor cost increase in the last optimization period, the marginal cost increases more considerably in the CO2+50 scenario. In the Gas+50 scenario it almost stays constant. By contrast, in the CO2+100 and in the IMP+ scenario, the marginal cost decreases considerably by 2030. In the CO2+100 scenario this is caused by a significant decrease in peak load marginal cost. This decrease in peak load marginal cost is caused, on the one hand, by a decrease in nodal prices in the last period that is due to the decreasing relevance of the congestion in the North and, on the other hand, by the abandonment of power generation from fuel oil. In the IMP+ scenario, the marginal cost of power supply decreases significantly in the last period because power generating capacities with comparatively higher marginal costs are replaced by the increasing power imports so that now power stations with lower marginal costs are price setting.

9.3. Development of the capacity and power generation mix

The nodal prices determined with PERSEUS-NET function as price signals for optimal regional power plant investments. Thus, not only the optimal fuel mix, but also the optimal location of power station siting can be determined using PERSEUS-NET. Total power generation in Germany decreases from 543.9 TWh in 2007 to 512.7 TWh by 2030 in all scenarios except for the IMP+ scenario, in which, by 2030, 81.5 TWh of electricity generated in Germany is replaced by power imports. Regarding the overall development of installed power station capacity in Germany, it increases from 131.0 GW in 2007 to 145.8 GW - 157.0 GW in 2030 depending on the scenario.

In the following, the main results of the scenario analysis regarding the structure of the capacity and generation mix as well as the regional distribution of power generation will be discussed.

9.3.1. Development of the structure of the capacity and generation mix

The development of power generation and generating capacity can be divided into two main segments with respect to time. The first segment ranges from 2007 to 2015, while the second segment covers the time horizon 2020 to 2030.

9.3.1.1. Development of the capacity and generation mix between 2007 and 2015

The development of the capacity and generation mix in the first time segment is characterized by the predefined development of nuclear energy and RES-E. In the first time segment, generation from nuclear energy still plays an important role. Yet, nuclear power generation decreases from 131.7 TWh in 2007 to 91.8 TWh in 2015. The volumes of RES-E in total power generation increase from 74.0 TWh in 2007 to 116.7 TWh in 2015. Since most of the power stations newly constructed between 2007 and 2015 have been predefined (because they are already under construction or in an advanced stage of planning) the development of power station capacity in the first segment is only to a marginal part a result of the optimization.

As a consequence, the capacity and generation mixes determined for the optimization periods 2007 and 2015 in the scenario calculations are almost identical to those of the BASE scenario. Regarding the structure of power generation, generation from lignite replaces nuclear power as the most important fuel in power generation by 2015. Moreover, coal remains the third most important fuel in power generation, while gas ranks on the fourth place. Due to the different typical average full load hours gas and coal-fired power stations rank before nuclear and lignite power stations in the capacity mix.

The only scenarios in which there are variations to the development of power generation in the BASE scenario are the GRID and in the IMP+ scenario. Minor differences in the capacity mix compared to the BASE scenario occur in the GRID scenario in 2015, where additional 190 MW of gas-fired power stations are installed. Variations in the generation mix occur in the GRID and in the IMP+ scenario in 2015. In the GRID scenario, 1.1 TWh of power from lignite are replaced by gas and coal. Moreover, in the IMP+ scenario, in which the increasing imports reduce power generation within Germany, power generation from coal decreases by 13.3 TWh, from lignite by 2.5 TWh, and from gas by 1.7 TWh.

9.3.1.2. Development of the capacity and generation mix between 2020 and 2030

In the second temporal segment, different developments of capacity and generation mixes are caused by the changes in the framework conditions in the analyzed scenarios. However, in all scenarios, both generating capacity and power generation developments are above all characterized by the strong increase in the share of RES. By 2020, power generation from RES exceeds power generation from any single carbon fuel. Moreover, nuclear power generation only plays a subordinate role in 2020, while in the following years it completely phases out.

In the following, the role of those fuels, whose developments are not predefined as it is the case with uranium and RES, will be discussed. Figure 9.3 compares the generation mix in 2020 and 2030 of the analyzed scenarios.

The role of lignite Lignite plays a dominant role in the German generation mix between 2020 and 2030. The lasting significance of lignite in power generation can be explained by comparatively low marginal costs of lignite-fired power stations. Moreover no restrictions of the power grid restricts the possibility to use lignite in power generation further on. In all scenarios, except for the CO2+100 scenario, lignite is the second most important fuel in power generation by 2030. Its share in total power generation by 2030 varies from 18.6% in the IMP+ scenario to 27.3% in the Gas+50 scenario. In the CO2+100 scenario, in which the increasing EUA prices compensate the marginal cost advantage of lignite-fired power stations, power generation from lignite decreases significantly. Since the level of utilization of lignite-fired power stations is very high, the installed capacity of lignite-fired power stations ranks only third among the carbon fuels. By 2030, the installed capacity of lignite-fired power stations is highest in the Gas+50 scenario, where it amounts to 20.0 GW and lowest in the IMP+ scenario, where it accounts for 11.4 GW.

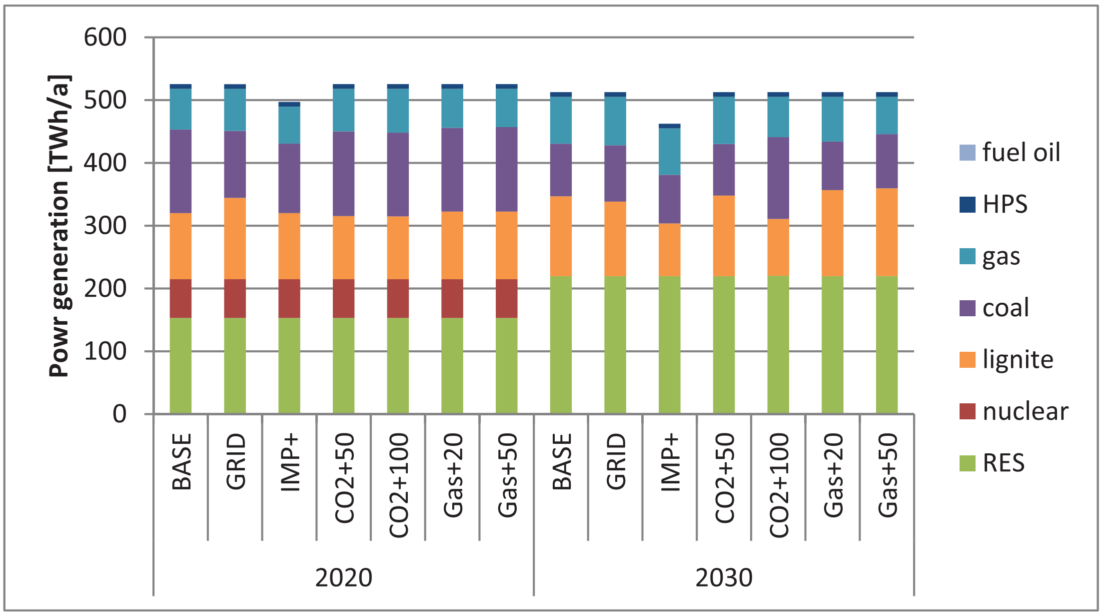

Figure 9.3.: Comparison of power generation mixes in 2020 and 2030 of the scenarios

The role of coal Coal-based power generation is used in all scenarios to replace the declining nuclear power generation. Nevertheless, in the last optimization periods, power generation from coal decreases, because of the rise in RES-E generation and the comparatively higher marginal cost in comparison with lignite. In most scenarios, power generation from coal reaches its maximum in 2020, where it replaces the decreasing nuclear power generation. In the GRID and IMP+ scenario, coal-based power generation reaches its maximum in 2025, while lignite replaces most of the declining nuclear power generation in 2020. In the CO2+100 scenario, in which the increase in EUA prices results in a comparative advantage of coal-fired power stations with CCS technology, coal is the most important fuel in power generation in 2030.

Regarding the development of the fossil capacity mix, coal-fired power stations remain the second most important technology among the thermal power stations until 2025 in all scenarios. By 2030, they are replaced by gas-fired power stations in all scenarios, except for the CO2+100 scenario. In the CO2+100 scenario 10.6 GW of coal-fired power stations with CCS technology are commissioned.

The role of gas The importance of gas in power generation increases in all scenarios, except for the CO2+100 and Gas+50 scenario. Its share in total power generation by 2030 in Germany is highest in the IMP+ scenario and in the GRID scenario. In the Gas+50 scenario, gas-based power generation decreases as a consequence of the strong increase in gas prices to 59.4 TWh by 2030, which corresponds to a share of 13.9% in total power generation. However, even in this scenario, gas has almost the same importance in power generation by 2030 as it has today. On the one hand, this is due to the model requirements for flexible reserve. On the other hand, the increasing congestion in the German power grid necessitates the operation of flexible power stations to counteract bottlenecks. This interpretation is supported by the increased shares of gas in power generation in the IMP+ and GRID scenario, in which higher system load leads to a more intensive utilization of gas (see also section 9.1). The most important advantage of gas-fired power stations is their high flexibility, expressed by low ramping costs and times.[3] Moreover, since according to the model assumptions no restrictions regarding the siting of gas-fired power stations exist, they can also be installed in remote areas, where neither lignite nor coal is available. As a consequence of their increasing utilization to influence power flows in the system network, the average full load hours of gas-fired power stations decrease over the covered time horizon. The decrease is highest in the IMP+ and GRID scenario, in which additional gas-fired power station capacity is built in deficit regions to counter power flows on congested corridors.

Others In all scenarios, power generation in HPS power stations plays an important role in times of peak load. By contrast, fuel oil-based power generation has only a subordinate relevance.

Summary To subsume, the structures of power generation and generating capacity are very similar until 2015, because of the limited degrees of freedom of the optimizer. However, between 2020 and 2030, differences depending on the scenario exist. In all scenarios except for the CO2+100 scenario, carbon intensive fuels remain the most important fuels alongside the RES. The reason for this is the comparative cost advantage of lignite and coal compared to the less carbon intensive gas. Moreover, by 2030 gas-fired power generation has almost the same share in total power generation as in 2007. Yet, it seems to be more frequently used to counteract congestion in the transmission grid.

In the following, the regional development of power generation in the considered scenarios will be discussed.

[3] In the model PERSEUS-NET, only ramping costs are considered.

9.3.2. Regional development of power generation

Regarding the regional development of power generation between 2007 and 2030, above all a considerable shift of power generation from Southern Germany to the North is obvious. The rise in power generation in the North is caused, above all, by the construction of large offshore wind parks in the North Sea. The reduction of power generation in Southern Germany results, among other things, from the decommissioning of large nuclear and coal-fired power stations in the South, which are only partly replaced by new conventional generation in the same area. In the BASE scenario, power generation in Southern Germany decreases by about 66 TWh between 2007 and 2030. In the South, new conventional power generating capacities are built close to the large load centers Munich, Ingolstadt, in the region Karlsruhe - Mannheim - Stuttgart, and Frankfurt. The shift from power generation from the southern part of Germany to the North is increased in the last optimization period by the construction of several large NGCC power stations that are installed at the deficit side of the bottleneck in Northwest Germany in all scenarios, except for the Gas+50 scenario. Their location is chosen so that the power stations can create a counter flow on the corridors congested in north - south direction, if needed. In case of delays in the extension of the German transmission grid (GRID), power generation increases in the southern and western parts of Germany, in particular in the directly affected optimization periods 2015 and 2020. In the scenario with increasing power imports (IMP+), power generation within Germany is reduced above all in South and Central Germany. Thus, the regional shift in power generation from the South to the North becomes more pronounced in the IMP+ scenario than in the other scenarios.

In addition to the shift in power generation and generating capacity from the South to the North, the lasting high relevance of power generation in the Ruhr district and at the lignite mining site can be noted. While power generation in the central German lignite mining district remains approximately at an equal level in all scenarios and over the considered time frame, power generation at the Lusatian mining area either remains at an equal level or decreases depending on the scenario. Power generation from lignite at Helmstedt disappears by 2030. Moreover, the development of power generation from lignite in the Rhineland depends on the scenario. It is closely linked to the development of power generation in the Ruhr district.

In the BASE scenario as well as in the gas price variation scenarios, power generation from lignite in the Rhineland increases over the covered time horizon. As a consequence, power generation in the Ruhr decreases. In all three scenarios, the shift is provoked by comparatively lower marginal cost of power generation from lignite compared to coal. In the BASE scenario, power generation from lignite in Lusatia is even partly shifted to the Rhineland. However, it has negative effects on congestion in the Northwest. Thus, in the BASE scenario, the natural gas combined cycle power stations at the deficit side of the bottleneck are built. In the gas variation scenarios, the increasing congestion costs are accepted to avoid higher cost of gas-fired power generation.

By contrast, in the IMP+ scenario, the increasing imports replace by 2030 in particular power generation from lignite in the Rhineland as well as, to some extent, power generation from lignite at Schwarze Pumpe in Lusatia. Likewise, in the GRID scenario, power generation in the lignite-fired power stations in the Rhineland is reduced, because, due to the bottlenecks in 2015 and 2020, lignite-fired power station capacity is replaced by gas.

The construction of power stations with CCS in the CO2+100 scenario also results in regional shifts in power generation. A considerable amount of power generation in the South and in the lignite mining district shifts to the Ruhr district, where the coal-fired power station with CCS technology are commissioned. The additional power station capacities with CCS are constructed at Frankfurt and near Saarbrucken.

Regarding the expected decentralization of power generation, it is above all caused by the predefined installation of RES-E. In addition, only a few small gas-fired power stations are built that would add to a further decentralization of the German power system.

While interpreting the results of the scenario analysis, it should be kept in mind that assumptions regarding the availability of fuels at the individual grid nodes had to be made. Moreover, neither regional preferences of individual competitors nor specifications of subordinate grids that could also have an effect on the choice of location and thus on the optimal siting of power stations are considered. Still, the results give an indication on the optimal regional power generation development under the chosen framework conditions.

Summary To subsume, a considerable shift of power generation from the southern parts to the northern parts of Germany can be made out, which result in particular from the fact that old conventional power station capacities in the South are replaced by power generation in offshore wind farms in the North Sea. New conventional power stations are either constructed close to the large load centers or at the lignite mining sites in the Rhineland and Lusatia. Moreover, in case of grid congestion, coal- and gas-fired power stations are commissioned at the deficit sides of the bottlenecks. Moreover, gas-fired power stations are used at the deficit side of the bottleneck, i.a. in order to create a counter flow on the congested corridor.

9.4. Carbon dioxide emissions

Figure 9.4 shows the development of the CO_2-emissions between 2007 and 2030 resulting in the seven scenarios. Comparing the first and the last optimization periods, the CO_2-emissions in the BASE scenario decrease by 29%. Until 2020, the CO_2-emissions are reduced by approximately 20%. The development of the CO_2-emissions in all scenarios, except for the CO2+100 and the IMP+ scenario, is almost identical to the one in the BASE scenario. In all scenarios, CO_2-emissions have a fluctuating development. In 2015, they increase slightly in all scenarios compared to 2010, above all because of an increase in power demand. Moreover, in 2020 CO_2-emissions decrease and increase again by 2025. In the BASE, gas price variation and EUA price variation scenarios the rise in CO_2-emissions in 2025 is caused by a significant increase in the use of lignite, while in the IMP+ and GRID scenario it results from an increased use of hard coal. Unlike it might be expected, the rise in gas prices has only little effect on the development of the CO_2-emissions, because the requirement of gas-fired power stations as flexible reserve results in only a minor reduction of power generation in gas-fired power stations.

Thus, the only changes in the framework conditions that lead to alternative developments of CO_2-emissions are the increase in EUA prices and the rise in power imports. However, the decrease in CO_2-emissions in the IMP+ scenario only reflects the significantly lower power generation within Germany. In the CO2+100 scenario, the doubling of EUA prices in the last period results in a considerable reduction of CO_2-emissions by 2030. Comparing 2007 and 2030, a 50% reduction is realized. In this scenario, the considerable, additional reduction of almost 60 Mt CO_2 is realized, above all, by the installation of 10.6 GW of coal-fired power stations with CCS technology. In the CO2+50 scenario, a single 1.0 GW power station with CCS technology is installed in the last period. Yet, since its share in power generation is comparatively low, the emission reductions realized are only marginal. In the other scenarios, the EUA prices are not high enough to trigger the use of CCS technology.

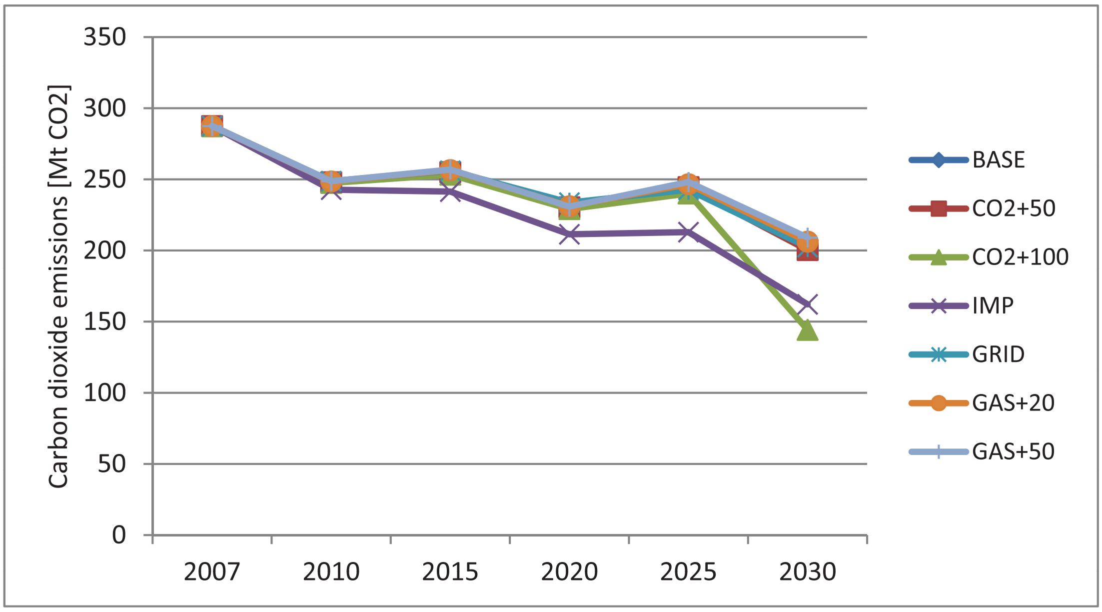

Figure 9.4.: Development of CO_2-emissions in the scenarios

To put the emission reductions realized in the scenarios into perspective, they can be compared to the emission reduction targets of the EU ETS. Furthermore, it is notable that the CO_2-emission volumes in the scenarios do not increase continuously, but rather increase in 2015 and 2025 and decrease in the following periods. This rise in CO_2-emissions is caused by changes in the fuel choice as well as by the phase-out of nuclear power stations. Due to the phase-out of nuclear power generation, the share of carbon emission free generation decreases.

Until 2020, the emission volumes of the sectors participating in the EU ETS are to be reduced by 1.74% per year. If we assume this annual reduction target for the energy sector considered in this work and if we extrapolate it until 2030, CO_2-emissions would have to be below 200.7 Mt CO_2 by 2030. This target is reached in the CO2+50 scenario and undercut in the CO2+100 and IMP+ scenario. The volumes emitted in the other scenarios lie by 1% - 4% above this level. Yet, if we assume that the energy sectors have to participate disproportionately in the fulfillment of the emission targets, the emission reductions realized in most scenarios are not sufficient to meet Germany's GHG emission reduction targets.

10. Conclusions and outlook

Within this work, an optimal power flow based energy system model has been developed, which allows us to determine the optimal point in time and location of power station capacity investment. It has been used to analyse the optimal future development of the German power system under predefined framework conditions.

The results of the scenario calculations presented in chapter 7 provide information regarding potential future development paths of the German power system under alternative framework conditions. In a base scenario, the reference development of the German power system has been modeled. Moreover, a scenario analysis has been conducted to evaluate the development of the German power system under alternative framework conditions. Since in this work special focus is given to the increasing relevance of grid constraints, two scenarios have been calculated in which two of the main influencing factors on the power flows in the German transmission grid have been varied. In the GRID scenario the influence of a delay in grid extensions has been evaluated, while in the IMP+ the relevance of a doubling of power imports combined with halving exports has been assessed. Moreover, input data whose development is subject to considerable uncertainties has been varied in the scenario analysis. Firstly, two scenarios with a more significant increase of the EUA prices[1] and secondly, two scenarios with a more fierce rise in gas and fuel oil prices have been presented.

In the following, main conclusions regarding the chosen modeling approach as well as regarding the development of the German power system until 2030 will be outlined. First, the most important characteristics of the chosen modeling approach will be summarized. In doing so, also the necessity to integrate grid constraints in energy system models, which has been the supposition of this work, will be discussed. Moreover, conclusions regarding the suitability of the chosen modeling approach for power plant investment planning will be addressed. In the second part of this chapter, general conclusions regarding the future development of the German power system in terms of regional capacity development, congestion, nodal prices, and CO_2-emissions will be drawn. In the last part of this chapter, an outlook on further model extensions as well as on further fields of applications will be given.

[1] Since only the German power system has been considered in the scenario analysis, an endogenous modeling of the ETS was not possible.

10.1. The developed nodal pricing based power system model

Due to the expected replacement of large conventional power stations that are today located close to the large load centers in the southern and western parts of Germany as well as due to the increasing use of offshore wind power, the system load in the German power system is expected to rise. As a result, congestion in the German transmission grid can be expected to rise in the future. For this reason, it is necessary to adequately consider grid constraints in the long-term modeling of power systems. Moreover, due to the increasing use of distributed RES-E, the consideration of regional characteristics becomes increasingly important in power system modeling.

Therefore, in this work, a modeling approach has been developed that allows for the analysis of the long-term development of power systems while respecting grid restrictions as well as the physical laws of power flow. The developed model PERSEUS-NET is part of the energy system model family PERSEUS. Its precursors, such as PERSEUS-CERT (Enzensberger [2003]), PERSEUS-HYDRO (Möst [2006]), or PERSEUS-RES-E (Rosen [2007]) have been used to analyze various questions regarding possible development paths of the European energy system. The PERSEUS models are multi-period optimization models which follow a cost minimizing approach to fulfill a given demand. Models of the PERSEUS model family allow for a very detailed representation of the techno-economic characteristics of power and heat generation technologies as well as energy flows. Moreover, the modular design of the PERSEUS models allows for an easy adaptation to various current questions and problems. The adapted model version PERSEUS-NET developed within this work is most suited to cope with the above mentioned new challenges for power system modeling. The chosen nodal pricing approach guarantees, on the one hand, an adequate consideration of grid constraints. The DC load flow model integrated in PERSEUS-NET provides a good approximation of the active power flows in the German transmission grid. On the other hand, PERSEUS-NET allows for a detailed regional representation of power systems.

PERSEUS-NET relies on an elaborated database, which comprises all grid nodes and transmission lines of the German extra high voltage grid. In total, PERSEUS-NET contains 442 individual grid nodes as well as 1302 power lines. Moreover, approximately 260 individual, large power stations as well as approximately 1600 existing small conventional units are considered. Furthermore, at each grid node up to five types of RES-E power generating technologies are considered. While the regional expansions of RES-E generating technologies in Germany is predefined, PERSEUS-NET enables a regional expansion of conventional power stations by defining regionally availabilities of expansion options and fuel choices. Moreover, regionally detailed demand levels allow for the consideration of regional changes in the demand levels due to different regional population and GDP developments. This comprehensive database enables a very precise modeling of the German power system, including its regional characteristics. Since the PERSEUS-NET database is coupled to a GIS, the regional input and output data can appropriately been displayed and edited.

Thus, a powerful tool has been developed, which can be used to analyze the long-term development of the German power system under different framework conditions. It particularly allows special focus, firstly on the significance of potential power grid constraints, and secondly on the regional development of the power system.

The results obtained with the model confirm the supposed need to consider grid constraints in long-term energy system modeling. In all scenarios, increasing congestion in the German power system has been determined. Moreover, the results of the scenario analysis show that grid constraints have an influence on the choice of location of power stations. In the case of bottlenecks, the siting of power stations is altered, as can be noticed by comparing the results of the BASE and the GRID or IMP+ scenario. The changes in the power system structure affect above all the location of the power stations, but also, to some extent the choice of fuel. Thus, the results of the model PERSEUS-NET give good indications regarding an optimal regional power station expansion in congested grids. Yet, since the PERSEUS-NET model does not consider extreme system loads, as they result from maximum offshore wind power feed-in, the grid access of power stations cannot be guaranteed only based on the results of the PERSEUS-NET model.

In policy advice or for the use of regulators the application of PERSEUS-NET seems most qualified, e.g. to evaluate giving incentives for an economically reasonable regional expansion of power stations. Moreover, market actors can use PERSEUS-NET as decision support in capacity investment planning. The application of PERSEUS-NET confirms the suitability of a nodal pricing-based power system model for power plant investment planning. With PERSEUS-NET nodal price signals have been determined that served as basis for a regional power station capacity investment planning under grid constraints. Thus, the regional development of the German power system until 2030 has been analyzed. In doing so, the optimal fuel choice, point in time, and location of power stations has been determined. However, as discussed in chapter 8, nodal pricing does not render correct long-term price signals, because the costs related to the construction and operation of the power grid are only partly captured. This is in particular true for PERSEUS-NET, because regarding the cost of the power grid, only the marginal cost of congestion are included in the optimization. By contrast, the marginal cost of losses and the cost arising from the investments in new transmission capacity are not considered.

Nevertheless, since nodal prices signal the correct “direction” for power station capacity investments, the results obtained with PERSEUS-NET can be used as a starting point for a more profound analysis. To finally decide whether the construction of a power station is optimal from an economic point of view, a comparative analysis using a techno-economic nodal pricing based model with a focus on power station capacity investments, such as PERSEUS-NET and an AC model with focus on transmission grid investments should to be conducted. In doing so, the different lead times of power station and grid investments should be kept in mind.

Yet, even though PERSEUS-NET has been proven to be a powerful tool for the analysis and evaluation of the long-term development of the German power systems, there are some limitations to the modeling approach, which have to be kept in mind when applying the model and interpreting the results obtained with PERSEUS-NET. They comprise the underlying market understanding as well as the simplified modeling of RES-E. In the following, the main conclusions that can be drawn from applying the model to the German power system are outlined.

10.2. Conclusions regarding the development of the German power system until 2030

10.2.1. Increasing congestion leading to regional price differences

Regarding the development of congestion in the German transmission system, it can be concluded that it is of utmost importance that the projects named in EnLAG [2009] are realized as fast as possible. As the analysis of the influence of delays in the extension of the transmission grid shows, the bottlenecks resulting from the delays cause significant differences in the locational marginal cost of power supply, which indicates the relevance of an early extension of the transmission grid.

Moreover, due to the significant increase in offshore wind power feed-in at the Frisian Coast, congestion occurs in all scenarios by 2025. The congestion is likely to increase, if increasing imports are to be expected. In addition, since strongly increasing gas prices result in a reduction of gas-fired power generation in remote areas in the scenario analysis, higher gas prices might provoke additional bottlenecks.

Due to the occurrence of an increasing number of bottlenecks in the German transmission grid, significant regional differences in the marginal cost of power supply occur in the scenarios by 2030. While they are very low or even negative at the East Frisian coast, they are considerably higher in the western and southwestern parts of Germany. If the power grid is additionally loaded, such as is the case when grid extensions are delayed or if power imports increase significantly, the regional price differences can reach levels of more than 500 €/MWh in certain time slots. Moreover, as the CO2+100 scenario shows, regional shifts in power generation can have a significant influence on the regional distribution of nodal prices. In particular a transfer of power generation from the East to the Ruhr districts seems to be a way to reduce large regional price differences.

Again, it should be noted that these results have to be interpreted taking into account the simplified modeling of the RES. In the real world, the effects are expected to be even higher, in particular in situations with high offshore wind power feed-in.

10.2.2. Lasting combination of renewable energy sources and carbon intensive technologies

The generation and capacity mixes obtained in the scenario analysis show a combination of a considerable share of RES-E and the carbon intensive fuels lignite and coal. Even though the share of RES in power generation increases to more than 40%, as it has been predefined in the model assumptions, lignite will most probably still be the most important fossil fuel in power generation in Germany, followed by coal.

The development of the fuels thus matches the development of their primary energy carrier prices. While today's very low lignite prices have been assumed to increase only slightly, more important price increases over time have been assumed for coal and, in particular, gas (see section 6.5.1). These differing developments in primary energy carrier prices counteract the increase in EUA prices that could make less carbon technologies more favorable from an economic point of view. The aspired transformation towards a more ecological power supply is therefore only partly achieved.

According to the model results, carbon capture and storage will only be used if the prices of EU emission allowances rise considerably. In the scenario analysis this first is the case when EUA prices rise above 67.50 €/t_{CO_2}. CCS is only be used to a considerable amount at an EUA price of 90.00 €/t_{CO_2} in 2030.

10.2.3. Increased use of flexible power stations to counteract congestion

In the scenario analysis, particularly gas-fired power stations are constructed at the deficit sides of bottlenecks to counteract congestion. The most prominent example are the natural gas combined cycle power stations that are commissioned at the deficit side of the bottleneck in the Northwest. They are used in particular in times of high system load and create a counterflow on the bottleneck. Moreover, e.g. in the GRID scenario, additional gas-fired power stations are built in South Germany at the deficit side of a bottleneck on the corridor connecting the east and the south of Germany. The results of the Gas+50 scenario have shown that if those power stations are not built due to too high gas prices, the cost of the congestion increases considerably.

Regarding the implication of the results for the development of the German power system, it is most likely that the number of rather small, flexible power stations will increase in the future. In particular, they are likely to be used to reduce temporal bottlenecks that only occur infrequently. In this context, it should also be investigated if the construction of additional flexible power stations might be beneficial compared to constructing new transmission lines. In some cases, the construction of additional flexible power stations at the deficit sides of bottlenecks might prove to make good economic sense as an alternative to the construction of additional transmission capacity. Furthermore, the right balance has to be found between the cost of congestion and the cost of constructing new power stations or grid capacities.

10.2.4. Further conclusions

Regarding the overall price level, there is a significant increase in the average marginal cost of power supply over the covered time horizon. By 2030, the average marginal cost of power supply is highest in the CO2+100 scenario and lowest in the IMP+ scenario.

Regarding the carbon dioxide emissions, the reductions necessary to meet the ambitious targets of Germany are only reached either if the EUA price increases significantly or if the investments of CCS decrease.

10.3. Outlook

The nodal pricing based modeling approach presented in this work has been proven very helpful in analyzing the long-term development of the German power system. Regarding the model development, the focus of this work was, on the one hand, on integrating the necessary DC optimal power flow equation in the energy system model source code. On the other hand, it was on digitizing the German transmission system and georeferencing the input data. Yet, the expected future developments in the energy industry as well as in energy system modeling evoke further research questions regarding potential model adaptations and applications that would have exceeded the scope of this work. In the following, the most interesting starting points for future research activities are outlined.

10.3.1. Extensions of the modeling approach

10.3.1.1. Modeling of renewable energy sources

In chapters 8 and 9 it has been discussed at length that due to the rough temporal structure and neglect of PV and wind power fluctuations, extreme grid situations cannot be modeled. This should also be the starting point for a first extension of the model. On the one hand, the model could be linked to an optimal power flow model with a higher temporal resolution. In that way, the feasibility of the results regarding the compliance with grid restrictions could be checked. Another approach to capture the fluctuating character of RES could be to revise the temporal structure. Even though a much higher temporal resolution seems not to be practical today, due to excessively high calculation times, the consideration of load profiles of wind power feed-in seems realizable. To consider such load profiles of PV or wind power, a comprehensive analysis of the temporal and regional distribution of wind speed and solar radiation data would have to be conducted. This approach would allow us to consider fluctuations in the feed-in of solar and wind power in a deterministic way. Extreme situations could be modeled too, such as high offshore wind power feed-in in combination with low system load or no offshore wind power feed-in at maximum system load. Therefore, the fluctuating stochastic character of RES-E feed-in cannot be captured. However, the integration of stochastic wind and solar power feed-in seems, at present, not advisable due to the computational restrictions.

10.3.1.2. Modeling of power grid investments

Using PERSEUS-NET optimal power station expansion paths can be determined for a predefined grid topology. In the scenarios, a grid expansion based on EnLAG [2009] is assumed. However, additional expansions, which will probably be necessary to integrate e.g. the increasing offshore wind power feed-in into the German transmission grid are not taken into account. Moreover, optimal locations for power grid investments are not determined. Thus, the interdependencies between regional power station and grid investments cannot be analyzed. Nor can be evaluated whether a further expansion of the transmission grid would be economically feasible to reduce differences in the locational marginal cost of power supply.

Therefore, thoughts should be given to modeling power grid expansion endogenously in PERSEUS-NET. For this purpose, the PERSEUS-NET source code would have to be adapted in a way to consider investments in power grid capacities. Since, a completely unrestricted expansion of power line capacities between all grid nodes of the transmissions system is not reasonable, appropriate regional investment options would have to be identified. Moreover, a comprehensive literature review on the techno-economic characteristics of potential grid expansion options would have to be carried out. The resulting model would allow for an integrated optimization of power station and grid investments. Thus, it could be applied e.g. to evaluate whether a further expansion of the power grid would be preferable over regional investments in distributed power stations and storage devices.

However, as the application of the current version of PERSEUS-NET as well as first approaches to develop an integrated power station and grid investment optimization model have shown (Apfelbeck [2009]) calculation time will become a crucial point. Therefore, it should be evaluated whether a scenario based analysis considering potential further power grid expansion projects would not be preferable over an integrated modeling approach (see also section 10.3.3).

10.3.1.3. Adoption of an AC optimal power flow approach

Another enhancement of the model that would allow for a better modeling of power grid restrictions is the adoption of an AC optimal power flow approach. Since the resulting optimizing problem is neither linear nor convex, iterative methods would have to be used to solve the problem. However, the methods typically used at present would be too time consuming, to be used for an analysis of the long-term development of the power system. Yet, if alternative solution procedures were available, the adoption of an AC OPF approach would be most beneficial. A first way to develop such an innovative modeling approach is presented in Schönfelder et al. [2011]. In addition, if an AC OPF approach was to be adopted, a comprehensive analysis of regional demands for reactive power as well as the consideration of additional power system elements such as FACTS and phase shifters would be necessary.

10.3.1.4. Considering a price-elastic power demand

In the model presented in this work, the power demand is considered as inelastic in the short-term as well as in the long-term (see section 3.2.2). One of the main reasons for this demand elasticity is that variations in generation costs are not mirrored in wholesale electricity prices. Furthermore, final customers often do not know the actual level and cost of the use of their electric appliances. Since the European energy savings directive EC [2006a] as well as the German EnWG [2005] supports the provision of final customers with smart meters and time-dependent tariffs reflecting the true costs of power consumption at each point in time, the price elasticity of power demand might increase during the next years. (Even more so, if technologies allowing for an automatic control of appliances penetrate the mass-market.)

Therefore, in the future, it might become necessary to consider a price-elastic power demand. To integrate a price-elastic demand in PERSEUS-NET an approach based on the cobweb model seems most appropriate (cf. e.g. Wietschel [1995]). PERSEUS-NET could be used to determine regional time-varying electricity prices, while the demand shifts would be determined in a demand side simulation model such as the model DS-Opt presented in Eßer et al. [2006b].

10.3.2. Supplementation of the data basis

In addition to extensions of the modeling approach, a supplementation of the data basis could be useful. The starting points for a supplementation of the data basis could be the integration of neighboring power systems as well as a more detailed modeling of the heat and power demand.

10.3.2.1. Integration of neighboring power systems

Germany is embedded in the core of the continental European power grid. Therefore, power exchanges with its neighboring power systems play an important role. Due to the extension of interconnectors, the inhomogeneously distributed potentials of RES, as well as due to an increasing number of regional cooperations to couple national markets (see section 3.4.2), power exchanges between Germany and its neighboring countries can be expected to increase in the future. However, in the current version of PERSEUS-NET the neighboring power systems are not considered, but rather the predefined power exchanges with the neighboring systems are modeled. Regarding future applications of the model, it is advisable to integrate other European power systems in the optimization model. Thus, regional shifts of power generation among different countries could be analyzed and the idea of a single European market could be better captured. Again, because the consideration of additional power systems would result in an increase in computing time, a trade-off between the necessary level of detail and simplifications to reduce computing time is necessary. Therefore, a modeling of the neighboring power systems as single grid nodes, as it is typical for conventional energy system models, is recommendable.

10.3.2.2. Modeling of the power and heat demand

In PERSEUS-NET, power demand has been modeled based on the regional population structure and the regional distribution of GDP. Regarding their future development, quantitative changes in population and GDP have been taken into account. Yet, scientific studies have shown a significant influence of the regional development of the demographic structure on energy demand (cf. e.g. Kronenberg and Engel [2008]). Among other things the age structure of a population can have an influence on power demand.

Therefore, the consideration of the influence of the evolution of regional demographic structures on electricity demand might be useful to further enhance the level of detail in modeling decentralized power systems. Moreover, the consideration of additional, new power demands, such as the power demand of electric mobility would be interesting.

Another option for further research is related to the modeling of the heat demand. Due to computational restrictions as well as the insufficient availability of relevant data, only the heat demand on those grid nodes, where there are power stations with considerable heat extraction, are modeled. To allow for an adequate modeling of co-generation, first of all, the regional heat demands (per temperature level) would have to be derived based on statistical data. Moreover, additional co-generation technologies, in particular for distributed heat and power generation, would have to be considered. This would allow for the evaluation of the implication on Germany's target to expand the use of co-generation on the power system. In doing so, regional characteristics in particular could be analyzed in detail. Furthermore, the expected further decentralization of power systems could be better captured. However, it should be noted that the consideration of additional generation process restrictions would increase computation time considerably.

10.3.3. Further fields of application

In this thesis, a modeling approach has been developed which allows for the analysis of the long-term development of power systems, while considering grid constraints as well as regional characteristics of the power system. The focus of the work was on the integration of power grid constraints into the model as well as on the modeling of the regional characteristics of the German power system, comprising regional power demands, RES-E potentials, as well as the regional availability of power station capacities. The model has been applied to analyse the development of the German power system until 2030.

Further fields of application could be orientated on current trends in energy research as well as on political ambitions. On the one hand, an evaluation of the influence of the use of stationary as well as mobile storages could be interesting. PERSEUS-NET would be most apt for such an analysis, because regional characteristics and potentials are of importance regarding the siting, in particular of stationary storages. Moreover, by using PERSEUS-NET it could be analyzed to what extent the use of storage capacities is suitable to decrease bottlenecks in the German transmission grid.

The evaluation of further expansions of the German transmission system could be a further field of application. For this purpose, a scenario analysis can be conducted, in which different likely expansion options are considered. In doing so, the influence of the considered expansion projects on the regional structures of power generation and nodal prices can be analyzed. Moreover, the influence of the grid expansions on the overall system cost can be estimated. Comparing the corresponding investments and the potential savings would allow to evaluated whether those investment projects would be economically reasonable (without modeling grid investments endogeneously).

Moreover, the model PERSEUS-NET is most suited to evaluate different market designs in Germany. Recently, the increasing relevance of grid constraints, which increasingly necessitate redispatches, has given rise to a discussion concerning adaptations of the market design in Germany. In this context, PERSEUS-NET could, for example be used to analyse the possible effects of the adoption of a market splitting approach in Germany. Furthermore, possible configurations of regionally differentiated network access charges for power stations, the socalled "G" component, could be analyzed.

A further field of application could be, as outlined in the previous section, an analysis of the influence of an increasing use of co-generation on the long-term development of the German power system. Moreover, other applications which have a focus on the local availability and expansion potential of RES are reasonable. In this case, it could be determined how and to what extent e.g. a decentralization of the power system could contribute to reducing congestion in Germany's future power system.

In addition, other fields of application are imaginable. PERSEUS-NET is particularly suitable whenever grid constraints or the regional characteristics of the energy system are of special importance.

A. Greenhouse gas emissions and Kyoto targets

Table A.1.: Greenhouse gas emissions in CO_2 equivalents (excl. LULUCF), Kyoto targets for 2008-2012, and emission projections (SEC(2008)2636 [2008])

Member states	**Base year**	**2006**	**Kyoto targets**	**Change base year - 2006**	**Kyoto targets**	**Projections for 2010 A**[1]	**Projections for 2010 B**[2]
	[Mt]			[%]			
Austria	79.0	91.1	68.8	15.2	-13.0	17.4	-13.3
Belgium	145.7	137.0	134.8	-6.0	-7.5	-3.7	-8.5
Bulgaria	132.6	71.3	122.0	-46.2	-8.0	-29.8	-34.9
Cypria	6.0	10.0	n/a	66.0	n/a	44.3	41.4
Czech Rep.	194.2	148.2	178.7	-23.7	-8.0	-25.1	-28.8
Denmark	69.3	70.5	54.8	1.7	-21.0	-2.2	-11.6
Estonia	42.6	18.9	39.2	-55.7	-8.0	-62.8	-65.7
Finland	71.0	80.3	71.0	13.1	0.0	19,7	-0.6
France	563.9	541.3	563.9	-4.0	0.0	0.8	-4.2
Germany	**1232.4**	**1004.8**	**973.6**	**-18.5**	**-21.0**	**-23.5**	**-26.2**
Greece	107.0	133.1	133.7	24.4	25.5	23.9	20.8
Hungary	115.4	78.6	108.5	-31.9	-6.0	-24.9	-25.4
Ireland	55.6	69.8	62.8	25.5	13.0	22.8	12.4
Italy	516.9	567.9	483.3	9.9	-6.5	7.5	-4.6
Latvia	25.9	11.6	23.8	-55.1	-8.0	-46.1	-46.1
Lithuania	49.4	23.2	45.5	-53.0	-8.0	-30.4	-30.4
Luxembourg	13.2	13.3	9.5	1.2	-28.0	3.1	-28.0
Malta	2.2	3.2	n/a	45.0	n/a	61.8	61.8
Netherlands	213.0	207.5	208.3	-2.6	-6.0	-2.2	-8.4
Poland	563.4	400.5	529.6	-28.9	-6.0	-28.4	-29.0
Portugal	60.1	83.2	76.4	38.3	27.0	44.2	22.7
Romania	278.2	156.7	256.0	-43.7	-8.0	-31.4	-35.3
Slovakia	72.1	48.9	66.3	-32.1	-8.0	-18.4	-21.6
Slovenia	20.4	20.6	18.7	1.2	-8.0	6.7	-13.2
Spain	289.8	433.3	333.2	49.5	15.0	52.0	20.5
Sweden	72.2	65.7	75.0	-8.9	4.0	-2.7	-5.7
UK	776.3	652.3	679.3	-16.0	-12.5	-19.4	-20.0
EU-15	4265.5	415.1	4110.2	-2.7	-8.0	-3.5	-11.3
EU-27	5768.0	5142.8	No targets	-10.8	No targets	-10.1	-16.3

[1]Considering existing policies and measures (stand: 16.10.2008).
[2]Additionally considering the use of Kyoto mechanisms, carbon sinks, and additional poicies and measures (stand: 16.10.2008).

B. Regional distribution of input data

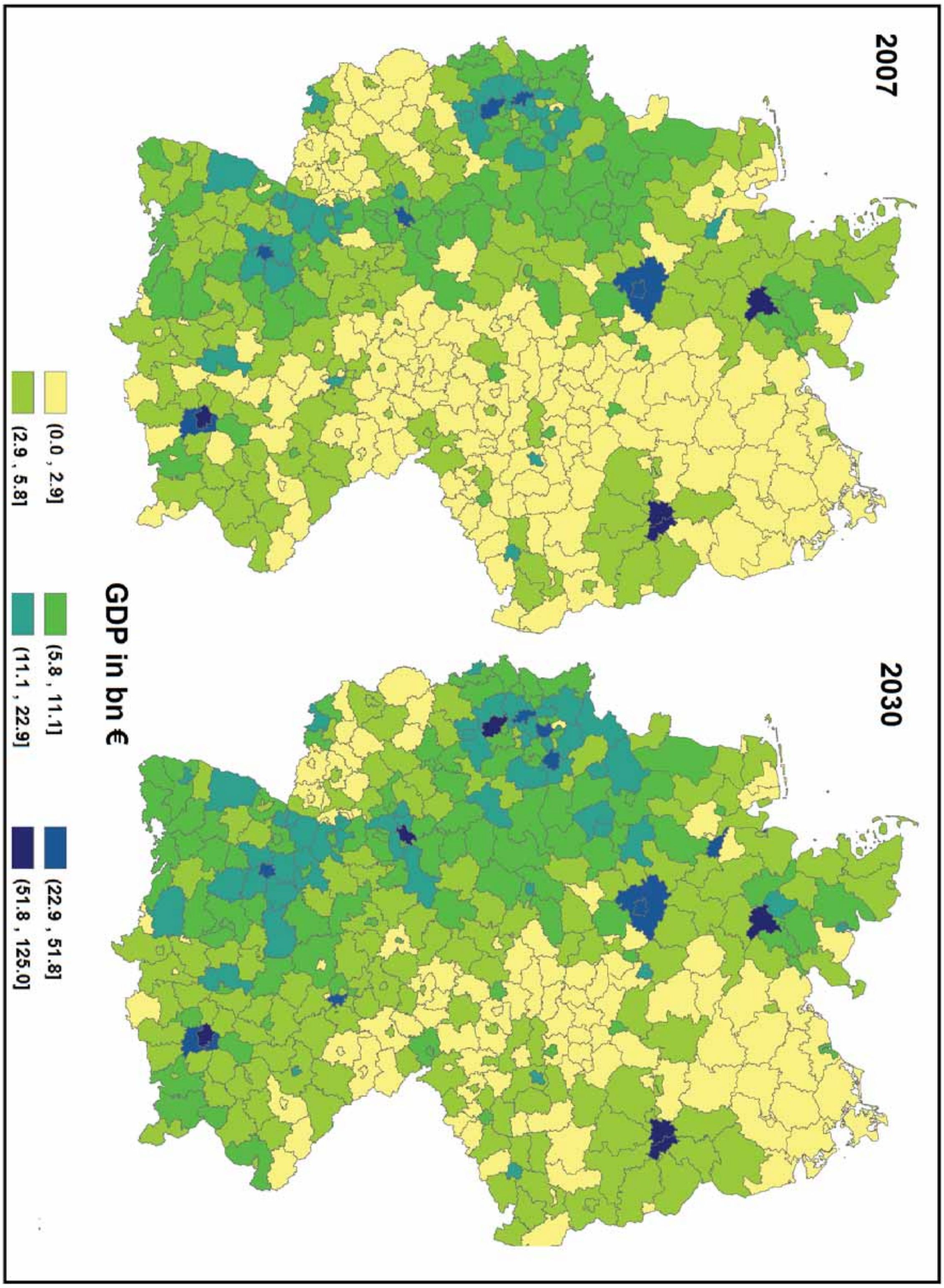

Figure B.1.: Regional distribution of the GDP (based on Prognos [2009], DESTATIS [2009])

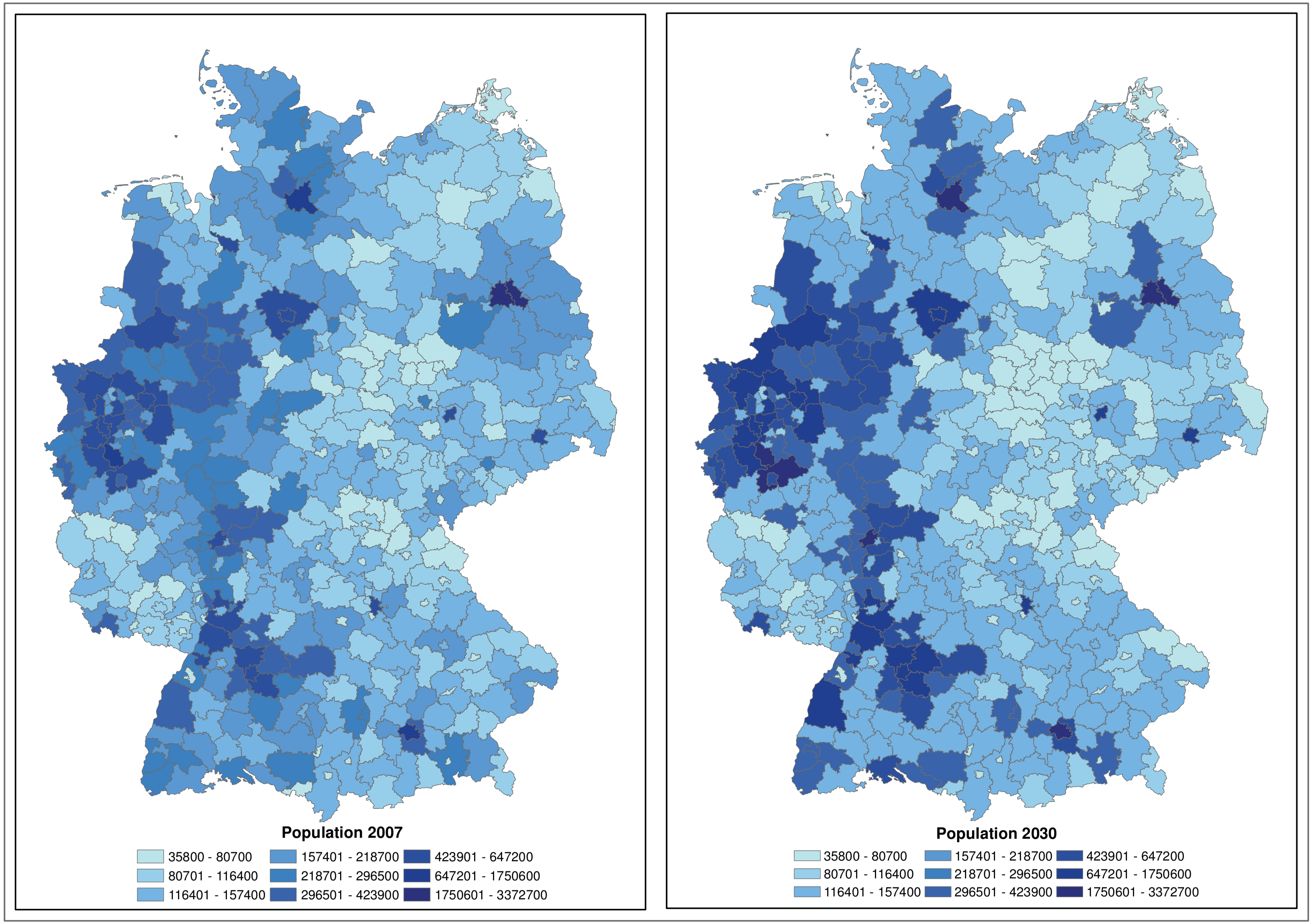

Figure B.2.: Regional population distribution (based on DESTATIS and BBR [2005])

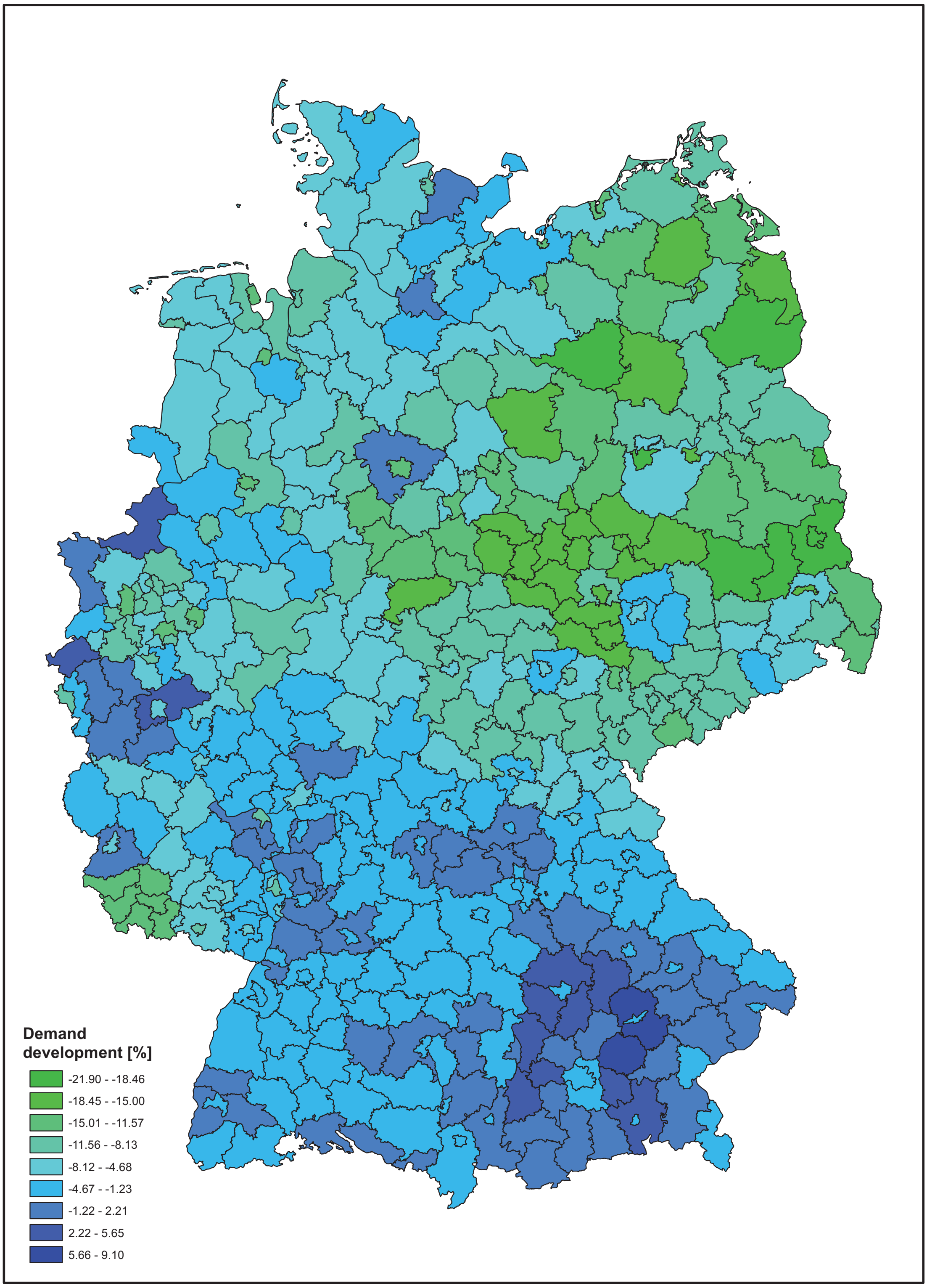

Figure B.3.: Spatial distribution of power demand development between 2007 and 2030

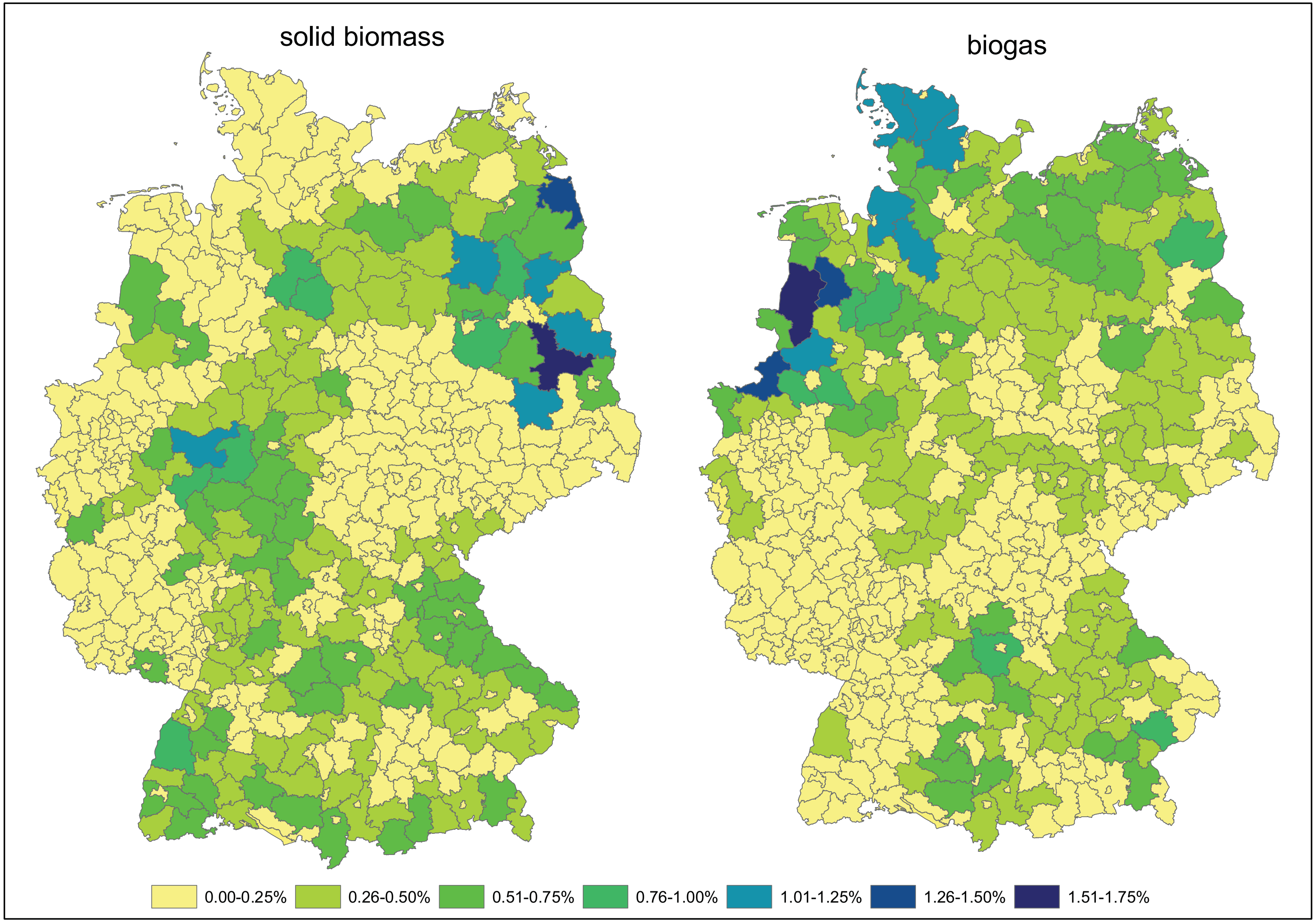

Figure B.4.: Spatial distribution of solid biomass and biogas potentials (based on Brökeland [1998], DESTATIS [2006])

C. Large power stations

Table C.1.: Power stations and generating units modeled individually in PERSEUS-NET

Name	Fuel	Year	Capacity [MW_{el}]	Capacity [MW_{th}]	Efficiency [%]
Ahrensfeld	gas	1991	150		31.0
Albbruck-Dogern	water	2009	80		50.0
Altbach	fueloil	1976	120		34.0
Altbach 4	fueloil	1974	238	180	45.0
Altbach 5	coal	1976	420	280	44.0
Altbach II 1	coal	1997	397	280	40.0
Bergkamen A	coal	1987	684	20	38.0
Bexbach C 1	coal	1983	714		38.0
Biblis A	uranium	1974	1167		30.5
Biblis B	uranium	1976	1240		30.5
Bocholt GuD	gas	2010	400		58.0
Bexbach	coal	2010	750		45.0
Boxberg N	lignite	1978	459		36.0
Boxberg P	lignite	1979	459		36.0
Boxberg Q	lignite	2000	845	71	42.0
Boxberg R	lignite	2011	670		43.9
Brokdorf 1	uranium	1986	1410		30.5
Brunsbuttel	fueloil	1974	252		34.0
Brunsbuttel 1	uranium	1976	771		30.5
Buschhaus A	lignite	1998	352		41.0
Charlottenburg	gas	2000	320	510	35.0
Chemnitz HKW	lignite	1986	170.2	732	35.0
Datteln 3	coal	1969	303	252	36.0
Datteln 4	coal	2011	1100		45.4
Dieselstraße	gas	2005	89	160	44.0
Dormagen RWE GT 2	gas	1979	185		41.0
Dormagen RWE GT 1	gas	2001	185		41.0

Dormagen RWE SC	gas	2001	190		41.0
Duisburg-Mitte 2	coal	1986	166	139	43.0
EDZ Huerth	lignite	1993	151	30	40.0
Eisenhuettenstadt	gas	1995	101.2		35.0
Emsland	uranium	1988	1329		30.5
Emsland B	gas	1974	410	37	40.0
Emsland C RWE C	gas	1975	410	37	40.0
Ensdorf RWE	coal	1971	296		35.0
Ensdorf VSE 2	coal	1963	114		33.0
Erzhausen	from-storage	1964	220		75.0
Farge 301	coal	1969	345		43.0
Flensburg	coal	1974	156.4	807	38.0
Fra West	coal	2004	168.4	448	30.0
Franken I 2	gas	1975	830		35.0
Frankfurt Nuon GuD	gas	2010	400		58.0
Frimmersdorf F	lignite	1960	143		31.0
Frimmersdorf G	lignite	1960	143		31.0
Frimmersorf H	lignite	1961	143		31.0
Frimmersorf 1	lignite	1960	143		31.0
Frimmersdorf J/CDE	lignite	1957	429		31.0
Frimmersdorf K	lignite	1962	143		31.0
Frimmersdorf L	lignite	1962	143		31.0
Frimmersdorf M	lignite	1962	143		31.0
Frimmersdorf N	lignite	1964	143		31.0
Frimmersdorf O	lignite	1964	143		31.0
Frimmersdorf P	lignite	1966	285		33.0
Frimmersdorf Q	lignite	1970	285		33.0
Gaisburg HKW	coal	1989	258	300	43.0
Gaisburg 5	gas	1973	59		35.0
Geesthacht	from-storage	1958	120		75.0
Gerstein K	coal	1984	720		43.0
Gerstein K GT	gas	1984	100		50.0
Gersteinwerk	gas	1973	460		42.0
Gersteinwerk F	coal	1973	406		35.0
Gersteinwerk G	coal	1973	406		35.0
GKM 3	coal	1966	200	131	36.0
GKM 4	coal	1970	200	131	36.0
GKM 6	gas	2006	251	167	45.0
GKM 7	coal	1983	432	283	40.0
GKM 8	coal	1993	437	287	43.0

GLEMS	from-storage	1968	89		75.0
Goldisthal 1	from-storage	2003	265		75.0
Goldisthal 2	from-storage	2003	265		75.0
Goldisthal 3	from-storage	2003	265		75.0
Goldisthal 4	from-storage	2004	265		75.0
Grafenrheinfeld 1	uranium	1981	1275		30.5
Grohnde 1	uranium	1985	1360		30.5
Grosskayna	fueloil	1994	127		34.0
Gundremmingen B	uranium	1984	1284		30.5
Gundremmingen C	uranium	1984	1288		30.5
Gustav Knepper C	coal	1971	325	15	38.0
Hafen 5	coal	1968	140	28	36.0
Hafen 6	coal	1979	300	28	40.0
Hallendorf	gas	1985	253	330	44.0
Hamborn RWE 1	gas	2003	225	535	43.0
Hamm D	coal	2011	800		46.0
Hamm E	coal	2012	750		46.0
Hamm-Uentrop	gas	2007	813		57.5
Hamm Trianel I	gas	2007	425		57.5
Hamm Trianel II	gas	2007	425		57.5
Hannover	coal	1989	230	100	36.0
Hastedt 14	gas	1972	170	130	35.0
Hastedt 15	gas	1989	130	130	43.0
Heilbronn 5	coal	1964	100		33.0
Heilbronn 6	coal	1966	100		33.0
Heilbronn 7	coal	1985	690	300	40.0
Herdecke	gas	2007	417		58.0
Herne 2	coal	1963	138	86.84	36.0
Herne 3	coal	1966	276	174	36.0
Herne 4	coal	1989	460	289.5	43.0
Heyden 4	coal	1987	865		38.0
HH Tiefstack HKW	gas	2008	125		60.0
Hohenwarte	from-storage	1963	382.75		75.0
Huerth	gas	2007	800		58.0
Huckingen A	gas	1975	290		39.0
Huckingen B	gas	1976	290		39.0
Ibbenburen B1	coal	1985	709		38.0
Iffezheim	water	1978	106.4		50.0
Iller	water		45.93		50.0
Ingolstadt 3	fueloil	1974	384		34.0
Ingolstadt 4	fueloil	1974	384		34.0
Irsching	gas	1969	878		35.0
Irsching 4	gas	2011	530		60.0

Irsching 5	gas	2009	845		60.0
Isar 1	uranium	1977	878		30.5
Isar 2	uranium	1988	1400		30.5
Janschwalde A	lignite	1980	460	58.2	36.0
Janschwalde B	lignite	1981	460	58.2	36.0
Janschwalde C	lignite	1982	460	58.2	36.0
Janschwalde D	lignite	1984	460	58.2	36.0
Janschwalde E	lignite	1986	460	58.2	36.0
Janschwalde F	lignite	1988	460	58.2	36.0
Jena Sued	gas	1996	196	225	55.0
Karlsruhe RDK 8	coal	2012	912		46.5
Karlsruhe RDK GuD	gas	2010	465		58.0
Karlsruhe West	coal	1985	116	191	40.0
Karlsruhe 7	coal	1985	501	220	42.0
Kiel A	coal	1970	323		58.0
Kirchlengern GT 1	gas	1980	176		50.0
Kirchmoder	gas	1996	160		50.0
Klingenberg	coal	1987	170.2	1010	40.0
Koepchenwerk II 1	from-storage	1989	153		75.0
Krummel 1	uranium	1983	1346		30.5
Lausward D	coal	1988	103	75	55.0
Lausward A	gas	1957	420	140	54.5
Lech	water		351		50.0
Leipzig Nord	gas	1996	176	53	65.1
Lichterfelde 1	fueloil	1970	150	240	35.0
Lichterfelde 2	gas	1970	150	240	35.0
Lichterfelde 3	gas	1974	150	240	35.0
Linden Hannover 1	gas	1999	91	100	50.0
Lingen	gas	2009	876		59.2
Lippendorf R	lignite	2000	891	155	43.0
Lippendorf S	lignite	1999	891	155	43.0
Ludwigshafen KW Sued GT 2	gas	1997	396		41.0
Luenen-1	coal	1973	120		43.0
Luenen-2	coal	1996	460	40	43.0
Lünen Trianel	coal	2012	750		46.0
Mainz 2	gas	1977	346		41.0
Mainz 3	gas	2001	401		58.0
Markersbach	from-storage	$<$2000	175		75.0
Mehrum-C	coal	1979	690		37.0
Meppen A1	gas		610		35.0
Merkenich	gas	1971	158	80	42.0

Mitte Berlin	gas	1996	411	630	57.0
Mittelsburen	gas	2001	80		35.0
Mittelsburen 1-4	gas	2001	360		35.0
Moabit 3	coal	1987	138	240	43.0
Moorburg	coal	2012	1680		46.5
Moorburg	fueloil	1980	150		34.0
Muenster GuD	gas	2005	96	115	40.0
Muenchen Nord	coal	1991	316	555	43.0
Muenchen Sued 6 GT 1	gas	1980	260	260	55.0
Muenchen Sued 6 GT 2	gas	2004	435	458	55.0
Muenchen Sud45	gas	2004	234	406	40.0
Neckar 1	uranium	1976	785		30.5
Neckar 2	uranium	1989	1310		33.0
Neurath A	lignite	1972	300		33.0
Neurath B	lignite	1972	300		33.0
Neurath BoA2	lignite	2010	1100		43.5
Neurath BoA3	lignite	2010	1100		43.5
Neurath C	lignite	1973	300		33.0
Neurath D	lignite	1975	600		35.0
Neurath E	lignite	1976	600		35.0
Niederaussem A	lignite	1963	132		31.0
Niederaussem B	lignite	1963	140		31.0
Niederaussem C	lignite	1965	308		31.0
Niederaussem D	lignite	1968	294		33.0
Niederaussem E	lignite	1970	290		33.0
Niederaussem F	lignite	1971	294		33.0
Niederaussem G	lignite	1974	580		33.0
Niederaussem H	lignite	1974	585		35.0
Niederaussem K	lignite	2002	931		41.0
Niederrad	gas	2006	73	90	55.0
Niehl 1	gas	2004	315	389	40.0
Niehl 2	gas	2005	382	370	55.0
Nossener Bruecke	gas	1995	258	480	50.0
Philippsburg 1	uranium	1979	890		30.5
Philippsburg 2	uranium	1984	1392		30.5
RDKarlsruhe 4	gas	1998	344		57.0
Reuter	coal	1988	244	230	36.0
Reuter West D	coal	1987	276	390	43.0
Reuter West E	coal	1988	276	390	43.0
Rheinfelden	water		25		50.0
Robert Frank 4	gas	1973	487		34.0

Roemerbruecke	gas	2005	113	230	55.0
Rostock 1	coal	1994	508	300	43.0
Rostock CHP	gas	1996	106	120	50.0
Saar	water		18.6		50.0
Sackingen	from-storage	1928	106	120	50.0
Sandreuth	gas	2006	190	320	57.0
Schkopau II A	lignite	1996	450		41.0
Schkopau II B	lignite	1996	450		41.0
Schluchsee	from-storage	2019	1000		75.0
Scholven B	coal	1968	345		33.0
Scholven C	coal	1969	345		33.0
Scholven D	coal	1970	345		35.0
Scholven E	coal	1971	345		35.0
Scholven F	coal	1979	676		37.0
Schwarze Pumpe A	lignite	1997	736		40.0
Schwarze Pumpe B	lignite	1997	736		40.0
Shamrock	coal	1957	152	300	33.0
Staudinger 1, 2	coal	1965	498	400	36.0
Staudinger 3	coal	1970	290		35.0
Staudinger 4	gas	1977	622		35.0
Staudinger 5	coal	1992	510	300	43.0
Stocken	coal	1989	230	425	43.0
Tiefstack Ersatz 1	coal	1993	180	785	43.0
Unterweser 1	uranium	1978	1345		30.5
Veltheim 3	coal	1970	320		35.0
Veltheim 4	gas	1974	300		47.0
Voerde A	coal	1970	710		43.0
Voerde B	coal	1971	710		43.0
Voelklingen-Fenne B 1	coal	1989	210	210	43.0
Voelklingen-Fenne C	coal	1982	210	185	43.0
Waldeck II 1	from-storage	1933	120		75.0
Waldeck II 2	from-storage	1974	440		75.0
Walheim 1	coal	1964	147	217	36.0
Walheim GT	fueloil	1982	97	142	36.0
Walsum	coal	2010	700		46.0
Walsum 7	coal	1959	150		36.0
Walsum 9	coal	1988	410		43.0
Wanheim	gas	2005	229.44	160	55.0
Wedel	fueloil	1971	108		34.0
Wedel	coal	1987	247	373	43.0
Wehr 1	from-storage	1968	225		75.0

Wehr 2	from-storage	1976	225		75.0
Wehr 3	from-storage	1976	225		75.0
Wehr 4	from-storage	1976	225		75.0
Weisweiler C	lignite	1955	143		31.0
Weisweiler D	lignite	1959	143		31.0
Weisweiler E	lignite	1965	300		33.0
Weisweiler F	lignite	1967	300		33.0
Weisweiler G	lignite	1974	600		35.0
Weisweiler GT 2	gas	2007	190		36.0
Weisweiler H	lignite	1975	600		35.0
Werdohl Elverlingsen 3	coal	1971	186		35.0
Werdohl Elverlingsen 4	coal	1982	301		37.0
Werdohl Elverlingsen E1/2	fueloil	1976	206		34.0
West (Voerde) 1	coal	1970	322		38.0
West (Voerde) 2	coal	1971	322		38.0
Westfalen A	coal	1962	152		33.0
Westfalen B	coal	1963	152		33.0
Westfalen C	coal	1969	284		33.0
WestGT	gas	1994	98	160	35.0
Wilhelmshaven Elec1	coal	2012	747		46.0
Wilhelmshaven A	coal	1976	744		37.0
Wolfsburg West 1	coal	1985	130	120	43.0
Wolfsburg West 2	coal	1985	130	120	43.0
Wolfsburg Nord	coal	2000	138	755	43.0
Zolling 5	coal	1985	450	150	40.0

D. Renewable energy potentials of the federal states

Table D.1.: Development potential of onshore wind energy (DEWI et al. [2005], Staiß [2007, p. 11] and own calculations

NUTS Code	Federal state	Full load hours [h/a]	Potential for expansion [MW]	Installed capacity 2007 [MW]	Remaining exp. potential 2007 [MW]	Repowering potential 2007 [MW]	Total remaining potential 2007 [MW]	Share in total remaining potential [%]
DE1	Baden-Württemberg	1150	542	404	138	95	233	1.6
DE2	Bavaria	1385	581	387	194	102	296	2.1
DE3	Berlin	1680	0	0	0	0	0	0.0
DE4	Brandenburg	1715	5,421	3,359	2,062	1,022	3,084	21.5
DE5	Bremen	1778	0	72	0	0	0	0.0
DE6	Hamburg	1752	0	34	0	0	0	0.0
DE7	Hesse	1572	860	476	384	195	579	4.0
DE8	Mecklenburg-Western-Pommerania	1830	1,724	1,327	398	459	856	6.0
DE9	Lower Saxony	1888	5,462	5,647	0	1,730	1,730	12.1
DEA	North Rhine-Westphalia	1758	5,522	2,558	2,964	974	3,938	27.4
DEB	Rhineland-Palatinate	1647	932	1,122	0	269	269	1.9
DEC	Saarland	1742	113	69	44	22	67	0.5
DED	Saxony	1738	883	808	75	287	363	2.5
DEE	Saxony-Anhalt	2002	3,920	2,786	1,134	688	1,822	12.7
DEF	Schleswig-Holstein	2065	2,327	2,522	0	913	913	6.4
DEG	Thuringia	1821	687	677	10	200	210	1.5
DE	Germany	-	28,974	22,247	7,403	6,957	14,360	100.0

The potential for expansion assumed for the base year 2007 of 7,403 MW results from subtracting the total capacity installed in 2007 from the technical potential of onshore wind energy use in the NUTS1-regions (DEWI et al. [2005, p. 11]). Furthermore, the remaining expansion potential and the repowering potential add up to a total remaining potential of 14,360 MW in 2007.

Table D.2.: Photovoltaic potential in the NUTS1-regions (cf. Staiß [2007])

NUTS codes	Federal state	Full load hours [h/a]	Roof area useable for PV [mill. m^2]	Share in total potential [%]	Open area useable for PV [km^2]	Share in total potential [%]
DE1	Baden-Württemberg	669	102	16	106	18
DE2	Bavaria	666	127	13	237	8
DE3	Berlin	550	24	3	0	0
DE4	Brandenburg	611	27	3	107	8
DE5	Bremen	412	7	1	0	0
DE6	Hamburg	442	16	2	0	0
DE7	Hesse	732	58	7	58	4
DE8	Mecklenburg-Western-Pommerania	619	18	2	109	8
DE9	Lower Saxony	513	90	11	213	16
DEA	North Rhine Westphalia	629	157	20	114	9
DEB	Rhineland-Palatinate	603	41	5	54	4
DEC	Saarland	732	12	1	6	0
DED	Saxony	566	41	5	70	5
DEE	Saxony-Anhalt	625	26	3	94	7
DEF	Schleswig-Holstein	603	29	4	83	6
DEG	Thuringia	530	28	4	61	5
DE	Germany	-	802	100	1312	100

Bibliography

AGEB. *Auswertungstabellen zur Energiebilanz für die Bundesrepublik Deutschland 1990 bis 2007*. Arbeitsgemeinschaft Energiebilanzen, 2008.

AGEB. *Stromerzeugung nach Energieträgern von 1990 bis 2008 (in TWh) Deutschland insgesamt*. Arbeitsgemeinschaft Energiebilanzen e. V., http://www.ag-energiebilanzen.de/, 2009.

AGEB. *Bruttostromerzeugung von 1990 bis 2010 nach Energieträgern*. http://www.ag-energiebilanzen.de/viewpage.php?idpage=65, Arbeitsgemeinschaft Energiebilanzen, 2011a.

AGEB. *Auswertungstabellen zur Energiebilanz für die Bundesrepublik Deutschland 1990 bis 2009*. Arbeitsgemeinschaft Energiebilanzen, 2011b.

M. Agnew, L. Schrattenholzer, and A. Voß. *A model for Energy Supply System Alternatives and their General Environmental Impact*. IIASA, Laxenburg, 1979.

J. Aguada, V. Quintana, and M. Madrigal. Optimization-Based Auction Mechanism for Inter-ISO Congestion Mangement. *Power Engineering Society Summer Meeting, 2001. IEEE*, 3:1647–1648, 2001.

Z. Alaywan and T. Wu. *Transitioning the California Markt from a Zonal to a Nodal Framework: An Operational Perspective*. 2004.

Amprion. *Netzausbau*. Amprion, http://www.amprion.net/netzausbau (retrieved: 2010-11-11), 2010.

G. Andersson. *Elektrische Energiesysteme - Vorlesungsteil Energieübertragung*. ETH Zürich, Power Systems laboratory, Zürich, 2009.

J. Apfelbeck. Simultane Optimierung des Kraftwerks- und Netzausbaus am Beispiel von Deutschland. *VDI-Berichte*, 2080:29–44, 2009.

A. Ardone. *Entwicklung einzelstaatlicher und multinationaler Treibhausgasminderungsstrategien für die Bundesrepublik Deutschland mit Hilfe von optimierenden Energie- und Stoffflussmodellen*. Peter Lang, Frankfurt a.M., 1999.

AregV. Verordnung über die Anreizregulierung der Energieversorgungsnetze. *BGBl*, (I), 2007.

AtG. Gesetz über die friedliche Verwendung der Kernenergie und den Schutz gegen ihre Gefahren (Atomgesetz). *BGBl*, I:1565, 1959.

AtG. Gesetz zur geordneten Beendigung der Kernenergienutzung zur gewerblichen Erzeugung von Elektrizität. *BGBl*, I:1351–1359, 2002.

AtG. Gesetz zur geordneten Beendigung der Kernenergienutzung zur gewerblichen Erzeugung von Elektrizität. *BGBl*, I:1817, 2010.

AtGÄndG. Dreizehntes Gesetz zur Änderung des Atomgesetzes (13. AtGÄndG). *BGBl*, (I):1704, 2011.

M. Ball. *Integration einer Wasserstoffwirtschaft in ein nationales Energiesystem am Beispiel Deutschlands: Optionen der Bereitstellung von Wasserstoff als Kraftstoff im Straßenverkehr bis zum Jahr 2030.* VDI-Verlag, Düsseldorf, 2006.

R. Barth, K. Rudion, C. Heyde, D. Swider, and Z. Styczynski. Improved consideration of the power grid in stochastic electricity market models dealing with distributed generation. In CIRED, editor, *19th International Conference on Electricity Distribution*, chapter 0636. 2007.

R. Barth, J. Apfelbeck, P. Vogel, P. Meiborn, and C. Weber. Load-flow based market coupling with large-scale wind power in Europe. *8th Workshop on Large-Scale Integration of Wind Power into Power Systems as well as on Transmission Networks for Offshore Wind Farms*, 2009.

BBR. *Raumordnungsprognose 2025.* Bundesamt für Bauwesen und Raumordnung, Berlin, 2008.

Bd.-Reg. *Eckpunkte für ein integriertes Energie- und Klimaprogramm.* Die Bundesregierung der Bundesrepublik Deutschland, 2009a.

Bd.-Reg. *Nationaler Entwicklungsplan Elektromobilität der Bundesregierung.* Die Bundesregierung der Bundesrepublik Deutschland, Berlin, 2009b.

Bd.-Reg. *Ausstieg aus der Kernkraft in einem Jahrzehnt.* Die Bundesregierung der Bundesrepublik Deutschland, http://www.bundesregierung.de/n_1264/Content/DE/Artikel/2011/06/2011-06-06-Schrittweiser_20-Atomausstieg.html (retrieved 06.06.2011), 2011.

BDEW. *Gutachten Flexibilisierung: Zentrale Ergebnisse und Bewertung.* Bundesverband der Energie- und Wasserwirtschaft e.V., Berlin, 2011.

P. Bellucci, D. Fernandez, S. La Monica, and L. Schirone. Assessment of the Photovoltaic Potential on Noise Barriers Along National Roads in Italy. In *Proceedings of the 3rd World Conference on Photovoltaic Energy Conversion*, pages 2474–2477. 2003.

BFS. *Erzeugte Elektrizitätsmengen (netto) der deutschen Kernkraftwerke, Übertragung von Produktionsrechten und Erfassung der Reststrommengen.* Bundesamt für Strahlenschutz, http://www.bfs.de/de/kerntechnik/strommengen.html, 2011.

BGR. *Reserven, Ressourcen und Verfügbarkeit von Energierohstoffen 2007 (Kurzstudie).* Bundesanstalt für Geowissenschaften und Rohstoffe, Hannover, 2007.

C. Böhringer and T. Rutherford. Combining bottom-up and top-down. *Energy Economics*, 30:574–596, 2008.

M. Biberacher. GIS-based modeling approach for energy systems. *International Journal of Energy Sector Management*, 2(3):368–384, 2008.

BioKraftQuG. Gesetz zur Einführung einer Biokraftstoffquote durch Änderung des Bundes-Immissionsschutzgesetzes und zur Änderung energie- und stromsteuerrechtlicher Vorschriften. *BGBl.*

M. Björndal and K. Jörnsten. Benefits from coordinating congestion management - The Nordic power market. *Energy Policy*, 35:1978–1991, 2007.

BMU. *Vereinbarung zwischen der Bundesregierung und den Energieversorgungsunternehmen vom 14. Juni 2000.* Bundesministerium für Umwelt, Naturschutz und Reaktorsicherheit, Berlin, 2000.

BMU. *Nationaler Allokationsplan für die Bundesrepublik Deutschland 2005-2007 (NAP I).* Bundesministerium für Umwelt, Naturschutz und Reaktorsicherheit, Berlin, 2004.

BMU. Nationaler Allokationsplan II- Eckpunkt und Vergleich mit NAP I. 2006a.

BMU. *Nationaler Allokationsplan für die Bundesrepublik Deutschland 2008-2012 (NAP II).* Bundesministerium für Umwelt, Naturschutz und Reaktorsicherheit, Berlin, 2006b.

BMU. *Weiterentwicklung der Ausbaustrategie Erneuerbare Energien - Leitstudie 2008.* Bundesministerium für Umwelt, Naturschutz und Reaktorsicherheit, Berlin, 2008.

BMU. *Kernkraftwerke in Deutschland.* Bundesministerium für Umwelt, Naturschutz und Reaktorsicherheit, http://www.bmu.de/atomenergie_sicherheit/kurzinfo/doc/42300.php, 2009.

BMU. *Erneuerbare Energien in Zahlen*, volume Dec. 2010. Bundesministerium für Umwelt, Naturschutz und Reaktorsicherheit, http://www.erneuerbare-energien.de/inhalt/2720/4590/, 2010.

BMU. *Restlaufzeiten der Atomkraftwerke in Deutschland.* Bundesministerium für Umwelt, Naturschutz und Reaktorsicherheit, http://www.bmu.de/atomenergie/doc/43032.php, 2011.

BMVBS. *Verkehr in Zahlen.* DVV Media Group, Hamburg, 37 edition, 2009.

BMWi. *Leuchtturm COORETEC der Weg zum zukunftsfähigen Kraftwerk mit fossilen Brennstoffen (Forschungsbericht Nr. 566).* Bundesministerium für Wirtschaft und Technologie, Berlin, 2007.

BMWi. *Zusammensetzung der Strompreise für Privathaushalte in Deutschland 2007.* Bundeministerium für Wirtschaft und Technologie, www.energie-verstehen.de, 2008.

BMWi. *Energiedaten - Zahlen und Fakten - Nationale und Internationale Entwicklung.* Bundesministerium für Wirtschaft und Technologie, www.bmwi.de, 2010.

BNetzA. *Begründung der Verfahrenseinstellung des Festlegungsverfahren zu Grundsatzfragen bei der Bewirtschaftung von Engpässen im Übertragungsnetz.* Bundesnetzagentur, http://www.bundesnetzagentur.de/enid/625f054b3f37dab1efcb36971ebba2fa,0/BK6-6-74/BK6-6-74Einstellung4s8.html (2010-03-25), 2008.

M. Boiteux. Peak-Load Pricing. *The Journal of Business*, 33(2):157–179, 1960.

R. Brökeland. *Planungsprogramm zur Nutzung von Biomasse für die Heizenergieversorgung von Gewächshäusern HORTEB*, volume 44. Institut für Technik in Gartenbau und Landwirtschaft - Universität Hannover, Hannover, 1998.

G. Brunekreeft, K. Neuhoff, and D. Newbery. Electricity transmission: An overview of the current debate. *Utilities Policy*, (13):73–93, 2005.

G. Brunekreeft, W. Pfaffenberger, J. Gabriel, and D. Balmert. *Optimal transmission networks - a discussion paper*. Bremer Energie Institut, Bremen, 2007.

BSH. *Nordsee: Offshore Windparks*. Bundesamt für Seeschifffahrt und Hydrographie, http://www.bsh.de/de/Meeresnutzung/Wirtschaft/CONTIS-Informationssystem/ContisKarten/NordseeOffshoreWindparksPilotgebiete.pdf (retrieved 01.06.2011), 2011a.

BSH. *Ostsee: Offshore Windparks*. Bundesamt für Seeschifffahrt und Hydrographie, http://www.bsh.de/de/Meeresnutzung/Wirtschaft/CONTIS-Informationssystem/ContisKarten/OstseeOffshoreWindparksPilotgebiete.pdf (retrieved 01.06.2011), 2011b.

Bundesnetzagentur. *Monitoringbericht 2009 - Monitoringbericht gemäß § 63 Abs. 4 EnWG i.V.m. § 35 EnWG*. Bundesnetzagentur für Elektrizität, Gas, Telekommunikation, Post und Eisenbahnen, Bonn, 2009.

Bundesnetzagentur. *Monitoringbericht 2009*. Bundesnetzagentur für Elektrizität, Gas, Telekommunikation, Post und Eisenbahnen - Monitoring, Marktbeobachtung, Bonn, 2010.

Bundesnetzagentur. *Monitoringbericht 2010*. Bundesnetzagentur für Elektrizität, Gas, Telekommunikation, Post und Eisenbahnen - Monitoring, Marktbeobachtung, Bonn, 2011a.

Bundesnetzagentur. *Auswirkungen des Kraftwerk-Moratoriums auf die Übertragungsnetze und die Versorgungssicherheit - Bericht der Bundesnetzagentur an das Bundesministerium für Wirtschaft und Technologie*. Bonn, 2011b.

Bundesnetzagentur. *Fortschreibung des Berichts der Bundesnetzagentur zu den Auswirkungen des Kernkraftwerksmoratoriums auf die Übertragungsnetze und die Versorgungssicherheit*. Bonn, 2011c.

J. Bushnell and S. Stoft. Electric grid investment under a contract network regime. *Journal of Regulatory Economics*, 10(1):61–79, July 1996.

CAISO. *Transmission Economic Assessment Methodology (TEAM)*. California Indepedent System Operator, http://www.caiso.com/docs/2004/06/03/2004060313241622985.pdf (2010-03-18), 2008.

CAISO. *Technical Bulletin - Market Optimization Details*. Califonia Independent System Operator, http://www.caiso.com/23cf/23cfe2c91d880.pdf (2010-03-16), 2009.

P. Capros. *Energy Systems Analysis of CCS technology*. Institute of Communication and Computer Systems, Energy-Economy-Environment Modelling Laboratory, National Technical University of Athens, Athens, 2007.

H. Chao and S. Peck. A Market Mechanism for Electric Power Transmission. *Journal of Regulatory Economics*, 10:25–59, 1996.

COM. *European Climate Change Programme - Long Report*. Commission of the European Communities, Brussels, 2001.

COM(1997)599. *Communication from the Commission - Energy for the future: renewable sources of energy - White Paper for a Community strategy and action plan*. European Commission, Brussels, 1997.

COM(1998)246. *Communication from the European Commission: Energy Efficiency in the European Communitiy - Towards a Strategy for the Rational Use of Energy*. Commission of the European Communities, Brussels, 1998.

COM(2000)247. *Communication from the Commission to the Council, the European Parliament, the Economic and Social Committee and the Committee of the Regions: Action Plan to Improve Energy Efficiency in the European Community*. Commission of the European Communities, Brussels, 2000.

COM(2000)769. *Green Paper: Towards a European strategie for the security of energy supply*. Commission of the European Communities, Brussels.

COM(2000)88. *Communication from the Commission to the Council and the European Parliament on EU policies and measures to reduce greenhouse gas emissions: Towards a European Climate Change Programme (ECCP)*. Commission of the European Communities, Brussels, 2000.

COM(2001)580. *Communication from the European Commission on the implementation of the first phase of the European Climate Change Programme* . Commission of the European Communities, Brussels, 2001.

COM(2005)265. *Green Paper on Energy Efficiency "Doing more with less"*. European Community, Brussels, 2005.

COM(2005)627. *The support of electricity from renewable energy sources*. Commission of the European Communities, Brussels, 2005.

COM(2006)105. *Green Paper: A European Strategy for Sustainable, Competitive and Secure Energy*. Commission of the European Communities, Brussels.

COM(2006)545. *Communication from the Commission: Action Plan for Energy Efficiency: Realising the Potential*. Brussels, 2006.

COM(2006)844. *Communication from the Commission to the Council of the European Parliament: Nuclear Illustrative Programme - Presented under Article 40 of the Euratom Treaty for the opinion of the European Economic and Social Committee*. Commission of the European Communities, Brussels, 2006.

COM(2007)1. *Communication from the European Commission to the European Council: An energy policy for Europe*. Commission of the European Communities, Brussels.

COM(2007)2. *Communication from the Commission to the Council, the European Parliament, the European Economic and Social Committee and the Committee of the Regions 'Limiting Global Climate Change to 2 degrees Celsius - The Way Ahead for 2020 and Beyond'*. Commission of the European communities, Brussels.

COM(2008)30. *Communication from the Commission to the European Parliament, the Council, the European Economic and Social Committee and the Committee of the Regions: '2020 by 2020 Europe's climate change opportunity'.* Commission of the European Communities, Brussels.

D. Conolly, H. Lund, B. V. Mathiesen, and M. Leahy. A review of computer tooks for analyzing the integration of renewable energy into various energy systems. *Applied Energy*, 87(4):1059–1082, 2009.

CONSENTEC, EWI, and IAEW. *Analyse und Bewertung der Versorgungssicherheit in der Elektrizitätsversorgung (Monitoringbericht nach §51 EnWG).* Bundesministerium für Wirtschaft und Technologie (BMWi), Berlin, 2008.

C. Cremer. *Integration regional aspects in modelling of electricity generation - the example of CO2 capture and storage*, volume 16119. Eidgenössische Technische Hochschule ETH Zürich, Zürich, diss., technische wissenschaften edition, 2005.

C. Cremer, A. Eskens, M. Fischedick, E. Gruber, F. Idrissova, W. Kuckshinrichs, J. Linßen, K. Pietzner, P. Radgen, A. Roser, N. Schnepf, D. Schumann, N. Supersberger, and P. Zapp. *Sozioökonomische Begleitforschung zur gesellschaftlichen Akzeptanz von Carbon Capture and Storage (CCS) auf nationaler und internationaler Ebene.* Gemeinschaftsprojekt des Wuppertal Instituts, des Forschungzentrum Jülich (STE), dem Fraunhofer Institut (ISI) und der BSR Sustainability GmbH, 2008.

CWE MC Project. *A report for the regulators of the Central West European (CWE) region on the final design of the market coupling solution in the region, by the CWE MC Project.* Resaux de transport d'electricite, 2010.

J. C. Das. *Power System Analysis - Short-Circuit Load Flow and Harmonics.* Marcel Dekker, Inc., New York, 2002.

DENA. *Kurzanalyse der Kraftwerks- und Netzplanung in Deutschland bis 2020 (mit Ausblick auf 2030).* Deutsche Energieagentur GmbH, Berlin, 2008.

DENA. *Initiative Energieeffizienz.* Deutsche Energieagentur, http://www.initiative-energieeffizienz.de/, 2009.

DENA. *DENA-Netzstudie II: Integration erneuerbarer Energien in die deutsche Stromversorgung im Zeitraum 2015 - 2020 mit Ausblick 2025.* DENA, Berlin, 2010a.

DENA. *Übersichtstabelle Windparks.* Deutsche Energie-Agentur, http://www.offshore-wind.de/page/index.php?id=4761, 2010b.

DESTATIS. *Statistik regional: Daten für die Kreise und kreisfreien Städte Deutschlands.* Statistische Ämter des Bundes und der Länder, 2006.

DESTATIS. *Bruttoinlandsprodukt - in jeweiligen Preisen - in Deutschland 1991 bis 2008 nach Bundesländern, in Mill.EUR.* Statistisches Bundesamt Deutschland, Berlin, 2009.

DESTATIS and BBR. *INKAR - Indikatoren und Karten zur Raumentwicklung.* Statistischen Ämter des Bundes und der Länder & Bundesamt für Raumwesen und Raumordnung, Bonn, 2005.

DEWI, E.On Netz, EWI, RWE Transportnetz Strom, and VE Transmission. *Energiewirtschaftliche Planung für die Netzintegration von Windenergie in Deutschland an Land und Offshore bis zum Jahr 2020.* Studie im Auftrag der Deutschen Energie Agentur GmbH, Köln, 2005.

DG for Energy and Transport. *Trends for 2030.* European Commission - Directorate General for Energy and Transport, Brussels, 2003.

K. Dietrich, F. Leuthold, and H. Weigt. Will the Market Get it Right? The Placing of New Power Plants in Germany. *Zeitschrift für Energiewirtschaft*, (34):255–265, 2010.

E. Dimson. The discount rate for a power station. *Energy Economics*, 1989(July): 175–180, 1989.

F. Ding and D. Fuller. Nodal, Uniform, or Zonal Pricing: Distribution of Economic Surplus. *IEEE Transactions On Power Systems*, 20(2):875–882, 2005.

DLR, IWES, and IFNE. *Leitstudie 2010 - Langfristszenarien und Strategien für den Ausbau der erneuerbaren Energien in Deutschland bei Berücksichtigung der Entwicklung in Europa und global.* BMU, Berlin, 2010.

D. Dolezilek and L. M. Ayers. Using Dynamic Real-Time Substation Information to Reinvest Asset Management. In *Proceedings of the 18th International Conference on Electricity Distribution*, pages 901–906. CIRED, 2005.

M. Dreher. *Analyse umweltpolitischer Instrumente zur Förderung der Stromerzeugung aus regenerativen Energieträgern im liberalisierten Energiemarkt.* Universität Karlsruhe, Dissertation, 2001.

C. Duthaler. Europe Nodal: A Simulation of the European Electricity Market based on the Full Network Model. In *Second Annual Conference on Competition and Regulation in Network Industries.* Center for European Studies, 2009.

E. Van der Voort. *Energy Supply Modelling Package, EFOM-12C Mark I, Mathematical Description.* Louvain-La-Neuve, 1984.

EC. Directive 96/92/EC of the European Parliament and of the Council of 19 December 1996 concerning common rules for the internal market in electricity. *Official Journal of the European Communities*, L. 27:20–29, 1996.

EC. *Combined heat and power production (CHP) in the EU - Summary of statistics.* Office for Official Publications of the European Communities, Luxembourg, 2001a.

EC. Directive 2001/77/EC of the European Parliament and of the Council of 27 September 2001 on the promotion of the electricity produced from renewable energy source in the internal electricity market. *Official Journal of the European Communities*, L. 283:33–40, 2001b.

EC. *Council Decision of 25 April 2002 concerning the approval, on behalf of the European Community, of the Kyoto Protocol to the United Nations Framework Convention on Climate Change and the joint fulfilment of commitments thereunder.* European Commission, Brussels, 2002a.

EC. Council Decision of 25 April 2002 concerning the approval, on behalf of the European Community, of the Kyoto Protocol to the United Nations Framework Convention on Climate Change and the joint fulfilment of commitments thereunder . *Official Journal of the European Communities*, (L 130):1–20, 2002b.

EC. Directive 2003/87/EC of the European Parliament and of the Council of 13 October 2003 establishing a scheme for greenhouse gas emission allowances trading within the Community and amending Council Directive 96/61/EC. *Official Journal of the European Union*, 275:32–46, 2003.

EC. Directive 2003/54/EC of the European Parliament and of the Council of 26 June 2003 concerning common rules for the internal market in electricity and repealing Directive 96/92/EC - Statements made with regard to decommissioning and waste management activities. *Official Journal of the European Communities*, L. 176:37–56, 2003a.

EC. Regulation (EC) No 1128/2003 of the European Parliament and of the Council of 26 June 2003 on 'Conditions for Access to the Network for Cross-border Exchanges in Electricity'. *Official Journal of the European Communities*, (L 176):1–10, 2003b.

EC. Directive 2004/8/EC of the European Parliament and of the Council of 11 February 2004 on the promotion of cogeneration based on a useful heat demand in the internal energy market. *Official Journal of the European Communities*, L. 52:50–51, 2004.

EC. Directive 2006/32/EC of the European Parliament and of the Council of 5 April 2006 on energy end-use efficiency and energy services and repealing Council Directive 93/76/EEC. *Official Journal of the European Communities*, L. 114:64–85, 2006a.

EC. Decision No 1982/2006/EC of the European Parliament and the Council of 18 December 2006 concerning the Seventh Framework Programme of the European Community for research, technological development and demonstration activities (2007-2013). *Official Journal of the European Union*, (L 412):1–41, 2006b.

EC. Directive 2006/32/EC of the European Parliament and the Council of 5 April 2006 on energy end-use efficiency and energy services and repealing Council Directive 93/76/EEC. *Official Journal of the European Union*, 114:64–85, 2006c.

EC. *Energy Star: Labelling Energy Efficient Office Equipment*. European Commission, http://www.eu-energystar.org/index.html, 2009a.

EC. *Intelligent Energy Europe*. European Commission, http://ec.europa.eu/energy/intelligent/, 2009b.

EC. Council resolution concerning new Community energy policy objectives for 1995 and convergence of the policies of the Member States. *Official Journal of the European Union*, (C 241):1–3, 2009.

EC. Directive 2009/31/EC of the European Parliament and the Council of 23 April 2009 on the geological storage of carbon dioxide and amending Council Directive 85/337/EEC, European Parliament and Council Directives 2000/60/EC, 2001/80/EC, 2004/35/EC, 2006/12/EC, 2008/1/EC and Regulation (EC) No 1013/2006. *Official Journal of the European Union*, (L 140):114–135, 2009a.

EC. Directive 2009/28/EC of the European Parliament and the Council of 23 April 2009 on the promotion of the use of energy from renewable sources and amending and subsequently repealing Directives 2001/77/EC and 2003/30/EC. *Official Journal of the European Communities*, (L 140):16–62, 2009b.

EC. Directive 2009/29/EC of the European Parliament and the Council of 23 April 2009 amending Directive 2003/87/EC so as to improve and extend the greenhouse gas emission allowance trading scheme of the Community. *Official Journal of the European Communities*, L 140:63–87, 2009c.

EC. Directive 2009/72/EC of the European Parliament and the Council of 13 July 2009 concerning common rules for the internal market in electricity and repealing Directive 2003/54/EC. *Official Journal of the European Communities*, L 211:55–93, 2009d.

EC. Regulation (EC) no 714/2009 of the European Parliament and the Council of 13 July 2009 on conditions for access to the network for cross-border exchanges in electricity and repealing Regulation (EC) No 1228/2003. *Official Journal of the European Communities*, L211:15–35, 2009e.

EC. *World Energy Technology Outlook - 2050*. European Commission, http://ftp.cordis.europa.eu/pub/fp7/energy/docs/weto-h2_en.pdf (retrieved: 2010-11-03), 2010.

EEA. *CORINE Land Cover Data 2000*. European Environmental Agency, Kopenhagen, (100 m x 100 m raster) edition, 2007.

EEA. *Emissions by Geographic entity by Year by Emission unit by EEA sector by Air pollutant*. European Environment Agency (12.5.2009), http://unfccc.int/resource/docs/convkp/kpeng.pdf (12.5.2009), 2009.

EEC. Council Directive 92/75/EEC of 22 September 1992 on the indication by labelling and standard product information of the consumption of energy and other resources by household appliances. *Official Journal of the European Communities*, L. 297:16–19, 1992.

EEG. Gesetz zur Neuregelung des Rechts der Erneuerbaren Energien im Strombereich. *BGBl*, (I):1918–1930, 2004.

EEG. Gesetz zur Neuregelung des Rechts der Erneuerbaren Energien im Strombereich und zur Änderung damit zusammenhängender Vorschriften. *BGBl*, (I):643, 2008.

EEG. Gesetz zur Neuregelung des Rechtsrahmens für die Förderung der Stromerzeugung aus erneuerbaren Energien (EEG) vom 28. Juli 2011. *BGBl*, (I):1634–1678, 2011.

A. Eßer, M. Franke, and A. Kamper. *SESAM Arbeitspaket 3.4: Modelle zur Steuerung, Planung und Optimierung in virtuellen Kraftwerken*. Universität Karlsruhe (TH), forschungsbericht edition, 2006a.

A. Eßer, A. Kamper, M. Franke, D. Möst, and O. Rentz. Scheduling of electrical household appliances with price signals. In K.-H. Waldmann and U. M. Stocker, editors, *Operations Research Proceedings 2006*. Springer, 2006b.

A. Eßer, M. Franke, A. Kamper, and D. Möst. Future electricity markets - impacts of consumer response and dynamic retail prices on electrictiy markets. *Wirtschaftsinformatik - Schwerpunktthema "IT in der Energiewirtschaft"*, 2007(5), 2008.

EEX. *Emission Spot History.* European Energy Exchange, http://www.eex.com/de/Downloads (19.04.2009), 2009.

EIA. *International Energy Outlook 2010.* Energy Information Administration, http://www.eia.doe.gov/oiaf/ieo/ (retrieved: 2010-11-03), 2010.

EMCC. *EMCC optimizer.* European Market Coupling Company GmbH, http://www.marketcoupling.com/document/1137/EMCC2010), 2009.

EnBW. *Grenzüberschreitende Lastflüsse und kommerzielle Fahrpläne der EnBW.* Energie Baden-Württemberg AG, http://www.enbw.com/content/de/netznutzer/strom/grenzlastfluesse/index.jsp (retrieved: 01/04/2008), 2008.

EnBW. *EEG Anlagenstammdatenmeldung an den Übertragungsnetzbetreiber.* Energie Baden Württemberg AG (retrieved July 27, 2009), http://www.enbw.com/content/de/netznutzer/stromverteilnetz/erneuerbare_energien/anlagenstammdatenmeldung/, 2009.

EnLAG. Gesetz zur Beschleunigung des Ausbaus der Höchstspannungsnetze vom 21. August 2009. *BGBl*, I(55):2870–2876, 2009.

Enquete-Kommission. *Nachhaltige Energieversorgung unter den Bedingungen der Globalisierung und der Liberalisierung (Endbericht)*, volume Drucksache 14/9400. 14. Deutscher Bundestag, Berlin, 2002.

ENTSO-E. *Statistical Yearbook 2008.* Regional group Continental Europe (former UCTE) produced under the responsibility of ENTSO-E, https://www.entsoe.eu/fileadmin/userupload/library/publications/ce/StatisticalYearbook2008.pdf (retrieved: 13/10/2010), 2008.

ENTSO-E. *Operation Handbook P1 - Policy 1: Load-Frequency Control and Performance.* European Network of Transmission System Operators for Electricity, http://www.entsoe.eu/fileadmin/user_upload/_library/publications/ce/oh/Policy1_final.pdf (Retrieved June 15, 2010), 2009.

EnVKW. Verordnung über die Kennzeichnung von Haushaltsgeräten mit Angaben über den Verbrauch an Energie und anderen wichtigen Ressourcen (Energieverbrauchskennzeichnungsverordnung - EnVKV). *BGBl*, I(Zuletzt geändert durch Art. 1 V v. 19. 2.2004 I 311):1632, 1997.

EnWG. Gesetz über die Elektrizitäts- und Gasversorgung (Energiewirtschaftsgesetz - EnWG). *BGBl*, I:730, 1998.

EnWG. Zweites Gesetz zur Neuregelung des Energiewirtschaftsrechts vom 7. Juli 2005. *BGBl*, I(Zuletzt geändert am 25.10.2008, BGBl I S. 2101):1970, 2005.

N. Enzensberger. *Entwicklung und Anwendung eines Strom- und Zertifikatmarktmodells für den europäischen Energiesektor.* VDI Verlag, Düsseldorf, 2003.

E.ON. *Grenzüberschreitende Lastflüsse und aggregierte abgestimmte kommerzielle Fahrpläne.* E.ON Netz GmbH, http://www.eon-netz.com/pages/ehnde/index.htm (retrieved: 01/08/2008), 2008.

E.ON. *Anlagen Stammdaten gem. art. 52.1 EEG.* E.ON Netz AG (retrieved July 27, 2009), http://www.eon-netz.com/pages/ehn_de/EEG__KWK-G/Erneuerbare-_Energien-Gesetz/Mitteilungs-_und_Veroeffentlichungspflichten/Leistungszeitraum_2009/index.htm, 2009.

ETSO. *Co-ordinated use of Power Exchanges for Congestion Management.* European Transmission System Operators, 2001.

ETSO. *Current state of balancing management in Europe.* European Transmission System Operators, http://www.etso-net.org/activities/BalanceManagement/e_default.asp (available on 10 February 2006), 2003.

ETSO. *Regional Flow-based allocations - State-of-play.* European Transmission System Operators, 2007.

EURATOM. *Annual Report 2007.* Office for Official Publications of the European Communities, Luxembourg, 2007.

EuroPEX and ETSO. *Development and Implementation of a Coordinated Model for Regional and Inter-Regional Congestion Management (Final Report).* http://www.europex.org/default.asp?kaj=news&id=277 (2010-03-22), 2009.

EUROSTAT. *Elektrizitätspreise - Preissysteme 2006.* EUROSTAT - EC, 2007a.

EUROSTAT. *Energy, transport and environment indicators.* Office for Official Publications of the European Communities, Luxembourg, 2007b.

EUROSTAT. Combined Heat and Power (CHP) in the EU, Turkey, and Norway - 2007 data. *Data in Focus*, 2009(28), 2009.

EUROSTAT. *Energieendverbrauch von Elektrizität (1 000 tRÖE).* http://epp.eurostat.ec.europa.eu/tgm/table.do?tab=table&init=1&language=de&pcode=ten00097&plugin=1 (retrieved: 31.05.2011), 2011.

EWI. *Bewertung energiepolitischer Optionen für eine sichere, wirtschaftliche und umweltgerechte Energieentwicklung in Deutschland - Analyse der Ursachen für negative Strompreise am 3./4. Oktober 2009 und mögliche Abhilfemaßnahmen.* Studie im Auftrag des Bundesministeriums für Wirtschaft und Technologie, Köln, 2010.

EWI and EEFA. *Energiewirtschaftliches Gesamtkonzept 2030.* Energiewirtschaftliches Institut an der Universität zu Köln & Energy Environment Forecast Analysis GmbH on behalf of the Verband der Elektrizitätswirtschaft (VDEW), Köln, 2007.

EWI and EEFA. *Energiewirtschaftliches Gesamtkonzept 2030.* Initiiert durch BDEW, BDI, DEBRIV, GVSt und VGB PowerTech, Köln, Berlin, 2008.

EWI and Prognos. *Die Entwicklung der Energiemärkte bis zum Jahr 2030 - Energiereport IVB.* Oldenbourg, München, 2005.

EWI and Prognos. *Auswirkungen höherer Ölpreise auf Energieangebot und -nachfrage: Ölpreisvariante der Energiewirtschaftlichen Referenzprognose 2030.* Untersuchung im Auftrag des Bundesministeriums für Wirtschaft und Technologie, Köln, Basel, 2006.

U. Fahl and M. Blesl. E^3Net-D2. In F. für Energiemodelle und Energiewirtschaftliche Systemanalysen in Deutschland, editor, *Energiemodelle zum Kernenergieausstieg in Deutschland: Effekte und Wirkungen eines Verzichts auf Strom aus Kernkraftwerken*, pages 265–315. Physika-Verlag, 2002.

FERC. *Remedying Undue Discrimination Through Open Access Transmission Service And Standard Market Design (Docket No. RM01-12-000).* United States of America Before the Ferderal Energy Regulatory Commission, 2002.

L. Ferreira, P. Carvalho, and L. Barruncho. An Evolutionary Approach to Decision-Making in Distribution Planning. In *CIRED Conference Publication No. 438*, pages 6.6.1–6.6.5. 1997.

W. Fichtner. *Strategische Optionen der Energieversorger zur CO2-Minderung - ein Energie- und Stoffflussmodell zur Entscheidungsunterstützung.* Erich Schmidt, Berlin, 1999a.

W. Fichtner. *Strategische Optionen der Energieversorger zur CO2 Minderung.* Oslo, 1999b.

Finanzagentur. *Bundeswertpapiere: Auszug - aktuelle Benchmarkanleihen des Bundes.* Finanzagentur GmbH der Bundesrepublik Deutschland, www.deutsche-finanzagentur.de (retrieval: 11/10/2010), 2010.

D. Finon. Optimization Model for the Energy Sector. *Energy Policy*, 1974(6):136–151, 1974.

G. Fiorese, G. Guariso, A. Lazzarin, and R. Razzano. Energy crops potential at regional scale: biomass yield and GHG flow. In *Proceedings of the International Conference on Clean Electrical Power*, pages 401–405. 2007.

L. G. Fishbone and H. Abilock. MARKAL: A linear programming model for energy systems analysis: Technical Description of the BNL version. *International Journal of Energy Research*, 4(5):353–375, 1981.

B. Flechner. *Die notwendige Modellierungsgenauigkeit bei der Energieeinsatzplanung in hydrothermischen Kraftwerkssystemen.* Fakultät für Elektrotechnik - Rheinisch-Westfälische Technische Hochschule, Aachen, 1996.

P. Fleeman. Gis based modeling of electricity networks. In *CIRED Conference Publications 438*. IEEE, 1997.

A. Fleury. *Eine Nachhaltigkeitsstrategie für den Energieversorgungssektor - dargestellt am Beispiel der Stromversorgung in Frankreich.* Universität Karlsruhe, Dissertation, 2005.

M. Frank. *Entwicklung und Anwendung einer integrierten Methode zur Analyse von betriebsübergreifenden Energieversorgunskonzepten.* Dissertation, Karlsruhe, 2003.

H. Fraser. Can FERC's Standard Market Design Work in Large RTOs? *Electricity Journal*, 15(6):19–30, 2010.

C. Frei, P.-A. Haldi, and G. Sarlos. Dynamic formulation of a top-down and bottom-up merging energy policy model. *Energy Policy*, 31:1017–1031, 2003.

R. Fronius and M. Gratton. Rural Electrification Planning Software. In *CIRED Conference Publications 482*. IEEE, 2001.

Frontier Economics. *International transmission pricing review*. Frontier Economics, Melbourne, 2009.

Frontier Economics and CONSENTEC. *Bedeutung von etablierten nationalen Gebotszonen für die Integration des europäischen Strommarkts - ein Ansatz zur wohlfahrtsorientierten Beurteilung*. Bundesnetzagentur, Bonn, 2011.

M. Förster, Y. Helms, A. Herberg, A. Köppgen, K. Kunzmann, D. Radtke, L. Ross, and S. Itzerott. A Site-Related Suitability Analysis for the Production of Biomass as a Contribution to Sustainble Regional Land-Use. *Environmental Management*, 41 (4):584–598, 2008.

FÖS. Gesetz zur Fortentwicklung der ökologischen Steuerreform. *BGBl*, I:4602, 2002.

S. Galati. *Geographic Information Systems Demystified*. Artech House Publishers, Norwood, 2006.

M. Göbelt. *Entwicklung eines Modells für die Investitions- und Produktionsprogrammplanung von Energieversorgungsunternehmen im liberalisierten Markt*. Universität Karlsruhe, Dissertation, 2001.

M. Göbelt, W. Fichtner, M. Dreher, M. Wietschel, and O. Rentz. A decision support tool for electric utility planning in liberalised energy markets under environmental constraints. In M. Khosrowpour, editor, *Challenges of Information Technology Management in the 21st Century - Proceedings of the IRMA 2000 Conference*, pages 674–675. Idea Group Publishing, 2000a.

M. Göbelt, W. Fichtner, M. Wietschel, and O. Rentz. Development and application of an optimizing energy and material flow model for strategic planning of energy utilities. In APORS, editor, *Conference Proceedings of the 5th Conference of Asian-Pacific Operational Research Societies within IFORS*. 2000b.

F. Genoese, M. Genoese, and M. Wietschel. Occurence of negative prices on the German spot market for electricity and their influence on balancing power markets. *Proceedings of the 7th Conference on the European Energy Market (EEM)*, 2010.

M. Genoese, D. Möst, and O. Rentz. Impact of emission allocation schemes on power market investments. In D. Möst, W. Fichtner, M. Ragwitz, and D. Veit, editors, *New methods for energy market modelling - Proceedings of the first European workshop on energy market modelling using agent-based computational economics*. Universitätsverlag, 2008.

H. J. Gerdey and W. Pfaffenberger. EMS (Modellbeschreibung). In Forum für Energiemodelle und Energiewirtschaftliche Systemanalysen in Deutschland, editor, *En-*

ergiemodelle zum Kernenergieausstieg in Deutschland: Effekte und Wirkungen eines Verzichts auf Strom aus Kernkraftwerken, pages 153–179. Physica-Verlag, 2002.

J. Goerten and E. Clement. *Electricity prices for second semester 2007*. EUROSTAT - EC, 2008.

K. Govender, A. Meyer, and B. Dwolatzky. The Automatic Clustering of Uniformly Distributed Loads for the use in Rural Electrification Planning. In *Proceedings of the Transmission and Distribution Conference*, pages 450–455. IEEE, 2001.

R. Green. *Electricity Transmission Pricing: How much does it cost to get it wrong?* CMI Working Paper, 2004.

M. Groschke, A. Eßer, D. Möst, and W. Fichtner. Neue Anforderungen an optimierende Energiesystemmodelle für die Kraftwerkseinsatz- und Zubauplanung bei begrenzten Netzkapazitäten. *Zeitschrift für Energiewirtschaft*, 33(1):14–22, 2009.

GtV. *Bestehende Projekte der Tiefen Geothermie*. Bundesverband Geothermie e.V. (GtV-BV), http://www.geothermie-dialog.de/index.php?option=com_content&view=category&id=4&Itemid=5 (retrieved 09.06.2011), 2011.

T. J. Hammons. International Practice in Distributed Generation Developments Worldwide. In *Proceedings of the 42nd Universities Power Engineering Conference*. IEEE, 2007.

E. Handschin, S. Kuhn, C. Rehtanz, R. Schultz, and D. Waniek. Optimaler Kraftwerkseinsatz in Netzengpasssituationen. In R. Schultz and H.-J. Wagner, editors, *Innovative Modellierung und Optimierung von Energiesystemen*, chapter 3, pages 39–68. LIT Verlag Dr. W. Hopf, 2009a.

E. Handschin, D. Mahlke, A. Martin, C. Rehtanz, D. Waniek, and A. Zelmer. Kostenoptimierte Planung gekoppelter Strom-, Gas- und Wärmenetze. In R. Schultz and H.-J. Wagner, editors, *Innovative Modellierung und Optimierung von Energiesystemen*, chapter 2, pages 9–38. LIT Verlag Dr. W. Hopf, 2009b.

S. Hao. Decentralized Approach to Intermarket Congestion Management. *IEEE Transactions On Power Systems*, 20(2):675–683, 2005.

E. Hausman, R. Fagan, D. White, K. Takahashi, and A. Napoleon. *LMP Electricity Markets: Market Operations, Market Power, and Value for Consumers*. Synapse Energy Economics Inc., 2006.

H. Heinrichs, A. Eßer-Frey, P. Jochem, and W. Fichtner. Zur Analyse der langfristigen Entwicklung des deutschen Kraftwerkparks. In V.-G. Energietechnik, editor, *Optimierung in der Energiewirtschaft*. VDI-Verlag, 2011.

A. Held. *Modelling the future development of renewable energy technologies in the European electricity sector using agent-based simulation*. Fraunhofer Verlag, Karlsruhe, 2011.

L. Hillemacher, A. Eßer-Frey, and W. Fichtner. Preis- und Effizienzsignale im MeRegio Smart Grid Feldtest - Simulationen und erste Ergebnisse. *Proceedings der IEWT 2011*, 2011.

B. Hobbs, M. Rothkopf, R. O'Neill, and H. Chao. *The Next Generation of Electric Power Commitment Models*. Kluwer Academic Publishers, 2001.

W. Hogan. Contract Networks for Electric Power Transmission. *Journal of Regulatory Economics*, (4):211–242, 1992.

W. Hogan. *Transmission Congestion: The Nodal-Zonal Debate Revisited*. 1999.

F. Hoster. *Auswirkungen des europäischen Binnenmarktes für Energie auf die deutsche Elektrizitätswirtschaft: ein Ansatz zur Analyse ordnungs- und umweltpolitischer Instrumente in der Elektrizitätswirtschaft* . Oldenbourg, München, 1996.

IEA. *World Energy Outlook*. International Energy Agency, 2008.

IEA and NEA. *Projected Costs of Generating Electricity: 2010 Edition*. International Energy Agency (IEA) and the OECD Nuclear Energy Agency (NEA), 2010.

R. Inderst and A. Wambach. Engpassmanagement im deutschen Übertragungsnetz. *Zeitschrift für Energiewirtschaft*, 31(4):333–342, 2007.

A. G. Isemonger. Market Redesign and Technology Upgrade: A Nodal Implementation. *The Electricity Journal*, 22(8):72–81, 2009.

E. Jochem, P. Radgen, C. Schmid, W. Mannsbart, W. Pfaffenberger, W. Schulz, A. Voß, M. Blesl, U. Fahl, J. Zschernig, J. Sager, D. Fahlenkamp, D. Hölder, and C. Dötsch. *Strategien und Technologien einer pluralistischen Fern- und Nahwärmeversorgung in einem liberalisierten Energiemarkt unter besonderer Berücksichtigung der Kraft-Wärme-Kopplung und erneuerbarer Energien - Kurzfassung der Studie*. AGFW, Frankfurt, 2000.

N. Johnson, C. Yang, and J. Ogden. A GIS-based assessment of coal-based hydrogen infrastructure deployment in the state of Ohio. *International Journal of Hydrogen Energy*, 33:5287–5303, 2008.

K. Jopp. Trend zu überkritischen Kohlekraftwerken der 800-MW-Klasse. *BWK*, 60 (7/8):50–52, 2008.

P. L. Joskow. Lessons learned form electricity market liberalization. *The Energy Journal*, (Special Issue - The future of electricity: Papers in Honor of David Newbery):9–40, 2008.

P. Jürgens. *Tageseinsatzplanung in hydrothermischen Kraftwerkssystemen - ein Verfahrensvergleich*, volume Band 25. Aachen, aachener beiträge zu energieversorgung edition, 1994.

M. Kaltschmitt, W. Streicher, and A. Wiese. *Erneuerbare Energien - Systemtechnik, Wirtschaftlichkeit, Umweltaspekte*, volume 4. Springer, Berlin, 2009.

S. Kearney. How Outage Management Systems Can Improve Customer Services. In *Proceedings of the 1998 ESMO IEEE 8th International Conference on Transmission and Distribution Construction, Operation and Live-Line Maintenance*, pages 172–178. 1998.

F. Kießling, P. Nefzger, J. Nolasco, and U. Kaintzyk. *Overhead power lines: planning, design, construction.* Springer, Berlin; Heidelberg; New York; Hong Kong; London; Milan; Paris; Tokyo, 2003.

M. Klobasa. *Dynamische Simulation eines Lastmanagements und Integration von Windenergie in ein Elektrizitätsnetz.* Fraunhofer IRB Verlag, Stuttgart, 2009.

KraftNAV. Verordnung zur Regelung des Netzanschlusses von Anlagen zur Erzeugung von elektrischer Energie (Kraftwerks-Netzanschlussverordnung - KraftNAV). *BGBl*, I:1187, 2007.

T. Krause. *Congestion Management in Liberalized Electricity Markets - Theoretical Concepts and International Application.* Zürich, 2005.

T. Krause. *Evaluating Congestion Management Schemes in Liberalized Electricity Markets Applying Agent-based Computational Economics.* Dissertation ETH Zürich, Zürich, 2007.

T. Kristiansen. Congestion management, transmission pricing and area price hedging in the Nordic region. *Electrical Power and Energy Systems*, (26):685–695, 2004.

T. Kronenberg and K. Engel. Demographischer Wandel und dessen Auswirkungen auf den Energieverbrauch in Hamburg und Mecklenburg Vorpommern. *Zeitschrift für Energiewirtschaft*, 2008(04):280–290, 2008.

C.-C. Kuo and Y.-T. Chao. Energy management based on AM/FM/GIS for phase balancing application on distribution systems. *Energy Conversion and Management*, 51:485–492, 2010.

KWKG. Gesetz für die Erhaltung, die Modernisierung und den Ausbau der Kraft-Wärme-Kopplung (Kraft-Wärme-Kopplungsgesetz). *BGBl*, (1):1092, 2002.

A. Le Dars and C. Loaec. Economic comparison of long-term nuclear fuel cycle management scenarios: The influence of the discount rate. *Energy Policy*, 35:2995–3002, 2007.

F. Leuthold. *Economic Engineering Modeling of Liberalized Electricity Markets: Approaches, Algorithms, and Applications in the European Context.* Technische Universtität Dresden (Dissertation), Dresden, 2010.

F. Leuthold and C. Todem. Flow-Based Coordinated Explicit Auctions: Auction Income Distribution. In *Proceedings of the Conference on "The Economics of Energy Markets"*. 2007.

F. Leuthold, H. Weigt, and C. v. Hirschhausen. Efficient pricing for European electricity networks - The theory of nodal pricing applied to feeding-in wind in Germany. *Utilities Policy*, (16):284–291, 2008.

F. Leuthold, H. Weigt, and C. v. Hirschhausen. A Large-Scale Spatial Optimization Model of the European Electricity Market. *Networks and Spatial Economics*, pages 1–31, 2010.

O. Lüth. *Strategien zur Energieversorgung unter Berücksichtigung von Emissionsrestriktionen.* VDI, Düsseldorf, 1997.

A. Luchmaya, B. Dwolatzky, and A. Meyer. Using Terrain Information in an Electrification Planning Tool. In *Proceedings of the Transmission and Distribution Conference*, pages 456–460. IEEE, 2001.

J. Malczewski. GIS-based multicriteria decision analysis: a survey of the literature. *International Journal of Geographical Information Science*, 20(7):703–726, 2006.

D. Martinsen, V. Krey, and P. Markewitz. Implication of high energy prices for energy systems and emissions - The response from an energy model for Germany. *Energy Policy*, 35:4504–4515, 2007.

F. Matthes and M. Cames. *Energiewende 2020: Der Weg in eine zukunftsfähige Energiewirtschaft.* Heinrich-Böll-Stiftung, Berlin, 2000.

P. Meiborn, H. Larsen, R. Barth, H. Brand, C. Weber, and O. Voll. *Wilmar Joint Market Model.* Risoe National Laboratory, Roskilde, 2006.

S. Messner. *Users guide for the matrix generator of message II.* IASA, Laxenburg, 1984.

S. Messner and L. Schrattenholzer. MESSAGE-MACRO: linking an energy supply model with a macroeconomic model and solving it iteratively. *Energy*, 25:267–282, 2000.

S. Messner and M. Strubegger. Model-based decision support in energy planning. *Internaional Journal Of Global Energy Issues*, (12):196–207, 1999.

MEX I. *Energiemodelle zum Klimaschutz in Deutschland - Strukturelle und gesamtwirtschaftliche Auswirkungen aus nationaler Perspektive.* Forum für Energiemodelle und Energiewirtschaftliche Systemanalysen in Deutschland, Physica-Verlag, Heidelberg, 1999.

MEX II. *Energiemodelle zum Kernenergieausstieg in Deutschland - Effekte und Wirkungen eines Verzichts auf Strom aus Kernkraftwerken.* Forum für Energiemodelle und Energiewirtschaftliche Systemanalysen in Deutschland, Physica-Verlag, Heidelberg, 2002.

MEX III. *Energiemodelle zum Klimaschutz in liberalisierten Energiemärkten - Die Rolle erneuerbarer Energieträger.* Forum für Energiemodelle und Energiewirtschaftliche Systemanalysen in Deutschland, Lit-Verlag, Münster, 2004.

MEX IV. *Energiemodelle zum europäischen Klimaschutz - Der Beitrag der deutschen Energiewirtschaft.* Forum für Energiemodelle und Energiewirtschaftliche Systemanalysen in Deutschland, Lit-Verlag, Münster, 2004.

V. Miranda, C. Monteiro, and I. Ramírez-Rosado. Negotiation Aid System For Promotion of Distributed Generation and Renewables. In *Proceedings of the IEEE Transmission and Distribution Conference*. IEEE, 2002.

T. Mohar, K. Bakic, and J. Curk. Advanced Planning Procedure and Operation of Distribution Network Supported by SCADA and GIS. In *Proceedings of the Power Engineering Society Winter Meeting*, pages 2780–2785. IEEE, 2000.

C. Monteiro, I. Ramírez-Rosado, V. Miranda, M. Sousa, P. Lara-Samtillan, E. Zorzano-Alba, and P. Zorzano-Santamaría. Spatial Analysis Tool to Evaluate Spatial Incremental Costs on Electric Distribution. In *Proceedings of the IEEE Porto Power Tech Conference*, pages 4–7. IEEE, 2001.

T. Morgenstern. *Dekomposition eines linearen Energieflussmodells*. Schulz-Kirchner Verlag, Idstein, 1991.

D. Möst. *Zur Wettbewerbsfähigkeit der Wasserkraft in liberalisierten Elektrizitätsmärkten - Eine modellgestützte Analyse dargestellt am Beispiel des schweizerischen Energieversorgungssystems*. Peter Lang, Frankfurt a.M., 2006.

D. Möst. *Energy economics and energy system analysis - Methods for decision support and its application in energy markets*. KIT, professorial dissertation, Karlsruhe, 2010.

D. Möst and W. Fichtner. Einführung zur Energiesystemanalyse. In D. Möst, W. Fichtner, and A. Grunwald, editors, *Energiesystemanalyse*, chapter 2, pages 11–32. Universitätsverlag Karlsruhe, 2008.

D. Möst and W. Fichtner. Renewable energy sources in European energy and interactions with emission trading. *Energy Policy*, 38(10):2898–2910, 2010.

D. Möst and M. Genoese. Market power in the German wholesale electricity market. *The Jounal of Energy Markets*, 2(2):47–74, 2009.

D. Möst, I. Tietze-Stöckinger, W. Fichtner, and O. Rentz. The use of optimizing energy models to derive electricity prices. In H. Fleuren, D. den Hertog, and P. Kort, editors, *Operations Research Proceedings 2004: Selected Papers of the Annual International Conference of the German Operation Research Society (GOR)*, pages 254–262. Springer-Verlag, 2004.

D. Möst, M. Genoese, A. Eßer, and O. Rentz. European electricity and emission market modeling - the design of emission allocation plans and its effects on investment planning. In *IEEE Proceedings of the 5th Conference on the Euroepean electricity market (EEM)*. 2008.

C. Murillo-Sánchez and R. J. Thomas. Thermal unit commitment with a nonlinear AC power flow network model. In H. et al., editor, *The next generation of electrical power unit commitment models*, chapter 5, pages 75–92. Kluwer Academic Publishers, 2001.

NERAC and GIF. *A Technological Roadmap for Generation IV Nuclear Energy Systems*. U.S. Nuclear Energy Research Advisory Committee (NERAC) and the Generation IV International Forum (GIF), 2002.

Niedersächsische Staatskanzlei. *Netzausbau in Niedersachsen*. Niedersächsische Staatskanzlei, http://www.netzausbau-niedersachsen.de, 2010.

A. Ockenfels, C. Gatzen, and M. Peek. Sind die Gesetze des Wettbewerbs auf dem Strommarkt außer Kraft gesetzt? Analyse der Strompreisbildung auf dem Großhandelsmarkt in Deutschland. *Energiewirtschaftliche Tagesfragen (ET)*, 55(11):4–11, 2005.

B. Oswald. *Vorlesung Elektrische Energieversorgung I - Skript Freileitungen.* Universität Hannover, Institut für Energieversorgung und Hochspannungstechnik, Hannover, 2005.

T. Overbye, X. Cheng, and Y. Sun. *A Comparison of the AC and DC Power Flow Models for LMP Calculations.* Proceedings of the 37th Hawai International Conference on System Science, 2004.

H. Perlwitz. *Der Erdgasmarkt für den Kraftwerkssektor unter CO2-Minderungsverpflichtungen: Eine modellgestütze Analyse des europäischen Energiemarktes.* Universitätsverlag, Karlsruhe, 2007.

W. Pfaffenberger and M. Hille. *Investitionen im liberalisierten Energiemarkt: Optionen, Marktmechanismen, Rahmenbedingungen.* Bremer Energieinstitut, Bremen, technical report edition, 2004.

Y. Ping and A. Sekar. Study of Linear Models in Steady State Analysis of Power Systems. *IEEE Power Engineering Society Winter Meeting*, pages 666–671, 2002.

Platts. *World Electric Power Plants Database.* Platts, Washington DC, 2005.

L. Powell. *Power System Load Flow Analysis.* McGra-Hill, New York, 2004.

Powernext. *Everything you need to know about TLC.* http://static.epexspot.com/document/3830/TLC(Mai 19, 2010), 2010.

R. Prest, T. Daniell, and B. Ostendorf. Using GIS to evaluate the impact of exclusion zones on the connection cost of wave energy to the electricity grid. *Energy Policy*, pages 4516–4528, 2007.

I. Pérez-Arriaga and L. Olmos. A Plausible Congestion Management Scheme for the Internal Electricity Market of the European Union. *Utilities Policy*, (13):117–134, 2005.

J. Price. Market-Based Price Differentials in Zonal and LMP Market Designs. *IEEE Transactions On Power Systems*, 22(4):1486–1494, 2007.

Prognos. *Prognos Deutschland Report 2030.* Prognos AG, Basel, 2009.

K. Purchala, L. Meeus, and R. Belmans. *Zonal network model of European interconnected electricity network.* 2005a.

K. Purchala, L. Meeus, D. M. V. Dommelen, and R. Belmans. Usefulness of DC power flow for active power flow analysis. In *Proceedings of the IEEE Power Engineering Society PES General Meeting.* 2005b.

A. Quelhas, E. Gil, and J. McCalley. Nodal prices in an integrated energy system. *International Journal on Critical Infrastructures*, 2(1):50–68, 2006.

M. Ragwitz, A. Held, G. Resch, T. Faber, R. Haas, C. Huber, R. Coenraads, M. Voogt, G. Reece, P. Morthorst, S. Jensen, I. Konstantinaviciute, and B. Heyder. *Assessment and optimisation of renewable energy support schemes in the European electricity market (OPTRES).* Intelligent Energy Europe, 2007.

G. Rahn. Energie und Emissionshandel. *BWK*, 60(4):62–68, 2008.

H. Ravn. *The Balmorel Model: Theoretical Background*. 2001.

O. Rentz, S. Cail, A. Fleury, I. Tietze-Stöckinger, and W. Fichtner. *Energy Efficiency through White Certificates*. French-German Institute for Environmental Research (DFIU/IFARE), 2004.

S. Rogge. *Geothermische Stromerzeugung in Deutschland - Ökonomie, Ökologie und Potentiale*. Fakultät VI Bauingenieurwesen und Angewandte Geowissenschaften, Berlin, 2004.

J. Rosen. *The future role of renewable energy sources in European electricity supply: A model-based analysis for the EU-15*. Universitätverlag Karlsruhe, Karlsruhe, 2007.

A. Rudkevich, K. Egilmez, M. Liu, P. Murti, P. Visudhiphan, R. Tabors, and T. Overbye. Identification and Congestion Analysis of Transmission Corridors of the Eastern Interconnection. In *Proceedings of the 40th Annual Hawaii International Conference on System Sciences*, pages 124–131. IEEE, 2007.

RWE. *Lastflüsse RWE*. RWE, http://www.rwe.com (retrieved: 01/08/2008), 2008.

RWE. *EEG Anlagenstammdaten*. RWE Transportnetze (retrieved July 27, 2009), http://www.rwetransportnetzstrom.com/web/cms/de/215900/rwe-transportnetz-strom/netznutzung/eeg-kwk/eeg-anlagenstammdaten-aktuell/, 2009.

P. Rychwalski. *Die Zukunkft der Energiemärkte in Deutschland: Auswirkungen und Perspektiven wettbewerbspolitischer Deregulierung am Beispiel des deutschen Strommarktes*. Münster, 2005.

R. Schemm. *Modell zur Untersuchung von Investitionsentscheidungen unter Unsicherheit in Stromerzeugungstechnologien*. genehmigte Dissertation der Technischen Universität Berlin, Berlin, 2011.

M. Schlesinger. Perspektiven und Chancen der Dienstleistungsindustrie in Baden-Württemberg. In *Festvortrag anlässlich der Preisverleihung "Wettbewerb Dienstleister des Jahres 2006"*. 2006.

D. Schmedding. *Erfassung und Bewertung von Straßenverkehrslärm auf der Basis von geographischen Informationssystemen*. Nomos, Baden-Baden, 2006.

M. Schönfelder, A. Eßer-Frey, M. Schick, W. Fichtner, V. Heuveline, and T. Leibfried. New Developments in Modeling Network Constraints in Techno-Economic Energy System Expansion Planning Models - An Overview of Existing Models and Prospects for Future Approaches. *Zeitschrift für Energiewirtschaft*, (4), 2011.

H. Schöttle. *Analyse des Least-Cost Planning Ansatzes zur rationellen Nutzung elektrischer Energie*. Universität Karlsruhe, Dissertation, 1998.

F. Schweppe, M. Caraminis, R. Tabor, and R. Bohn. *Spot pricing of Electricity*. Kluver Academic Publishers, New York, 1988.

SEC. *Third Benchmarking Report on the Implementation of the Internal Electricity and Gas Market*. Staff of the European Commission, Brussels, 2004.

SEC(2001)1957. *First benchmarking report on the implementation of the internal electricity and gas market*. Staff of the European Commission, Brussels, 2001.

SEC(2002)1038. *Second benchmarking report on the implementation of the internal electricity and gas market* . Staff of the European Commission, Brussels, 2002.

SEC(2008)2636. *Commission staff working document accompanying document to the Communication from the Commission 'Progress towards achieving the Kyoto objectives'.* Staff of the European Commission, Brussels, 2008.

SEC(2009)1581. *Commission Staff Working Document Accompanying the Report from the Commission to the European Parliament and the Council: Progress Towards Achiving the Kyoto Objectives.* Commission of the European Communities, Brussels, 2009.

F. Sensfuß, M. Genoese, M. Ragwitz, and D. Möst. Agent-based simulation of electricity markets - a literature review. *Energy Studies Review*, 2008.

P. Seydel, M. Wietschel, and C. Cremer. Die Rolle regionaler Energieträger beim Wasserstoffinfrastrukturaufbau. In *Proceedings of the 5. Internationale Energiewirtschaftstagung an der TU Wien*. 2007.

Y. Smeers. Computable equilibrium models and the restructuring of the European electricity and gas markets. *Energy Journal*, 18(4):1–31, 1997.

Y.-H. Song and X.-F. Wang. *Operation of Market-oriented Power Systems.* Springer, London, 2003.

E. Spring. *Elektrische Energienetze.* VDE Verlag, Berlin, 2003.

F. Staiß. *Jahrbuch Erneuerbare Energien 2007.* Bieberstein Verlag & Agentur, Radebeul, 2007.

G. Stamtsis. *Power Transmission Cost Calculation in Deregulated Electricity Market.* Logos, Berlin, 2004.

G. Stamtsis, J. Christensen, and I. Erlich. Evaluation of Power Systems Congestion Using Nodal Price Analysis. In *Proceedings of the International Symposium MEPS*, pages 25–30. 2002.

G. Stamtsis, M. Björndal, I. Erlich, and K. Jörnsten. *Assessment of the Norwegian Transmission Pricing Rules by Using a Modified AC-OP (Discussion Papers)*, volume 8/2004. Department of Finance and Management Science, Norwegian School of Economics and Business Administration, 2004.

A. Stangeland. A model for the CO2 capture potential. *International Journal of Green House Gas Control*, 2007(1):418–429, 2007.

SteinkohleFinG. Gesetz zur Finanzierung der Beendigung des subventionierten Steinkohlenbergbaus zum Jahr 2018 (Steinkohlefinanzierungsgesetz). *BGBl*, I:3086, 2007.

H. Stigler and C. Todem. Optimization of the Austrian Electricity Sector (Control Zone of VERBUND APG) under the Constraint of Network Capacities by Nodal Pricing. *Central European Journal of Operations Research*, (13):105–125, 2004.

H. Stigler, C. Todem, U. Bachhiesl, M. Zambelli, C. Huber, G. Hafner, and A. Schweiger. *Sicherung der heimischen Elektrizitätsversorgung.* 2004.

S. Stoft. *Power System Economics - Designing Markets for Electricity*. IEEE-Press, Wiley-Inderscience, New York, 2005.

B. Stojkovska, V. Glamocanin, and R. Golob. Towards effective geographic information system for the liberalized markets. In *Proceedings of the Transmission and Distribution Conference*, pages 870–874. IEEE, 2002.

StromNEV. Verordnung über die Entgelte für den Zugang zu Elektrizitätsversorgungsnetzen (Stromnetzentgeltverordnung) vom 25. Juli 2005. *BGBl*, 1:2225, 2005.

StromNZV. Verordung über den Zugang zu Elektrizitätsversorgungsnetzen (Stromnetzzugangsverordnung) vom 25. Juli 2005. *BGBl*, (I):2243, 2005.

D. Sun, X. Ma, and K. Cheung. The Application of Optimization Technology for Electric Market Operation. In *IEEE PES Transmission and Distribution Conference 2005*. 2005.

J. Sun and L. Tesfatsion. *DC Optimal Power Flow Formulation and Solution Using QuadProgJ - Department of Economics Working Paper Series*, volume 06014. Iowa State University, 2006.

S. Szabo, A. Jäger-Waldau, and L. Szabo. Risk adjusted financial costs of photovoltaics. *Energy Policy*, 38:3807–3819, 2010.

I. Tietze-Stöckinger. *Kosteneinsparpotentiale durch Erweiterung von betrieblichen Systemgrenzen - dargestellt an Beispielen von Kooperationen aus den Bereichen Energieversorgung und Abfallentsorgung*. Universitätsverlag, Karlsruhe, 2005.

C. Todem. *Methoden und Instrumente zur gesamtsystemischen Analyse und Optimierung konkreter Problemstellungen im liberalisierten Elektrizitätsmarkt*. Graz University of Technology, Graz, 2004.

transpower. *Stand der Umsetzung der Netzausbaumaßnahmen*. Transpower GmbH, http://www.transpower.de/pages/tennettso_de/Transparenz/Veroeffentlichungen/Berichte_und_aktuelle_Informationen/Netzausbau_undbr_-zustand/pdf_berichte_service/Bericht_zum_3.Quartal_2010_ber_den_Stand_der_Umsetzung_der_Netzausbauvorhaben.pdf (retrieved: 2010-11-11), 2010.

D. TREN. *European Energy and Transport: Trends towards 2030*. Office for Official Publications of the European Communities, Luxembourg Office for Official Publications of the European Communities, update 2007 edition, 2008.

UBA. *Datenbank "Kraftwerke in Deutschland" - Liste der sich in Betrieb befindlichen Kraftwerke bzw. Kraftwerksblöcke ab einer elektrischen Bruttoleistung von 100 MW*. Umweltbundesamt, www.umweltbundesamt.de, 2007.

UBA. *Klimaschutz und Versorgungssicherheit - Entwicklung einer nachhaltigen Stromversorgung*, volume 13/2009. Umweltbundesamt, Dessau, 2009.

UCTE. *Interconnected network of the UCTE*. UCTE - printed publications, 2008.

UN. *United Nations Framework Convention on Climate Change*. United Nations, New York, 1992.

UN. *Kyoto Protocol to the United Nations Framework Convention on Climate Change.* United Nations, Kyoto, 1998.

S. Vajjhala. *Siting Renewable Energy Facilities*, volume Discussion Paper 06-34. RFF, 2006.

L. Vandezande, L. Meeus, and R. Belmans. *Introduction to cross-border balancing in the Central West region.* 2008.

Vattenfall. *Lastflüsse des Übertragungsnetzes der Vattenfall Europe Transmission GmbH an den Kuppelstellen zum Ausland.* Vattenfall Transmission GmbH, www.vattenfall.com (retrieved: 01/04/2008), 2008.

Vattenfall. *EEG Stammdaten Vattenfall.* Vattenfall Europe AG (retrieved July 27, 2009), http://www.vattenfall.de/cps/rde/xchg/trm_de/hs.xsl/165.htm, 2009.

VDEW. *Repräsentative VDEW-Lastprofile.* VDEW, 1999.

M. Ventosa, A. Baillo, A. Ramos, and M. Rivier. Electricity market modeling trends. *Energy Policy*, 33:897–913, 2005.

D. Waniek, U. Häger, C. Rehtanz, and E. Handschin. Influences of Wind Energy on the Operation of Transmission Systems. In *IEEE Power and Energy Society General Meeting - Conversion and Delivery of Electrical Energy in the 21st Century*, pages 1–8. 2008.

D. Waniek, C. Rehtanz, and E. Handschin. Flow-based evaluation of congestions in the electric power transmission system. *EEM 2010 - 7th Converence on the European Energy Market*, 2010.

C. Weber. *Uncertainty in the Electric Power Industry - Methods and Models for Decision Support.* Springer, New York, 2004.

H. Weigt. A time-variant welfare economic analysis of a nodal pricing mechanism in Germany. In *Proceeding of the 5th Conference on Applied Infrastructure Research.* 2006.

H. Weigt. *Modeling Competition and Investment in Liberalized Electricity Market.* Fakultät Wirtschaftswissenschaften - Technische Universität Dresden (dissertation), Dresden, 2009.

H. Weigt, T. Jeske, F. Leuthold, and C. v. Hirschhausen. "Take the long way down": Integration of large-scale North Sea wind using HVDC transmission. *Energy Policy*, (38):3164–3173, 2010.

M. Wietschel. *Die Wirtschaftlichkeit klimaverträglicher Energieversorgung - Entwicklung und Bewertung von CO2-Minderungsstrategien in der Energieversorgung und -nachfrage.* Schmidt, Berlin, 1995.

M. Wietschel, O. Rentz, A. Ardone, W. Fichtner, O. Lüth, and H. Schöttle. PERSEUS: Modellentwicklungsstand, Anwendungsfälle und Perspektiven. In J. F. Hake and P. Markewitz, editors, *Modellinstrumente für CO2-Minderungsstrategien, Konferenzband 42003 (IKARUS-Schriften)*, pages 223–240. Forschungszentrum, 1997.

M. Wietschel, J. Balduf, H. Schöttle, and O. Rentz. Least-Cost Planning im liberalisierten Markt: Chancen und Risiken. *Energiewirtschaftliche Tagesfragen (ET)*, 49 (5):318–323, 1999.

I. Wing. The synthesis of bottom-up and top-down approaches to climate policy modeling: Electric power technology detail in a social accounting framework. *Energy Economics*, 30:547–573, 2008.

F. Wolak, B. Barber, J. Bushnell, and B. Hobbs. *Comments on the California ISO's Transmission Expansion Assessment Methodology (TEAM)*. 2004.

D. Wolter and E. Reuter. *Preis- und Handelskonzepte in der Stromwirtschaft*. Deutscher Universitätsverlag, Wiesbaden, 2005.

H. Wu, C. Tsai, and C. Lu. Load Forecast In A Competitve Retail Market. In *Proceedings of the Transmission and Distribution Conference*, pages 160–164. 1999.

J. Q. Xin, E. Bompard, and R. Napoli. Security Coordinated Economic Dispatch for Joint Energy and Reserve Markets. In *IEEE International Conference on Power System Technology 2006*. 2006.

E. Yeh and H. Tram. Information Integration in Computerized Distribution System Planning. *IEEE Transactions On Power Systems*, 12(2):1008–1013, 1996.

C.-D. Yue and M.-H. Yang. Exploring the potential of wind energy for coastal state. *Energy Policy*, 37:3925–3940, 2009.

ZEP. *EU Demonstration Programme for CO2 Capture and Storage (CCS)*. European Technology Platform for Zero Emission Fossil Fuel Power Plants (ZEP), 2008.

L. Zhang, J. Zhao, X. Han, and P. Yang. A new approach for security constrained unit commitment. In *IEEE International Conference on Power System Technology 2006*. 2006.

Q. Zhou and J. Bialek. *Approximate Model of European Interconnected System as a Benchmark System to Study Effects of Cross-Border Trades*, volume 20. IEEE Transactions On Power Systems, 2nd edition, 2005.

S. Zhou. *Comparison of Market Designs - Market Oversight Division Report*. Public Utility Commission of Texas, 2003.

L. Zifa and Z. Jianhua. Optimal Planning of Substation of Locating and Sizing Based on GIS and Adaptive Mutation PSO Algorithm. In *Proceeding of the International Conference on Power System Technology*. IEEE, 2006.